**CONTRACTOR REPORT**

SAND92—7347
Unlimited Release
UC—721

# Hydrogen Generation by Metal Corrosion in Simulated Waste Isolation Pilot Plant Environments:

## Progress Report for the Period November 1989 through December 1992

M. R. Telander and R. E. Westerman
Pacific Northwest Laboratory
Operated for the US Department of Energy
by Battelle Memorial Institute

Prepared by Sandia National Laboratories Albuquerque, New Mexico 87185
and Livermore, California 94550 for the United States Department of Energy
under Contract DE-AC04-76DP00789

Printed July 1993

Issued by Sandia National Laboratories, operated for the United States Department of Energy by Sandia Corporation.

**NOTICE:** This report was prepared as an account of work sponsored by an agency of the United States Government. Neither the United States Government nor any agency thereof, nor any of their employees, nor any of their contractors, subcontractors, or their employees, makes any warranty, express or implied, or assumes any legal liability or responsibility for the accuracy, completeness, or usefulness of any information, apparatus, product, or process disclosed, or represents that its use would not infringe privately owned rights. Reference herein to any specific commercial product, process, or service by trade name, trademark, manufacturer, or otherwise, does not necessarily constitute or imply its endorsement, recommendation, or favoring by the United States Government, any agency thereof or any of their contractors or subcontractors. The views and opinions expressed herein do not necessarily state or reflect those of the United States Government, any agency thereof or any of their contractors.

Printed in the United States of America. This report has been reproduced directly from the best available copy.

Available to DOE and DOE contractors from
Office of Scientific and Technical Information
PO Box 62
Oak Ridge, TN 37831

Prices available from (615) 576-8401, FTS 626-8401

Available to the public from
National Technical Information Service
US Department of Commerce
5285 Port Royal Rd
Springfield, VA 22161

NTIS price codes
Printed copy: A10
Microfiche copy: A01

SAND92-7347
Unlimited Release
Printed September 1993

Distribution
Category UC-721

# Hydrogen Generation by Metal Corrosion in Simulated Waste Isolation Pilot Plant Environments:

## Progress Report for the Period November 1989 through December 1992[a]

M. R. Telander and R. E. Westerman
Pacific Northwest Laboratory
Operated for the US Department of Energy
by Battelle Memorial Institute

## ABSTRACT

The corrosion and gas-generation characteristics of three material types: low-carbon steel (the current waste packaging material for the Waste Isolation Pilot Plant), Cu-base materials, and Ti-base materials were determined in both the liquid and vapor phase of Brine A, a brine representative of an intergranular Salado Formation brine. Test environments included anoxic brine and anoxic brine with overpressures of $CO_2$, $H_2S$, and $H_2$. Low-carbon steel reacted at a slow, measurable rate with anoxic brine, liberating $H_2$ on an equimolar basis with Fe reacted. Presence of $CO_2$ caused the initial reaction to proceed more rapidly, but $CO_2$-induced passivation stopped the reaction if the $CO_2$ were present in sufficient quantities. Low-carbon steel immersed in brine with $H_2S$ showed no reaction, apparently because of passivation of the steel by formation of a protective iron sulfide reaction product. Cu- and Ti-base materials showed essentially no corrosion when exposed to brine and overpressures of $N_2$, $CO_2$, and $H_2S$ except for the rapid and complete reaction between Cu-base materials and $H_2S$. No significant reaction took place on any material in any environment in the vapor-phase exposures.

---

[a] *Prepared for Sandia National Laboratories Waste Isolation Pilot Plant Gas Generation Program, Albuquerque, New Mexico under Contract No. 67-8608.*

## ACKNOWLEDGMENTS

The authors acknowledge the excellent programmatic guidance of the present work provided by Drs. L. H. Brush and M. A. Molecke, Sandia National Laboratories; the technical assistance of D. J. Criswell, S. M. Faber, R. F. Klein, N. D. Stice, and R. B. Watson, PNL, for their contributions to performance of the experimental work; the contributions of K. H. Pool, PNL, and his analytical laboratory staff, for makeup and analysis of the test brines as well as valuable insights into the chemistry of the test environments; D. E. McCready, PNL, for his unflagging interest in performing XRD analyses; R. E. Brinson and M. W. Goheen, PNL, for their cooperation in performing the many gas analyses required; B. L. Hopkins, Westinghouse Hanford Corporation, for performing the He leak checks of the test containers; B. O. Barnes, for his assistance with the Quality Assurance (QA) aspects of the program; D. N. Anderson, PNL, and B. Rutherford, SNL, for their assistance with the statistical analyses; and P. L. Novak, PNL, for her invaluable assistance in editing the final report.

## CONTENTS


EXECUTIVE SUMMARY . . . . . ES-1

1.0 INTRODUCTION . . . . . 1-1

2.0 OBJECTIVE . . . . . 2-1

3.0 SCOPE OF WORK . . . . . 3-1

4.0 TECHNICAL BACKGROUND . . . . . 4-1

4.1 Fe-Anoxic Brine . . . . . 4-1
4.2 Fe-$CO_2$ . . . . . 4-3

4.2.1 General Mechanisms of Corrosion . . . . . 4-4
4.2.2 Thermodynamic Considerations . . . . . 4-6
4.2.3 Corrosion Kinetics, Experimental Studies . . . . . 4-7

4.2.3.1 Effect of Temperature on the Corrosion Product Film . . . . . 4-7
4.2.3.2 Corrosion Rates . . . . . 4-8

4.3 Fe-$H_2S$ . . . . . 4-11

4.3.1 General Mechanism of Corrosion . . . . . 4-11
4.3.2 Thermodynamic Considerations . . . . . 4-15
4.3.3 Corrosion Kinetics, Experimental Studies . . . . . 4-16

4.4 Fe-$CO_2$-$H_2S$ . . . . . 4-18
4.5 Cu-Anoxic Brine . . . . . 4-21
4.6 Cu-$CO_2$ . . . . . 4-22
4.7 Cu-$H_2S$ . . . . . 4-23

4.7.1 Thermodynamic Considerations . . . . . 4-23
4.7.2 Kinetics of the Cu-$H_2S$ Reaction . . . . . 4-24

4.8 Ti-Anoxic Brine . . . . . 4-25
4.9 Ti-$CO_2$ and Ti-$H_2S$ . . . . . 4-26

5.0 APPROACH . . . . . 5-1

5.1 Testing Methods . . . . . 5-1

5.1.1 Seal-Welded-Container Test Method . . . . . 5-1
5.1.2 Autoclave Test Method . . . . . 5-7

## CONTENTS (Continued)


5.2 Materials . . . . . 5-7

5.2.1 Low-Carbon Steels . . . . . 5-8
5.2.2 Alternative Packaging Materials . . . . . 5-12
5.2.3 Brine . . . . . 5-13
5.2.4 Salt (Halite) . . . . . 5-14

6.0 RESULTS . . . . . 6-1

6.1 Low-Carbon Steel Tests . . . . . 6-2

6.1.1 Seal-Welded-Container Tests . . . . . 6-3

6.1.1.1 Anoxic Brine (Brine/$N_2$) . . . . . 6-3
6.1.1.2 Brine/$CO_2$ . . . . . 6-14
6.1.1.3 Brine/$H_2S$ . . . . . 6-27

6.1.2 High-Pressure Autoclave Tests . . . . . 6-29

6.1.2.1 High $H_2$ Pressure Tests . . . . . 6-30
6.1.2.2 High $N_2$ Pressure Test . . . . . 6-32
6.1.2.3 High $CO_2$ Pressure Tests . . . . . 6-34

6.1.3 Salt-Phase Autoclave Tests . . . . . 6-40

6.1.3.1 Post-Test Observations, Test AUT-5 . . . . . 6-41
6.1.3.2 Post-Test Observations, Test AUT-6 . . . . . 6-42
6.1.3.3 Corrosion Rates, Tests AUT-5 and AUT-6 . . . . . 6-43

6.2 Alternative Material Tests . . . . . 6-44

6.2.1 Cu in Brine A with $N_2$ . . . . . 6-46
6.2.2 Cu in Brine A with $CO_2$ . . . . . 6-47
6.2.3 Cu in Brine A with $H_2S$ . . . . . 6-47
6.2.4 Ti in Brine A with $N_2$, $CO_2$, and $H_2S$ . . . . . 6-49

7.0 CONCLUSIONS . . . . . 7-1

8.0 FUTURE WORK . . . . . 8-1

9.0 REFERENCES . . . . . 9-1

## CONTENTS (Continued)


APPENDIX A: PRESSURE HISTORIES, ANOXIC BRINE (BRINE/$N_2$) AND BRINE/$CO_2$ SEAL-WELDED-CONTAINER TESTS . . . . . A-1

APPENDIX B-1: INDIVIDUAL-SPECIMEN CORROSION RATE DATA, ANOXIC BRINE ENVIRONMENT, SEAL-WELDED-CONTAINER TEST METHOD . . . . . B-1

APPENDIX B-2: INDIVIDUAL-SPECIMEN CORROSION RATE DATA, ANOXIC BRINE ENVIRONMENT, SEAL-WELDED-CONTAINER TEST METHOD . . . . . B-11

APPENDIX B-3: INDIVIDUAL-SPECIMEN CORROSION RATE DATA, ANOXIC BRINE ENVIRONMENT, SEAL-WELDED-CONTAINER TEST METHOD . . . . . B-21

APPENDIX B-4: INDIVIDUAL-SPECIMEN CORROSION RATE DATA, ANOXIC BRINE ENVIRONMENT, SEAL-WELDED-CONTAINER TEST METHOD . . . . . B-31

APPENDIX B-5: INDIVIDUAL-SPECIMEN CORROSION RATE DATA, AUTOCLAVE TEST AUT-1 . . . . . B-41

APPENDIX B-6: INDIVIDUAL-SPECIMEN CORROSION RATE DATA, AUTOCLAVE TEST AUT-3 . . . . . B-43

APPENDIX B-7: INDIVIDUAL-SPECIMEN CORROSION RATE DATA, AUTOCLAVE TEST AUT-4 . . . . . B-45

APPENDIX B-8: INDIVIDUAL-SPECIMEN CORROSION RATE DATA, AUTOCLAVE TEST AUT-2 . . . . . B-47

APPENDIX B-9: INDIVIDUAL-SPECIMEN CORROSION RATE DATA, AUTOCLAVE TEST AUT-7 . . . . . B-49

APPENDIX B-10: INDIVIDUAL-SPECIMEN CORROSION RATE DATA, AUTOCLAVE TEST AUT-5 . . . . . B-51

APPENDIX B-11: INDIVIDUAL-SPECIMEN CORROSION RATE DATA, AUTOCLAVE TEST AUT-6 . . . . . B-53

## CONTENTS (Continued)

APPENDIX B-12: INDIVIDUAL-SPECIMEN CORROSION RATE DATA, Cu-BASE MATERIALS, ANOXIC BRINE ENVIRONMENT, SEAL-WELDED-CONTAINER TEST 7A . . . . . B-55

APPENDIX B-13: INDIVIDUAL-SPECIMEN CORROSION RATE DATA, Cu-BASE MATERIALS, BRINE/$CO_2$ ENVIRONMENT, SEAL-WELDED-CONTAINER TEST 8A . . . . . B-59

APPENDIX B-14: INDIVIDUAL-SPECIMEN CORROSION RATE DATA, Cu-BASE MATERIALS, BRINE/$H_2S$ ENVIRONMENT, SEAL-WELDED-CONTAINER TEST 3A AND 9A . . . . . B-63

APPENDIX B-15: INDIVIDUAL-SPECIMEN CORROSION RATE DATA, Ti-BASE MATERIALS, ANOXIC BRINE ENVIRONMENT, SEAL-WELDED-CONTAINER TEST 10A . . . . . B-69

APPENDIX B-16: INDIVIDUAL-SPECIMEN CORROSION RATE DATA, Ti-BASE MATERIALS, BRINE/$CO_2$ ENVIRONMENT, SEAL-WELDED-CONTAINER TEST 11A . . . . . B-73

APPENDIX B-17: INDIVIDUAL-SPECIMEN CORROSION RATE DATA, Ti-BASE MATERIALS, BRINE/$H_2S$ ENVIRONMENT, SEAL-WELDED-CONTAINER TEST 12A . . . . . B-77

APPENDIX C: METHOD OF DETERMINING DEGREE OF MOLAR EQUIVALENCE BETWEEN $H_2$ FORMED AND Fe REACTED IN ANOXIC BRINE (BRINE/$N_2$) AND BRINE/$CO_2$ SEAL-WELDED-CONTAINER TESTS . . . . . C-1

APPENDIX D: TOTAL STEEL SPECIMEN AREA, SEAL-WELDED-CONTAINER TESTS . . . . . D-1

## Figures

5-1. Seal-welded test container with specimen rack in place . . . . . 5-2

5-2. Seal-welded test container, fully charged, ready for placement in oven . . . . . 5-3

5-3. Microstructure of steel, lots J and K . . . . . 5-10

5-4. Microstructure of steel, lots L and M . . . . . 5-11

## CONTENTS (Continued)


6-1. Pressure-time curves, low-carbon steel anoxic brine tests . . . . . 6-4

6-2. Post-test appearance of steel specimens, immersed, 6- and 24-month anoxic brine tests . . . . . 6-7

6-3. Post-test appearance of steel specimens, vapor-phase exposure, 24-month anoxic brine tests . . . . . 6-8

6-4. XRD results obtained from the unidentifiable 12- and 24-month-test corrosion products, anoxic brine tests . . . . . 6-12

6-5. Pressure-time curves, low-carbon steel/brine-$CO_2$ tests . . . . . 6-17

6-6. Post-test appearance of steel specimens, immersed, 24-month brine/$CO_2$ tests . . . . . 6-22

6-7. Post-test appearance of steel specimens, vapor-phase exposure, 24-month brine/$CO_2$ tests . . . . . 6-23

6-8. Pressure-time curves, controlled-$CO_2$-addition tests . . . . . 6-26

6-9. Pressure-time curves, Fe-$H_2S$ tests, test containers 40-43 . . . . . 6-29

6-10. Pressure-time curves, tests AUT-7 and AUT-8 . . . . . 6-39

6-11. Test arrangements, tests AUT-5 and AUT-6 . . . . . 6-41

6-12. Method of mounting specimens on specimen rack for alternative packaging materials tests . . . . . 6-45

6-13. Pressure-time curves, tests 3A, 9A, and 15A . . . . . 6-48


## Tables


3-1. Test matrix, low-carbon-steel tests . . . . . 3-2

3-2. Test matrix, alternative packaging materials tests . . . . . 3-3

4-1. Summary of corrosion rate data, aqueous $H_2S$ systems . . . . . 4-17

5-1. Compositions of low-carbon steels . . . . . 5-9

## CONTENTS (Continued)


5-2. Compositions of alternative materials used in corrosion/gas-generation study . . . . . 5-13

5-3. Composition of brines used in tests . . . . . 5-14

6-1. Composition of gas at conclusion of test, anoxic brine (brine/$N_2$) tests . . . . . 6-6

6-2. Summary of corrosion-rate data, immersed specimens, anoxic brine (brine/$N_2$) tests . . . . . 6-10

6-3. Results of brine analyses, anoxic-brine seal-welded container tests . . . . . 6-10

6-4. Comparison of moles of $H_2$ formed (by pressure increase) with moles of Fe reacted . . . . . 6-13

6-5. Composition of gas at conclusion of test, brine/$CO_2$ tests . . . . . 6-18

6-6. Summary of corrosion-rate data, immersed specimens, brine/$CO_2$ tests . . . . . 6-19

6-7. Comparison of moles of $H_2$ formed (gas analysis) with moles of Fe reacted (by specimen weight change), brine/$CO_2$ tests . . . . . 6-20

6-8. Results of brine analyses, brine/$CO_2$ seal-welded-container tests . . . . . 6-24

6-9. Summary of test conditions, controlled-$CO_2$-addition tests . . . . . 6-25

6-10. Summary of test conditions, $H_2$-overpressure tests AUT-1, AUT-3, and AUT-4 . . . . 6-31

6-11. Corrosion rates of steel specimens in high $H_2$ pressure tests compared with corrosion rates in brine/$N_2$ seal-welded container tests . . . . . 6-32

6-12. Corrosion rates of steel specimens in high $N_2$ pressure tests compared with corrosion rates in brine/$N_2$ seal-welded container tests . . . . . 6-34

6-13. Corrosion rates of steel specimens, test AUT-7 . . . . . 6-37

6-14. Corrosion rates of steel specimens in solid-salt tests, compared with corrosion rates in brine/$N_2$ seal-welded container tests . . . . . 6-43

6-15. Initial conditions, tests 1A through 19A . . . . . 6-46

# EXECUTIVE SUMMARY

A mined geologic repository site for demonstrating the safe management and disposal of defense-related transuranic (TRU) waste is being developed by the US Department of Energy near Carlsbad, New Mexico. The site, designated the Waste Isolation Pilot Plant (WIPP), is located in the bedded salt of the Salado Formation, at a depth of 655 m (2150 ft) below the land surface.

If brine should enter the repository and contact the low-carbon steel waste containers (and metallic items in the waste), the possibility exists that corrosion product $H_2$ could pressurize the facility. The rate of $H_2$ formation and the ultimate $H_2$ pressure attained would be dependent on the amount of brine available, the corrosion products formed, the kinetics of the specific corrosion reactions involved, and the available storage volume.

Sandia National Laboratories (SNL), WIPP Gas Generation Program, issued a subcontract to Pacific Northwest Laboratory (PNL)[a] authorizing the performance of laboratory experiments to assist in resolving the gas generation and performance assessment-related questions. The present report summarizes the laboratory corrosion results obtained through December 1992.

The experimental work has focused on the corrosion/gas generation characteristics of three material types: low-carbon steel (the current packaging material); Cu-base materials; and Ti-base materials. The latter two classes are considered to be alternative packaging materials should low-carbon steels prove unusable. Four basic test environments are being used in the tests: Brine A (a Na, Mg, K chloride-sulfate brine simulating a WIPP intergranular Salado Formation brine) with a $N_2$ overpressure; Brine A with a $CO_2$ overpressure; Brine A with an $H_2S$ overpressure; and Brine A with an $H_2$ overpressure.

Test specimens of low-carbon steel have been exposed to the test environments in the entirely immersed condition as well as the vapor-phase-only condition. Limited testing has been done with steel specimens embedded in nearly pure particulate halite (NaCl) obtained from the WIPP site. All testing has been done at 30°C. The experimental work has involved a determination of the rate at which pressure ($H_2$ gas) builds in test containers; the gravimetric determination of the metal lost from the test specimens because of the corrosion reaction; correlation between $H_2$ formed and metal reacted, where possible; identification of the corrosion products formed; and post-test determination of the compositions of gases and brines in the test containers.

It has been shown that the long-term (last 12 months of 24-month corrosion tests) corrosion rate of steel in anoxic Brine A is 0.71 $\mu$m/yr, producing 0.10 mol $H_2/m^2$-steel-yr. The corrosion product is not adherent and not identifiable by x-ray diffraction analysis (XRD). The long-term corrosion rate is approximately linear. Increasing the pressure of $N_2$ increases the corrosion rate.

A dichotomy exists in the case of $CO_2$ overpressures, in that increasing the gas overpressure increases the initial corrosion rate and also increases the probability of passivation due to the formation of an impermeable corrosion product film, either $FeCO_3$ or a close relative.

In the low-carbon steel corrosion studies, the molar equivalency between Fe reacted and $H_2$ formed was satisfactory in both the $N_2$/immersed and the $CO_2$/immersed tests. Steel exposed to the vapor phase over Brine A only, with either $N_2$ or $CO_2$ present, showed essentially no evidence of corrosion.

Steel specimens exposed to a $H_2S$ pressure of 5 atm, either immersed in Brine A or suspended in Brine A vapor, showed essentially no reaction. This is attributed to the passivating effect of pyrite ($FeS_2$) or a similar protective higher-sulfide corrosion product.

Limited anoxic corrosion studies were performed in which steel specimens were embedded in particulate salt (halite) that had been obtained from the Salado Formation in the WIPP underground workings. The particulate salt was either (a) contacting a pool of Brine A in a test autoclave (a "wicking" test) or (b) suspended above the Brine A (an attempt to form a "vapor transport" test). The corrosion rates observed in the former test were similar to those observed in tests in which steel specimens were immersed in Brine A with a $N_2$ overpressure. In the latter test, the intended vapor-transport process was compromised by an unexpected condensation-drip process from the underside of the autoclave head. The corrosion rates were relatively low, because of (a) lack of reactant $H_2O$, or (b) the low-Mg test environment resulting from the condensed-$H_2O$ drip.

Alternative packaging materials (Cu-base and Ti-base alloys) showed essentially no corrosion when exposed to environments of Brine A and overpressures of $N_2$, $CO_2$, and $H_2S$, except for the rapid and complete reaction between the Cu-base materials and $H_2S$. Cu-base materials would appear to be a poor choice for use in the WIPP repository if $H_2S$ is expected to be present in the environment, for example, through generation by microbial sulfate-reduction processes. It appears as though Ti-base materials could be used without concern for significant gas production.

# 1.0 INTRODUCTION

A mined geologic repository for demonstrating the safe management and disposal of defense-related transuranic (TRU) waste is being developed by the US Department of Energy near Carlsbad, New Mexico. The site, designated the Waste Isolation Pilot Plant (WIPP), is located in the bedded salt of the Salado Formation, at a depth of 655 m (2150 ft) below the land surface. Eight storage panels of seven rooms each will be mined. The panels, access ways, and shafts will be sealed before the site is decommissioned.

At the present time, a large quantity of transuranic (TRU) wastes are being temporarily stored in steel drums and steel waste boxes at waste generator sites. Under current plans, these wastes would be transported to and emplaced within the WIPP site without additional modification of the original packaging. Additional metal pieces (Fe- and Al-based alloys, for example) are contained within the waste containers as contaminated waste materials.

A number of scenarios have been advanced whereby brine could intrude into the repository (Guzowski, 1990). Should brine contact the metallic waste containers (and certain of the metallic wastes within the containers), anoxic corrosion product $H_2$ would be expected to form (Lappin et al., 1989; Brush et al., 1991b; Brush et al., 1991a). The amount of $H_2$ and the ultimate $H_2$ pressure attained would be dependent on the amount of brine available for reaction, the corrosion products formed, and the kinetics of the corrosion reactions involved. The effect of microbes in the brine/waste repository environment and the possible formation of $CO_2$ and/or $H_2S$ by microbial activity have also been cited as being potentially important gas-generation processes.

Butcher (1990) has discussed the potential negative effects of gas pressure on the WIPP site. This pressure will tend to retard room closure; it can contribute to fractures within the disturbed rock zone; it has the potential of leaking from the site, possibly causing perceptual, technical, or regulatory concerns; it can contribute to two-phase gas-driven flow from the repository; and it could possibly degrade the repository sealing system.

The site-pressurization concerns led to a selection of alternative container materials; that is, materials that would not be expected to generate significant quantities of gas in the WIPP repository environment. A Waste Container Materials Panel was convened by the WIPP Project in 1990 (EATF, 1991) to make a preliminary selection of alternative packaging materials. Of the metallic

container materials considered, copper-base and titanium-base alloys were judged to offer the best combination of properties when fabricability, availability, technology status, cost, and gas-generation potential were taken into account. Though no programmatic decision has yet been made regarding the use of these alternative materials, verification of their corrosion and gas-generating characteristics has been considered to be an important task in support of the WIPP Project so that their use could be invoked if deemed necessary.

Past studies have not permitted an unambiguous resolution of the WIPP gas generation and repository pressurization question, because of 1) use of test temperatures different from those expected in WIPP disposal rooms, 2) inadequate test durations, 3) inadequate backpressure of corrosion product gases, and 4) an inadequate simulation of the brine chemistry specific to the WIPP site. For these reasons, the Sandia National Laboratories (SNL) WIPP Gas Generation Program, on behalf of the WIPP Project, issued a subcontract to Pacific Northwest Laboratory (PNL) authorizing the performance of laboratory experiments to assist in resolving the gas-generation question as it relates to low-carbon steel and alternative material corrosion. This report summarizes all available results obtained since the receipt of work authorization at PNL in November 1989 through the end of calendar year 1992.

## 2.0 OBJECTIVE

The major objective of the present WIPP-PNL project is to determine the rate of hydrogen generation and the hydrogen pressurization potential associated with the reaction of steel drum and waste box materials, alternative packaging materials, and metal wastes contained in drums and waste boxes with simulated, repository-relevant WIPP environments.

# 3.0 SCOPE OF WORK

The initial (and major) effort in the present project has been directed toward characterizing the behavior of low-carbon steels in simulated WIPP environments: namely, environments consisting of liquid Brine A or water vapor in equilibrium with Brine A, with overpressures of $N_2$, $CO_2$, $H_2$, or $H_2S$ gas. Four lots (heats) of steel have been included in the tests: two lots of ASTM Grade A366, representative of 55-gallon steel waste drums, and two lots of ASTM Grade A570, representative of steel waste boxes and steel waste components. The $N_2$ overpressure is used in the anoxic test environments in which only the brine constituents are to react with the metal specimens. Because microbial degradation activity on organic-matrix waste materials isolated in the WIPP repository may produce significant quantities of $CO_2$ and $H_2S$, these species have been included in selected tests. This is an important focus of this laboratory program. The test matrix describing the gas-generation studies performed to date involving low-carbon steel is presented in Table 3-1. Discussions of specific low-carbon-steel tests and test results in the present report will be keyed to this matrix by test environment (i.e., gas, brine or vapor, overpressure) and container (test) identification.

The scope of work of the present study was extended beyond low-carbon-steel studies in 1991 to include an assessment of the anoxic corrosion and gas-generation behavior of four alternative WIPP metal packaging materials. These materials are unalloyed copper, cupronickel 90-10, Ti Grade 2 (a grade of commercial-purity Ti), and Ti Grade 12 (a crevice-corrosion-resistant Ti-base alloy containing 0.7-0.9% Ni and 0.2-0.4% Mo). As in the case of the low-carbon-steel studies, the corrosion rates of these materials are being investigated in brine environments with overpressures of $N_2$, $CO_2$, and $H_2S$. The test matrix describing the gas-generation studies performed to date on alternative materials is presented in Table 3-2.

Throughout this report, "psig" refers to psi gauge and "psia" refers to psi absolute, where psig + 14.7 is equivalent to psia. The term "atm" always refers to atmospheres pressure absolute. In describing pressure differences "psi" is used.

The "brine" environment referred to in the test matrices refers to a saturated Na-Mg-K chloride-sulfate brine designated "Brine A." This brine simulates intergranular Salado Formation brines at or near the stratigraphic horizon of the WIPP repository (Molecke, 1983). It is discussed in detail in Section 5.2.3 of this report.

Table 3-1. Test Matrix, Low-Carbon Steel Tests. Pressures given in table are approximate. Test temperature = 30 ±5°C

| Test Type | Overpressure Gas | Container (or Test) Identification | Test Time, Months Aim | Test Time, Months Actual | Initial Gas Overpressure or Amount | Steel Lot(s)[a] in Test | Remarks |
|---|---|---|---|---|---|---|---|
| Specimens immersed in Brine A | $N_2$ | 1, 2 | 3 | 3 | 10 atm | J, K, L, M | Tests concluded, specimens examined |
| | | 9, 10 | 6 | 6 | | | |
| | | 17, 18 | 12 | 12 | | | |
| | | 25, 26 | 24 | 24 | | | |
| SWC[b] | $CO_2$ | 3,[c]4[c] | 3 | 3 | 12 atm | | |
| | | 11,[c] 12[c] | 6 | 6 | | | |
| | | 19,[c] 20[c] | 12 | 12 | | | |
| | | 27,[c] 28[c] | 24 | 24 | | | |
| | | 33 | Open | | 0.32 mol/m$^2$ steel | | Test duration not defined, to be based on observed results |
| | | 34 | | | 0.16 mol/m$^2$ steel | | |
| | | 35 | | | 0.063 mol/m$^2$ steel | | |
| | | 36 | | | 0.032 mol/m$^2$ steel | | |
| | | 37 | | | 0.016 mol/m$^2$ steel | | |
| | | 38[e] | | | 0.00 mol/m$^2$ steel | | |
| | $H_2S$ | 40[c] | | | 5 atm | | |
| | | 41[c] | | | | | |
| Specimens in vapor phase | $N_2$ | 5, 6 | 3 | 3 | 10 atm | | Tests concluded, specimens examined |
| | | 13, 14 | 6 | 6 | | | |
| | | 21, 22 | 12 | 12 | | | |
| SWC | | 29, 30 | 24 | 24 | | | |
| | $CO_2$ | 7, 8 | 3 | 3 | | | |
| | | 15, 16 | 6 | 6 | | | |
| | | 23, 24 | 12 | 12 | | | |
| | | 31, 32 | 24 | 24 | | | |
| | $H_2S$ | 42 | Open | | 5 atm | | Test duration not defined |
| | | 43 | | | | | |
| Specimens immersed in Brine A | $H_2$ | AUT-1 | 3 | 6 | 70 atm | J, K | Tests concluded, specimens examined |
| | | AUT-3 | 6 | 12 | 36 atm | | |
| | | AUT-4 | | | 70 atm | | |
| AUT[d] | $N_2$ | AUT-2 | 3 | 6 | 73 atm | | |
| | $CO_2$ | AUT-7 | 6 | 6 | 36 atm | J, K, L, M | |
| | | AUT-8 | 12 | Open | | | In progress |
| Specimens embedded in salt | $N_2$ | AUT-5 | 3 | 3 | 10 atm | J | Salt mass contacting brine - concluded |
| AUT | | AUT-6 | | | | | Salt mass above brine - concluded |

[a] J = ASTM A366; K = ASTM A366; L = ASTM A570; M = ASTM A570.
[b] SWC = seal-welded test containers.
[c] Containers equipped with 300-psig full-range gauges. All other SWC tests equipped with 200-psig full-range gauges.
[d] AUT = high-pressure autoclave system.
[e] Part of test series directed toward determining the effect of $CO_2$, but contains only $N_2$ as a control.

Table 3-2. Test Matrix, Alternative Packaging Materials Tests. Specimens immersed in brine in seal-welded test containers. Temperature = 30 ±5°C

| Material | Overpressure Gas | Container (or Test) Identification | Test Time, Months Aim | Actual | Remarks |
|---|---|---|---|---|---|
| Copper and cupronickel 90-10 | $N_2$, 10 atm | 1A | 6 | 10 | Tests concluded, specimens examined |
| | | 7A | 12 | 15 | |
| | | 13A | 24 | Open | Aim test duration not yet attained |
| | $CO_2$, 10 atm | 2A | 6 | 10 | Tests concluded, specimens examined |
| | | 8A[a] | 12 | 15 | |
| | | 14A[a] | 24 | Open | Aim test duration not yet attained |
| | $H_2S$, 5 atm | 3A | 6 | 9 | Tests concluded, specimens examined |
| | | 9A[a] | 12 | 15 | $H_2$ vented, container re-pressurized with $H_2S$ at 9 months |
| | | 15A[a] | 24 | Open | Aim test duration not yet attained ($H_2$ vented, container re-pressurized with $H_2S$ at 9 months) |
| Ti Grade 2 and Ti Grade 12 | $N_2$, 10 atm | 4A | 6 | 10 | Tests concluded, specimens examined |
| | | 10A | 12 | 15 | |
| | | 16A | 24 | Open | Aim test duration not yet attained |
| | $CO_2$, 10 atm | 5A | 6 | 10 | Tests concluded, specimens examined |
| | | 11A | 12 | 15 | |
| | | 17A[a] | 24 | Open | Aim test duration not yet attained |
| | $H_2S$, 5 atm | 6A | 6 | 9 | Tests concluded, specimens examined |
| | | 12A | 12 | 15 | |
| | | 18A[a] | 24 | Open | Aim test duration not yet attained |
| None | $H_2S$, 5 atm | 19A | Open | | "Control" container |

[a] Tests equipped with 300-psig full-range gauges. All others equipped with 200-psig full-range gauges.

The principal metal wastes contained within the existing TRU waste receptacles capable of participating in $H_2$-generating reactions are alloys of Fe and Al. The gas-generating behavior of Fe alloys is currently being investigated because of the obvious potential importance of the low-carbon-steel drums and waste boxes currently in use. The behavior of Al alloys has not yet been addressed. Initiation of Al alloy investigations is planned for CY 1993.

# 4.0 TECHNICAL BACKGROUND

The present study has focused on the corrosion and gas-generation characteristics of low-carbon steel, Cu-base materials, and Ti-base materials in simulated WIPP environments consisting of brine with overpressures of $N_2$, $CO_2$, $H_2$, and $H_2S$. Relevant background information obtained from the literature will be presented in this section of the report, in the following order:

- Fe-anoxic brine
- Fe-$CO_2$
- Fe-$H_2S$
- Cu-anoxic brine
- Cu-$CO_2$
- Cu-$H_2S$
- Ti-anoxic brine
- Ti-$CO_2$
- Ti-$H_2S$

## 4.1 Fe-Anoxic Brine

On a thermodynamic basis, iron is capable of reacting with water to form high hydrogen overpressures. Brush et al. (1991a; 1991b) have estimated the hydrogen fugacities to be $\sim$400 atm in equilibrium with an $Fe_3O_4$ reaction product and $\sim$60 atm in equilibrium with an $Fe(OH)_2$ reaction product. Simpson and Schenk (1989) presented similar thermodynamic conclusions. Brush et al. noted that the $Fe(OH)_2$ product is unstable compared to the $Fe_3O_4$ product. The high potential pressures predicted by such thermodynamic calculations provided the WIPP Project incentive for laboratory studies (such as the present PNL study) designed to determine the kinetics of the corrosion

and gas-generation reactions and the nature of the reaction products formed. Also, such calculations have provided the incentive for investigating the potential replacement of low-carbon steels with alternative packaging materials.

The tendency for steels to corrode in anoxic brine at significant rates with concomitant production of hydrogen has been documented in recent studies. For example, Haberman and Frydrych (1988) investigated the corrosion of cast low-carbon steels in synthetic anoxic Permian Basin brines at temperatures of 90, 150, and 200°C. They found significant corrosion rates and reported that the corrosion rates increased with the Mg concentration in the brine. Simpson and Schenk (1989) studied the corrosion of low-carbon steel in natural and synthetic granitic ground waters and NaCl solutions at 25, 50, and 80°C over a pH range of 7-10 and concluded that the resulting reactions could produce $H_2$ at a rate faster than it could diffuse through the compacted bentonite backfill proposed for a Swiss nuclear repository. They reported a corrosion (penetration) rate of 3.6 μm/yr (0.14 mil/yr, or "mpy") for a low-carbon steel in a neutral (pH 7) anoxic NaCl brine containing 8000 ppm $Cl^-$ (0.23 M) at 50°C; the corresponding rate in 800 ppm $Cl^-$ (0.023 M) brine is 1.4 μm/yr (0.055 mpy). The test duration was described only as that required to reach a steady-state corrosion rate, with a minimum test duration of 16 days. By contrast, Braithwaite and Molecke (1980) reported the linearized corrosion rate of low-carbon steel (AISI 1018) in both Brine A, a concentrated Na-Mg-K brine, and Brine B, a nearly saturated NaCl brine, under anoxic test conditions at 25°C, to be 30 μm/yr (1.2 mpy). The test duration was 28 days. The relatively high corrosion rate reported by Braithwaite and Molecke (1980) was apparently due either to the relatively corrosive brine media used in their tests or to the possibility that the test duration used by Simpson and Schenk (1989) was much longer than 28 days, allowing the corrosion rate to decrease to a relatively low level due to the formation of a corrosion product film on the surface of the steel specimens that retarded the corrosion rate.

Grauer et al. (1991) investigated the corrosion/gas generation of steel under anoxic conditions in aqueous cementitious (alkaline) environments. Their work clearly demonstrates the profound effect of pH on steel corrosion under anoxic conditions. The low-temperature data of Grauer et al. (1991)

and Simpson and Schenk (1989) illustrate the effect of pH on the corrosion rate of steel over a range of anoxic aqueous environments:

| pH | Approximate Relative Corrosion Rate |
|---|---|
| 7 | 1 |
| 10 - 11 | 0.1 - 0.01 |
| 12 | 0.01 - 0.001 |
| 13 | <0.001 |

Although these conclusions are approximate, they provide some guidance in evaluating the potential beneficial effect of additions of alkaline reagents to the WIPP backfill material to decrease the corrosion rate of steel containers.

## 4.2 Fe-$CO_2$

The corrosive effects of aqueous solutions of $CO_2$ on low-carbon and low-alloy steels have been well known and have been the subject of many research investigations over the past 50 years. Most of the work has been sponsored by oil and gas producers. The subject has received increased attention in recent years with the increased use of $CO_2$ pressurization in enhanced oil recovery techniques, and with the occurrence of $CO_2$ in deep gas-producing wells. The nature of the research sponsorship explains the general nature of the work found in the literature: corrosion studies done under flowing conditions at elevated temperature over short test durations, frequently with the aqueous solutions not saturated with corrosion products. The objective of such work is, of course, to improve the economics of gas and oil production by determining optimal alloys for tubular products and developing effective corrosion inhibition methods. These conditions are not generally relevant to expected WIPP conditions, so only a small fraction of the large body of research results available in the literature are directly applicable to or comparable with the present PNL studies.

### 4.2.1 General Mechanisms of Corrosion

Aqueous $O_2$-free solutions of $CO_2$ are corrosive to iron and low-carbon steels because they form weak acids:

$$CO_2 + H_2O = H_2CO_3 = H^+ + HCO_3^- \quad (1)$$

$$HCO_3^- = H^+ + CO_3^{2-} \quad (2)$$

$$Fe = Fe^{2+} + 2e^- \quad (3)$$

$$2H^+ + 2e^- = H_2 \quad (4)$$

$$H_2CO_{3ads} + 1e^- = H_{ads} + HCO_{3ads}^- \quad (5)$$

The corrosion rate of bare steel in carbonic acid solutions is controlled by the kinetics of the $H_2$ evolution at the cathode [Equations (4) and (5)]. It has been determined that the hydrogen evolution from steel surfaces in contact with $CO_2$ solutions can occur by the two fundamentally different mechanisms shown in Equations (4) and (5). One mechanism involves the electrochemical reduction of $H^+$ ions that diffuse to the surface of the steel, in common with general acid corrosion phenomena [Equation (4)]. The other mechanism involves the direct reduction of adsorbed $H_2CO_3$ molecules, as shown in Equation (5) (Schmitt, 1983a). The relative rapidity of the hydrogen reduction by the two parallel mechanisms makes corrosion in aqueous $CO_2$ solutions relatively rapid compared to corrosion in other acids, such as HCl, at the same pH (Schmitt, 1983a; Hausler and Stegmann, 1988).

The increase generally found in steel corrosion rates (prior to stable corrosion product film formation) in aqueous $CO_2$ solutions with increasing pressure of $CO_2$ (see Section 4.2.3.2 of this report) is consistent with Equations (4) and (5). The pH decreases with increasing $CO_2$ pressure, attaining values as low as 4.3 at 0.1 atm, 3.9 at 1 atm, and 3.4 at 10 atm $CO_2$ over a 0.5 M NaCl solution at

25°C (Crolet and Bonis, 1984). Seki et al. (1982) report pH values of 5.1 and 4.3 at $CO_2$ pressures of 0.1 atm and 1 atm, respectively, using an artificial seawater solution. These results are consistent with an increase in the rate of Equation (4) with increased $CO_2$ pressure. The increasing concentration of $H_2CO_3$ with $CO_2$ pressure, according to the Henry's Law constant for the specific solution involved, would of course be consistent with an increase in the rate of Equation (5) with increasing $CO_2$ pressure. As the reaction of the iron or steel surface in aqueous $CO_2$ solutions proceeds, the corrosion product $FeCO_3$ (siderite) will form if the solubility of $Fe^{2+}$ in the solution near the metal surface has attained the saturation concentration:

$$Fe^{2+} + CO_3^{2-} = FeCO_3 \tag{6}$$

by the overall reaction

$$Fe + CO_2 + H_2O = FeCO_3 + H_2 \tag{7}$$

Formation of an $FeCO_3$ film on a given low-carbon or low-alloy steel is favored by static or low-flow-rate conditions. These conditions permit the concentration of $Fe^{2+}$ ions to increase near the corroding steel surface and eventually attain the saturation concentration. Other conditions that favor $FeCO_3$ deposition are alkaline conditions from addition of alkaline corrosion inhibitors, for example, and increased temperature due to the retrograde solubility of $FeCO_3$. On the other hand, increasing $CO_2$ partial pressure and the concentration of calcium or magnesium ions in the brine increases the iron carbonate solubility (Hausler, 1983).

It has been generally found that chloride ion concentration is not an important factor in the corrosion of steels in aqueous $CO_2$ environments (Ikeda et al., 1984).

Another possible corrosion product in the corrosion of steels in aqueous $CO_2$ environments is $Fe_3O_4$. Its formation is favored by low $CO_2$ and $H_2$ fugacities and elevated temperatures. Dunlop et al. (1983) have computed the stability fields of $FeCO_3$ and $Fe_3O_4$ as a function of the $CO_2$ and $H_2$

fugacities and temperature. Also, Ca can be found in siderite films when the environment contains Ca salts. Murata et al. (1983) suggested the possibility that this is due to codeposition of $CaCO_3$ with $FeCO_3$.

Conditions in the WIPP (i.e., essentially static conditions, limited brine volume, and high $Fe^{2+}$ availability) are consistent with a rapid formation of corrosion product film on the surface of corroding steel. The corrosion product is expected to exert ultimate rate control through the control of reactant transport kinetics. Hausler (1983) postulated that the transport processes through the siderite film involved simultaneous migration of $Fe^{2+}$ ions, by an interstitial diffusion process, and electron transport via protonation of carbonate ions in the siderite lattice. After testing the model with experimental results, he concluded that the model was overly simple and could not readily explain all of the complex corrosion processes observed. The detailed corrosion-product-layer transport processes that control the corrosion rates of steel in static aqueous environments containing $CO_2$ remain largely undefined.

### 4.2.2 Thermodynamic Considerations

The overall reaction of Fe with $H_2O$ and $CO_2$ to form $FeCO_3$ and $H_2$ [Equation (7)] is strongly favored thermodynamically. If the $\Delta G^\circ$ values for $H_2O$, $CO_2$, and $FeCO_3$ at 25°C are assigned (Rossini et al., 1952), and if the fugacity of $H_2O$ is assigned the value 0.03 atm (Brush, 1991b), the following equilibrium constant results:

$$\frac{f_{H_2}}{f_{CO_2}} = 6 \times 10^5 \qquad (8)$$

Equation (8) shows that, under equilibrium conditions, the fugacity of $H_2$ could equal $6 \times 10^5$ times the fugacity of $CO_2$. This information provides incentive for a study of the kinetic processes involved, as a $CO_2$ fugacity of less than 0.001 atm could, in theory, produce an $H_2$ pressure sufficient to affect the integrity of the repository.

### 4.2.3 Corrosion Kinetics, Experimental Studies

As previously mentioned, the major part of the reported research work performed to date has been done at temperatures higher than the expected WIPP operating temperature of ~30°C and has also utilized flowing systems and short-term (typically 1-7 days) test durations. A great deal of work has been done under test conditions that do not permit formation of adherent corrosion product films. And, of course, no corrosion investigations have been performed by others in test media equivalent to Brine A with $CO_2$ overpressures. In spite of these obvious problems of relevance of results, that experimental work which appears to be in some way related to the WIPP site conditions or that would tend to augment the PNL investigations will be described here.

#### 4.2.3.1 EFFECT OF TEMPERATURE ON THE CORROSION PRODUCT FILM

A profound effect of temperature has been observed on the nature of the corrosion product film formed on steel in aqueous $CO_2$ solutions. In corrosion tests utilizing a flowing 5% NaCl brine with a 30 atm overpressure of $CO_2$ (equilibrated with the brine at 25°C in a different portion of the loop), Ikeda et al. (1983) found that at temperatures <60°C the $FeCO_3$ that formed on the steel surface was "soft and not adhesive." The corrosion observed was uniform. At temperatures in the vicinity of 100°C, the film was "thick and not tight," and deep pitting attack was observed. At temperatures >150°C, the $FeCO_3$ film was "fine, tight, and adhesive," and uniform corrosion was again observed. According to Schmitt (1983b), "considering the present knowledge on $CO_2$ corrosion, it appears that the temperature is obviously the most important parameter." Schmitt (1983b), in an admittedly overly simplified analysis, characterized $CO_2$ corrosion of steels at temperatures <60°C as forming non-protective films, with the rate of corrosion being dependent on $H_2$ evolution and independent of flow rate. He went on to state that the corrosion rate under these low-temperature circumstances would be expected to be predicted by the relation

$$\log \text{rate} = 0.67 \log P_{CO_2} + C \qquad (9)$$

where $P_{CO_2}$ is the pressure of $CO_2$ in atmospheres and C is a constant. This relation was first described by de Waard and Milliams (1975a; 1975b) and has been shown to predict corrosion rates reasonably well under a variety of $CO_2$-charged-brine conditions *that essentially preclude formation of an adherent $FeCO_3$ film* (Schmitt, 1983a; Videm and Dugstad, 1987; Ikeda et al., 1983). In a separate review of low-temperature corrosion, Schmitt (1983a) stated that the corrosion dependence on $CO_2$ pressure [per Equation (9)] has been shown to be reliable to low partial pressures of $CO_2$ (<2 atm) and temperatures up to 60°C "under laminar flow conditions."

It should be further noted that de Waard and Milliams (1975b) were forced to reject data from a significant number of tests in developing their corrosion rate-$CO_2$ pressure relationship [Equation (9)] because of an $FeCO_3$ film forming on their corrosion specimens and yielding corrosion-rate results that were too low. This generally occurred at temperatures >60°C in their "vigorously stirred" solutions, but also happened at 40°C if the solution (0.1 or 1.0% NaCl) was stagnant. Based on the results of the work performed by the investigators cited, and bearing in mind the inherent WIPP-relevance questions already described, it appears that the corrosion product films expected to form on steel under $CO_2$-charged repository conditions will have protective characteristics, but that they may not be as protective as films formed at higher temperatures, i.e., temperatures >60°C.

#### 4.2.3.2 CORROSION RATES

Summaries of the corrosion kinetics observed in a large number of steel corrosion studies in aqueous $CO_2$ systems were presented by Videm and Dugstad (1987), Burke (1984), and DeBerry and Clark (1984).

The corrosion rates in flowing environments at 25°C and $CO_2$ pressures >1 atm [one study only, due to A. A. Abramyan, reported by DeBerry and Clark (1984)] show steel corrosion rates of >5 mm/yr (>200 mpy) at 10 atm pressure of $CO_2$, and a rate of >10 mm/yr (>400 mpy) at 35 atm pressure of $CO_2$. These data were obtained in an aqueous environment (unspecified by DeBerry and Clark) flowing at 1 cm/s. The tests were only 12 h in duration. The corrosion rate

versus $P_{CO_2}$ plot is in excellent agreement with Equation (9), suggesting that the metal surfaces were unencumbered by corrosion product films. This could be due to the flow rate, the very-short-term nature of the tests, or both.

Loop test results at higher temperatures and more rapid flow rates show even higher corrosion rates than those of Abramyan. The grouping (60 to 100°C, 1 m/s to 20 m/s, variable pH, variable $Fe^{2+}$ concentrations) of loop data presented by Videm and Dugstad (1987) shows a range of corrosion rates from 4 mm/yr (160 mpy) to 20 mm/yr (800 mpy) at 1 atm $CO_2$ pressure; from 20 mm/yr (800 mpy) to 60 mm/yr (2400 mpy) at 10 atm $CO_2$ pressure; and from 40 mm/yr (1600 mpy) to ~100 mm/yr (~4000 mpy) at 35 atm $CO_2$ pressure.

It appears that only two quantitative, low-temperature (20 to 30°C) static (unstirred, unflowing) studies have been reported on steel corrosion in aqueous $CO_2$ environments wherein corrosion product films have been obviously permitted to form on the corrosion specimens. In one study, Rhodes and Clark (1936) exposed specimens of two lots of steel (0.18 C, 0.39 Mn; 0.22 C, 0.66 Mn) to distilled water at various pressures of $CO_2$ at 22.5°C. Test durations were ~3 days. The penetration rates observed ranged from 1.2 mm/yr (47 mpy) at 10 atm $CO_2$ pressure to 1.5 mm/yr (60 mpy) at 31 atm (450 psia). These rates are only about one-fourth as high as the rates determined by Abramyan under flowing conditions, consistent with the formation of a partially protective film on the specimens in the static test. Rhodes and Clark did report a "loose black coating" on their specimens that was easily removed by "wiping with cloth." The corrosion rates obtained in the low-$CO_2$-pressure range agreed well with Equation (9). The high-$CO_2$-pressure data showed lower-than-expected rates, suggesting a higher degree of corrosion product film integrity at the higher $CO_2$ concentrations. The second static-environment, film-forming study was performed by Greco and Wright (1962). They used a somewhat lower range of $CO_2$ pressures than Rhodes and Clark (0.25-4.5 atm), a 400-ppm NaCl solution, a test duration of 2 days, and a test temperature of 30°C. The test material is described as "shim stock," as "mild steel," and as "iron"; its exact composition is not clear. Greco and Wright reported corrosion rates of 0.25 mm/yr (9.9 mpy) at 0.25 atm $CO_2$; 0.35 mm/yr (14 mpy) at 1 atm $CO_2$; and 0.93 mm/yr (37 mpy) at 5 atm $CO_2$. These data provide a very satisfactory continuation (extrapolation) of the data of Rhodes and Clark to lower $CO_2$ pressures. The corrosion-rate data of Greco and Wright exhibit the $CO_2$ pressure dependency shown in Equation (9) over the entire pressure range, consistent with only partial protection from the "extremely slight and gray in color" film that formed on the specimens in the course of the short (2-day) test periods.

Three additional autoclave studies deserve mention here. Murata et al. (1983) described the results obtained from autoclave studies using a simulated seawater environment, temperatures of 25°and 60°C, a 5-day test duration, a low-carbon steel (0.12% C, 1.28% Mn, 0.021% Nb, 0.03% Al) test material, and a $CO_2$ pressure range of $10^{-2}$ to $10^2$ atm. Unfortunately, it was not reported whether the specimens were covered with corrosion product during the test exposure, and a lack of description of the degree of agitation of the test medium makes it difficult to determine. The authors imply clean specimen surfaces during the 25°C test to explain the test results because they refer to the presence of a $CaCO_3$ layer on the specimens during the 60°C test, when the pressure of $CO_2$ was above 1 atm. However, the corrosion rates presented are similar to those of Rhodes and Clark (1936), which strongly suggests presence of a corrosion product film.

The second study, by Masamura et al. (1983), involved exposure of a low-carbon steel to water at 40°C with a $CO_2$ pressure of approximately 30 atm in a refreshed autoclave system. The water was equilibrated with $CO_2$ before entering the autoclave. The duration of the test was 4 days. The corrosion rate observed (5.6 mm/yr, or 220 mpy) lies between the filmed-specimen data of Rhodes and Clark (1936) and the bare-specimen-data of Abramyan (DeBerry and Clark, 1984). This intermediate rate suggests that specimen filming occurred and that it occurred partway through the test. However, no detailed description of the specimen(s) after the test is given, so relevant inferences are not possible.

In the third study (Seki et al., 1982), truly static conditions were apparently employed. Specimens of two low-carbon steels were immersed in synthetic seawater at 25°C for 4 days, using $CO_2$ pressures ranging from 1 to 10 atm. The corrosion rates observed under these conditions ranged from 0.47 mm/yr (19 mpy) at 1.0 atm $CO_2$ pressure to 0.76 mm/yr (30 mpy) at 10 atm $CO_2$ pressure, in reasonably good agreement with the filmed-specimen corrosion rate results of Greco and Wright. Nothing is mentioned in the paper, however, about the nature of the specimen surfaces when the test was concluded, though the results are consistent with transport control through semi-protective corrosion product layers. The limited data of Seki et al. (1982) do not show the same degree of $CO_2$ pressure dependence as the data of Greco and Wright, though there is plainly an increase in corrosion rate with increasing $CO_2$ pressure.

## 4.3 Fe-$H_2S$

As in the case of the Fe-$CO_2$ studies described in the previous section of this report, existing Fe-$H_2S$ corrosion data derive primarily from work sponsored by oil and gas producers. The primary focus has been on sulfide-induced cracking of steels; however, some corrosion data exist, and those considered relevant to the WIPP site will be presented in this section of the report.

### 4.3.1 General Mechanism of Corrosion

Weak acid solutions are formed when $H_2S$ gas is dissolved in aqueous solutions:

$$H_2S + H_2O = H^+ + HS^- + H_2O \quad (10)$$

$$HS^- + H_2O = H^+ + S^{2-} + H_2O \quad (11)$$

Crolet and Bonis (1984) and Seki et al. (1982) determined the relationship between the pressure of $H_2S$ gas and the resultant pH in water, 0.5 M NaCl, and simulated seawater solutions. The acidifying effect of $H_2S$ is similar to, but slightly less than, the acidifying effect of $CO_2$ at equivalent pressures. For example, for a 0.5 M NaCl solution at 25°C, Crolet and Bonis give pH values of 4.0 and 3.9 for $H_2S$ and $CO_2$ at 1 atm, respectively. At 10 atm $H_2S$ and $CO_2$, the pH values are 3.6 and 3.4, respectively.

The corrosion of iron or steel in aqueous $H_2S$ solutions can be described by combining the anodic reaction

$$Fe = Fe^{2+} + 2e^- \quad (12)$$

with the cathodic reaction

$$2H^{+} + 2e^{-} = H_2 \quad (13)$$

which utilizes the $H^+$ produced in Equations (10) and (11). The overall reaction is

$$Fe + H_2S = FeS + H_2 \quad (14)$$

or

$$Fe + 2H_2S = FeS_2 + 2H_2 \quad (15)$$

The reaction product $H_2$ is, of course, a matter of concern to the WIPP Project.

A wide range of iron sulfide reaction products can form depending on factors such as pressure of $H_2S$, temperature, and time of exposure. Equation (14) represents the formation of iron sulfides that are approximated by the composition FeS; namely, mackinawite ($FeS_{1-x}$), troilite (FeS), and pyrrhotite ($Fe_{1-x}S$), whereas Equation (15) describes the formation of either marcasite or pyrite ($FeS_2$).[a]

Wikjord et al. (1980) have presented a much more complete description of the sulfides that can form on steels.

In a static environment, the expected corrosion product formation sequence in the reaction of steels with aqueous $H_2S$ solutions is mackinawite[b] ($FeS_{1-x}$) → troilite (FeS) → pyrrhotite ($Fe_{1-x}S$) → pyrite/marcasite ($FeS_2$). Mackinawite, the lowest sulfide, is considered to be the least protective of the sulfide corrosion products; pyrrhotite and pyrite are considered to offer the most protection to the metal substrate (Meyer et al., 1958; Wikjord et al., 1980; Tewari et al., 1979; Tapping et al., 1983; Thomason, 1978).

---

[a] Marcasite and pyrite have the same stoichiometry, but different crystal structures. Marcasite is orthorhombic, pyrite is cubic.

[b] Mackinawite is frequently referred to as "kansite" in older publications. Milton (1966) demonstrated the equivalence of mackinawite and kansite, and recommended that the term "kansite" be dropped.

The sulfide corrosion product formation sequence shown is logical, as the corrosion product layer would be expected to exhibit a greater proportion of higher sulfides as the cation concentration gradient became slower due to film thickening. Differences in system conditions and uncertainty regarding the corrosion product formation kinetics make a prediction of corrosion product(s) difficult, if a specific system has not been previously studied experimentally.

Sardisco et al. (1963) and Sardisco and Pitts (1965) have reported the only data (known to the authors of this report) that tend to contradict the corrosion product sequence noted. In the course of tests of short (3-day) duration in an aqueous environment at 24°C, they observed the formation of a relatively protective film of marcasite/pyrite and troilite, with some mackinawite, at a low $H_2S$ partial pressure (0.0068 atm) in $CO_2$. At greater partial pressures of $H_2S$ (to 0.22 atm), a relatively non-protective film formed, consisting primarily of mackinawite. They found that the best mathematical description of the metal reacted as a function of time could be made, in general, using a mixed-parabolic kinetic expression

$$Ay^2 + By + C = t \tag{16}$$

where A, B, and C are constants

y = metal reacted

t = time

The mixed-parabolic expression is consistent with the overall reaction being controlled partially by an interface reaction and partially by the passage of ions and electrons across the reaction product film. At the lowest $H_2S$ pressure employed (0.00065 atm, or 0.00958 psia), the reaction kinetics tended toward parabolic, expected in the case of protective films. A troilite + pyrite/marcasite film was present on the specimen surfaces. At the highest $H_2S$ pressures employed (0.22 atm, or 3.25 psia), the kinetic expression tended toward linear, consistent with the lack of protectiveness expected from the predominantly mackinawite film.

Meyer et al. (1958) noted an initial protective mackinawite "tarnish film" on steel specimens exposed at room temperature to moist $H_2S$ at ~1 atm pressure. After a time period of 5 to 10 days

the tarnish film changed to a "rough flaky scale" of mackinawite and lost its original highly protective character. When the $H_2S$ was humidified by a 5% NaCl brine, or when $CO_2$ was present in the system, the mackinawite remained the predominant phase. In experiments in which the $H_2S$ was humidified with water alone the initial mackinawite layer became a triple corrosion-product layer, with mackinawite next to the steel surface, a layer of pyrrhotite next, and a layer of pyrite at the gas-corrosion product interface. (It should be noted that the effect of the NaCl solute in the humidifying medium is not at all clear, unless some mechanical transfer of brine from the solution to the specimens occurred. The possibility of this happening was not mentioned by the authors.) The tests of Meyer et al. had a duration of ~125 days.

Thomason (1978) studied the corrosion kinetics of a mild steel in a 3% NaCl solution saturated with $H_2S$ at 1 atm pressure. Testing was done over the temperature range 30 to 90°C; the corrosion tests typically lasted for 6 days. Thomason found that the corrosion rates were highest at the lowest temperatures (30 to 50°C). Only mackinawite was observed, however, on any of the specimens.

Tapping et al. (1983) described methods for producing relatively protective sulfide films on steels, using a combination of exposure times and temperatures. They reported formation of pyrite at 50°C during a 12.2-day exposure in a loop containing "$H_2S$-saturated water," whereas films primarily composed of troilite and pyrrhotite (considered almost as protective as pyrite) formed at 150°C at a 7.1-day exposure. After 9 days at 150°C the film was primarily pyrrhotite.

Wikjord et al. (1980) exposed specimens of SAE 1010 mild steel to water solutions of $H_2S$ at a total system pressure of 1.5 MPa (14.8 atm) at temperatures of 30°C, 100°C, and 160°C. The minimum test time was 30 days. The test specimen was a spinning disk, to simulate velocity effects of flowing process plant fluids. The disks, 51 mm (2.0 in.) in diameter, were typically rotated at 100 rpm.

At 30°C, mackinawite was found at test durations up to 3 h. At 72 h troilite was the principal reaction product. Troilite remained the principal product to the conclusion of the test (30 days). At 60°C, the principal corrosion product changed from troilite to the higher sulfide pyrrhotite over the 30-day test period. At 160°C, troilite converted quickly to the higher sulfide pyrrhotite (1 day), but pyrite did not evidence itself until near the end of the 35-day test. These tests show that higher sulfides are indeed favored by increased exposure time and increased temperature. However, the spinning-disk specimen makes it difficult to extrapolate the findings to a static system.

Tewari et al. (1979) provided qualitative insights into the effect of fluid velocity on the sulfide corrosion products formed on mild steel. They essentially duplicated the work of Wikjord et al. (1980), except that they varied the rotational speed of the disk from 0 to 1440 rpm while maintaining the temperature at 120°C. The total system pressure was 1.6 MPa (15.8 atm). They found that at high rotational speeds the predominant sulfide corrosion product on the disk was mackinawite, which continually dissolved in a steady-state fashion, whereas at low speeds (or static-solution conditions) pyrrhotite or pyrite would form. Presence of bubbles in contact with the disk also promoted the formation of the pyrrhotite/pyrite phases, as mass transport of the mackinawite constituents into the liquid phase was hampered by the bubbles. The high resultant concentration of $Fe^{2+}$ ions induced a series of reactions leading to the formation of pyrrhotite and pyrite. Tewari et al. concluded that "the transformation of mackinawite to higher phases of iron sulphide will, therefore, be favored on corroding carbon steel exposed to aqueous $H_2S$ solutions in a stagnant solution."

Tewari et al. (1979) also showed that a disk pre-filmed with pyrite would undergo no further observable corrosion when exposed to the aqueous $H_2S$ environment.

Based on the investigations reported in the literature, it would be difficult to predict exactly which sulfide corrosion products would be produced on a low-carbon steel surface in static WIPP-relevant brine as a function of $H_2S$ partial pressure and exposure time. It appears certain that long exposure times and high $H_2S$ fugacities favor the protective high-sulfide corrosion products. The effect of the WIPP-site brine constituents on the reaction products, or the overall rate of reaction, cannot be predicted from the literature data.

### 4.3.2 Thermodynamic Considerations

The reaction of Fe with $H_2S$ to form either FeS [Equation (14)] or $FeS_2$ [Equation (15)] and $H_2$ is strongly favored thermodynamically. Assigning $\Delta G°$ values at 27°C for $H_2S$ and troilite, FeS (Chase et al., 1985) results in the expression

$$\frac{f_{H_2}}{f_{H_2S}} = 7 \times 10^{11} \quad (17)$$

The equivalent expression, also at 27°C, with pyrite, $FeS_2$ (Chase et al., 1985), as the product instead of troilite, is

$$\frac{f_{H_2}}{f_{H_2S}} = 1 \times 10^{8} \quad (18)$$

The hydrogen fugacity potentially resulting from a reaction between steel and $H_2S$ could, on an equilibrium thermodynamics basis, become extremely high, even at low $H_2S$ fugacities. The same considerations hold true for $H_2S$ as previously stated for $CO_2$ [Equation (8)], except that the theoretical pressurization potential associated with $H_2S$ is even higher than that of $CO_2$ at equivalent fugacities. These considerations provide the incentive for the present PNL study of the kinetics of the reaction between steel and aqueous $H_2S$ solutions.

### 4.3.3 Corrosion Kinetics, Experimental Studies

A wide range of corrosion kinetics of iron and low-carbon steel in aqueous $H_2S$ environments have been reported. It has been shown that the specific sulfide corrosion product largely dictates the corrosion response, and the film formed depends on exposure time, $H_2S$ activity, temperature, and other environmental factors such as fluid velocity, presence of $CO_2$, and (possibly) brine constituents.

The Fe-aqueous $H_2S$ corrosion data available in the literature possibly having relevance to WIPP site conditions are presented in Table 4-1. The tests are of short duration (very short relative to expected WIPP conditions), and protective layers of higher sulfides would not, in general, be expected to have formed on the specimens. An exception would be the data of Meyer et al. (1958), in the "vapor over $H_2O$" environment, in which a layer of pyrite was shown to have eventually formed over layers of troilite and mackinawite, contributing some undefined degree of protection.

Table 4-1. Summary of Corrosion Rate Data, Aqueous $H_2S$ Systems

| Investigator | Specimen Material | $H_2S$ Pressure, atm | Aqueous Medium | Temp. °C | Test Exposure, Days | Corrosion Rate mm/yr (mpy) | Comments |
|---|---|---|---|---|---|---|---|
| Sardisco and Pitts, 1965 | unalloyed Fe | $6.5 \times 10^{-4}$ to 0.22 in $CO_2$ (1 atm total) | $H_2O$ | 24 | ~3 | 0.46(18) | rate at 0.22 atm $H_2S$ |
| Greco and Wright, 1962 | low-C steel | $4 \times 10^{-6}$ to 0.45 in $CO_2$ (1 atm total) | 400 ppm NaCl brine | 30 | 2 | 0.46(18) | rate at 0.45 atm $H_2S$ |
| Meyer et al., 1958 | low-C steel | ~1 | • vapor over $H_2O$ | room | to 125 | 0.63(25) to 0.25(10) | rates after ~10 days |
| | | ~1 | • vapor over 5% NaCl solution | room | to 125 | 0.63(25) to 1.7(68) | |
| | | ~0.5 + 0.5 atm $CO_2$ | • vapor over 5% NaCl solution | room | to 125 | ~0.63(25) | |
| Thomason, 1978 | low-C steel | ~1 | 3% NaCl solution | 30-90 | ~6 | 0.45(18)<br>1.8(71)<br>0.45(18)<br>0.12(4.7) | - 30°C<br>- 40°C<br>- 50°C<br>- 60°C |
| Bruckhoff et al., 1985 | low-C steel | ~16 | triethyleneglycol + 10% $H_2O$, 0-2% NaCl | 25 | 42 | 0.2(7.9) to 0.5(20) | rates at 2% NaCl (maximum) |
| Hudgins and McGlasson, 1981 | N-80 steel (0.45 C, 1.52 Mn) | 1, 2 | 5% NaCl | 25 to 204 | 30 | 0.4(16)<br><0.03(0.1)<br>0.2(8) | - 25°C<br>- 50°C<br>- 204°C |
| Tewari et al., 1979 | low-C steel | ~23 | $H_2O$ | 120 | 3-10 | nil | rotating disk with preformed pyrite |
| Seki et al., 1982 | low-C steel | 0-10 | synthetic sea water | 25 | 4 | ~0.1(4)<br>~0.6(24) | - 1 atm $H_2S$<br>- 10 atm $H_2S$ |
| Dougherty, 1988 | low-C steel | 4, with 51 atm $CO_2$ and 23 atm $CH_4$ | 0.6% NaCl brine | 27 | 2, 14 | 3.9(154)<br>0.5(20) | - 2-day exposure<br>- 14-day exposure |

The data in Table 4-1 show some degree of consistency in a variety of liquid media over a wide range of $H_2S$ pressures at temperatures of about 30°C. Under these conditions, the observed corrosion rate of steel is ~0.4 mm/yr (~16 mpy). This rate would be expected to diminish with increasing exposure times, based on 1) the expectation that thicker films of any corrosion product, even mackinawite, will eventually slow the kinetics of the sulfidation reaction; and 2) existing data correlating increased protectiveness with higher sulfide corrosion products.

## 4.4 Fe-$CO_2$-$H_2S$

The corrosive effect of mixtures of $CO_2$ and $H_2S$ on low-carbon and alloy steels is of great interest to oil producers, because the two species frequently occur together in deep hot wells. The presence of both $CO_2$ and $H_2S$ is relevant to WIPP waste isolation because of the potential occurrence of various microbial processes on both the waste and sulfate-bearing minerals, e.g., anhydrite. The simultaneous presence of the two gases complicates the already complex and aggressive corrosion situation caused by the presence of either one alone. The existing data are extremely limited and not obviously directly applicable to the WIPP site, but they will be presented here for the insights they might provide.

Sardisco and Pitts (1965) attributed no influence on rate or sulfide reaction product formed to the presence of $CO_2$ at ~1 atm pressure in their tests of iron corrosion at 24°C (see item 1, Table 4-1). This may be justified; on the other hand, $CO_2$ may be a causative factor in their observations of highest sulfides (e.g., pyrite) being formed at low $H_2S$ pressures and the lowest sulfide (mackinawite) at the highest $H_2S$ pressures used in their experiments. These results, which are contrary to Fe/$H_2S$ kinetic expectations, have been noted in the previous section of this report. Greco and Wright (1962) also performed tests at ~1 atm total pressure with $H_2S$ admixed in a $CO_2$ carrier gas. The $H_2S$ ranged in partial pressure from $4 \times 10^{-6}$ atm to 0.45 atm. The tests were performed using low-carbon steel specimens immersed in a dilute (400 ppm NaCl) static brine solution at a temperature of 30°C (item 2, Table 4-1). The tests were very short term (2 days). Greco and Wright found that the corrosion rates in pure $CO_2$ (~0.4 mm/yr, or 16 mpy) sharply decreased with the addition of small amounts of $H_2S$. At a partial pressure of $1.6 \times 10^{-5}$ atm $H_2S$, the rate had decreased to ~1/5 of the pure-$CO_2$ rate. The corrosion rate stayed constant with $H_2S$ partial pressure

until the $H_2S$ partial pressure was greater than ~0.03 atm, at which time the corrosion rate began to increase. At a pressure of 0.45 atm $H_2S$ (~0.5 atm $CO_2$) the corrosion rate was slightly higher (0.46 mm/yr, or 18 mpy) than the pure-$CO_2$ corrosion rate. Greco and Wright did not attempt to correlate the corrosion rates observed with the sulfide corrosion product, as the corrosion products were apparently not analyzed.

The rapid reduction of corrosion rate with $H_2S$ additions to $CO_2$ was also reported by Seki et al. (1982), who tested mild steels in synthetic seawater solutions at 25°C. They employed $H_2S$-$CO_2$ gas mixtures at a maximum total pressure of ~15 atm. At a given $CO_2$ pressure, the corrosion rate decreased sharply with $H_2S$ partial pressure, remained constant over a range of $H_2S$ pressure, then increased to a rate similar to the $CO_2$-pressure rate. Seki et al. did not correlate corrosion rates with corrosion product compositions.

Meyer et al. (1958) determined the corrosion rates of steel samples in water vapor at room temperature with $H_2S$ and $CO_2$, each present at ~0.5 atm partial pressure (see item 3, Table 4-1). Presence of the $CO_2$ diluent produced corrosion rates lower than those in pure $H_2S$. Meyer et al. reported that the corrosion product film formed in the presence of $CO_2$ was predominantly kansite and speculated that $CO_2$ might inhibit the formation of pyrrhotite and pyrite.

Dougherty (1988) immersed specimens of mild steel in a 0.6% NaCl brine, equilibrated with a mixture of $H_2S$ (5%), $CO_2$ (65%), and $CH_4$ (30%) at 78 atm total pressure. The test temperature was 27°C and test durations were 2 days and 14 days (see item 9, Table 4-1). The corrosion rate started relatively high (2-day test), but decreased to a fairly typical value after 14 days. Dougherty apparently did not identify the corrosion product on his test specimens, so a correlation of rate with corrosion product is not possible.

The work described by the foregoing investigations apparently all involved specimens that became coated with sulfide corrosion products early in the course of the specimen exposures to the $H_2S$-containing environment, in spite of the presence of $CO_2$ at relatively high pressures. This is not surprising, as an examination of Equations (8), (17), and (18) clearly shows the thermodynamic stability of the FeS and $FeS_2$ corrosion products relative to the $FeCO_3$ corrosion product. If the previously used $\Delta G°$ values are assigned to the constituents of the equation

$$FeCO_3 + H_2S = FeS + H_2O + CO_2 \quad (19)$$

the equilibrium constant at 30°C is found to be

$$\frac{f_{CO_2} \times f_{H_2O}}{f_{H_2S}} = 3 \times 10^4 \quad (20)$$

At the low fugacity of $H_2O$ expected (Brush et al., 1991b) in equilibrium with Brine A at 30°C ($\sim$0.03 atm)

$$\frac{f_{CO_2}}{f_{H_2S}} = 1 \times 10^6 \quad (21)$$

Equation (21) states that FeS will form rather than $FeCO_3$, if the fugacity of $H_2S$ is $>1 \times 10^{-6} \times f_{CO_2}$. Higher fugacities of $H_2O$, of course, would decrease the value of the ratio of Equation (21), in effect stabilizing $FeCO_3$ relative to FeS. The ratio of Equation (21) is consistent with the results of investigators who found sulfide corrosion products on steel specimens exposed to very low $H_2S$ partial pressures in a $CO_2$ environment.

In their experimental corrosion studies, Ikeda et al. (1984) used an $H_2S$ partial pressure in $CO_2$ insufficient to maintain a sulfide film on specimens of "pure iron" exposed to a flowing 5% NaCl solution. They used a temperature range of 25 to 250°C, a total gas pressure of 30 atm, and a $H_2S$ addition of 3.3, 33, and 330 ppm (by volume). The $H_2S$ was not replenished during the 4-day tests. At 25°C, the $H_2S$ additions of 3.3 ppm and 33 ppm caused an acceleration of the corrosion reaction relative to "no $H_2S$ addition" by the activation of the cathodic reaction. At 33 ppm $H_2S$ the corrosion reaction was slowed relative to the 3.3 ppm $H_2S$ test by the temporary deposition of FeS. Ikeda et al. postulated that, because the $H_2S$ was not replenished, the deposited FeS redissolved and was eventually replaced by a $FeCO_3$ film.

The work of Ikeda et al. is relatively complex, in that 1) the flowing system was capable of affecting the formation kinetics of an $FeCO_3$ film, and 2) the $H_2S$ was not replenished, so the available reactant disappeared with time, allowing $FeCO_3$ films to form.

## 4.5 Cu-Anoxic Brine

The gas-generation potential of unalloyed Cu and Cu-Ni alloys in WIPP-relevant brines is expected to be extremely low, as these metals are noble with respect to hydrogen. The thermodynamic driving force for the reaction

$$2Cu + H_2O = Cu_2O + H_2 \tag{22}$$

[using $\Delta G°$ values obtained from Rossini et al. (1952) for $H_2O$ and $Cu_2O$] is positive, and leads to an equilibrium relationship at 25°C of

$$\frac{f_{H_2}}{f_{H_2O}} = 2 \times 10^{-16} \tag{23}$$

If $f_{H_2O}$ is assigned the expected value at 30°C of ~0.03 atm (Brush et al., 1991b), then

$$f_{H_2} = 6 \times 10^{-18} \tag{24}$$

The $f_{H_2}/f_{H_2O}$ ratio of Equation (23) is so small that one could well suspect that Cu would not react at all with deaerated water. This has been shown to be the case. Simpson and Schenk (1987) found that no $H_2$ evolution could be detected from the corrosion of Cu in dilute chloride solutions at 50 and 80°C, "supporting the thermodynamic evidence that water cannot be an oxidant for copper in pure water or dilute chloride media." They concluded that the small weight changes that the Cu specimens exhibited were due to a Cu chloride complex solubility and possible reaction with residual $O_2$ in the system.

Findings of Westerman (1988) are consistent with the same thermodynamic argument. Specimens of unalloyed Cu, 90-10 Cu-Ni, and 70-30 Cu-Ni were exposed to saturated Na-Ca-Mg-K chloride brine under anoxic test conditions at 90°C and 150°C for 3 months. At the conclusion of the test the specimens were found to be bright, with no apparent oxide or corrosion product layer. The linearized corrosion rates of the specimens at 90°C from weight loss determination were all

$<0.2$ $\mu$m/yr ($<0.008$ mpy). Thus, if the reaction of Cu with a given brine results in the formation of a corrosion product of no greater thermodynamic stability than $Cu_2O$, the fugacity of $H_2$ resulting from the reaction is expected to be negligible.

## 4.6 Cu-$CO_2$

The reaction between Cu and Cu-Ni alloys to produce $H_2$ from aqueous $CO_2$ solutions would be expected to take the form

$$Cu + CO_2 + H_2O = CuCO_3 + H_2 \quad (25)$$

If $\Delta G°$ values at 25°C are assigned to $CO_2$ and $H_2O$ (Rossini et al., 1952) and $CuCO_3$ (Silman, 1958), an expression relating $H_2$ fugacity to the fugacities of $CO_2$ and $H_2O$ results:

$$\frac{f_{H_2}}{f_{CO_2} \times f_{H_2O}} = 4 \times 10^{-23} \quad (26)$$

Again setting $f_{H_2O} = 0.03$ atm, the expected fugacity of $H_2O$ in equilibrium with a repository-relevant brine at 30°C, we have the expression

$$\frac{f_{H_2}}{f_{CO_2}} = 1 \times 10^{-24} \quad (27)$$

The expected fugacity of $H_2$, according to Equations (26) and (27), would be expected to be minimal if a corrosion product no more thermodynamically stable than $CuCO_3$ formed in the aqueous $CO_2$ solution. For lack of other insights as to what such a product might be, it would be reasonable to assume that no significant gas generation would take place due to the reaction of Cu or Cu-Ni alloys with a repository brine in equilibrium with even very high pressures of $CO_2$.

## 4.7 Cu-$H_2S$

Unlike anoxic aqueous solutions, or aqueous $CO_2$ solutions, aqueous sulfide solutions are known to readily attack Cu and Cu-base alloys (ASM, 1987). Because of the need to use natural waters, such as polluted seawater, as a coolant in heat exchangers tubed with Cu-base alloys, a great deal of research has been done in an attempt to understand and control the corrosion of Cu and Cu-base alloys by sulfides. Most of the corrosion research has therefore been done using oxygenated solutions that simulate natural waters (Vreeland, 1976; Macdonald et al., 1979; Gudas and Hack, 1979; Popplewell, 1980; Eiselstein et al., 1983; Gehring et al., 1983). Such studies have shown that the co-presence of sulfide and $O_2$ in seawater results in very high corrosion rates (tens of mm/yr metal penetration) of Cu-Ni alloys, far higher than if sulfide ion alone were present. The accelerated corrosion appears to be the result of the sulfide preventing the formation of a protective oxide corrosion product layer, supported by a cathodic reduction of $O_2$ (Eiselstein et al., 1983). Kato et al., 1984 have postulated that the sulfide layer's dominant role is that of a catalyst for $O_2$ reduction. Gudas and Hack (1979) demonstrated that sulfide concentrations as low as 0.01 $g/m^3$ (10 ppb by weight) can cause high corrosion rates of Cu-Ni alloys in aerated seawater.

### 4.7.1 Thermodynamic Considerations

In the absence of $O_2$, the reaction between $H_2S$ and Cu can be written

$$Cu + H_2S = Cu_2S + H_2 \qquad (28)$$

Chalcocite, $Cu_2S$, is the corrosion product generally observed. The cathodic reduction of $H^+$ has been shown to take the place of $O_2$ reduction in anoxic systems (Macdonald et al., 1979). A thermodynamic analysis of Equation (28) shows a strong potential for $H_2$ generation. Assigning $\Delta G°$ values to $Cu_2S$ (Rossini et al., 1952) and $H_2S$ (Chase et al., 1985) results in the expression

$$\frac{f_{H_2}}{f_{H_2S}} = 1 \times 10^9 \quad (29)$$

for temperatures in the vicinity of 25°C. It is apparent that the fugacity of corrosion-product $H_2$ is very much higher than the fugacity of $H_2S$. The relationship shown in Equation (29) obviously gives incentive to determining 1) the availability of $H_2S$ and 2) the rate of the Cu-$H_2S$ reaction, should the use of a Cu-base alloy be considered as an alternative waste container material.

### 4.7.2 Kinetics of the Cu-$H_2S$ Reaction

As previously noted, the literature on the kinetics of Cu-$H_2S$ reactions in anoxic systems is sparse. Syrett (1977) studied the reaction kinetics of Cu with dilute $H_2S$ solutions at 30°C with and without dissolved $O_2$. In his tests, a cylindrical copper specimen was rotated to produce turbulent flow conditions in an aqueous environment. Total system pressure was 1 atm. $H_2S$ gas was bubbled through the solution at an unspecified partial pressure to produce a concentration in the solution of 1.94 ppm sulfide ion. Syrett calculated a Cu corrosion rate of ~0.01 mm/yr (0.4 mpy) at the end of the 2-day test. Addition of ~0.9 ppm $O_2$ to the solution accelerated the rate of attack by a factor of 30.

Booker et al. (1984) determined the corrosion behavior of a Cu-1.8% Be alloy in simulated oil field environments consisting of simulated sea water in equilibrium with various mixtures of $H_2S$, $CO_2$, and $N_2$. The total system pressure was 68 atm. Booker et al. used three test temperatures—66°, 121°, and 149°C—and test durations up to 30 days. They found average corrosion rates of 0.0078 mm/yr (0.31 mpy) at 66°C in a gas mixture of 1% $H_2S$ and 20% $CO_2$, and an average corrosion rate of 0.019 mm/yr (0.75 mpy) at 66°C in a gas mixture of 10% $H_2S$ and 20% $CO_2$. The corrosion rates over a 30-day test duration showed no tendency for corrosion rate reduction with time. The 30-day corrosion rates increased by a factor of ~4 between 66°C and 121°C in the 1% $H_2S$ environment, and by a factor of ~10 in the 10% $H_2S$ environment.

## 4.8 Ti-Anoxic Brine

Ti is an active metal that relies on its stable oxide film for its oxidation resistance. The thermodynamic driving force for the reaction

$$Ti + 2H_2O = TiO_2 + 2H_2 \tag{30}$$

is extremely high. Assigning $_{\Delta}G°$ values at 25°C for $H_2O$ (Rossini et al., 1952) and $TiO_2$ (Turkdogan, 1980) yields the expression

$$\frac{f_{H_2}}{f_{H_2O}} = 4 \times 10^{35} \tag{31}$$

If the repository is at 30°C and the water vapor is in equilibrium with a halite-saturated brine, then

$$f_{H_2} = \sim 1 \times 10^{34} \text{ atm} \tag{32}$$

A container made of a Ti-base alloy reacting in an active manner with a brine solution would obviously be capable of compromising the integrity of the WIPP. An active reaction with brine at the expected temperature of 30°C is not expected, however, and there is a great deal of corrosion data to support that conclusion.

In an excellent summary of the corrosion behavior of Ti and Ti alloys relevant to nuclear repository conditions, Soo (1983) shows, from the data of several investigators, that the uniform corrosion rates of both commercial-purity Ti and Ti Grade 12 [a Ti-Ni-Mo alloy that exhibits a high degree of crevice (and uniform) corrosion resistance] are $<0.1$ μm/yr ($<0.004$ mpy) in deoxygenated WIPP Brine A at 30°C.

Braithwaite and Molecke (1980) and Molecke et al. (1983) investigated the corrosion behavior of Ti-base alloys in nuclear waste disposal applications and concluded that Ti-base alloys offered an excellent degree of corrosion resistance for this service.

In a saturated NaCl brine, over a pH range of 0 to 14, both commercial-purity Ti and Ti Grade 12 are expected to be essentially completely resistant to both uniform corrosion and crevice corrosion at temperatures $<70°C$. In saturated NaCl brine at pH of 8, the "nil corrosion" temperature is $\sim 150°C$ for commercial-purity Ti and $\sim 270°C$ for Ti Grade 12 (ASM, 1980). Similar findings were recently published by Japanese investigators, who used an electrochemical repassivation method to establish permissible operating conditions for commercial-purity Ti as a function of $Cl^-$ concentration and system temperature. They concluded that, in saturated NaCl brine, an exposure temperature below $\sim 55°C$ would preclude crevice corrosion (Asano et al., 1992).

Conditions anticipated in the WIPP would appear to be totally compatible with the use of a Ti or a Ti Grade 12 container as long as the repository temperature lies in the vicinity of 30°C. The amount of gas generated by corrosion reactions under these circumstances would be expected to be extremely small.

## 4.9 Ti-$CO_2$ and Ti-$H_2S$

The passive film formed on the surface of Ti makes the metal resistant to attack by a broad range of chemical environments, including aqueous $H_2CO_3$ and $H_2S$ solutions (Jones, 1992; Schutz, 1986). Titanium is considered to be "excellent" in carbonic acid service, at temperatures to 100°C (Schweitzer, 1986). It is expected to exhibit corrosion rates $<0.05$ mm/yr ($<2$ mpy) under these conditions. Schutz (1986) stated that Ti can be used to temperatures "in excess of 200°C" in wet or dry $CO_2$ and $H_2S$. Aqueous solutions of $H_2S$, in equilibrium with $H_2S$ pressures as high as 15 atm are routinely contained in titanium autoclaves (Tewari et al., 1979; Wikjord et al., 1980).

It appears from the foregoing accounts of Ti applications in aqueous $H_2CO_3$ and $H_2S$ solutions that no significant reaction would be expected between Ti containers and aqueous $CO_2$ or $H_2S$ solutions in the WIPP.

# 5.0 APPROACH

All of the $H_2$-generation studies are being performed using laboratory test equipment and laboratory facilities. Each test follows one of two basic testing methods, according to the type of reaction vessel employed. The test methods, the metallic test materials, and the brine used in the testing program are described in this section of the report.

## 5.1 Testing Methods

Two test methods are being used in the program: the seal-welded-container test method and the autoclave test method.

### 5.1.1 Seal-Welded-Container Test Method

Tests performed in the presence of brine and low-to-intermediate gas pressures (e.g., 0 to 20 atm) make use of seal-welded containers made of Hastelloy C-22,® a corrosion-resistant Ni-Cr-Mo alloy (Figures 5-1 and 5-2). The specimen rack shown in Figure 5-1 is used for low-carbon-steel tests, and is discussed in more detail in Section 6.1.1 of this report. The alternative packaging material tests used a somewhat different arrangement, described in Section 6.2. In both cases, the same specimen support rack geometry is used. The rack shown in Figure 5-1 is in the position used for immersed-specimen testing. For vapor-phase testing the rack would be inverted.

Because the course of the reaction is monitored by the pressure of $H_2$ retained within the container by means of the pressure gauge, and because atmospheric gases must be rigorously excluded from the test environment, it is imperative that the containers be leak-free. To that end, the containers are of all-welded construction (with the exception of the gauge's pipe-thread joint with the

® Hastelloy C-22 is a registered trademark of Haynes International, Kokomo, IN.

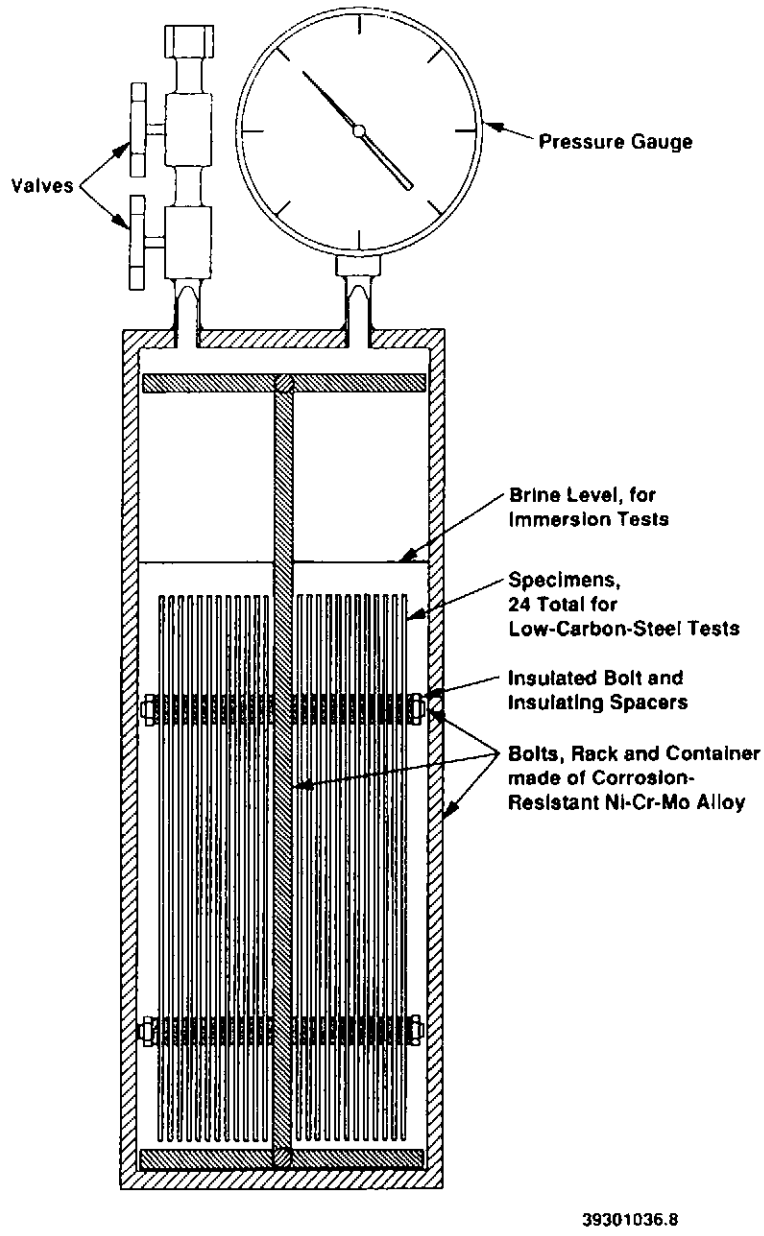



Figure 5-1. Seal-welded test container with specimen rack in place. Inside dimensions (typical): 28.9 cm (11.4 in.) high, 10.2 cm (4.0 in.) diameter.

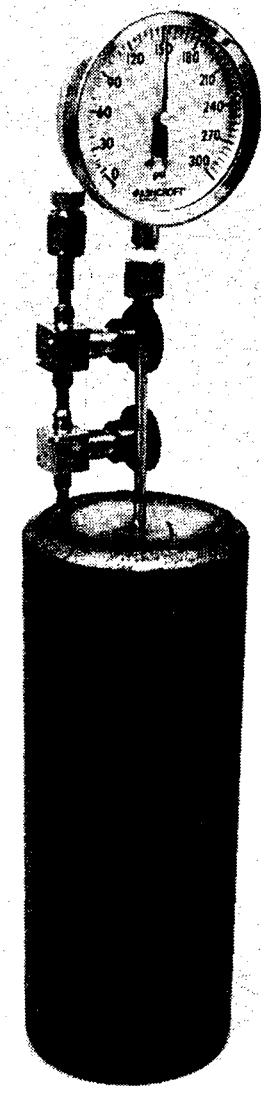


Figure 5-2. Seal-welded test container, fully charged, ready for placement in oven.

body of the container, which is made up very tightly, with Teflon® tape applied to the threads). The pre-weighed test specimens (of large area, to expedite rapid quantification of gas generation) and the brine are placed in the container before welding the top on the container. The sealed containers are then pressurized with He gas (at 4.4 atm, or 50 psig). Two He fills with intermediate evacuations are made to ensure minimization of contamination with residual air. The containers are then given a standard He leak-check test capable of sensing a He leak rate of $1.2 \times 10^{-10}$ atm-cc/s. A container that does not pass the leak test is not used. If the leak test is successfully passed, the He is evacuated from the container and the appropriate overpressure gas is added. The containers are then placed in forced-convection (incubator) ovens maintained at $30 \pm 5°C$, and the course of the gas-generating reaction is monitored by observing the pressure changes on the pressure gauges. Gas samples can be obtained from the containers at any time for gas analysis, though taking such a sample greatly perturbs the container gas inventory and gas pressure. For this reason, gas sampling is generally performed at the conclusion of a test, after the final pressure readings have been obtained.

In the seal-welded-container tests, two methods are used to determine the rates of the corrosion and gas-generation reactions: 1) determination of the container gas pressure as a function of time and 2) determination of the amount of metal lost from each specimen at the conclusion of a test by gravimetric methods. The former method has the advantage of yielding real-time information on the course of the gas-generating reaction. Confidence in the results obtained in any given test environment is dependent on accurate pressure gauge information and accurate estimations of specimen area and the plenum volume (vapor space) of the test container. The result obtained represents the gross integrated reaction of the specimen assembly, without quantifying the contribution of each specimen, hence each lot of material, to the $H_2$ being generated. The latter method has the advantage of being capable of specifying the contribution of each specimen to the $H_2$ generated during the test. Confidence in the results obtained using any given set of test conditions is dependent on accurate pre- and post-test specimen weights, accurate determination of specimen areas, and carefully controlled specimen surface preparation and corrosion-product-stripping procedures.

Because pressure gauge accuracy is an important factor in the quantitative determination of gas produced by the pressure-volume method, the inherent accuracy of the pressure gauges used in the tests was investigated by analyzing the pressure readings of new gauges in comparison with a

calibration standard.[a] Two gauge ranges were used in the tests; 200-psig full-scale and 300-psig full-scale. All were supplied by the same manufacturer, and all were basically the same type of simple bourdon-tube gauge. All gauges were tested against a calibration standard before use to ensure that the accuracy of the gauge met the manufacturer's specifications (±3% of full-scale reading). Each 200-psig gauge was tested at five pressure levels; each 300-psig gauge was tested at six pressure levels. The full statistical experiment consisted of calibration data from sixteen new 200-psig gauges and eight new 300-psig gauges. A one-way random-effects analysis of variance was used to characterize the bias in the gauges and the gauge-to-gauge and experimental variabilities. These estimates of bias and variability were then used to construct a confidence on a true pressure value.

If M is a single reading obtained from a 200-psig gauge, the confidence limits associated with this single reading have been determined to be

90% confidence: M -2.9/+1.9 psi

95% confidence: M -3.4/+2.4 psi

99% confidence: M -4.3/+3.3 psi.

For a single reading obtained from a 300-psig gauge, the confidence limits have been determined to be

90% confidence: M -7.9/+5.8 psi

95% confidence: M -9.2/+7.1 psi

99% confidence: M -11.8/+9.7 psi.

Repeated readings of the same gauge or use of more than one gauge to report a given pressure would increase the level of confidence in the reading obtained.

The 200-psig gauges are clearly more accurate than the 300-psig gauges. At the 95% confidence level, the 200-psig gauges can be approximately characterized as being within ±1.5% of the

---

[a] All gauges used in the present test series were tested against calibration standards by the Westinghouse Hanford Company Standards Laboratory. The pressure standards (250 psig full-scale for the 200-psig gauges; 500 psig full-scale for the 300-psig gauges) have a reported accuracy of 0.1% of the full-scale reading. In the statistical analysis described here the calibration standard was assumed to be absolutely accurate.

full-scale reading; the 300-psig can be approximately characterized as being within ±3% of the full-scale reading. The volume of the plenum of the test containers can be known with a high degree of confidence to ±3%. The error in determining the area of the sample array is much less than that associated with the gauge pressure and the plenum volume (< ±1%). If a simple propagation-of-error approach is used, it can be seen that, at pressures near the full-scale range, the amount of gas in moles (proportional to pressure x volume) present in the test container equipped with a 300-psig gauge is given to ±6% by the pressure gauge/plenum volume method. If the pressure gauge is not near its limit, the error, by the same reasoning, can increase. For example, in the case of a 300-psig gauge reading 150 ±9 psig (95% confidence level), the contribution of gauge error in estimating the moles of gas present in the test container is ±6%, with a total error of ±9%.

The tables summarizing the test conditions for all of the seal-welded-container test, Tables 3-1 and 3-2, call out the tests that were equipped with 300-psig gauges. All other tests were equipped with 200-psig gauges.

The sources of variability in the gravimetric data include

- container-to-container variability, reflecting differences in the handling of the containers and the conditions within the containers throughout the experiment;
- alloy-to-alloy variability, reflecting differences between alloys (or heats of the same alloy) that affect the corrosion rate;
- sample-to-sample variability, which includes variability in alloy composition from location to location within the parent sheet stock; differences in surface preparation; errors associated with weighing and surface area determination; and differences in the local environment within the sample container.

At the conclusion of a test, the container is opened by means of a milling operation that removes the top closure weld. The specimens are quickly lifted from the container, removed from the specimen rack, rinsed, and placed in desiccators. X-ray diffraction (XRD) analyses of the corrosion products are typically performed on selected specimens, usually within 24 h if there is judged to be a possibility of oxidation of the corrosion product by contact with air. The brine from the test container is retained for chemical analysis. The corrosion product is stripped from the specimens by means of an inhibited acid solution, and the amount of metal lost from each specimen is determined. The gravimetric analysis permits an estimate to be made of the metal loss from (or penetration of)

each specimen. These metal-loss data are compared with the quantity of $H_2$ generated and the corrosion product formed, for determination and corroboration of the overall corrosion/gas generation processes.

### 5.1.2 Autoclave Test Method

Tests performed at high gas overpressures, e.g., pressures greater than ~20 atm, utilize heavy-wall autoclave systems. The autoclaves are typically of 3.8-L capacity. Because autoclaves have high-pressure gasket seals, they cannot be expected to be as gas tight as the seal-welded containers. However, pressure-time data can be obtained from an autoclave pressure gauge when the autoclave is extremely well sealed. Otherwise, the data from an autoclave system consist of the gravimetric results and the analysis of the corrosion product film by XRD or other methods.

While autoclave systems are often employed for high-pressure studies, they have additional uses associated with their relatively large volume. For example, if it is considered necessary to keep major components of a test separate, as in the case of a mass of salt containing test specimens suspended in the vapor phase over a pool of brine, the autoclave can provide the flexibility and volume required.

## 5.2 Materials

The $H_2$-generation study has focused on two major material classes: low-carbon steel, intended to closely represent the drum steel and the waste-box steel materials while approximately representing the steel wastes within the containers; and alternative packaging materials, consisting of unalloyed Cu and Ti and selected alloys of these two materials.

### 5.2.1 Low-Carbon Steels[a]

The drums and waste boxes containing the TRU waste will make by far the greatest contribution of metallic Fe to the WIPP repository (Brush, 1990). This Fe will be in the form of low-carbon steel, ranging in composition from the low-C, low-Mn material used in the fabrication of the Department of Transportation (DOT) 17-C drums (0.04 to 0.1% C, 0.25 to 0.5% Mn) to the somewhat more highly alloyed material used in the waste boxes (for example, ASTM Grade A36 steel, with 0.25% C maximum and 0.8 to 1.2% Mn; and ASTM Grade A569 steel, with 0.15% C and 0.60% Mn maximum). The steel waste contained within the waste boxes can be expected to range widely in composition, from low-carbon steel (for example, nails, wire, structured steel) to highly alloyed material (for example, tools, high-strength fasteners, machine components).

Ideally, a corrosion or a gas-generation study would utilize test specimens and a test environment that exactly duplicate the field conditions. In the present case, this is of course not possible, as a very wide range of steel compositions will exist in the repository, and the compositions cannot ever be known with a high degree of certainty. It is therefore necessary to simulate the WIPP site conditions by using a range of steel compositions approximating the range of material compositions expected in the WIPP site. To this end, four lots (heats) of steel were obtained for test specimens, two lots each of ASTM Grade A366 (standard specification for cold-rolled sheet), representative of steel waste drums, and ASTM Grade A570 (standard specification for hot-rolled carbon steel sheet and strip), representative of steel waste boxes and other steel waste materials. The two lots of ASTM Grade A366 steel are designated "J" and "K," and the two lots of ASTM Grade A570 steel are designated "L" and "M." The thickness of the as-received material is given below:

---

[a] The term "low-carbon steels" is a broad material classification, generally considered to include steels having less than 0.25% C, 1.65% Mn, and 0.60% Cu, along with small amounts of other elements (ASM, 1978). According to this definition, the drum materials and the waste box materials are "low-carbon steels."

| Lot | Thickness, mm (in.) |
|---|---|
| J | 0.70 (0.028) |
| K | 0.86 (0.034) |
| L | 1.5 (0.059) |
| M | 1.6 (0.063) |

The compositions of the four lots of steel are presented in Table 5-1. Two values are presented for the C content of each lot of steel, representing analyses provided by 1) the steel vendor and 2) an independent testing laboratory.[a] The discrepancies in C concentration noted for the J and K lots between the two analyses are not considered important to the results of the study.

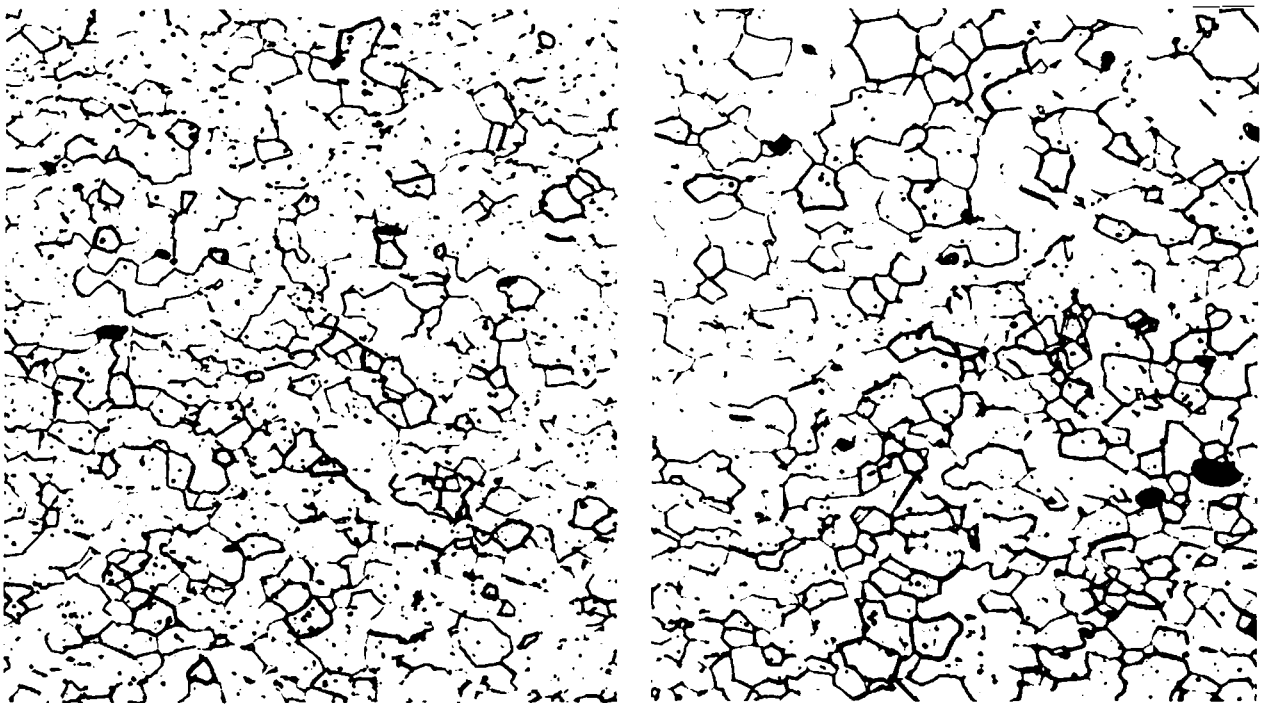
Table 5-1. Compositions of Low-Carbon Steels

| | ASTM A366 | | ASTM A570 | |
|---|---|---|---|---|
| Specie | Lot J | Lot K | Lot L | Lot M |
| C | 0.06/0.10 | 0.05/0.09 | 0.13/0.14 | 0.13/0.13 |
| Mn | 0.30 | 0.30 | 0.77 | 0.75 |
| Si | 0.08 | 0.07 | 0.11 | 0.10 |
| P | 0.015 | 0.015 | 0.017 | 0.020 |
| S | 0.012 | 0.009 | 0.015 | 0.015 |
| Cu | 0.015 | 0.020 | 0.015 | 0.040 |
| Fe | bal | bal | bal | bal |

In all of the calculations conducted in the present work equating molar equivalencies of corrosion reactants and corrosion products, and in all calculations equating corrosion (penetration) rates with metal lost, the steels are treated as though they are pure Fe, with a molecular weight of 55.85 and a density of 7.86.

[a] Koon-Hall Testing Corporation, 5687 S.E. International Way #A, Portland, OR 97222.

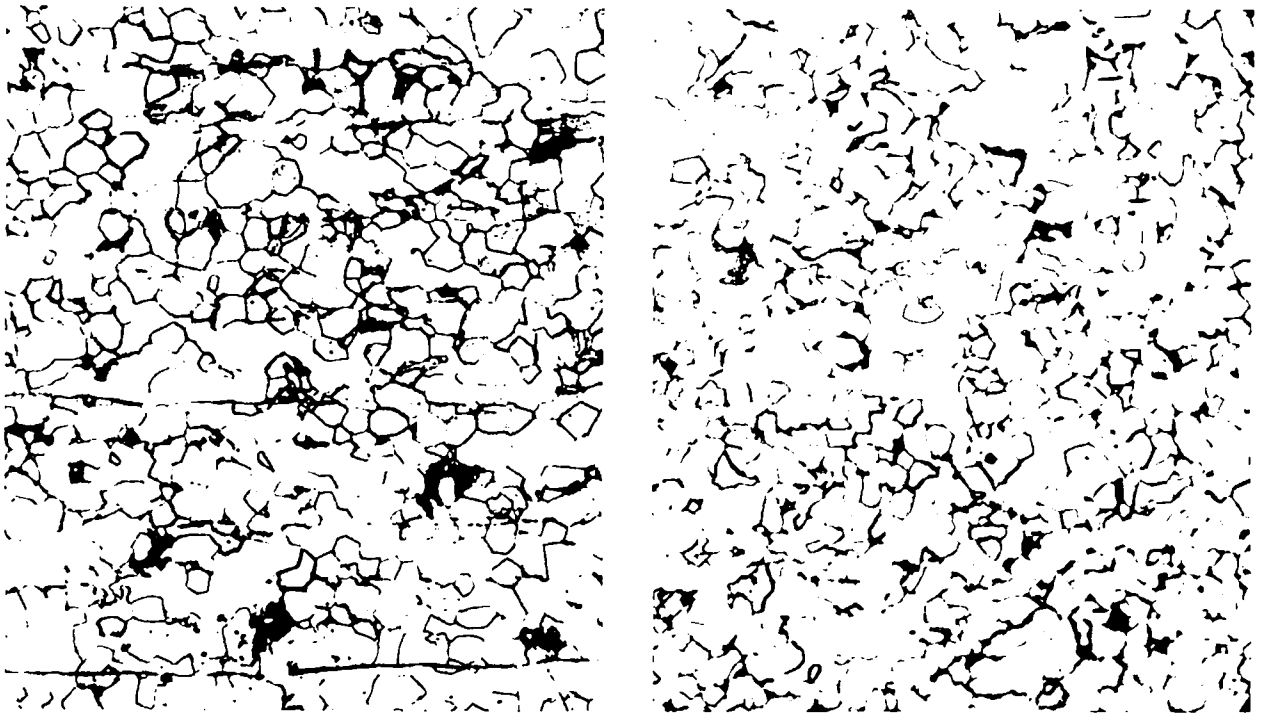
The microstructures of the steel are shown in Figures 5-3 and 5-4. The microstructures appear quite similar, from lot to lot, except for 1) the carbon-content-related effects, e.g., the amount of carbide-rich phases (notably pearlite) present; and 2) the fact that the as-received hot-rolled materials (lots L and M) have a layer of mill scale (iron oxide) 5 to 13 $\mu$m (0.2 to 0.5 mil) thick on their surfaces. This oxide was abraded off before the gas-generation tests. All of the microstructures appear to be in the annealed condition, and all of the grain sizes are similar (60 to 90 grains/cm$^2$ at 100x). The "cold-rolled" material exhibits little, if any, evidence of cold work.



Lot J Lot K

Figure 5-3. Microstructure of steel, lots J and K. 350X.

It is expected that the corrosion and gas-generation characteristics of steel lots procured for test would closely simulate the characteristics not only of the drums and waste boxes, but of the low-alloy steels contained within the wastes as well. The reason for this is that many studies have shown that the alloying elements present within carbon and low-alloy steels do not have a very strong effect on



Lot L Lot M

Figure 5-4. Microstructure of steel, lots L and M. 350X.

their corrosion behavior in aqueous brine environments. As an example of such a study, Reinhart and Jenkins (1972) reported corrosion results obtained from exposure of a large number of low-carbon and low-alloy steels to seawater at various depths (to 1,830 m or 6,000 ft), hence different $O_2$ activities and temperatures, for time periods up to 18 months. Low-carbon steels, hardenable low-alloy steels (e.g., AISI types 4140 and 4340), Fe-Ni alloys containing up to 9% Ni, and many other wrought and cast alloys were included in the study. Little effect of steel composition on corrosion rates was found at the conclusion of these studies. General corrosion behavior was dominated by duration of exposure, depth in the ocean, and $O_2$ availability. Southwell and Alexander (1969) reported corrosion results obtained from 10 low-alloy steels exposed for 16 yr at a depth of 14 ft in the ocean near the Panama Canal. The corrosion rates of the alloys within the group, which included a low-carbon steel and steels containing up to 5% Cr, up to 0.9% Cu, and up to 5.5% Ni, were all 97 $\pm$30 $\mu$m/yr (3.8 $\pm$ 1.2 mpy) after 16 yr. Again, little effect of alloy composition was observed in the brine environment. Given findings such as these, it appears reasonable to deduce the approximate

behavior of low-carbon steel packaging materials and low-alloy-steel wastes contained within the packages from the four lots of steel procured for laboratory testing in the present project, where "approximate behavior" would mean to within a factor of $\sim 2$.

### 5.2.2 Alternative Packaging Materials

The potential for gas pressurization of the WIPP underground facility due to corrosion of packaging materials and metal waste has necessitated consideration of several different options for waste form modification. One possible option involves repackaging the waste in containers that do not have the gas-generation characteristics of mild steel. To identify suitable alternative materials for waste packaging, an expert panel referred to as the Waste Container Materials Panel (WCMP) was convened August 20 and 21, 1990, by the DOE WIPP Project Office, as a part of the Engineered Alternatives Task Force (EATF) activities. The panel evaluated a wide range of metallic, ceramic, cementitious, polymeric, and coating materials for their applicability to WIPP containers (EATF, 1991).

An important criterion for the selection of suitable metallic materials was absence or significant minimization of gas-generation tendency. Additional criteria were fabricability, availability, fabrication capacity (industrial production capacity), status of technology development, cost, and mechanical properties.

The metal categories selected by the panel for in-depth consideration were

- Cu and Cu alloys
- Ti and Ti alloys
- high-Ni alloys
- Zr and Zr alloys
- stainless steels.

The panel then determined the degree to which each metal class met the previously set container material requirements. The overall ranking of materials indicated that the Cu-base and Ti-base

material classes offered the best combination of material properties and overall economic incentive for replacing carbon steel as a metallic container material at the WIPP site. Cu-base materials, though obviously susceptible to attack by and reaction with certain chemical species such as nitrates and sulfides, offer a high degree of thermodynamic stability in near-neutral aqueous solutions. Ti-base materials are extremely corrosion resistant in a wide variety of low- and intermediate-temperature brines because of the protection afforded by their oxide film (see Sections 4.8 and 4.9 of this report). Unalloyed Cu (oxygen-free, electronic) and unalloyed Ti (Ti Grade 2) were accordingly selected from the candidate material list for an investigation of their corrosion/gas-generation characteristics in simulated WIPP environments. In addition, cupronickel 90-10 was chosen for study, as its mechanical properties are far superior to unalloyed Cu due to the presence of 10% Ni, Ti Grade 12, a Ti-Ni-Mo alloy, was also selected because of its well known resistance to crevice corrosion. The chemical compositions of the specific materials procured for study are presented in Table 5-2.

Table 5-2. Compositions of Alternative Materials Used in Corrosion/Gas-Generation Study

| | Weight Percent, or (ppm) | | | | | | | | | | |
|---|---|---|---|---|---|---|---|---|---|---|---|
| Material[a] | Cu | Ti | Ni | Zn | Mn | Mo | Fe | Pb | O | S | C |
| Unalloyed Cu (C10100) | 99.99 | -- | -- | -- | -- | -- | -- | (3) | (2) | (10) | -- |
| Cupronickel 90-10 (C70600) | 87.58 | -- | 10.4 | 0.2 | 0.5 | -- | 1.3 | 0.01 | -- | 0.005 | 0.01 |
| Ti Grade 2 (R50400) | -- | Bal | -- | -- | -- | -- | 0.16 | -- | 0.13 | -- | 0.01 |
| Ti Grade 12 (R53400) | -- | Bal | 0.80 | -- | -- | 0.30 | 0.14 | -- | 0.12 | -- | 0.01 |

a Unified Numbering System (UNS) designations are in parentheses.

### 5.2.3 Brine

The brine used in the present study is based on the WIPP Brine A composition described by Molecke (1983). It is a high Mg, K, and Na chloride-sulfate brine and is used as a simulant for intergranular Salado Formation brine that might intrude into the WIPP repository horizon. The composition of Brine A, as well as the average value and range of compositions of the three lots of brine made up to date for usage at PNL in the present study, are given in Table 5-3.

Table 5-3. Composition of Brines Used in Tests

| Chemical Specie | Concentration, mg/L | |
|---|---|---|
| | Brine A (target) | PNL Brines |
| Na | 42,000 | $39{,}400^{+1200}_{-1100}$ |
| Mg | 30,000 | $34{,}700^{+1000}_{-1500}$ |
| K | 35,000 | $29{,}900^{+600}_{-400}$ |
| Ca | 600 | $560^{+40}_{-60}$ |
| B | 220 | $220^{+1}_{-4}$ |
| Cl | 190,000 | $188{,}300^{+2700}_{-4300}$ |
| $SO_4$ | 3,500 | $4{,}130^{+50}_{-60}$ |
| $HCO_3$ | 700 | $680^{+30}_{-60}$ |
| pH | 6.5 | $7.4^{+0.5}_{-0.7}$ |

Only the major constituents of the brine as described by Molecke (1983) were used to make up the PNL brines. Omitted minor constituents, deemed to have little or no effect on the corrosiveness of the brine, were Fe, Cs, Rb, Li, Sr, and I. These minor elements totaled only 58 mg/L in the composition described by Molecke.

### 5.2.4 Salt (Halite)

Two corrosion and gas-generation tests (tests AUT-5 and AUT-6) were conducted in which the specimens were packed in particulate salt (halite). The salt used in the tests was shipped to PNL from SNL in two 1-gallon containers, identified as "WIPP Salt E 140-N635." The salt was originally gathered from the floor of "E 140 drift, 194 m (635 ft) north of the salt shaft." It was assumed to be essentially pure (>95%) NaCl, and was not analyzed.

# 6.0 RESULTS

Two major efforts were undertaken in the present corrosion and gas-generation laboratory study: experiments directed toward determining the behavior of current packaging materials (low-carbon steels in simulated WIPP environments); and experiments directed toward determining the behavior of alternative packaging (Cu- and Ti-base) materials in simulated WIPP environments. The experimental results associated with each major materials group will be discussed separately in this section of the report. (This basic division in the experimental work is reflected in the summary test matrices for the project, presented in Tables 3-1 and 3-2. Reference may be made to these tables for information on the individual tests described in this section of the report.)

In general, each test was designed to provide 1) time-dependent container pressure, from which $H_2$ pressure data could be determined; 2) gas composition data, for quantification of corrosion-product gas generation rates in conjunction with item 1; 3) corrosion rate (metal penetration) data, obtained gravimetrically after corrosion-product film stripping; and 4) corrosion product identification. Post-test brine analyses were also obtained. Items 1 and 2 have the most value and are most defensible when obtained from a demonstrably leak-tight container, such as the seal-welded containers used in the present tests. Information from items 1, 2, and 3 permit a comparison of the moles of $H_2$ formed versus moles of metal reacted, to verify the legitimacy of the conclusions drawn. Item 4 provides insights into the potential protectiveness of the corrosion product film and also ensures that the appropriate reaction is being considered when the molar equivalency of metal and $H_2$ are being compared.

The raw data describing container pressure as a function of time for the anoxic brine (brine/$N_2$) and the brine/$CO_2$ seal-welded container tests are contained in Appendix A to this report. All of the individual specimen data from all concluded corrosion tests are contained in Appendix B. These data are presented to permit additional, independent evaluation and corroboration of the results presented and conclusions drawn in the present report and to facilitate statistical treatment of the data according to the specific future needs of the WIPP Project modelers. Such treatments were not attempted in the present report because of the many different approaches to the data that could be taken in such statistical analyses.

## 6.1 Low-Carbon Steel Tests

The corrosion and gas-generation behavior of low-carbon steels was evaluated in three environments: anoxic brine (brine/$N_2$)[a], brine/$CO_2$, and brine/$H_2S$. In each environment specimens were exposed either fully immersed in the brine (Brine A) or in the vapor phase over the brine. All tests were performed at 30 $\pm$5°C. The test conditions are summarized in Table 3-1.

All steel specimens were surface ground using 60-grit emery cloth to remove mill scale or other surface deposits. After grinding, they were dimensionally measured, degreased (using trisodium phosphate followed by a water rinse, and an absolute alcohol rinse), and weighed. The specimen dimensions were obtained to a minimum accuracy of $\pm$0.025 mm ($\pm$0.001 in.); the specimen weights (pre- and post-test) were obtained to $\pm$0.0001 g. After the final degreasing and weighing operations, the specimens were stored in a desiccator until needed. At this time, the steel specimens exhibited a bright, clean, as-ground appearance.

Upon conclusion of a test, the specimens were removed from the test container, rinsed in deionized water and alcohol, and placed in a desiccator to minimize the possibility of further reactions. Selected specimens were held in reserve for analysis of corrosion products, usually accomplished by x-ray diffraction (XRD). The corrosion product layer was removed from the remainder of the specimens by immersing the specimens in an inhibited HCl corrosion-product stripping solution per National Association of Corrosion Engineers (NACE) standard TM-01-69, 1976 revision. The stripping solution is made by adding 12 ml formaldehyde to 1 L of 50% HCl solution. A final weighing was then performed so that the mass of metal lost from each specimen by corrosion could be calculated.

---

[a] Strictly speaking, each of the environments investigated consists of anoxic brine, as $O_2$ has been excluded from the test containers. The term "anoxic brine" as used here to describe the environment having no reactive gas ($CO_2$, $H_2S$) overpressure signifies that the reactant is anoxic brine alone, without an added reactive constituent.

### 6.1.1 Seal-Welded-Container Tests

Each seal-welded container test described in this section of the report contained a rack of 24 test specimens, comprising six replicate test specimens of each of the four lots of low-carbon steel previously described in Section 5.2. The six test specimens of each lot of steel consisted of three wide specimens, 86 mm (3.4 in.) x 190 mm (7.5 in.), and three narrow specimens, 51 mm (2.0 in.) x 190 mm (7.5 in.). Each specimen had two holes, 8 mm (0.31 in.) in diameter, to accommodate the insulated rack supports. The narrow specimens were placed on the outer part of the rack to optimize material loading in the container. The total specimen area in each container lay in the range 0.60 to 0.64 $m^2$. In the immersed-specimen tests, sufficient Brine A (1.34 to 1.39 L) was added to the container to cover the tops of the specimens to a depth of ~6.4 mm (~0.25 in.). In the vapor-phase exposure tests, 0.25 L of brine was placed in the bottom of the test container. The level of the brine was below the racked specimens, though the brine unintentionally splashed on the bottoms of the specimens during container handling. The immersed-specimen containers had a calculated vapor-space plenum volume of 0.634 L. The plenum volume in the vapor-phase exposure tests was 1.74 L. The specimen area-to-plenum volume ratio was made large to promote a rapid response on the test container pressure gauge to the $H_2$ generated by corrosion reactions.

#### 6.1.1.1 ANOXIC BRINE (BRINE/$N_2$)

The anoxic brine tests were intended to provide basic information on the corrosion/gas-generation proclivity of low-carbon steel in the absence of reactants other than low-carbon steel and Brine A. The anoxic brine immersed-specimen testing regimen includes test containers 1, 2; 9, 10; 17, 18; and 25, 26; the vapor-phase-specimen testing regimen includes test containers 5, 6; 13, 14; 21, 22; and 29, 30. Proximate identification numbers (e.g., 1, 2) signify duplicate tests. These test container identification data are also contained in Table 3-1.

All of the pressure-time plots from the brine/$N_2$ test series are presented in Figure 6-1. The corresponding raw data are presented in Appendix A. In each case, the initial starting pressure of $N_2$ gas (99.99% $N_2$ by analysis) was approximately 10 atm absolute (~9 atm gauge). At 30°C the partial pressure of water vapor in equilibrium with Brine A is ~0.03 atm, so the pressure gauge reading

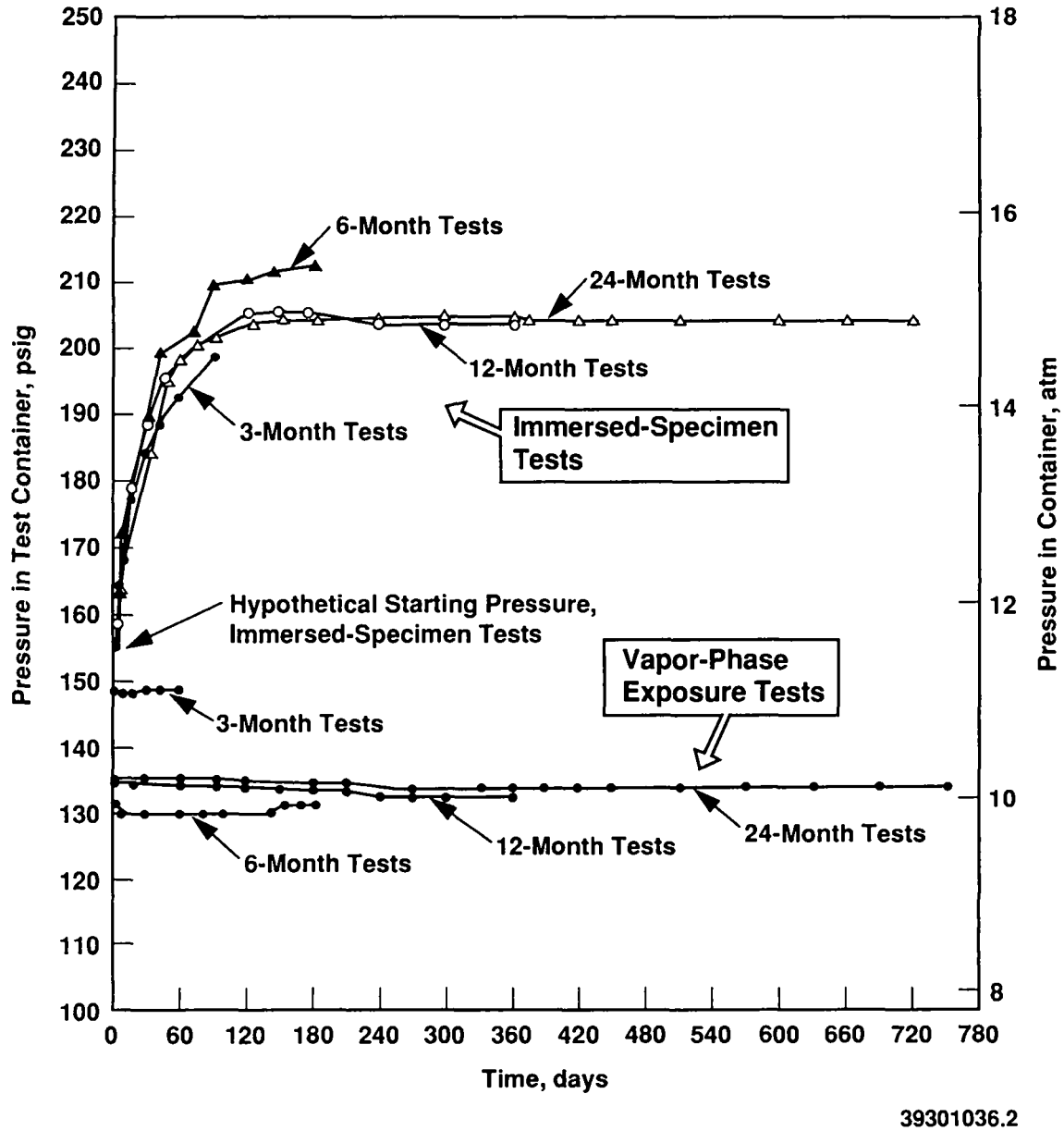



Figure 6-1. Pressure-time curves, low-carbon steel anoxic brine tests. Each curve represents two (duplicate) tests.

essentially represents the starting $N_2$ pressure plus the pressure of corrosion-product $H_2$. Because of the very close agreement in pressure between duplicate containers (typically within 2 to 3 psi), the pressure readings of duplicate containers were averaged in all cases to develop the curves shown in

Figure 6-1. The eight curves shown, therefore, represent the results of all 16 tests. Pressures were recorded at a minimum frequency of weekly; the test temperature was continually plotted to ensure conformity with the specified 30 $\pm 5$°C temperature range.

The test containers used for the 24-month tests had been equipped with pressure gauges limited to a maximum pressure of slightly over 200 psig. For this reason, the 24-month test containers were vented approximately halfway through the test, as it could be seen that the pressure limit of the gauges would be exceeded by the end of the test if some of the corrosion-product $H_2$ were not released.

The curves of Figure 6-1 show 1) that a good test-to-test agreement in the pressure-generation-rate results between the various tests had been attained; 2) that the immersed-specimen tests can be characterized by a steady, approximately linear $H_2$ generation rate; and 3) that the vapor-phase exposure of the mild steel did not produce measurable $H_2$ after an initial short period of pressure increase. The pressure increase at the beginning of these latter tests is ascribed to corrosion taking place on the bottom of the specimens, because the brine in the bottom of the vapor-phase-exposure containers contacts the bottom of the specimens by unintentional splashing when the containers are handled after brine-charging and container closure. Approximately 10% of the surface area of the test specimens in these tests is typically affected in this manner.

An analysis of the gas samples taken from the containers just before they were opened is presented in Table 6-1. The analyses confirm that the pressure increase observed in the containers was due to corrosion-product $H_2$. The consistency in the gas generation between duplicate test containers is evident from the table. Significant differences are evident between the $H_2$ contents of the vapor-exposure containers. This is attributed to the varying test specimen surface area splashed by brine from one container to another.

The post-test appearance of the steel specimens is shown in Figure 6-2 (immersed specimens, 6 and 24 months exposure) and Figure 6-3 (vapor-phase-exposure specimens, 24 months exposure).

The appearance of the specimens (Figure 6-2) changed somewhat between 6 and 24 months exposure, with the specimens maintaining a general metallic appearance, but darkening with increasing exposure time. The 3- and 12-month test specimens resembled the 6-month-exposure specimens more than the 24-month-exposure specimens. The bulk of the greenish-gray, flocculent corrosion

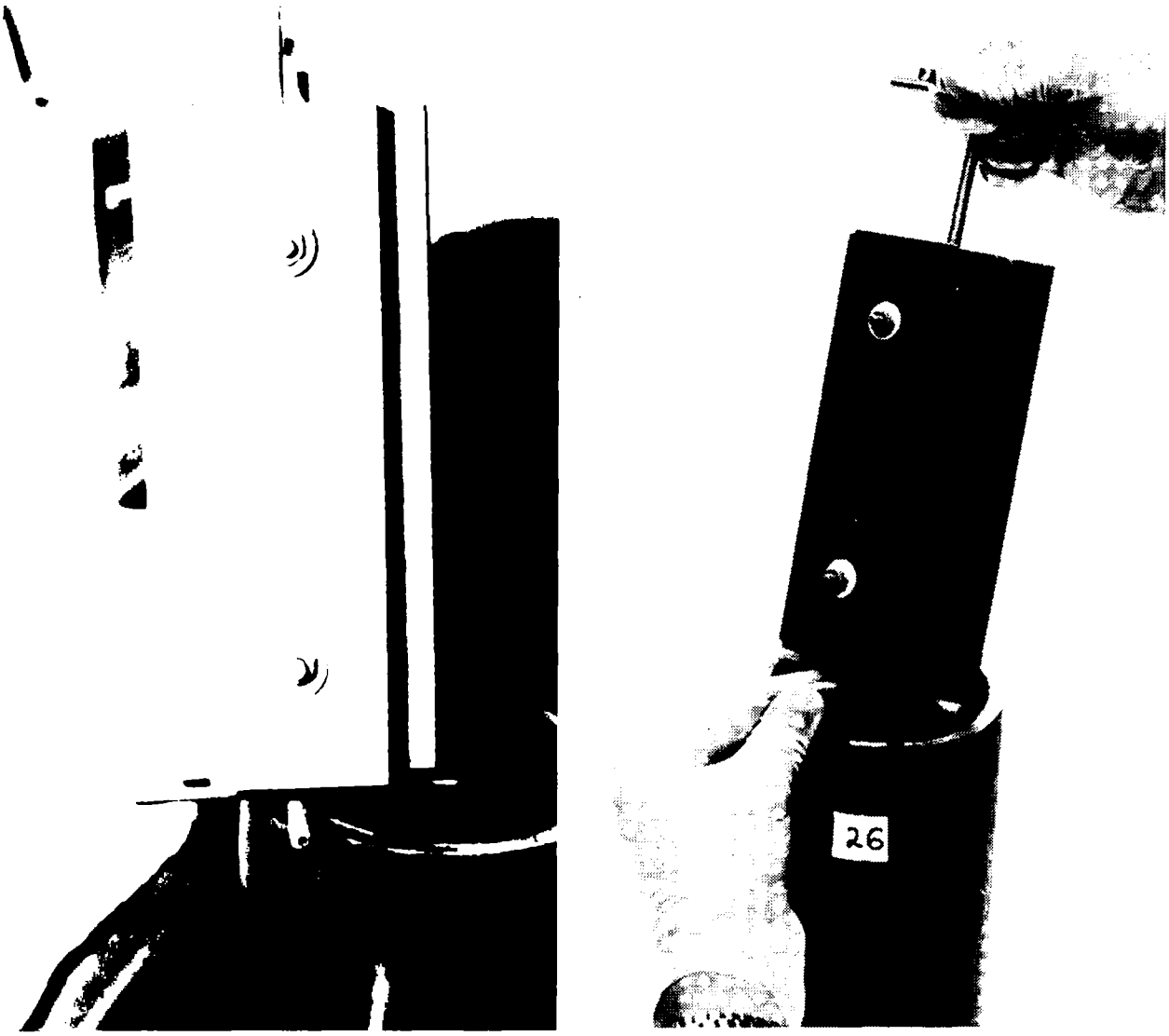
Table 6-1. Composition of Gas at Conclusion of Test, Anoxic Brine (Brine/$N_2$) Tests. Each tabulated value is average of two analyses. Results are given in vol% (mol%).

| | Immersed-Specimen Tests | | | | Vapor-Phase-Exposure Tests | | | |
|---|---|---|---|---|---|---|---|---|
| | Test Numbers | | | | Test Numbers | | | |
| | 3-mo | 6-mo | 12-mo | 24-mo | 3-mo | 6-mo | 12-mo | 24-mo |
| Specie | 1/2[a] | 9/10 | 17/18 | 25/26 | 5/6 | 13/14 | 21/22 | 29/30 |
| $N_2$ | 89.5<br>89.8 | 80.2<br>81.1 | 74.5<br>73.1 | 60.1<br>61.5 | 99.6<br>99.8 | 99.5<br>99.4 | 99.7<br>99.5 | 99.2<br>99.2 |
| $H_2$ | 10.5<br>10.1 | 19.5<br>18.7 | 25.5<br>26.8 | 39.7<br>38.5 | 0.42<br>0.15 | 0.20<br>0.32 | 0.20<br>0.35 | 0.66<br>0.56 |
| He | <0.01<br>0.08 | 0.34<br>0.30 | 0.08<br>0.09 | 0.06<br>0.06 | 0.02<br>0.02 | 0.26<br>0.24 | 0.10<br>0.13 | 0.19<br>0.28 |
| $O_2$ | <0.1, all tests | | | | | | | |

[a] 1/2, 9/10, etc. indicates that tests numbered 1 and 2 are duplicate tests, 9 and 10 are duplicate tests, etc. In the table, the average of two separate gas analyses for test 1 is over the average analyses for 2, the average of two separate gas analyses for test 9 is over the average of two separate gas analyses for 10, etc. In all cases the two separate analyses made on gas samples from one container showed excellent agreement.

product that typically forms in these tests does not adhere to the surface of the specimens, but instead settles to the bottom of the test container. The darkening with exposure time suggests a change in the nature of the surface and the film associated with the specimen surface.

The appearance of the specimens in Figure 6-3 is also typical of the appearance of the specimens from the 3-, 6-, and 12-month anoxic-brine-vapor exposures. The specimens removed from the vapor-phase (humid) tests typically appeared to be shiny and unreacted except for the bottom ~10% of the specimens that had been splashed by brine placed in the bottom of the test containers (see Figure 6-3). This description implies that corrosion products did not form on the specimen surfaces contacted by vapor only. An effort was undertaken to quantify the limits of oxidation/metal consumption that can take place on the surfaces of such specimens while the corrosion product film remains undetectable by the human eye.




6-Month Exposure

24-Month Exposure

Figure 6-2. Post-test appearance of steel specimens, immersed, 6- and 24-month anoxic brine tests. The 24-month specimens appear dark, though essentially none of the corrosion product is found on the specimen surfaces.

Preliminary scoping tests confirmed that visible films could be readily produced on surface-ground low-carbon steel specimens by heating them in air for ~10 min at temperatures of 250°C (straw color) and 300°C (dark blue color). Accordingly, two specimens of Lot J steel, each 51 mm (2.0 in.) x 190 mm (7.5 in.) x 0.70 mm (0.028 in.), were carefully cleaned, then weighed five times




Figure 6-3. Post-test appearance of steel specimens, vapor-phase exposure, 24-month anoxic brine tests. No reaction is evident except where brine has contacted the bottoms of the specimens.

each (once on each of five successive days), using the same 4-place (0.0001 g) balance. The average weight of the five weighings was taken as the starting weight. The specimens were then heated for 18 min each at either 250°C or 300°C, to produce the straw-colored and dark-blue-colored oxide films. The post-treatment weights of the specimens were then obtained in the same manner as the

pre-treatment weights, and the average of the five weights was taken as the final weight of each specimen. It was ascertained that the specimen heated at 250°C showed a net weight change of -0.0001 g; the specimen heated at 300°C showed a net weight change of +0.0009 g. The effective zero net weight change exhibited by the straw-colored specimen justifies the conclusion of zero corrosion on a "clean and shiny" specimen, as the clean, shiny specimen has obviously formed less surface corrosion product than the straw-colored specimen. Even the maximum weight change found in the investigation, +0.0009 g on the dark-blue specimen, represents a metal loss (assuming FeO formation) of only ~1% of that taking place on an immersed specimen of Lot J steel in anoxic 30°C Brine A with a $N_2$ overpressure during a 1-year exposure. Thus, assumption of essentially zero corrosion on a specimen that emerges "clean and shiny" from a vapor-phase corrosion test is justified by the test described. Such a conclusion is also consistent with the lack of pressure increase in the test container after the first few days of exposure, signifying essentially a complete lack of water vapor reaction between the steel and the test environment.

All of the specimen weight-change data from the 3-, 6-, 12-, and 24-month immersed-specimen tests are presented in Appendix B-1; data from the vapor-phase-exposure tests are presented in Appendix B-2. The data from the immersed-specimen tests are summarized in Table 6-2 in terms of metal penetration (uniform corrosion) rate.

Later in this report section the equivalence between metal lost to corrosion and container pressure increase will be demonstrated, and the corrosion and gas generation rate followed during the last 12 months of the 24-month test will be the rate recommended for WIPP repository modeling purposes. This rate is lower than the lowest rate shown in Table 6-2.

The four lots of steel exhibited similar corrosion characteristics in the anoxic brine environment. The rates are obviously decreasing with time; this is also evident from the pressure-time curves of Figure 6-1.

The post-test compositions of the brines obtained from the test containers after the 6-, 12-, and 24-month tests are compared with the starting brine composition in Table 6-3. It is evident from the table that 1) there are no significant differences in brine composition between the immersed-specimen tests and the vapor-phase-specimen tests, at the same test duration; and 2) there is no significant

Table 6-2. Summary of Corrosion-Rate Data, Immersed Specimens, Anoxic Brine (Brine/$N_2$) Tests. Penetration rate means and standard deviations are presented. Each penetration rate value in the columns J, K, L, and M represents an average of five specimens; the sixth specimen of each lot was reserved for XRD and archive. Penetration rate is expressed in $\mu$m/yr.

| Test Duration, Months | Test Containers | Steel Lot and Penetration Rate[a] | | | | |
|---|---|---|---|---|---|---|
| | | J | K | L | M | All Lots |
| 3 | 1, 2 | 1.94±0.16 | 2.03±0.26 | 2.10±0.19 | 1.79±0.16 | 1.96±0.22 |
| 6 | 9, 10 | 1.61±0.07 | 1.65±0.37 | 1.91±0.04 | 1.71±0.08 | 1.72±0.13 |
| 12 | 17, 18 | 1.05±0.05 | 1.26±0.04 | 1.31±0.04 | 1.29±0.03 | 1.23±0.11 |
| 24 | 25, 26 | 0.95±0.05 | 1.14±0.08 | 0.91±0.04 | 0.95±0.04 | 0.99±0.11 |

[a] To convert from a penetration rate expressed in $\mu$m/yr to moles Fe reacted/$m^2$ - yr, multiply the penetration rate by 0.141 mol/$\mu$m - $m^2$.

Table 6-3. Results of Brine Analyses, Anoxic-Brine Seal-Welded Container Tests. Comparison of brine compositions after 6-, 12-, and 24-month tests with original brine composition. Concentrations given in mg/L.

| | | Test Duration and Specie Concentration | | | | | |
|---|---|---|---|---|---|---|---|
| | | 6 month | | 12 month | | 24 month | |
| Specie | Brine A | Imm[a] | Vapor[b] | Imm[c] | Vapor[d] | Imm[e] | Vapor[f] |
| Na | 38,300 | 43,000 | 42,000 | 40,900 | 39,800 | 40,200 | 41,000 |
| Mg | 35,700 | 35,800 | 35,400 | 35,100 | 34,700 | 32,900 | 34,000 |
| K | 29,500 | 29,900 | 29,700 | 30,500 | 30,700 | 31,000 | 31,000 |
| Ca | 560 | 600 | 610 | 630 | 590 | 581 | 572 |
| B | 230 | 230 | 230 | 240 | 230 | 230 | 228 |
| Fe[g] | <10 | <10 | <10 | <10 | <10 | <10 | <10 |
| Cl | 190,000 | 196,000 | 196,000 | 190,000 | 187,000 | 192,000 | 192,000 |
| $SO_4$ | 4070 | 4240 | 4190 | 3600 | 3800 | 4660 | 4620 |
| pH | 6.7 | 8.3 | 8.0 | 8.3 | 8.0 | 8.4 | 8.4 |

[a] Test container 10; [b] 14; [c] 17; [d] 21; [e] 25; [f] 29.

[g] Fe not detectable in these solutions. Solutions were exposed to air prior to analysis, permitting Fe oxidation and precipitation from solution.

difference between any brine composition and the starting brine composition. These observations suggest that the diminution in corrosion rate observed with increasing test time is not due to a decrease in concentration of a potential reactant (e.g., $Mg^{2+}$) supplied by the brine, but a steadily increasing inhibition of corrosion by a corrosion product adhering to the surface of the steel.

XRD analyses of the corrosion product collected from the bottoms of the test containers used in the immersed-specimen tests were unsuccessful in defining the corrosion product.[a] The XRD results showed that similar corrosion products formed after all exposure durations. As an example, the diffraction results obtained from the 12- and 24-month corrosion products are presented graphically in Figure 6-4.

The XRD analysis was completed within a few hours of collecting the corrosion product from the test container to minimize oxidation of the corrosion product through contact with air. A color change, from gray-green to orange-red, over a period of several days of exposure to air confirmed the air-oxidizability of the corrosion product and is consistent with a 2+ valence state of the iron in the corrosion product as it existed in the anoxic test container environment.

The corrosion product adhering to the bottoms of the specimens removed from the vapor-phase-exposure tests was $\beta Fe_2(OH_3)Cl$, beta iron chloride hydroxide, in all cases. This tan-to-dark brown corrosion product bore no visual resemblance to the corrosion product formed in the immersed-specimen tests.

The corrosion product in all cases is expected to contain iron in the reduced ($Fe^{2+}$) valence state, which would require that the Fe reactant and the $H_2$ reaction product be equivalent on a molar basis:

$$Fe + 2H^+ = Fe^{2+} + H_2 \qquad (33)$$

---

[a] The principal XRD reference database used in the XRD corrosion product analyses is that of the International Center for Diffraction Data (ICDD) Powder Diffraction File on CD-ROM (PDF-2), including all entries through Sec 41 (1991). The database comparison was effected by means of the search/match code Micro-ID Plus, available from MDI, Inc., Livermore, CA.

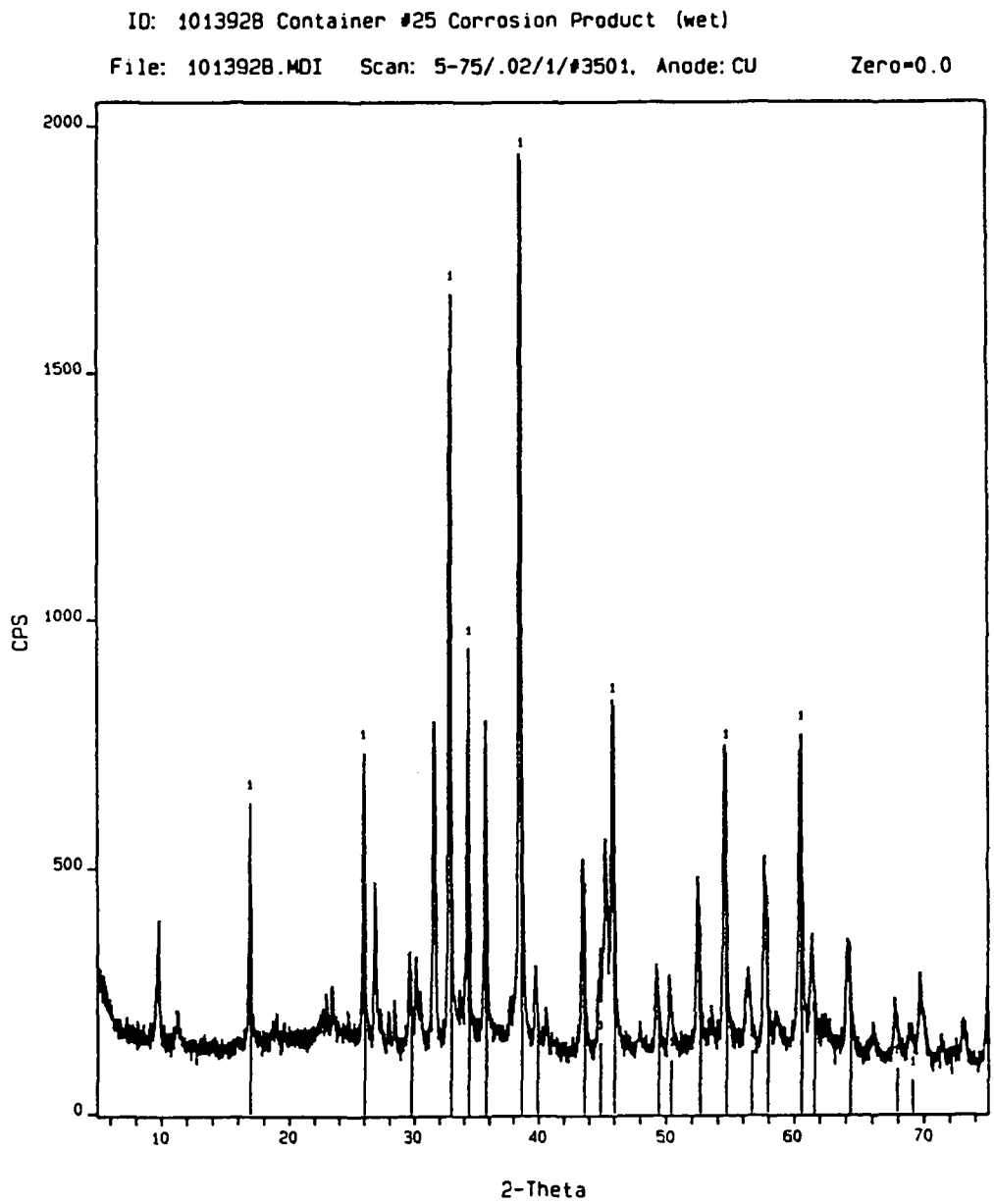



Figure 6-4. XRD results obtained from the unidentifiable 12- and 24-month-test corrosion products, anoxic brine tests. The vertical lines (labeled "1") correspond to the principal 12-month corrosion-product diffraction peaks; they are superimposed on the raw data obtained from the 24-month corrosion product. More than one compound may be present in each lot of corrosion product.

Knowledge of the plenum volume in the test containers, the test temperature, the container pressure at the end of a test, and the final gas composition permits a calculation to be made of the moles of $H_2$ present in a test container at the conclusion of a test. This can be compared with the amount of steel reacted, determined by a gravimetric analysis of the specimens exposed to the test medium. The results of this analysis for the anoxic brine seal-welded container tests are shown in Table 6-4.[a] The results from the two duplicate test containers are averaged in the table. $H_2$ was considered to be insoluble in the brine for the purpose of these calculations.

Table 6-4. Comparison of Moles of $H_2$ Formed (by pressure increase) with Moles of Fe Reacted (by specimen weight change), Anoxic Brine Tests

| Test Duration, Months | Average Moles Fe Reacted, $mol/m^2$ - yr | Average Moles $H_2$ Formed, $mol/m^2$ - yr | Moles $H_2$/ Moles Fe |
|---|---|---|---|
| 3 | 0.276 | 0.190 | 0.69 |
| 6 | 0.243 | 0.209 | 0.86 |
| 12 | 0.173 | 0.156 | 0.90 |
| 24 | 0.140 | 0.141 | 1.0 |

The tabulated data show that for tests of >6 months duration the agreement between container pressure increase and gravimetric data are very good. This finding validates the use of pressure-time data as a means of describing the rate at which hydrogen is produced per unit area of steel exposed to the simulated WIPP environment, as it ties observed pressure to actual metal reacted. This finding supports the use of pressure-time curve slopes (tangents) to estimate the rate at which $H_2$ is being generated as a f(t), as long as the slopes are not determined at short (<6 month) test times where they will under-represent the rate of Fe reaction.

The improvement in agreement in molar equivalence between $H_2$ formed and Fe reacted with increasing test time can be explained by a *relatively* greater loss of corrosion-product $H_2$ in the short-term tests, due to

[a] The calculations involved in arriving at the values presented in Table 6-4 are shown in Appendix C.

- $H_2$ reactions with iron oxides on the specimen surfaces
- $H_2$ reactions with other oxides or residual $O_2$, present in the system
- $H_2$ absorption by the steel and the container walls
- some $H_2$ solution in the brine phase.

Pressure-time data[a] from the long-term tests and from the longest-term portions of the long-term tests are believed to have the most credibility in repository-behavior modeling because long-term tests would be more relevant to the time scales used in repository performance assessment. Thus, from Figure 6-1, the relatively low rate of $H_2$ evolution over the last 12 months of the 24-month test, amounting to 0.71 $\mu$m/yr metal penetration or 0.10 mol $H_2/m^2$ steel-yr,[b] would be considered the best basis for estimating $H_2$ generation by steel in the WIPP repository of the data bases available, *assuming* that the steel in the repository is totally immersed in brine. Over long periods of time, this rate would be expected to continually decrease if the environment were maintained static and unrefreshed. The rate of 0.71 $\mu$m/yr is one-fourth to one-half the $H_2$-generation rates determined by Simpson and Schenk (1989) in relatively dilute (800 to 8000 ppm $Cl^-$) NaCl brines at 50°C. This is considered to be good agreement, considering the relatively long duration of the PNL tests and the difference in test temperatures between the two investigations.

#### 6.1.1.2 BRINE/$CO_2$

The brine/$CO_2$ tests were intended to provide information on the corrosion and gas-generation proclivity of low-carbon steel in the presence of Brine A and $CO_2$. The presence of $CO_2$ in the WIPP at significant fugacities is considered to be a distinct possibility because it is an expected byproduct of the microbially mediated degradation of cellulosic materials and other organic materials that will presumably be disposed of in the WIPP in large quantities.

---

[a] This statement is not meant to imply that gas-generation estimates based on container pressure are superior to those based on gravimetric data, as the equivalence of the two methods has been demonstrated (Table 6-4). The pressure-time curves, however, provide a means of estimating gas-generation (or corrosion) rates as a f(t) over the course of a test, something the gravimetric data do not permit.

[b] Obtained from the final slope of the 24-month curve, Figure 6-1.

Two types of brine/$CO_2$ experiments were performed: experiments in which $CO_2$ was present in the test containers in quantities so large that its complete consumption was not possible (the "excess-$CO_2$" tests); and tests in which the quantities of $CO_2$ added to the test containers were controlled so as to permit the essentially complete consumption of the $CO_2$ in some of the tests, but not in others (the "controlled-$CO_2$-addition" tests). These tests will be discussed separately in the following subsections.

### Excess-$CO_2$ Tests

The excess-$CO_2$ tests were intended to provide information on the corrosion and gas-generation characteristics of low-carbon steel in the presence of Brine A and excess $CO_2$. The brine/$CO_2$ immersed-specimen testing regimen includes test containers 3, 4; 11, 12; 19, 20; and 27, 28. The brine/$CO_2$ vapor-phase-specimen testing regimen includes containers 7, 8; 15, 16; 23, 24; and 31, 32. Proximate identification numbers (e.g., 3, 4) signify duplicate tests.

In the immersed-specimen tests the $CO_2$ was added to the test containers at an initial hypothetical starting pressure of $\sim 155$ psig ($\sim 170$ psia, or $\sim 12$ atm). This starting pressure is termed "hypothetical" because, in general, equilibration between the $CO_2$ present in the plenum of the test container and $CO_2$ present in the brine was not achieved for several days after test initiation, in spite of the fact that each container was agitated (by hand-shaking) for a period of 10 to 15 min after addition of the final $CO_2$ charge. (The containers with specimens exposed only to $CO_2/H_2O$ vapor were not purposefully shaken to effect $CO_2$ dissolution in the brine. Any agitation that these containers received was inadvertent.) Though this agitation effected a fairly good dissolution of the $CO_2$ in the brine phase, for the first few days of each test the pressure tended to decrease as gaseous $CO_2$ continued to dissolve in the brine. The amount of $CO_2$ added to these test containers was determined both by knowledge of the gas added to the plenum of each container and by weighing each test container after the gas addition on a balance sensitive to $\pm 1$ g. The two months showed good agreement. The average quantity of $CO_2$ added to each of the immersed-specimen test containers was 19.3 g, or 0.44 mol. As the average steel area in each test container in this series of tests was 0.604 $m^2$, the initial $CO_2$ charge in each test container was equivalent to 0.73 mol per square meter of steel in an $FeCO_3$-forming reaction.

The Henry's Law coefficient, S, for $CO_2$ in equilibrium with Brine A

$$S = \frac{\text{moles } CO_2 \text{ in solution}}{\text{pressure } CO_2, \text{ atm}} \tag{34}$$

was experimentally determined to be equal to 0.012 at 20°C, and 0.010 at 30°C. During a 30°C test, assuming equilibrium conditions, the major portion of the $CO_2$ (~65%) would be expected to be present in the gas phase with the remainder (~35%) dissolved in the brine. The $H_2$ generated by the corrosion reaction, on the other hand, would collect in the plenum region of the test container only, as it is essentially insoluble in the brine phase. As the $CO_2$ is consumed by the corrosion reaction [Equation (7)], the pressure will tend to decrease in the plenum, but not to the extent that the pressure increases due to $H_2$ formation because the brine phase will continually supply a fraction of the $CO_2$ involved in the corrosion reaction. Thus, a pressure buildup in the plenum will be observed on the pressure gauge as the reaction proceeds, even though Equation (7) states that a mole of $CO_2$ will be consumed for each mole of $H_2$ formed.

The pressure-time curves for the excess-$CO_2$ tests are presented in Figure 6-5. The corresponding raw data are presented in Appendix A. The starting pressure of the immersed-specimen tests is given as 155 psig in the figure; the pressure variations that occurred during the first few days of the tests are not shown for clarity. The actual starting pressures of the vapor-phase-exposure tests are those given in the figure.

All of the container pressures of the duplicate tests have been averaged, so that the curves of Figure 6-5 actually represent data obtained from 16 test containers. The close agreement in pressure between duplicate containers, typically within 2 to 3 psi, justifies this averaging. An exception to this close agreement was the pressure data from the 6-month immersed-specimen tests, where the pressure disparity between the two tests (containers 11 and 12) attained a value of 8 psi during the fourth month of the test and 10 psi during the last two months (the highest system pressure was associated with container 11). In spite of this relatively large disparity between the two test containers, the data were averaged to produce the single curve shown for simplicity of presentation.

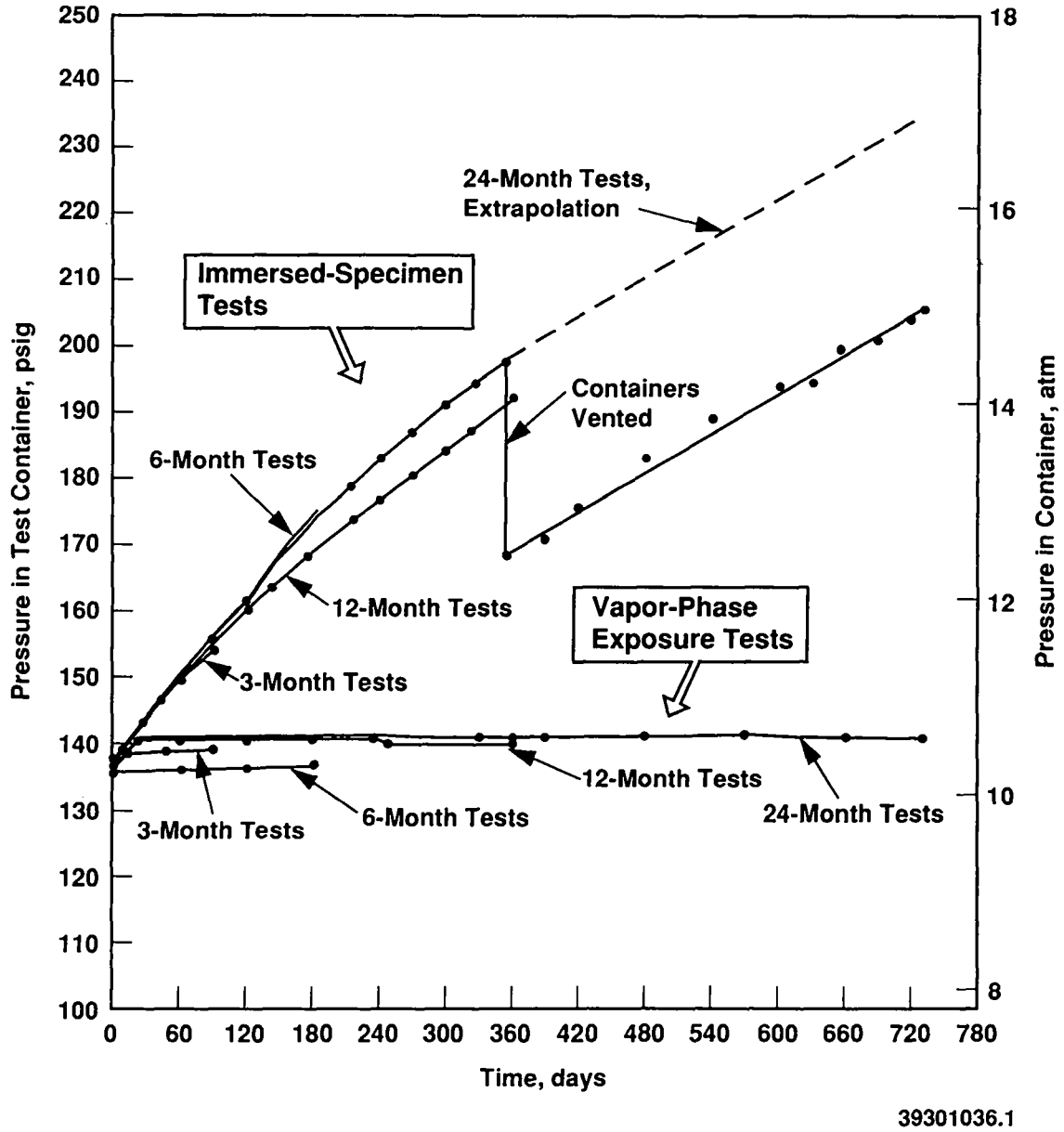



Figure 6-5. Pressure-time curves, low-carbon steel/brine-$CO_2$ tests. Each curve represents two (duplicate) tests.

The curves of Figure 6-5 show generally good agreement. The immersed-specimen tests are characterized by a rapid increase in pressure for a period of about 100 days, followed by a period in which the specimens appear to have become totally non-reacting (passivated).

An analysis of the gas samples taken from the containers just before they were opened is presented in Table 6-5. The analyses confirm that the pressure increase observed in the containers was due to corrosion-product $H_2$. Though not as good as that evidenced in the anoxic-brine tests, the consistency in the composition of gas generated between the duplicate immersed-specimen test containers is observable in the tabulated data. A significant unexplained disparity exists between the two 6-month test containers; container 11 shows a significantly higher $H_2$ generation rate than container 12. The difference in the pressure-time curves in the 6-month tests (as much as 10 psi) has already been alluded to. Significant differences are also evident between the $H_2$ contents of the vapor-exposure containers. As in the case of the anoxic brine (brine/$N_2$) tests, this is attributed to the varying test specimen surface area splashed by brine from one test container to another.

Table 6-5. Composition of Gas at Conclusion of Test, Brine/$CO_2$ Tests. Each tabulated value is average of two analyses. Results are given in vol% (mol%).

| | Immersed-Specimen Tests | | | | Vapor-Phase-Exposure Tests | | | |
|---|---|---|---|---|---|---|---|---|
| | Test Numbers | | | | Test Numbers | | | |
| | 3-month | 6-month | 12-month | 24-month | 3-month | 6-month | 12-month | 24-month |
| Specie | 3/4[a] | 11/12 | 19/20 | 27/28 | 7/8 | 15/16 | 23/24 | 31/32 |
| $CO_2$ | 51.1 | 28.0 | 40.0 | 41.3 | 98.8 | 97.4 | 98.6 | 98.5 |
| | 50.8 | 35.6 | 43.7 | 38.4 | 98.9 | 97.5 | 98.4 | 97.7 |
| $H_2$ | 47.7 | 71.1 | 59.0 | 58.0 | 0.12 | 1.65 | 0.25 | 0.48 |
| | 47.9 | 63.4 | 64.4 | 61.0 | 0.12 | 1.62 | 0.48 | 1.25 |
| He | 0.13 | 0.11 | 0.05 | 0.09 | 0.02 | 0.25 | 0.22 | 0.24 |
| | 0.27 | 0.27 | 0.05 | 0.07 | 0.02 | 0.30 | 0.24 | 0.27 |
| $N_2$ | 1.08 | 0.79 | 0.90 | 0.63 | 1.08 | 0.72 | 0.92 | 0.76 |
| | 1.01 | 0.83 | 0.85 | 0.57 | 0.98 | 0.63 | 0.91 | 0.81 |
| $O_2$ | <0.1, in all tests | | | | | | | |

[a] 3/4, 11/12, etc. indicates that tests numbered 3 and 4 are duplicate tests, 11 and 12 are duplicate tests, etc. In the table, the average of two separate gas analyses for test 3 is over the average of two separate gas analyses for 4, the average of two separate gas analyses for test 11 is over the average of two separate gas analyses for 12, etc. In all cases the two separate analyses made on gas samples from one container showed excellent agreement.

The brine/$CO_2$ corrosion rate data are summarized in Table 6-6. The corrosion rates of Table 6-6 are far lower than the corrosion rates found by other investigators who used only short-term tests (see Section 4.2.3.2 of this report). All of the individual-specimen data from the immersed-specimen tests with $CO_2$ overpressure are shown in Appendix B-3; data from the vapor-phase-exposure tests are shown in Appendix B-4.

Table 6-6. Summary of Corrosion-Rate Data, Immersed Specimens, Brine/$CO_2$ Tests. Penetration rate means and standard deviations are presented. Each penetration rate value in the columns labeled J, K, L, and M represents an average of five specimens; the sixth specimen of each lot was reserved for surface analysis/archive. Penetration rate is expressed in $\mu$m/yr.

| Test Duration, Months | Test Containers | Steel Lot and Penetration Rate,[a] $\mu$m/yr | | | | |
|---|---|---|---|---|---|---|
| | | J | K | L | M | All Lots |
| 3 | 3, 4 | 12.7±3.1 | 9.59±1.02 | 5.29±0.85 | 7.41±2.43 | 8.76±3.44 |
| 6 | 11, 12 | 8.47±1.91 | 7.91±2.50 | 3.82±0.74 | 5.00±0.90 | 6.31±2.54 |
| 12 | 19, 20 | 3.68±0.70 | 3.58±0.78 | 1.72±0.20 | 2.69±2.61 | 2.91±1.00 |
| 24 | 27, 28 | 1.63±0.34 | 1.85±0.43 | 1.12±0.49 | 1.26±0.20 | 1.46±0.47 |

[a] To convert from a penetration rate expressed in $\mu$m/yr to moles Fe reacted /$m^2$ - yr, multiply the penetration rate by 0.141 mol/$\mu$m - $m^2$.

Unlike the corrosion results obtained from the anoxic brine tests (summarized in Table 6-2), the four lots of steel immersed in the brine/$CO_2$ environment showed a significant difference in corrosion rate from lot to lot of steel. The corrosion rates of the higher-carbon lots of steel (lots L and M) average ~60% of the corrosion rates exhibited by the low-carbon lots (lots J and K).[a] Also, in comparison with the anoxic brine data, the specimen-to-specimen variability of the brine/$CO_2$ test is much greater. This is believed to be at least partly caused by the much greater difficulty encountered in stripping the $FeCO_3$ corrosion product films from the brine/$CO_2$ test specimens. For example, the immersion time for stripping a specimen in the inhibited HCl stripping solution varied from ~1 min

[a] This behavior reverses at high $CO_2$ overpressures. Possible reasons for the corrosion dependence exhibited is discussed in Section 6.1.2.3.

for the anoxic brine test to 6 to 7 min for the brine/$CO_2$) tests. Accordingly, there was a possibility of 1) over-etching the steel substrate while attempting to remove the last traces of corrosion product, or 2) leaving small quantities of corrosion product unremoved, even after long exposure times.

Knowledge of the plenum volume in the test containers, the test temperature, the container pressure at the end of a test, and the final gas composition permits a calculation to be made of the moles of $H_2$ present in a test container at the conclusion of a test. This can be compared with the amount of steel reacted, determined by a gravimetric analysis of the specimens exposed to the test medium. The results of this analysis for the brine/$CO_2$ seal-welded container tests are shown in Table 6-7. (The calculations are presented in Appendix C.)

Table 6-7. Comparison of Moles of $H_2$ Formed (gas analysis) with Moles of Fe Reacted (by specimen weight change), Brine/$CO_2$ Tests

| Test Duration, Months | Average Moles Fe Reacted, mol/m$^2$ - yr | Average Moles $H_2$ Formed, mol/m$^2$ - yr | Moles $H_2$ / Moles Fe |
|---|---|---|---|
| 3 | 1.24 | 1.11 | 0.89 |
| 6 | 0.890 | 0.877 | 0.99 |
| 12 | 0.410 | 0.386 | 0.94 |
| 24 | 0.206 | 0.186 | 0.90 |

The agreement between moles $H_2$ formed and moles Fe reacted is good throughout the test, validating the proposed reaction given by Equation (7). Even in the case of the long-term tests, however, the moles of $H_2$ formed are not quite equivalent to the moles Fe lost from the test specimens, as was the case in the anoxic brine tests (Table 6-4). A possible reason for this is the difficulty of stripping the Fe $CO_3$ from the steel specimens prior to final weighing, which can lead to some over-etching of the steel and an exaggeration of the metal apparently lost to the corrosion reaction.

The corrosion rates are obviously decreasing strongly with time, in accordance with the specimen-passivation information provided by the pressure-time curves (Figure 6-5). A comparison of the 12- and 24-month corrosion rates in Table 6-6 shows that no corrosion occurred in the last 12 months of the 24-month test, suggesting eventual complete passivation of the steel in the test

environment. XRD analyses of the corrosion-product films formed on these specimens showed them to be composed of siderite, $FeCO_3$, as expected. No $CaCO_3$ was observed by XRD. The ability of siderite to passivate a steel substrate, especially in stagnant solutions in the presence of high fugacities of $CO_2$, has been reported by a number of investigators, though the passivating ability generally has been reported to be most effective at temperatures $>60°C$ (see Section 4.2 of this report).

The amount of $CO_2$ required to passivate the steel under the test conditions employed can be estimated from the data of Table 6-6 and the information provided in Figure 6-5. From the figure, the steel has apparently passivated at a time period $<6$ months. If it is assumed that no reaction has taken place on any specimen after 6 months, and that the corrosion reaction can be expressed by Equation (7), then the amount of Fe lost to corrosion during the 6-, 12- and 24-month tests can be averaged to determine the amount of $CO_2$ (and Fe) contributing to the corrosion reaction and the attainment of the passivated state. From Table 6-6 the average Fe loss to corrosion during the 6-month test was 6.31 $\mu$m/yr x 1/2 yr, or 3.16 $\mu$m; during the 12-month test it was 2.91 $\mu$m; and during the 24-month test it was 1.46 $\mu$m/yr x 2 yr, or 2.92 $\mu$m. The average penetration over these three tests was therefore 3.00 $\mu$m prior to passivation. A penetration of 1 $\mu$m over 1 $m^2$ is equivalent to 1 $cm^3$ (7.86 g) Fe/$\mu$m - $m^2$, or 0.141 mol/$\mu$m - $m^2$. The 3.00 $\mu$m penetration observed is therefore equivalent to 3.00 $\mu$m x 0.141 mol/$\mu$m - $m^2$, or 0.42 mol $CO_2$ (or Fe)/$m^2$ of steel required for passivation.

The post-test appearance of the steel specimens is shown in Figure 6-6 (immersed specimens, 24 months exposure) and Figure 6-7 (vapor-phase exposure specimens, 24 months exposure). The dark gray, adherent corrosion product observed on the specimens is $FeCO_3$.

The post-test compositions of the brines obtained from the test containers after the 6-, 12- and 24-month tests are compared with the starting brine composition in Table 6-8. The brines from the immersed-specimen tests differ significantly from the starting brine composition, in that the pH is considerably lower and the Fe composition has attained a significant value. In addition, the Ca concentration of the brine has been reduced significantly, though no evidence of Ca compounds was found in the XRD investigations of the corrosion product layer. [The reduction of Ca concentration in the brine is consistent with the observations of Murata et al. (1983), who found $CaCO_3$ in the $FeCO_3$ layers formed on steels corroding in $CO_2$-saturated brines containing Ca.]

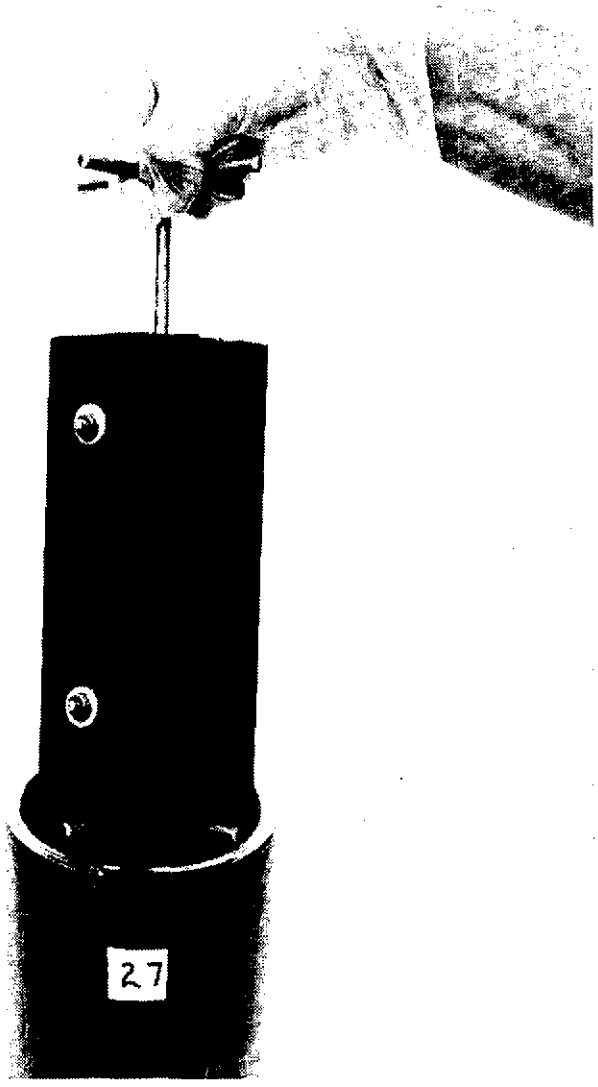



Figure 6-6. Post-test appearance of steel specimens, immersed, 24-month brine/$CO_2$ tests. Specimens are coated with an adherent black $FeCO_3$ corrosion product.

The pH and Fe concentration in the brine shown in Table 6-8 cannot be taken as representative of the conditions existing within the test container during an actual test, as $CO_2$ escapes from the system as soon as the container is opened, and $Fe^{2+}$ oxidizes rapidly and precipitates from solution as the

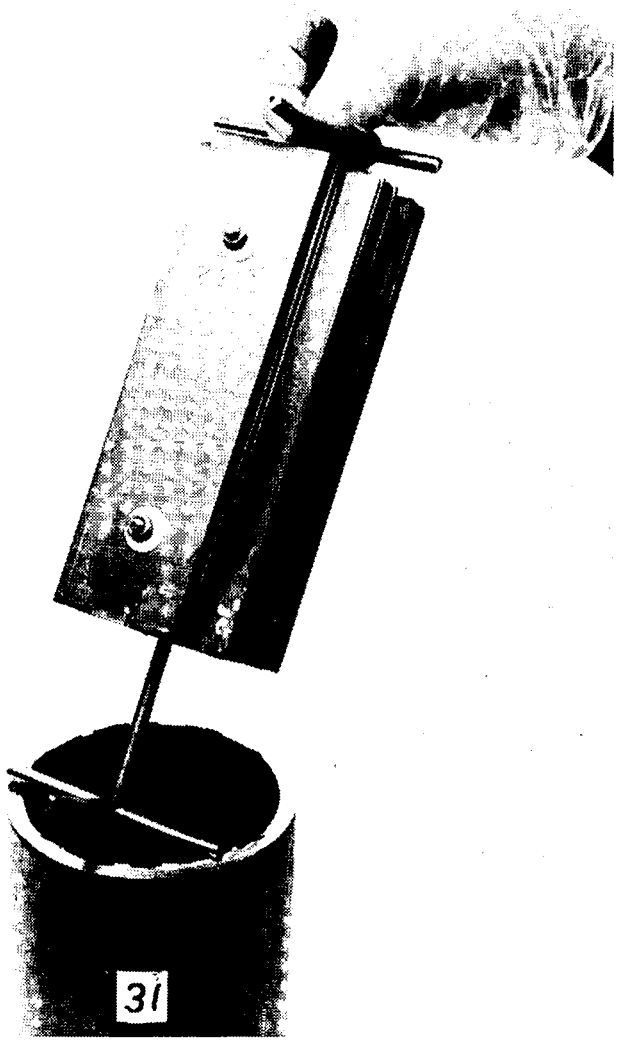



Figure 6-7. Post-test appearance of steel specimens, vapor-phase exposure, 24-month brine/$CO_2$ tests. No significant corrosion reaction is evident except where brine has contacted the bottoms of the specimens.

solution comes in contact with air. Also, the concentration of $Fe^{2+}$ reported as being in solution in the $CO_2$/brine tests may actually be high, as a fine particulate suspension may be contributing to the concentration values reported.

Table 6-8. Results of Brine Analyses, Brine/$CO_2$ Seal-Welded-Container Tests. Comparison of brine compositions after 6-, 12- and 24-month tests is made with original brine composition. Concentration given in mg/L.

| | | Test Duration | | | | | |
|---|---|---|---|---|---|---|---|
| | | 6 months | | 12 months | | 24 months | |
| Specie | Brine A | Imm.[a] | Vapor[b] | Imm.[c] | Vapor[d] | Imm.[e] | Vapor[f] |
| Na | 38,300 | 42,600 | 41,000 | 40,300 | 40,500 | 40,500 | 40,300 |
| Mg | 35,700 | 35,500 | 34,900 | 34,500 | 35,000 | 33,200 | 33,500 |
| K | 29,500 | 30,600 | 29,900 | 29,800 | 30,200 | 30,000 | 30,000 |
| Ca | 560 | 240 | 590 | 270 | 600 | 230 | 567 |
| B | 230 | 220 | 230 | 230 | 240 | 220 | 226 |
| Fe | < 10 | 1,480 | 5 | 1,230 | < 10 | 1,320 | < 10 |
| Cl | 190,000 | 196,000 | 196,000 | 191,000 | 189,000 | 194,000 | 188,000 |
| $SO_4$ | 4,070 | 4,230 | 4,240 | 3,900 | 4,200 | 4,540 | 3,920 |
| pH | 6.7 | 5.1 | 7.1 | 3.4 | 7.3 | 5.9 | 6.9 |

[a] Test container 12; [b] 16; [c] 19; [d] 23; [e] 27; [f] 31.

### Controlled-$CO_2$-Addition Tests

When the activity of $CO_2$ dissolved in Brine A is increased, two opposing effects are manifested: the brine becomes a more aggressive corrodant toward steel due to effects already discussed [Equations (1) through (7)]; and the presence of $CO_2$ tends to stop the reaction through the formation of a stable $FeCO_3$ layer. The controlled-$CO_2$-addition tests were intended to provide information on the amount of $CO_2$ required/unit area of steel to attain a passivated state, such as was attained in the excess-$CO_2$ tests after $CO_2$ had reacted with the steel to the extent of $\sim 0.42$ mol $CO_2/m^2$ steel.

The controlled-$CO_2$-addition tests comprised test containers 33 through 38. The test conditions are summarized in Table 6-9. A $N_2$ addition was made to test containers 36 through 38 so that the pressure gauges would provide a positive reading.

Table 6-9. Summary of Test Conditions, Controlled-$CO_2$-Addition Tests

| Test Container | Initial $CO_2$ Charge Pressure, atm (psia)[a] | $N_2$ Pressure, atm (psia) | Mol $CO_2/m^2$ Steel[b] |
|---|---|---|---|
| 33 | 7.8 (115) | no $N_2$ | 0.32 |
| 34 | 3.8 (56) | no $N_2$ | 0.16 |
| 35 | 1.5 (22) | no $N_2$ | 0.063 |
| 36 | 0.75 (11) | 2.0 (30) | 0.032 |
| 37 | 0.39 (5.7) | 2.0 (30) | 0.016 |
| 38 | 0 (0) | 3.1 (45) | 0.0 |

[a] Assumes plenum = 0.634 L, T = 30°C, no $CO_2$ dissolution in brine at the time of $CO_2$ charging.

[b] Total area of steel specimens in each test container = 0.629 $m^2$.

The highest ratio of mol $CO_2/m^2$ steel (0.32) employed in the test series was intended to approximate the 0.42 mol/$m^2$ value causing passivation in the excess-$CO_2$ tests (Table 6-6). Lesser quantities of $CO_2$ were also used to determine if passivation, or temporary passivation, would develop under conditions of relatively low concentrations of $CO_2$.

The pressure-time curves for the controlled-$CO_2$-addition tests are shown in Figure 6-8. It is apparent that at least some degree of passivity has been attained in the test containers with the maximum amount of $CO_2$ added (containers 33 and 34). Though the pressure-time curves for these two containers appear to attain a near-zero slope after a time period of ~150 days, the curves indicate some degree of reaction even to the maximum test duration shown in the figure. This test will be allowed to continue so that the ability of the steel to passivate completely under the test conditions can be more fully evaluated. A continual pressure increase was not observed in the excess-$CO_2$ tests after passivation of the specimens was achieved (see Figure 6-5 and Table 6-6).

The raw pressure-time data for the test containers 33 through 38 corresponding to the curves of Figure 6.8 are presented in Appendix A. The gravimetric data for the individual specimens will not be available until the study is concluded.

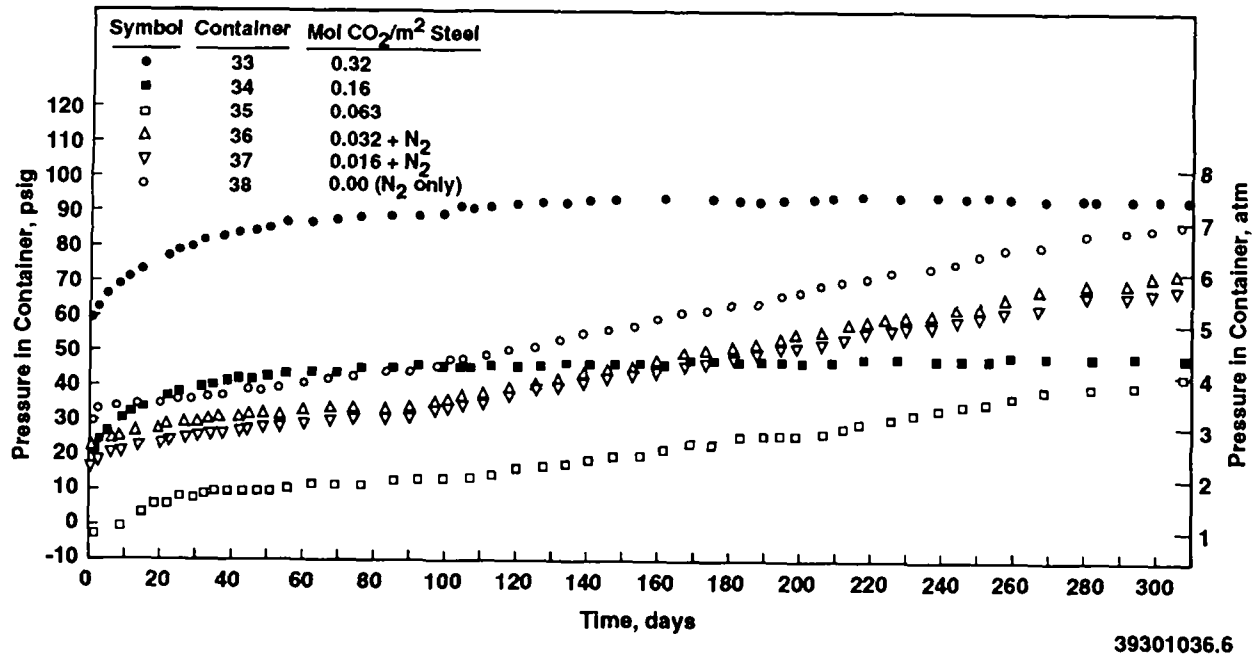



Figure 6-8. Pressure-time curves, controlled-$CO_2$-addition tests.

Assuming that all of the $H_2$ resulting from the corrosion reaction collects in the plenum of the test container, that all of the $H_2$ resulting from the corrosion reaction is accounted for, that passivation of the steel does not stop the corrosion reaction, and that the reaction

$$Fe + CO_2 + H_2O = FeCO_3 + H_2 \qquad (35)$$

is the only $H_2$-producing reaction, then the reaction will stop when the $H_2$ pressure in the plenum equals the original starting $CO_2$ charge pressure (i.e., the $CO_2$ pressure in the container plenum before its dissolution in the brine).[a] The initial charge pressures are given in Table 6-9. From these data

[a] Strictly speaking, there will always be some $CO_2$ remaining unreacted, as equilibrium conditions [as given by the equilibrium constant of Equation (8)] require a residual $CO_2$ fugacity equal to $\sim 2 \times 10^{-4} f_{H2}$. In the practical terms of the present test, this $CO_2$ fugacity will not be sensed by the pressure gauges employed, nor will it affect the conclusions drawn in the subsequent discussion.

and associated assumptions it can be calculated that the reaction in container 33 has consumed 95% of the original $CO_2$ charge at 250 days, that the reaction in container 34 has consumed the equivalent of 110% of the original $CO_2$ charge at 250 days, and that the reaction in container 35 has consumed the equivalent of 220% of the original $CO_2$ charge at 250 days. Obviously, an Fe-$H_2O$ reaction is proceeding and producing $H_2$ in the latter two cases cited. The containers with less $CO_2$ than container 35 essentially behaved as though no $CO_2$ had been added at all, as their pressure-time curves closely simulate that of the $CO_2$-free control, container 38.

The pressure-time curve of container 35 appeared to temporarily passivate in the time period 30-50 days. If it is assumed as before that $H_2$ generated is equivalent to $CO_2$ consumed, at 50 days the initial $CO_2$ charge has been 110% consumed. This good agreement between apparent passivation and $CO_2$ consumption suggests that a state of imperfect passivation was produced by the available $CO_2$, perhaps produced by a siderite layer containing defects that could not remain "healed" due to the absence of a continuing supply of $CO_2$. The defective film then eventually lost its protectiveness entirely, and permitted the competing Fe-$H_2O$ reaction to proceed at a normal rate, as in the case of the Fe-anoxic brine (brine/$N_2$) tests or the case of container 38.

The controlled-$CO_2$-addition tests are still in progress, so the final assessment of the results of the test cannot yet be made. The test results obtained to date suggest, however, that the best passivation obtained under the conditions used in the controlled-$CO_2$-addition study is still questionable and does not yet evoke confidence as a true, stable state of corrosion prohibition.

#### 6.1.1.3 BRINE/$H_2S$

The brine/$H_2S$ tests were intended to provide information on the corrosion and gas generation proclivity of low-carbon steel in the presence of Brine A and $H_2S$. Like $CO_2$, $H_2S$ is a potential byproduct of microbial activity through sulfate reduction in the WIPP, so its presence in the site environment is considered to be a credible possibility. As has been shown [Equations (17) and (18)], the thermodynamic tendency for reaction of Fe with $H_2S$ is strong. There is a possibility, however, of passivating steel in the presence of $H_2S$ at sufficient activity to form the high sulfides, such as pyrite (see Section 4.3 of this report).

The brine/$H_2S$ tests of low-carbon steel were performed in test containers 40, 41, 42, and 43. In replicate test containers 40 and 41, the specimens were exposed under immersed conditions; in test containers 42 and 43 the specimens were suspended in the vapor phase over Brine A. The method of racking the specimens in test containers was similar to that used in the anoxic brine (brine/$N_2$) and the $CO_2$-brine tests previously described, and the amount of brine used in each test container was essentially the same as that used in the previous tests: 1.4 L in the immersed-specimen tests, 250 mL in the vapor-phase tests. The area of steel specimens present in each test container was 0.497 $m^2$.

The partial pressure of $H_2S$ in these initial Fe/$H_2S$ tests was purposefully chosen to be a high value relative to $H_2S$ concentrations expected in the WIPP. An arbitrary (equilibrium) partial pressure of 5 atm was selected for these tests. For $H_2S$, the gas-charging method employed was similar to that used for $N_2$ and $CO_2$ in tests previously described, in that the $H_2S$ gas was charged into the plenum of a previously evacuated test container with both steel specimens and Brine A already in place.

The $H_2S$ gas dissolved much more rapidly into the brine than did the $CO_2$. The Henry's Law coefficient, S, for $H_2S$ was determined to be

$$S = 0.050 \text{ mol/atm-L} \tag{36}$$

at the gas-charging temperature of ~25°C. As a consequence of the high solubility of the $H_2S$ in Brine A, the major amount of the $H_2S$ charged into the immersed-specimen test containers is dissolved in the brine phase.[a]

The pressure-time curves for tests 40 through 43 are shown in Figure 6-9. After an initial period of activity lasting about 6 days, the specimens appear to be essentially nonreactive in the brine/$H_2S$ environment. During the initial period of activity the immersed specimens appeared to generate corrosion-product $H_2$. The vapor-phase tests appeared to simply show the effect of continued $H_2S$ dissolution in the brine phase present (the vapor-phase test containers were not shaken after gas addition to expedite equilibration of gas between vapor space and brine).

---

[a] Because $H_2S$ shows significant non-ideal behavior, even at pressures as low as 5 atm, a van der Waals relationship was used to determine the relationship between moles $H_2S$ and pressure of $H_2S$ throughout all of the $H_2S$ investigations (Lange's Handbook, 1985).

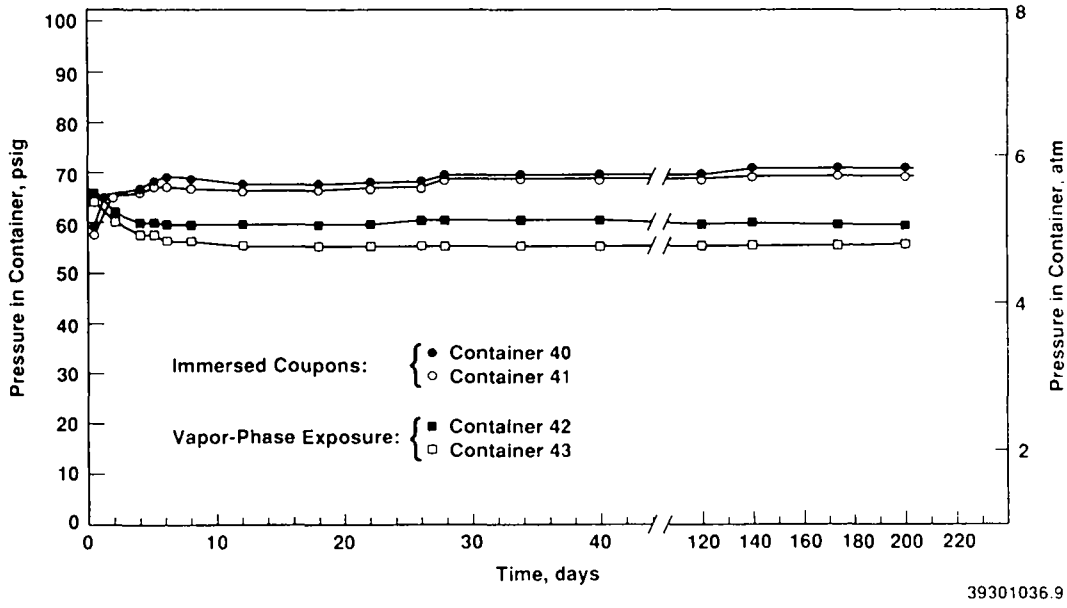



Figure 6-9. Pressure-time curves, Fe-$H_2S$ tests, test containers 40-43.

The lack of continued reaction after a time period of about 6 days in the immersed-specimen test condition suggests that pyrite or other high sulfide had rapidly formed on the specimen surfaces and stopped further reaction from taking place. This could be considered at least partially consistent with the observations of other investigators (see Section 4.3 of this report), in that higher sulfides are highly passivating, and high pressures of $H_2S$ are consistent with formation of higher sulfides. However, other investigators (such as Meyer et al., 1958) have found that 1 atm $H_2S$ is not readily passivating, in that nonprotective lower sulfides form under these conditions. The preliminary results of the present tests suggest that 5 atm partial pressure is passivating even though 1 atm partial pressure $H_2S$ may not be.

### 6.1.2 High-Pressure Autoclave Tests

The seal-welded container tests were charged with overpressure gas to equilibrium pressures in the range of 5 to 12 atm. These pressures are, of course, low by comparison with total pressure expected when the WIPP approaches lithostatic pressure. High-pressure autoclave tests were conducted to gain insights into the effect of high $CO_2$, $H_2$ and $N_2$ pressures on the reaction kinetics, with

equilibrium pressures in the range 36 to 73 atm. The high-pressure testing regimen comprised tests AUT-1, -2, -3, -4, -7, and -8 (Table 3-1). In general, the steel specimens were prepared pre-test and examined post-test in the same manner as that used for the seal-welded-container tests. The specimen area per test was much smaller in the autoclave tests because emphasis was placed on gravimetric analysis of the specimens rather than following the pressure as a function of time. This basic difference in test approach is based on the fact that an autoclave system cannot be relied upon to be (essentially) leak free for very long periods of time, even though this is sometimes observed to be the case in practice.

#### 6.1.2.1 HIGH $H_2$ PRESSURE TESTS

Tests AUT-1, AUT-3, and AUT-4 were initiated to determine to what extent, if any, high $H_2$ pressures inhibit the progress of the Fe-$H_2O$ (Brine A) reaction. The steel test specimens, five specimens of lot J and five of lot K, were completely immersed in Brine A in this test series. A summary of these tests, extending the data of Table 3-1, is presented in Table 6-10. The individual specimen-corrosion data for tests AUT-1, AUT-3, and AUT-4 are tabulated in Appendices B-5, B-6, and B-7, respectively.

At the conclusion of the high $H_2$ pressure tests, the specimens were clean and shiny in appearance. A small amount of corrosion product was present in the autoclave at the conclusion of each test. XRD analysis of the dark gray particulate corrosion-product residues left after the 6-month test (AUT-1) showed evidence of reevesite, $(Ni,Fe)_6Fe_2(CO_3)(OH)_{16} \cdot 4H_2O$, nickel iron carbonate hydroxide hydrate, with perhaps as many as two additional unidentifiable phases. Because of the small amount of corrosion product recovered and because of the nickel content exhibited by the identifiable phase (suggesting a possible autoclave-wall contribution),[a] little significance was attached to the XRD results obtained. Chemical analysis of the corrosion product revealed a significant Mg presence

[a] The autoclaves used in these studies were made of Ni-Cr-Mo alloys.

Table 6-10. Summary of Test Conditions, $H_2$-Overpressure Tests AUT-1, AUT-3, and AUT-4. Number of specimens of each material lot: 5. Test temperature: 30°C.

| Test | Initial Mean $H_2$ Overpressure | Brine Volume, L | Total Specimen Area, $m^2$ | Test Duration, Months |
|---|---|---|---|---|
| AUT-1 | 1030 psia (70 atm) | 2.79 | 0.199 | 6 |
| AUT-3 | 515 psia (35 atm) | 2.79 | 0.199 | 12 |
| AUT-4 | 1010 psia (69 atm) | 2.78 | 0.198 | 12 |

(15%) and a Ni concentration of 4%. The high Mg concentration suggests that the portion of the corrosion product unidentifiable by XRD could be of the form $Fe,Mg(OH)_2$, a corrosion product found in another study where steel was allowed to react with a high-Mg brine at elevated temperatures (Westerman et al., 1987).

The gravimetrically determined corrosion rates obtained from the high $H_2$ pressure tests are presented in Table 6-11. The corrosion rates are compared in the table with results obtained from seal-welded corrosion tests of 6- and 12-month test durations having a $N_2$ overpressure, to aid in evaluating the effect of the $H_2$ overpressure on the reaction kinetics.

The data of Table 6-11 show that presence of a high $H_2$ pressure can significantly inhibit the corrosion rate of low-carbon steels in Brine A, relative to tests having an $N_2$ overpressure only. A $H_2$-induced factor of five reduction in corrosion rate, at the same test times, is evident from the table when the autoclave and the $N_2$/immersed seal-welded-container tests are compared. (Reduction in steel corrosion rate in a high-Mg-brine environment by a $H_2$ overpressure at 150°C has been reported previously by Westerman et al., 1987.)

Doubling the $H_2$ pressure from 35 to 69 atm (Tests AUT-3 and AUT-4) did not exert an inhibiting effect on the corrosion rate beyond that observed at the lower pressure. It is believed that this is due to the rate-decreasing effect of the additional $H_2$ pressure being effectively counterbalanced by the rate-increasing effect of the additional system pressure. This pressure-induced increase in

Table 6-11. Corrosion Rates of Steel Specimens in High $H_2$ Pressure Tests Compared with Corrosion Rates in Brine/$N_2$ Seal-Welded Container Tests

| Test | Corrosion Rate, $\mu$m/yr[a] | |
|---|---|---|
| | Steel Lot J | Steel Lot K |
| AUT-1 70 atm $H_2$, 6 months | 0.32±0.01 | 0.40±0.04 |
| AUT-3 35 atm $H_2$, 12 months | 0.20±0.01 | 0.25±0.02 |
| AUT-4 69 atm $H_2$, 12 months | 0.20±0.01 | 0.27±0.03 |
| Seal-Welded Container $N_2$/Immersed Tests, 10 atm $N_2$ | | |
| 6-month test | 1.61±0.07 | 1.65±0.37 |
| 12-month test | 1.05±0.05 | 1.26±0.04 |

[a] Average linearized corrosion rate of all specimens of each material lot in each test, with standard deviation.

corrosion rate has been observed in other studies in which steel-brine systems were subjected to an overpressure of inert gas (Westerman et al., 1987), and will be discussed further in the next section of this report.

It is interesting to note that steel lot J corroded at a consistently lower rate than lot K in the $H_2$-overpressure studies, as it did in all of the $N_2$/immersed seal-welded container tests. Because the two steels are alike in composition and microstructure, no explanation can be offered for the observed corrosion differences on the basis of the available information.

#### 6.1.2.2 HIGH $N_2$ PRESSURE TEST

The effect of high $N_2$ pressure on the reaction rate of steel in Brine A was investigated by determining the corrosion rate of low-carbon steel under a relatively high $N_2$ pressure. The test, designated AUT-2, was performed in a manner similar to that described for the high-pressure $H_2$ tests in the preceding section of this report. The initial $N_2$ pressure was 1070 psia (73 atm); the volume of the brine in the 4 L autoclave was 2.79 L; the total area of the steel specimens was 0.199 $m^2$. Five

specimens of steel lot J and five of lot K were exposed to the brine in the completely immersed condition. The test duration was 6 months. The individual-specimen data from test AUT-2 are presented in Appendix B-8.

The test specimens appeared clean and shiny when removed from the autoclave and were free of adherent corrosion products. The corrosion product, present in copious quantities compared to the $H_2$-overpressure tests, was found adhering to the specimen rack and the autoclave walls. It was of a cream-beige color when removed from the autoclave (with a spatula); upon exposure to the air it gradually turned a dark yellow-brown color. In texture and distribution it resembled the corrosion product associated with the $N_2$/immersed seal-welded-container tests.

A specimen of the corrosion product was analyzed by XRD within an hour of its being removed from the test autoclave. It proved to be unidentifiable. The diffraction pattern had the same characteristics as the unidentifiable patterns obtained from the $N_2$/immersed seal-welded container tests (see Section 6.1.1.1 of this report).

The chemical composition of the corrosion product was determined in an attempt to gain some insights into its nature. The analysis showed the cationic constituents of the corrosion product to be essentially Fe, with $\sim 12\%$ Mg. As in the case of the high $H_2$ pressure tests, this suggests a corrosion product of the form $Fe,Mg(OH)_2$. The averaged corrosion rates, determined gravimetrically using all of the 10 specimens included in the test, are shown in Table 6-12.

The $N_2$ overpressure substantially increased the corrosion rate over that observed in the seal-welded container test. This same phenomenon was observed in studies by Westerman et al. (1987), in steel-brine systems pressurized with Ar.

Apparently, that portion of the overall cathodic reaction

$$HOH + 1e = \frac{1}{2}H_2 + (OH)^- \qquad (37)$$

responsible for the actual rate control has associated with it an activated complex with a smaller net volume than the reactants it comprises. Increasing the total system pressure would cause this decrease in volume to decrease the activation energy required for its production and thereby cause an increase

Table 6-12. Corrosion Rates of Steel Specimens in High $N_2$ Pressure Tests Compared with Corrosion Rates in Brine/$N_2$ Seal-Welded Container Tests

| Test | Corrosion Rate, $\mu$m/yr[a] | |
|---|---|---|
| | Steel Lot J | Steel Lot K |
| AUT-2: 73 atm $N_2$, 6 months | 2.76±0.24 | 3.17±0.04 |
| Seal-Welded-Container, $N_2$/Immersed Test, 10 atm $N_2$, 6 months | 1.61±0.07 | 1.65±0.37 |

[a] Average linearized corrosion rate of all specimens included in category, with standard deviation.

in the cathodic reaction rate. Because either $N_2$ or $H_2$ could cause such an activation energy decrease, increasing a $H_2$ overpressure could decrease the reaction rate (back reaction tendency) while increasing the reaction rate by the mechanism just described, whereas under the same circumstances increasing the $N_2$ overpressure would be expected to increase only the reaction rate.

The foregoing explanation of the effects of system pressure on corrosion reaction rate is obviously highly qualitative and not capable of explaining the quantitative relationships between reaction inhibition by back-reaction and reaction promotion by system pressure. The reaction mechanisms involved, and the pressure dependence of the mechanisms, are not specifically known.

#### 6.1.2.3 HIGH $CO_2$ PRESSURE TESTS

The dichotomy in $CO_2$ behavior toward steel, in which increasing the pressure of $CO_2$ increases the reactivity of the system while enhancing the ability of steel to passivate itself through formation of a relatively stable and impervious layer of $FeCO_3$, has already been described. The tendency of the $FeCO_3$ reaction product to dissolve in the test solution, and the fairly high $Fe^{2+}$ concentrations associated with the terminal solubility of $FeCO_3$ in solutions having high $CO_2$ concentrations, complicates the prediction of corrosion rates and ultimate disposition of reaction products. The high $CO_2$ pressure

tests AUT-7 and AUT-8 were intended to further the understanding of the $CO_2$-steel system by providing steel corrosion data obtained at the relatively high $CO_2$ pressure of 36 atm.

Tests AUT-7 and AUT-8 utilized two 4L autoclaves. Each autoclave contained four specimens of each of the following steel lots: J, K, L, and M. The total area of the steel specimens was 0.095 $m^2$ in AUT-7, and 0.094 $m^2$ in AUT-8. Each autoclave was charged with 3.1 L of Brine A at the beginning of the test. The specimens were completely immersed in the brine phase throughout the tests. Test AUT-7 was terminated after 6 months; test AUT-8 has a projected test duration of 12 months. At the present time, only data from test AUT-7 are available. Individual-specimen data for test AUT-7 are presented in Appendix B-9 of this report.

Before opening the AUT-7 test autoclave for specimen examination, a complete analysis was made of the gas in the autoclave plenum. The gas was composed almost entirely of $CO_2$ (87.4%) and $H_2$ (12.3%). The pressure in the autoclave increased from 535 psia to 590 psia during the test as corrosion-product $H_2$ was generated.

The steel specimens were covered with a brownish-black, adherent corrosion product when they were removed from the autoclave. XRD analysis of the corrosion product showed that the corrosion product was closely approximated by $(Fe,Mn,Zn)CO_3$, "oligonite." The crystal structure of oligonite differs somewhat from the $FeCO_3$ (siderite) diffraction patterns obtained from specimens exposed in the past to $CO_2$-brine environments. To clarify the compositional question, especially the implication of the presence of Zn, a small amount of corrosion product was scraped from the surface of a specimen and its composition was determined by x-ray fluorescence analysis (XRFA). The composition of the corrosion product so determined is given below, in weight percent:

| | |
|---|---|
| Fe | 92.2 |
| Ca | 6.1 |
| Mn | 0.76 |
| Ni | 0.31 |
| Zn | 0.18 |
| Cu | 0.17 |

Other than Fe, the major constituent of the corrosion product is obviously Ca derived from the brine. The coprecipitation of Ca in the carbonate film has been mentioned previously (Section 6.1.1.2 of this report); its presence in the corrosion product film is therefore not surprising. The small amount of

Zn present belies the crystal structure nomenclature derived from the XRD database. It is most likely not a major crystal-structure-defining constituent in the corrosion product at the level of concentration observed. The source of Zn is not known; it may have been derived from the chemicals used to make up the brine. The relatively high level of Mn could have as its source the steel itself, as the steels exposed to the brine contain 0.3 to 0.8 wt% Mn.

Both the AUT-7 and the seal-welded container test environments (36 atm and 12 atm overpressure $CO_2$, respectively) are potentially highly reactive with unprotected steel. The pH values associated with these $CO_2$ pressures, in a 0.5 M NaCl medium, have been estimated to be 3.1 and 3.3, respectively (Crolet and Bonis, 1984).

The linearized corrosion rates over the 6-month test period of the specimens from test AUT-7 are presented in Table 6-13.

It is interesting to note that in test AUT-7 the lots of steel having a relatively low C content, J and K, corroded at significantly lower rates than steel lots L and M. This is contrary to the findings from the 3-, 6-, and 12-month seal-welded container tests with immersed specimens and an initial overpressure of 12 atm $CO_2$ (Section 6.1.1.2).

The corrosion rates of the specimens from test AUT-7 are considerably higher (by a factor of 4.7) than those determined in seal-welded container tests of 6-month duration originally charged with 12 atm $CO_2$, as listed in Table 6-6. However, the specimens in the seal-welded container tests passivated well before the end of the 6-month test exposure, with the corrosion process coming essentially to a complete stop at that time.

The complexities associated with the explanation and prediction of corrosion rates of specimens of nearly identical commercial steels has been long recognized. Cleary and Greene (1967) attempted to isolate the factors contributing to the corrosion of carbon steels by subjecting a large number of steel specimens having widely varying compositions and microstructures to an anoxic environment of dilute sulfuric acid at 30°C. By means of a multiple correlation analysis they were able to deduce the compositional and microstructural factors important to the corrosion of the steels. They found that C and P were particularly detrimental to corrosion resistance. Mn was beneficial to ~0.6 wt%; beyond 1.0 wt% it was detrimental. Si is also detrimental, whereas Cu is beneficial. If the environment

Table 6-13. Corrosion Rates of Steel Specimens, Test AUT-7

| Sample Identification | Corrosion Rate, μm/yr | Average Corrosion Rate, μm/yr with Standard Deviation |
|---|---|---|
| J71 | 23.7 | 22.1±1.8 |
| J72 | NA | |
| J73 | 20.1 | |
| J74 | 22.5 | |
| K71 | 23.6 | 24.9±1.0 |
| K72 | 25.2 | |
| K73 | 25.0 | |
| K74 | 25.8 | |
| L71 | 34.4 | 36.0±1.3 |
| L72 | 37.6 | |
| L73 | 35.9 | |
| L74 | 36.3 | |
| M71 | 37.8 | 35.8±1.7 |
| M72 | 35.8 | |
| M73 | 35.8 | |
| M74 | 33.7 | |

employed by Cleary and Greene can be considered analagous to the anoxic, $CO_2$-overpressured brine environments used in present study, the composition of the steels used (Table 5-11) gives possible insights into the pre-passivation corrosion behavior observed. In the seal-welded container tests, lots L and M showed the highest corrosion resistance. These alloys have a higher Mn content than lots J and K, and this factor could be responsible for the corrosion rate differential observed. At the higher $CO_2$ overpressures (higher $H^+$ activities) it is reasonable to expect the C content to have a more profound effect, because of its direct involvement in the cathodic $H^+$-reduction process, usually rate-limiting. One might therefore postulate that the Mn content of lots L and M could contribute to their corrosion resistance at low $CO_2$ overpressures, while their high C-content could be responsible for

their higher corrosion rates at higher $CO_2$ overpressures. These considerations apply only to the corrosion occurring prior to the formation of the passivating film. The processes associated with the film formation and the transport-inhibiting properties of the resulting film, ignored in the foregoing speculative analysis, could be more important than the considerations presented.

In order to gain some insight into the kinetics of the corrosion process taking place in test AUT-7 over the 6-month test period, an analysis was made of the pressure data from the autoclave pressure gauge. This is a necessarily limited analysis, because of the characteristics of the autoclave gauge (2000-psig range; smallest division 20 psi; reading accuracy approximately $\pm 5$ psi); the fact that all autoclave systems can be expected to leak gas to some extent, especially low-molecular-weight gases such as $H_2$; and the fact that $CO_2$ is consumed as $H_2$ is generated, complicating the pressure-time analysis. Also, the non-ideal nature of $CO_2$ precludes use of the ideal gas law under all high-pressure conditions, if a reasonable degree of accuracy is expected, and the high solubility of $CO_2$ in the brine phase has to be considered in all gas-accounting analyses. In all of the computations it was assumed that the $H_2$ produced was insoluble in the brine phase, and that the Henry's Law constant governing the solubility of $CO_2$ in the brine phase had a value of 0.0102 mol/atm under all pressure conditions. The van der Waals equation was used to define the $CO_2$ pressure/volume/mole relationships. The pressure-time curves for tests AUT-7 and AUT-8 are presented in Figure 6-10.

The experimentally determined increase in total system pressure for test AUT-7 over the 6-month test duration was 55 psi. This value was in reasonably good agreement with the pressure increase expected if all of the Fe lost from the specimens (0.199 mole) was converted on an equimolar basis to $H_2$ (102 psia in the autoclave plenum region), and if the corresponding $CO_2$ pressure drop in the autoclave (44 psi) was subtracted from this $H_2$ pressure (102 psi - 44 psi = 58 psi). This agreement gives assurance that the autoclave was extremely well sealed and that the pressure-time data of Figure 6-10 have a strong measure of credibility. Not surprisingly, in spite of this good pressure agreement, some of the theoretical $H_2$ is not accounted for, as evidenced by comparing the $CO_2/H_2$ ratio from the gas analysis results ($\sim 7.1$) with the calculated $CO_2/H_2$ ratio assuming complete $H_2$ accountability in the plenum of the autoclave ($\sim 5.9$). This lack of complete $H_2$ accountability was encountered in the short-term seal-welded-container tests as well. It can be ascribed to a) reaction of $H_2$ with metal oxides present in the system; b) solution of $H_2$ in both brine and metal; and/or c) some $H_2$ leakage from the system. The loss of $H_2$ from the system does not appear severe enough to call

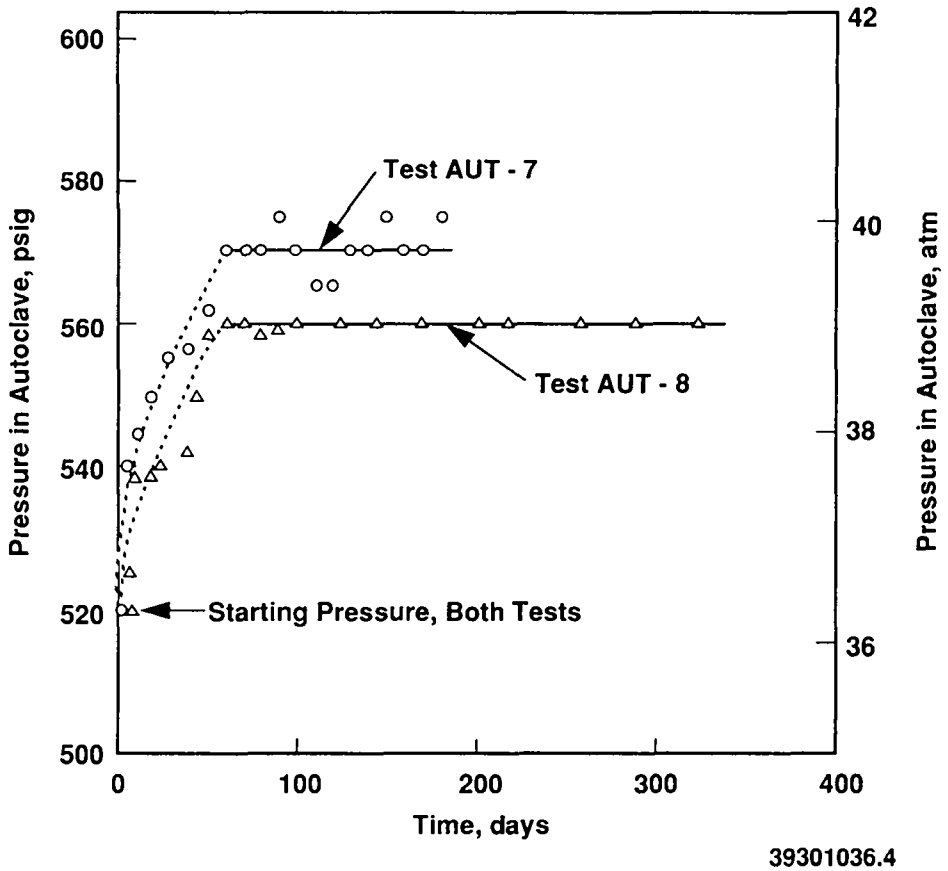



Figure 6-10. Pressure-time curves, tests AUT-7 and AUT-8.

the AUT-7 pressure-time curve of Figure 6-10 into question. The value of the AUT-8 pressure-time curve in predicting corrosion kinetics will not be known until the test is concluded and the amount of steel lost in the course of that test is determined. These results will be reported in the future.

The curves of Figure 6-10 suggest that the steel specimens first underwent a significant attack, due to the high $CO_2$ activity present in the system, but that either passivation of the specimens or saturation of the brine with $Fe^{2+}$ occurred after a time period of ~2 months. The saturation of the brine phase with $Fe^{2+}$ is currently not considered a totally satisfactory explanation for the complete stopping of the corrosion process, either in the AUT-7 test or in the seal-welded container tests. The amount of corrosion taking place in the AUT-7 test amounted to 4.0 g Fe/L of brine; in the case of the seal-welded-container tests, the corrosion amounted to 11.0 g Fe/L of brine. The fact that the higher-pressure test showed a lower Fe loss per liter of solution than the lower-pressure test is not

consistent with the expectations of siderite solubility as a function of $CO_2$ pressure. Also, both tests lost far more Fe/L than can be accounted for by estimating the solubility of $Fe^{2+}$ in the brine phase. (Ikeda et al., 1983 attempted to calculate the concentration of $Fe^{2+}$ in a brine solution in equilibrium intruding with $FeCO_3$, but an error in their reasoning produced results that were as much as three orders of magnitude too high at 30°C.) The concentration of $Fe^{2+}$ in equilibrium with $FeCO_3$ in Brine A at 30°C is currently not known. The gravimetric data from the 12-month test (test AUT-8) will be required in order to make a definitive judgment on whether or not the surface passivation suggested by the pressure-time curves of Figure 6-10 in fact took place.

### 6.1.3 Salt-Phase Autoclave Tests

A probable scenario in the corrosion of steel in the WIPP involves the contact of steel by a moist mass of salt rather than brine. The moisture could be derived from intruding brine from a distant source "wicked" to the surface of the steel by capillary action or water vapor from a distant source equilibrating with the salt contacting the steel.

Two autoclave scoping tests, designated AUT-5 and AUT-6, were conducted to determine the approximate corrosion kinetics associated with the two scenarios described. The test arrangements are shown schematically in Figure 6-11. Test AUT-5 was designed to investigate the effect of wicking. The bottom of the salt mass was below the level of the brine, but the bottom of the specimens was above the brine liquid level. Test AUT-6 was designed to investigate the effect of vapor transport, so the bottom of the salt mass was above the liquid level of the brine. In each test 12 specimens of lot J steel were embedded in particulate salt (natural halite from the WIPP site) contained in a stainless steel mesh basket suspended from the top of the autoclave. The specimens were 51 mm x 25 mm (2 in. x 1 in.). Care was taken to prevent the specimens from contacting the basket or each other. A coarse fraction of the salt supplied was used (particles approximately 2 to 6 mm in major dimension) to permit at least initial vapor transport through the salt mass. Approximately 2 kg of salt was placed in each basket. The volume of Brine A placed in the bottom of the autoclave in test AUT-5 was 890 mL; in test AUT-6 the brine volume added was 350 mL. The initial $N_2$ overpressure in each test was 10 atm; the test duration was three months.

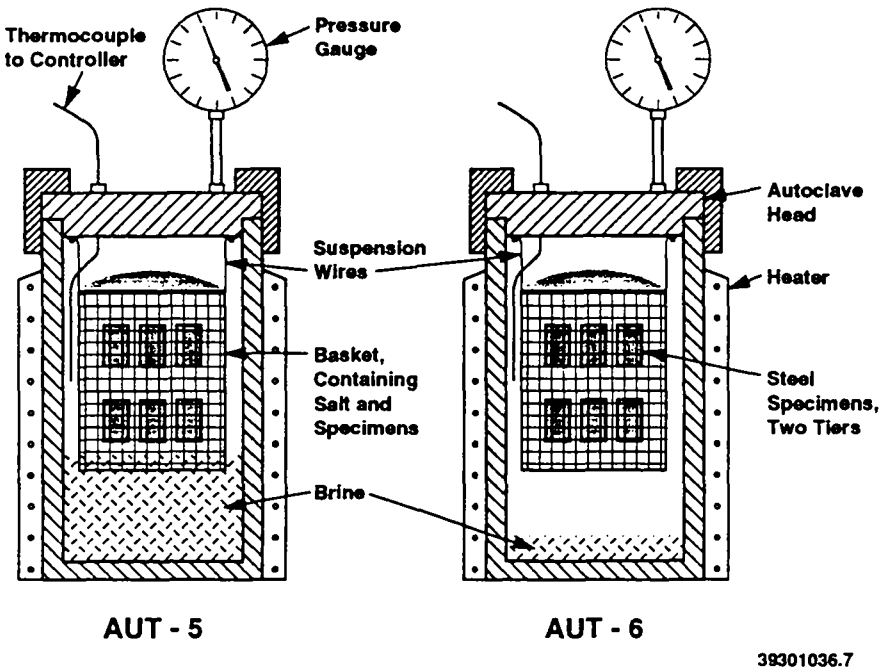



Figure 6-11. Test arrangements, tests AUT-5 and AUT-6.

#### 6.1.3.1 POST-TEST OBSERVATIONS, TEST AUT-5

This wicking test functioned as intended. At the conclusion of the test the salt was still mounded in the basket, and the specimens were all entirely covered with salt. Salt crystals were adhering to both the basket and the autoclave wall above the liquid level. A mass of crystalline salt was present in the bottom of the autoclave in the brine. The salt in the basket was hard, and the samples were chipped out with difficulty. No red oxides (traces of ferric ion) were present in the test assembly. The samples were mottled due to a discontinuous tarnish film, but had an essentially metallic appearance when removed from the salt. Predictably, the mottled regions rapidly darkened and assumed a reddish hue when the specimens were exposed to air. The specimens were washed sequentially in deionized water and ethanol and stored in a desiccator.

The brine was "water-white" when removed from the autoclave, but developed a light yellow hue upon standing for a few hours, indicating the presence of $Fe^{2+}$ ions in the brine removed from the autoclave.

### 6.1.3.2 POST-TEST OBSERVATIONS, TEST AUT-6

In this test the bottom of the salt mass was above the level of the brine. The intent of the test arrangement was to make the vapor-phase transport of water the only method of water transport. Because of the reduced activity of water in the Brine A water source and the expectation that at the low test temperature employed a large temperature gradient between the underside of the autoclave head and the contents of the autoclave would not exist, it was assumed that no water would condense on the bottom of the autoclave head and drip onto the salt. Such was not the case. For some period of time water apparently dripped from the underside of the autoclave head onto the salt, as the top of the salt was partially eroded in a non-uniform manner, and the top of one top-tier specimen was slightly exposed. Also, as the autoclave head was lifted from the autoclave, some water droplets were noted clinging to the tubing.

At 30°C, the partial pressure of $H_2O$ over saturated Brine A is 0.03 atm or 23 mm Hg (Brush, 1990). At this pressure, pure $H_2O$ will condense at a temperature equal to or less than 25°C. This means that a temperature gradient of at least 5°C existed in the autoclave, permitting $H_2O$ to condense on the head of the autoclave. Though this magnitude of temperature gradient was not expected, it apparently occurred for at least some portion of the 3-month operating period of the autoclave test. The test employing the partially submerged salt (AUT-5) did not show any evidence of water transport by dripping, as the salt dome was smooth with no signs of dripping-induced erosion. The dripping transport obviously precludes characterizing the test as a vapor-phase-transport test. Instead, it can best be characterized as a vapor-phase-transport, dripping-transport test, with the time period of dripping and the amount of water transported by dripping unknown.

As in test AUT-5, salt crystals were found clinging to the outside of the basket and to the inside wall of the autoclave above the brine level, and a mass of salt crystals was in the bottom of the autoclave in the brine. The brine was "water-white" when removed from the autoclave, but developed a light yellow hue upon standing for a few hours, indicating some iron specie(s) in solution. As in the case of test AUT-5, the steel specimens were removed from test AUT-6 with some difficulty, as the salt particles in the salt adhered strongly to one another. The steel specimens removed from test AUT-6 were shinier and more metallic in appearance than those removed from AUT-5; i.e., the extent of corrosion tarnish was somewhat less, though the mottled appearance was similar. No red corrosion product was observed anywhere in the system.

### 6.1.3.3 CORROSION RATES, TESTS AUT-5 AND AUT-6

The corrosion rates of the steel specimens from tests AUT-5 and AUT-6 were determined by the conventional gravimetric method. These results are presented in Table 6-14, compared to 3- and 6-month corrosion data from $N_2$/immersed seal-welded container tests. Individual-specimen data for tests AUT-5 and AUT-6 are tabulated in Appendices B-10 and B-11, respectively.

The corrosion rates obtained from specimens lying in the bottom tier of the wicking test AUT-5 are the only ones that approach the corrosion rates of specimens actually immersed in Brine A with a $N_2$ overpressure, as reflected by the seal-welded-container test results. The reason for the relatively low corrosion rates observed in the top tier of test AUT-5, or the generally low rates observed in test AUT-6, could be due to either 1) a reduced $H_2O$ availability or 2) a reduced Mg availability, as the corrosiveness of brines toward steel are markedly dependent on their Mg concentration (Westerman et al., 1987).

Table 6-14. Corrosion Rates of Steel Specimens in Solid-Salt Tests, Compared with Corrosion Rates in Brine/$N_2$ Seal-Welded Container Tests

| Test | Tier | Corrosion Rate, $\mu$m/yr[a] |
|---|---|---|
| AUT-5 3 months | Top | 1.15±0.22 |
| | Bottom | 1.92±0.45 |
| AUT-6 3 months | Top | 0.79±0.04 |
| | Bottom | 0.64±0.09 |
| $N_2$/Immersed, Seal-Welded Container Tests, Steel Lot J | | |
| 3-month test | | 1.94±0.16 |
| 6-month test | | 1.61±0.37 |

[a] Average linearized corrosion rate of all specimens included in category, with standard deviation.

As previously mentioned, the corrosion rates that would be obtained under a strictly controlled vapor-transport test cannot be estimated from the results of the tests described above. If a vapor-transport test were to be repeated, an insulating cover on the autoclave head and a drip shield over the salt basket would be reasonable precautions. Further wicking and vapor-phase tests, with steel specimens embedded in simulated backfill material, will be conducted in the future. The results of those tests will be compared with the results of the tests described here.

## 6.2 Alternative Material Tests

The corrosion and gas-generation behavior of the four candidate alternative packaging materials [high-purity Cu; cupronickel 90-10; commercial-purity Ti (Ti Grade 2) and Ti Grade 12] was investigated in three environments—anoxic brine (Brine A with $N_2$); Brine A with $CO_2$; and Brine A with $H_2S$. Only the seal-welded-container method of testing was used, as reliance was placed on gas-pressure measurements as well as gravimetric analyses of the test specimens to establish the behavior of the materials in the test environments. The test matrix summarizing these tests is shown in Table 3-2.

The manner of racking the specimens in the alternative material tests was different from the method of racking used in the low-carbon steel tests. In the latter tests, the specimens were held on a specimen rack with no effort made to produce well defined crevices between the test specimens. In the alternative material tests, two specimen geometries were used: rectangular specimens 19.1 cm x 6.35 cm (7.5 in. x 2.5 in.), and circular specimens 3.81 cm (1.50 in.) in diameter. The rectangular specimens were provided with two holes, each 0.79 cm (0.31 in.) in diameter for rack mounting; the circular specimens had one centrally located hole of the same size. The manner of racking the specimens is shown in Figure 6-12.

Each test involved 16 rectangular specimens and 16 circular specimens. The 16 circular specimens were tightly compressed between adjacent rectangular specimens, as shown in Figure 6-12, to provide regions for crevice corrosion if the tendency for that degradation mode existed in a given test system.

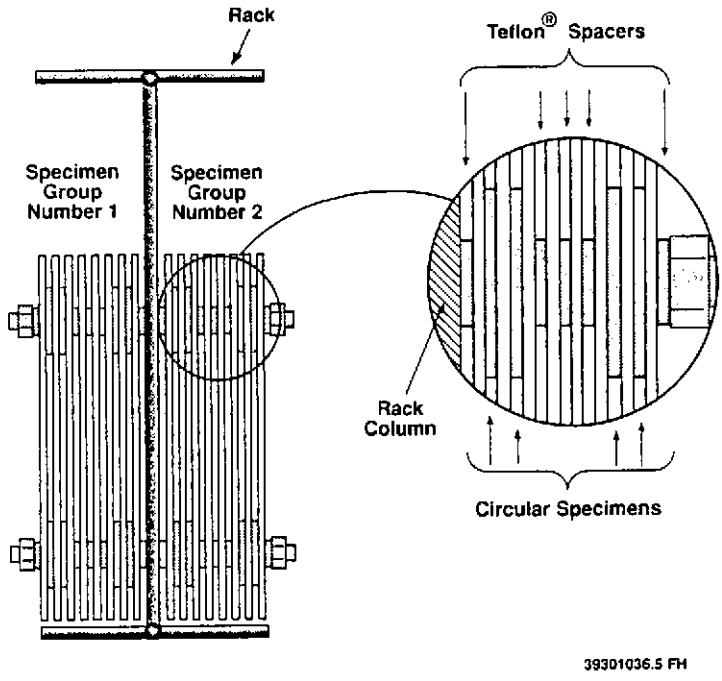



Figure 6-12. Method of mounting specimens on specimen rack for alternative packaging materials tests.

During alternative material testing, Cu-base and Ti-base materials were always tested in separate containers. In tests of Cu-base materials, all of the high-purity-Cu specimens (8 rectangular, 8 circular) were placed on one side of a specimen rack, and 16 equivalent specimens of cupronickel were situated on the other side of the rack. In a similar manner, in a test of Ti-base materials, specimens of Ti Grade 2 were placed on one side of a rack, and specimens of Ti Grade 12 on the other. The specimens were always completely immersed in Brine A during a test. All tests were conducted at 30 $\pm 5$°C.

The alternative packaging materials investigation comprised tests 1A through 19A. Details of the tests, expanding on the information presented in Table 3-2, are presented in Table 6-15. Individual-specimen data for completed tests are presented in Appendices B-12 through B-17.

### 6.2.1 Cu in Brine A with $N_2$

Cu and cupronickel 90-10 specimens exposed to anoxic Brine A showed no significant reaction, as indicated by either pressure increase within the test container or by consumption of metal by a corrosion reaction. This is consistent with thermodynamic expectations [Equation (24)].

Specimens removed from test containers 1A and 7A after test periods of 10 and 15 months, respectively, exhibited freshly ground, as-received surface conditions reminiscent of the pre-test specimen conditions. A gravimetric analysis of specimens from test 7A (see Appendix B-12 for individual

Table 6-15. Initial Conditions, Tests 1A through 19A

| Test Identification | Material Base | Initial Overpressure Gas/atm[a] | Total Specimen Area, $m^2$ | Brine Volume, L | Actual Test Duration, Months |
|---|---|---|---|---|---|
| 1A | Cu | $N_2$/10.6 | 0.43 | 1.415 | 10 |
| 2A | Cu | $CO_2$/11.5 | 0.43 | 1.375 | 10 |
| 3A | Cu | $H_2S$/4.9 | 0.43 | 1.390 | 9 |
| 4A | Ti | $N_2$/10.7 | 0.44 | 1.435 | 10 |
| 5A | Ti | $CO_2$/11.6 | 0.44 | 1.360 | 10 |
| 6A | Ti | $H_2S$/4.7 | 0.44 | 1.415 | 9 |
| 7A | Cu | $N_2$/10.4 | 0.43 | 1.420 | 15 |
| 8A | Cu | $CO_2$/11.0 | 0.43 | 1.405 | 15 |
| 9A | Cu | $H_2S$/5.1 | 0.43 | 1.405 | 15 |
| 10A | Ti | $N_2$/10.5 | 0.44 | 1.420 | 15 |
| 11A | Ti | $CO_2$/10.9 | 0.44 | 1.400 | 15 |
| 12A | Ti | $H_2S$/5.1 | 0.44 | 1.360 | 15 |
| 13A | Cu | $N_2$/10.2 | 0.43 | 1.380 | open |
| 14A | Cu | $CO_2$/10.9 | 0.43 | 1.410 | open |
| 15A | Cu | $H_2S$/4.9 | 0.43 | 1.420 | open |
| 16A | Ti | $N_2$/10.2 | 0.44 | 1.365 | open |
| 17A | Ti | $CO_2$/10.8 | 0.44 | 1.360 | open |
| 18A | Ti | $H_2S$/5.1 | 0.44 | 1.360 | open |
| 19A | Control | $H_2S$/4.5 | -- | 1.740 | open |

[a] At attainment of 30°C test temperature.

specimen weight-change data) showed that the weight changes undergone by the circular specimens were within the accuracy limits of the four-place balance used for the analysis. The rectangular specimens showed weight gains up to 0.0117 g. The pressure changes in the two test containers over the entire period of the tests were within ±1 psi. Thus, it can be concluded on the basis of the evidence currently available that Cu and cupronickel 90-10 will not react with Brine A to form significant $H_2$ under the anoxic test conditions employed. The container pressure of the continuing test (test 13A) is consistent with this observation; the pressure has not increased over a 16-month test period.

### 6.2.2 Cu in Brine A with $CO_2$

Cu and cupronickel 90-10 specimens exposed to Brine A with $CO_2$ showed no significant reaction, as indicated by either pressure increase within the test container or by consumption of metal by a corrosion reaction. This is consistent with thermodynamic expectations [Equation (27)].

Specimens removed from test containers 2A and 8A after test durations of 10 and 15 months, respectively, appeared clean and uncorroded. The pressure in both these containers dropped during the test periods by approximately 2 psi. The test specimens from test 8A lost a small amount of weight during the test, possibly due to Cu dissolution or Cu-complex dissolution effects. (See Appendix B-13 for individual specimen weight-change data.) It can be concluded, on the basis of the available evidence, that Cu and cupronickel 90-10 will not react with Brine A to form significant $H_2$ under the test conditions used. The container pressure of the continuing test (test 14A) is following a course consistent with these observations, in that the pressure has not increased after 16 months.

### 6.2.3 Cu in Brine A with $H_2S$

Cu and cupronickel 90-10 specimens exposed to Brine A with $H_2S$ show a rapid $H_2$-generating reaction. These observations can be said to be consistent with thermodynamic predictions [Equation (29)], though the upper limits of $H_2$ pressure suggested by those limits have not been nearly approached in the present tests.

The pressure histories of the three tests 3A, 9A, and 15A, originally charged with Cu-base materials, Brine A, and $H_2S$ gas, are summarized in Figure 6-13. Test 3A was opened for specimen examination after a 3-month test exposure. Test 15A is an ongoing test. Containers 9A and 15A

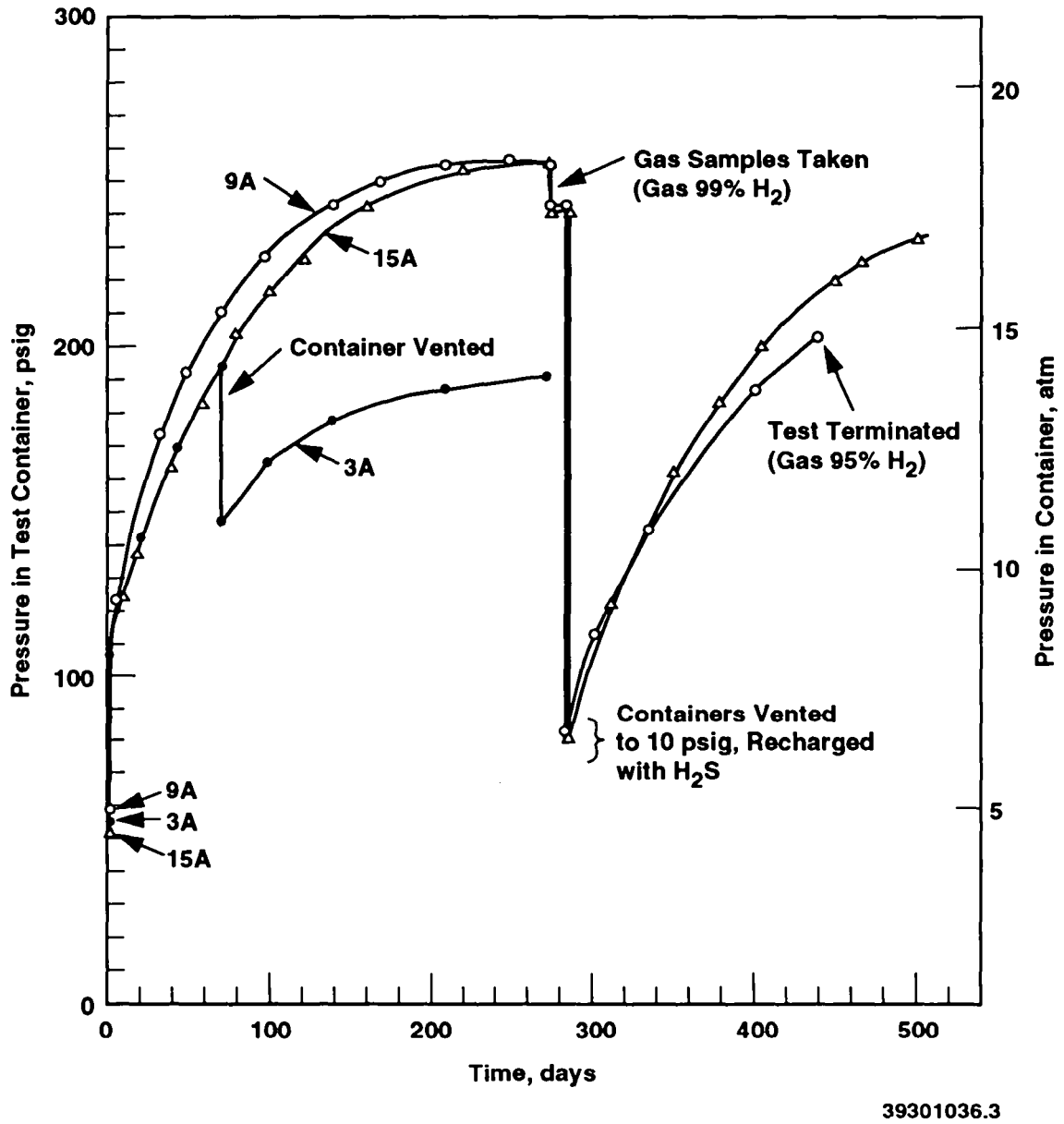



Figure 6-13. Pressure-time curves, tests 3A, 9A, and 15A.

were vented and repressurized with $H_2S$ gas after 9 months exposure. (The intent of the venting and repressurization was to reveal whether the specimens had originally stopped reacting due to formation of a protective sulfide film, or whether the decrease in reaction rate with time was simply a result of $H_2S$ consumption.) The vented gas was essentially pure $H_2$ in both cases. The pressure buildup as a function of time in the vented-and-repressurized test containers has approximately duplicated the initial pressure buildup in the containers.

These observations demonstrate that the reduction of apparent reaction rate observed was due to consumption of the $H_2S$ reactant, not formation of a passive film. Further supporting this conclusion are two additional observations: 1) the buildup in pressure before venting and refilling the containers at nine months was caused by an amount of $H_2$ calculated to be equivalent, on a molar basis, to the $H_2S$ originally charged into the containers; and 2) a gravimetric determination of the amount of Cu lost from a sampling of the test specimens in the two containers in which the specimens were examined (3A and 9A) showed a close agreement in molar equivalency between the metal lost to the corrosion reaction and the $H_2$ generated, assuming the reaction of 2 moles of Cu with 1 mole of $H_2S$ to form 1 mole of $Cu_2S$ and 1 mole of $H_2$. $Cu_2S$, chalcocite, is the only reaction product found on the surface of the specimens. Individual specimen weight-change data for tests 3A and 9A are presented in Appendix B-14.

At this time it can be concluded that Cu and cupronickel 90-10 react rapidly and essentially completely with $H_2S$ under the test conditions imposed to form $Cu_2S$ and $H_2$ in the expected quantities, with little if any inhibition of reaction rate ascribable to the corrosion product film forming on the specimen surface. Because the reaction proceeds at a rapid rate (on a WIPP-relevant time scale) to very low activities of $H_2S$, it is difficult to conceive of a useful Cu-alloy container if $H_2S$ has a significant probability of being present in the environment.

### 6.2.4 Ti in Brine A with $N_2$, $CO_2$, and $H_2S$

All alternative-material tests of Ti Grade 2 and Ti Grade 12 have shown essentially complete stability of the Ti-base materials in the test environments. The pressure changes observed in the Ti with $N_2$ and Ti with $CO_2$ tests have been within 4 psi of the starting pressure over the entire period of the tests; the pressure changes observed were pressure drops. The Ti with $H_2S$ tests, on the other

hand, all showed a pressure increase of 9 to 10 psi within the first 30 h of gas addition, after which time the pressure stabilized, within ± 2 psi, for the remainder of the test period. Gas taken from the 15-month-exposure test (test 12A) before test termination showed a trace of $H_2$ (0.5%), consistent with a limited corrosion reaction at the beginning of the test.

All of the Ti-base specimens appeared clean, shiny, and unreacted upon removal from the containers of terminated tests. A gravimetric analysis of a random sample of specimens from the 15-month tests (tests 10A, 11A, and 12A)[a] showed that the majority of specimens from the $N_2$/brine tests gained weight, up to 0.0018 g; whereas all of the specimens from the other two environments (brine/$CO_2$ and brine/$H_2S$) lost weight, as much as 0.0014 g. As in the case of the Cu-base alloys, weight changes to the extent observed in the present tests have little significance in an assessment of gas-generation potential.

It appears, on the basis of the information obtained to date, that Ti Grade 2 and Ti Grade 12 could be used as alternative packaging materials in the WIPP without concern about gas generation.

---

[a] Individual-specimen data from test 10A, an anoxic brine (brine/$N_2$) test, are presented in Appendix B-15; specimen data from test 11A, a brine/$CO_2$ test, are presented in Appendix B-16; and specimen data from test 12A, a brine/$H_2S$ test, are presented in Appendix B-17.

# 7.0 CONCLUSIONS

The present report describes progress made through December 1992 toward achieving the objectives of the Sandia National Laboratories support project at PNL. Because several of the corrosion and gas-generation tests are still in progress, not all of the areas of investigation initiated can be completely assessed and summarized. The current conclusions that can be made are presented in this section of the report.

- The corrosion rate of low-carbon steel immersed in anoxic Brine A at 30°C for test durations of 24 months decreased slowly with time. The corrosion rate of the steel during the final 12-month period of the 24-month test was 0.71 $\mu$m/yr, equivalent to the generation of 0.10 mol $H_2/m^2$-Fe-yr.

- The corrosion rate of low-carbon steel in anoxic Brine A (Brine A with $N_2$) increased with increasing $N_2$ pressure and decreased with imposition of a 36-atm $H_2$ overpressure. A 70-atm $H_2$ overpressure caused no further reduction in rate, possibly because of a balance between the rate-reduction effect of the reactant back-pressure and the rate enhancement caused by pressure per se.

- In the long-term tests (12 and 24 months) of steel immersed in anoxic brine there was excellent agreement between moles of Fe reacted and moles of $H_2$ produced, assuming the Fe in the corrosion product is only in the divalent state. The non-adherent, greenish-gray corrosion product could not be identified by XRD.

- Steel specimens exposed only to the vapor phase of Brine A under anoxic conditions showed no discernible corrosion reaction. The corrosion product adhering to the bottoms of these specimens where they were contacted by the brine during handling of the containers was $\beta Fe_2(OH)_3Cl$ in all cases investigated.

- $CO_2$ in Brine A causes an initial increase in the reaction rate of steel, relative to anoxic conditions. The initial reaction rate increases with the $CO_2$ pressure imposed. Additions of $CO_2$ beyond a certain threshold amount cause the reaction to essentially stop, however, typically in $\sim$100 days, due to the formation of an adherent carbonate reaction product [$FeCO_3$, siderite, or Fe,Mn,Zn($CO_3$), oligonite]. The "threshold" $CO_2$ required is the subject of a continuing investigation.

- The immersed-specimen tests in Brine A with $CO_2$ showed fairly good agreement between moles of Fe reacted and moles of $H_2$ produced, assuming that Fe is only in the divalent state in the corrosion product.

- Steel specimens exposed to a 10 atm $CO_2$ pressure and vapor of Brine A at 30°C showed insignificant corrosion. Corrosion product in the splash zone of the test specimens was siderite, $FeCO_3$.

- The brine in the test containers does not, in general, undergo an appreciable change in composition during the $N_2$/immersed or the $CO_2$/immersed tests. Exceptions are the relatively high Fe concentration and the relatively low Ca concentration and low pH of the brines at the conclusion of the $CO_2$/immersed tests.

- Steel specimens exposed in the immersed and vapor-phase test conditions to Brine A and a 5-atm pressure of $H_2S$ have shown no significant ongoing reaction. It is assumed that a high sulfide, such as $FeS_2$, pyrite, rapidly formed on the specimen surfaces and prevented further reaction. These tests are continuing.

- Steel specimens embedded in a mass of particulate salt wicking brine from a pool of Brine A under anoxic test conditions corroded at a rate slower but not dissimilar to the rate observed under anoxic brine-immersed conditions. The test lasted only 3 months. Specimens in a similar test in which condensate dripped from the underside of the autoclave lid onto the salt produced significantly lower corrosion rates, presumably because of the lower Mg concentration in the specimen environment.

- The Cu-base alternative packaging materials showed insignificant reaction in $N_2$/immersed and $CO_2$/immersed test conditions. Reaction with $H_2S$ was rapid and complete and produced $H_2$ equivalent to the $H_2S$ added. Cu-base packaging materials are unsuitable if $H_2S$ is considered to be a likely environmental constituent, such as from microbial degradation or sulfate reduction processes.

- The Ti-base alternative packaging materials showed insignificant reaction in all test environments; i.e., in $N_2$/immersed, $CO_2$/immersed, and $H_2S$/immersed environments. It appears at the present time that Ti-base packaging materials could be used in the WIPP site without concern for corrosion or gas generation.

# 8.0 FUTURE WORK

PNL and Sandia-WIPP Gas Generation Program personnel will continue to work cooperatively in interpreting the existing and forthcoming corrosion and gas generation data. Such data results, conclusions, predictions, etc., will be tailored to satisfy the informational needs of the WIPP Project gas generation modeling and performance assessment efforts. PNL and Sandia personnel will also continue to update or modify the current PNL corrosion program to help satisfy these informational needs as the WIPP Project evolves. Significant expansions to the laboratory program are being contemplated or proposed to evaluate gas generation impacts due to potential interactions of corrosion (and corrosion byproducts) with microbial degradation and/or brine-radiolysis reaction products.

The following ongoing or new laboratory efforts are planned for CY 1993:

- The seal-welded-container tests of low-carbon steel in $CO_2$ and $H_2S$ will be continued. A decision will be made, perhaps at mid-year, as to the conclusion of, or possible alteration to, these tests. Further evaluations of the passivating nature of these gases, in WIPP-specific environments, are planned.

- The high-pressure autoclave test (AUT-8) of low-carbon steels in $CO_2$ will be terminated in January 1993 for specimen examination. Further high-pressure studies are being considered by the WIPP Gas Generation Program and may be initiated.

- The corrosion testing of two Al-base materials, high-purity Al and alloy 6061, will be initiated. These materials represent metallic Al in the waste. Test environments utilizing Brine A with $N_2$, $CO_2$, and $H_2S$ are planned, with both immersed and vapor-phase exposure of test specimens. Tests as a f(pH) will also be conducted

- The long-term seal-welded container tests of Cu-base and Ti-base materials will be continued as a longer-term monitoring effort. A decision on their continuation will be made at mid-year.

- It is anticipated that one or more tests will be initiated that will involve the corrosion testing of low-carbon steel specimens in contact with a simulated backfill materials. The test parameters and overall matrix have not yet been finalized.

- Gravimetric data obtained in past studies will be statistically analyzed in order to provide confidence limits for the resulting metal consumption-time curves.

- WIPP-brine-specific, anoxic steel corrosion and gas generation studies as a f(pH) are being considered and may be initiated.

## 9.0 REFERENCES


Asano, H., H. Wakamatsu, and M. Akashi. 1992. "Corrosion Lifetime Assessment for Candidate Materials of Geological Disposal Overpack for High-Level Nuclear Waste Canisters: Perspective of R&D in Japan," *High Level Radioactive Waste Management Proceedings of the Third International Conference, Las Vegas, NV, April 12-16, 1992.* La Grange Park, IL: American Nuclear Society, Inc.; New York, NY: American Society of Civil Engineers. Vol. 2, 1658-1669.

ASM (American Society for Metals). 1978. *Metals Handbook, Volume 1 Properties and Selection: Irons and Steels.* 9th ed. Metals Park, OH: American Society of Metals. 161.

ASM (American Society for Metals). 1980. *Metals Handbook. Volume 3 Properties and Selection: Stainless Steels, Tool Materials, and Special-Purpose Materials.* 9th ed. Metals Park, OH: American Society for Metals. 381.

ASM International. 1987. *Metals Handbook. Volume 13 Corrosion.* 9th ed. Metals Park, OH: ASM International. 618-619, 632.

Booker, J., W.R. Cribb, J.C. Turn, Jr., and R.D. Kane. 1984. "Corrosion Behavior of Beryllium Copper and Other Nonmagnetic Alloys in Simulated Drilling Environments," *Corrosion '84, New Orleans, LA, April 2-6, 1984.* Paper No. 220. Houston, TX: National Association of Corrosion Engineers.

Braithwaite, J.W., and M.A. Molecke. 1980. "Nuclear Waste Canister Corrosion Studies Pertinent to Geologic Isolation," *Nuclear and Chemical Waste Management.* Vol. 1, 37-50.

Bruckhoff, W., O. Geier, K. Hofbauer, G. Schmitt, and D. Steinmetz. 1985. "Rupture of a Sour Gas Line Due to Stress Oriented Hydrogen Induced Cracking Failure Analyses, Experimental Results and Corrosion Prevention," *Corrosion/85, Boston, MA, March 25-29, 1985.* Paper No. 389. Houston, TX: National Association of Corrosion Engineers.

Brush, L.H. 1990. *Test Plan for Laboratory and Modeling Studies of Repository and Radionuclide Chemistry for the Waste Isolation Pilot Plant.* SAND90-0266. Albuquerque, NM: Sandia National Laboratories.

Brush, L.H., M.A. Molecke, A.R. Lappin, R.E. Westerman, X. Tong, J.N.P. Black, D. Grbic-Galic, R.E. Vreeland, and D.T. Reed. 1991a. "Laboratory and Bin-Scale Tests of Gas Generation for the Waste Isolation Pilot Plant," *Waste-Generated Gas at the Waste Isolation Pilot Plant: Papers Presented at the Nuclear Energy Agency Workshop on Gas Generation and Release from Radioactive Waste Repositories, Aix-en-Provence, France, September 23-26, 1991.* Eds. P.B. Davies, L.H. Brush, M.A. Molecke, F.T. Mendenhall, and S.W. Webb. SAND91-2378. Albuquerque, NM: Sandia National Laboratories. 2-1 through 2-13.

Brush, L.H., D. Grbic-Galic, D.T. Reed, X. Tong, R.H. Vreeland, and R.E. Westerman. 1991b. "Preliminary Results of Laboratory Studies of Repository Chemistry for the Waste Isolation Pilot Plant," *Scientific Basis for Nuclear Waste Management XIV, Materials Research Society Symposium Proceedings, Boston, MA, November 26-29, 1990.* Eds. T.A. Abrajano, Jr. and L.H. Johnson. SAND90-1031C. Pittsburgh, PA: Materials Research Society. Vol. 212, 893-900.

Burke, P.A. 1984. "Synopsis: Recent Progress in the Understanding of $CO_2$ Corrosion," *Advances in $CO_2$ Corrosion in the Oil and Gas Industry, Proceedings of the Corrosion/83 Symposium, Anaheim, CA, April 18-19, 1983.* Ed. R.H. Hausler. Houston, TX: National Association of Corrosion Engineers. Vol. 1, 3-9.

Butcher, B.M. 1990. *Preliminary Evaluation of Potential Engineered Modifications for the Waste Isolation Pilot Plant (WIPP).* SAND89-3095. Albuquerque, NM: Sandia National Laboratories.

Chase, M.W., Jr., C.A. Davies, J.R. Downey, Jr., D.J. Frurip, R.A. MacDonald, and A.N. Syverud. 1985. *JANAF Thermochemical Tables.* 3rd ed. [Washington, DC]: American Chemical Society; New York, NY: American Institute of Physics. Pts. I-II.

Cleary, H.J., and N.D. Greene. 1967. "Corrosion Properties of Iron and Steel," *Corrosion Science.* Vol. 7, no. 12, 821-831.

Crolet, J.L., and M.R. Bonis. 1984. "pH Measurements Under High Pressures of $CO_2$ and $H_2S$," *Corrosion '84, International Corrosion Forum Devoted Exclusively to the Protection and Performance of Materials, New Orleans, LA, April 2-6, 1984.* Paper no. 294. Houston, TX: National Association of Corrosion Engineers.

DeBerry, D.W., and W.S. Clark. 1984. "Corrosion Due to Use of Carbon Dioxide for Enhanced Oil Recovery," *$CO_2$ Corrosion in Oil and Gas Production—Selected Papers, Abstracts, and References.* Compiled and edited by NACE Task Group T-13. Houston, TX: National Association of Corrosion Engineers. 7-74.

de Waard, C., and D.E. Milliams. 1975a. "Prediction of Carbonic Acid Corrosion in Natural-Gas Pipelines," *Proceedings of the First International Conference on the Internal and External Protection of Pipes, University of Durham, Durham, England, September 1975.* Paper F1. Bedford, England: BHRA Fluid Engineering.

de Waard, C., and D.E. Milliams. 1975b. "Carbonic Acid Corrosion of Steel," *Corrosion.* Vol. 31, no. 5, 177-181.

Dougherty, J.A. 1988. "Factors Affecting $H_2S$ and $H_2S/CO_2$ Attack on Carbon Steels Under Deep Hot Well Conditions," *Corrosion '88, St. Louis, MO, March 21-25, 1988.* Paper no. 190. Houston, TX: National Association of Corrosion Engineers.

Dunlop, A.K., H.L. Hassell, and P.R. Rhodes. 1983. "Fundamental Considerations in Sweet Gas Well Corrosion," *Corrosion '83, Anaheim, CA, April 18-22, 1983.* Paper no. 46. Houston, TX: National Association of Corrosion Engineers.

EATF (Engineered Alternatives Task Force). 1991. "Appendix H: Report of the Waste Container Materials Panel," *Evaluation of the Effectiveness and Feasibility of the Waste Isolation Pilot Plant Engineered Alternatives: Final Report of the Engineered Alternatives Task Force.* DOE/WIPP 91-007, Rev. 0. Carlsbad, NM: Waste Isolation Pilot Plant. Vol. II, H-i through H-39.

Eiselstein, L.E., B.C. Syrett, S.S. Wing, and R.D. Caligiuri. 1983. "The Accelerated Corrosion of Cu-Ni Alloys in Sulphide-Polluted Seawater: Mechanism No. 2," *Corrosion Science.* Vol. 23, no. 3, 223-239.

Gehring, G.A., Jr., R.L. Foster, and B.C. Syrett. 1983. "Effect of Sulfide on the Corrosion and Protection of Seawater-Cooled Condenser Alloys," *Corrosion '83, International Corrosion Forum, Anaheim, CA, April 18-22, 1983.* Paper no. 76. Houston, TX: National Association of Corrosion Engineers.

Grauer, R., B. Knecht, P. Kreis, and J.P. Simpson. 1991. "Hydrogen Evolution from Corrosion of Iron and Steel in Intermediate Level Waste Repositories," *Scientific Basis for Nuclear Waste Management XIV, Materials Research Society Symposium Proceedings, Boston, MA, November 26-29, 1990.* Eds. T.A. Abrajano, Jr. and L.H. Johnson. Pittsburgh, PA: Materials Research Society. Vol. 212, 295-302.

Greco, E.C., and W.B. Wright. 1962. "Corrosion of Iron in an $H_2S$-$CO_2$-$H_2O$ System," *Corrosion.* Vol. 18, no. 3, 119t-124t.

Gudas, J.P., and H.P. Hack. 1979. "Sulfide Induced Corrosion of Copper Nickel Alloys," *Corrosion.* Vol. 35, no. 2, 67-73.

Guzowski, R.V. 1990. *Preliminary Identification of Scenarios That May Affect the Escape and Transport of Radionuclides from the Waste Isolation Pilot Plant, Southeastern New Mexico.* SAND89-7149. Albuquerque, NM: Sandia National Laboratories.

Haberman, J.H., and D.J. Frydrych. 1988. "Corrosion Studies of A216 Grade WCA Steel in Hydrothermal Magnesium-Containing Brines," *Scientific Basis for Nuclear Waste Management XI, Materials Research Society Symposium Proceedings, Boston, MA, November 30-December 3, 1987.* Eds. M.J. Apted and R.E. Westerman. Pittsburgh, PA: Materials Research Society. Vol. 112, 761-772.

Hausler, R.H. 1983. "Laboratory Investigations of the $CO_2$ Corrosion Mechanism as Applied to Hot Deep Gas Wells," *Corrosion '83, International Corrosion Forum, Anaheim, CA, April 18-22, 1983.* Paper no. 47. Houston, TX: National Association of Corrosion Engineers.

Hausler, R.H., and D.W. Stegmann. 1988. "$CO_2$ Corrosion and Its Prevention by Chemical Inhibition in Oil and Gas Production," *Corrosion '88, National Association of Corrosion Engineers Meeting, St. Louis, MO, March 21-25, 1988.* Houston, TX: National Association of Corrosion Engineers.

Hudgins, C.M., Jr., and R.L. McGlasson. 1981. "The Effect of Temperature (75°F-400°F) on the Aqueous Sulfide Stress Cracking Behavior of an N-80 Type Steel," *$H_2S$ Corrosion in Oil and Gas Production—A Compilation of Classic Papers.* Eds. R.N. Tuttle and R.D. Kane. Houston, TX: National Association of Corrosion Engineers. 90-94.

Ikeda, A., M. Ueda, and S. Mukai. 1983. "$CO_2$ Corrosion Behavior and Mechanism of Carbon Steel and Alloy Steel," *Corrosion '83, Anaheim, CA, April 18-22, 1983.* Paper no. 45. Houston, TX: National Association of Corrosion Engineers.

Ikeda, A., S. Mukai, and M. Ueda. 1984. "Prevention of $CO_2$ Corrosion of Line Pipe and Oil Country Tubular Goods," *Corrosion '84, New Orleans, LA, April 2-6, 1984.* Paper no. 289. Houston, TX: National Association of Corrosion Engineers.

Jones, D.A. 1992. *Principles and Prevention of Corrosion.* New York, NY: Macmillan Publishing Company. 523.

Kato, C., H.W. Pickering, and J.E. Castle. 1984. "Effect of Sulfide on the Corrosion of Cu-9.4Ni-1.7Fe Alloy in Aqueous NaCl Solution," *Journal of the Electrochemical Society.* Vol. 131, no. 6, 1225-1229.

Lange's Handbook. 1985. *Lange's Handbook of Chemistry.* 13th ed. Ed. J.A. Dean. New York, NY: McGraw-Hill. 11-21.

Lappin, A.R., R.L. Hunter, D.P. Garber, and P.B. Davies, eds. 1989. *Systems Analysis, Long-Term Radionuclide Transport, and Dose Assessments, Waste Isolation Pilot Plant (WIPP), Southeastern New Mexico; March 1989.* SAND89-0462. Albuquerque, NM: Sandia National Laboratories.

Macdonald, D.D., B.C. Syrett, and S.S. Wing. 1979. "The Corrosion of Cu-Ni Alloys 706 and 715 in Flowing Sea Water. II - Effect of Dissolved Sulfide," *Corrosion.* Vol. 35, no. 8, 367-378.

Masamura, K., S. Hashizume, K. Nunomura, J. Saki, and I. Matsushima. 1983. "Corrosion of Carbon and Alloy Steels in Aqueous $CO_2$ Environment," *Corrosion '83, Anaheim, CA, April 18-22, 1983.* Paper no. 19. Houston, TX: National Association of Corrosion Engineers.

Meyer, F.H., O.L. Riggs, R.L. McGlasson, and J.D. Sudbury. 1958. "Corrosion Products of Mild Steel in Hydrogen Sulfide Environments," *Corrosion.* Vol. 14, no. 2, 109t-115t.

Milton, C. 1966. "'Kansite'=Mackinawite, FeS (Technical Note)," *Corrosion.* Vol. 22, no. 7, 191-193.

Molecke, M.A. 1983. *A Comparison of Brines Relevant to Nuclear Waste Experimentation.* SAND83-0516. Albuquerque, NM: Sandia National Laboratories.

Molecke, M.A., J.A. Ruppen, and R.B. Diegle. 1983. "Materials for High-Level Waste Canister/ Overpacks in Salt Formations," *Nuclear Technology.* Vol. 63, no. 3, 476-510.

Murata, T., E. Sato, and R. Matsuhashi. 1983. "Factors Controlling Corrosion of Steels in $CO_2$— Saturated Environments," *Advances in $CO_2$ Corrosion in the Oil and Gas Industry, Proceedings of the Corrosion/83 Symposium, Anaheim, CA, April 18-19, 1983.* Ed. R.H. Hausler. Houston, TX: National Association of Corrosion Engineers. Vol. 1, 64-71.

National Association of Corrosion Engineers. 1976. *Laboratory Corrosion Testing of Metals for the Process Industries.* TM-01-69. Houston, TX: National Association of Corrosion Engineers.

Popplewell, J.M. 1980. "The Effect of Sulfides on the Corrosion Resistance of Copper Base Alloys in Salt Water," *Corrosion '80, International Corrosion Forum Devoted Exclusively to the Protection and Performance of Materials, Chicago, IL, March 3-7, 1980.* Paper No. 180. Houston, TX: National Association of Corrosion Engineers.

Reinhart, F.M., and J.F. Jenkins. 1972. *Corrosion of Materials in Surface Seawater After 12 and 18 Months of Exposure, Final Report.* NCEL-TN-1213. Port Hueneme, CA: US Naval Civil Engineering Laboratory.

Rhodes, F.H., and J.M. Clark, Jr. 1936. "Corrosion of Metals by Water and Carbon Dioxide Under Pressure," *Industrial Engineering Chemistry.* Vol. 28, 1078-1079.

Rossini, F.D., D.D. Wagman, W.H. Evans, S. Levine, and I. Jaffe. 1952. *Selected Values of Chemical Thermodynamic Properties.* National Bureau of Standards Circular 500. Washington, DC: US Government Printing Office.

Sardisco, J.B., and R.E. Pitts. 1965. "Corrosion of Iron in an $H_2S$-$CO_2$-$H_2O$ System—Mechanism of Sulfide Film Formation and Kinetics of Corrosion Reaction," *Corrosion.* Vol. 21, no. 8, 245-253.

Sardisco, J.B., W.B. Wright, and E.C. Greco. 1963. "Corrosion of Iron in an $H_2O$-$CO_2$-$H_2O$ System: Corrosion Film Properties on Pure Iron," *Corrosion.* Vol. 19, no. 10, 354t-359t.

Schmitt, G. 1983a. "Fundamental Aspects of $CO_2$ Corrosion," *Advances in $CO_2$ Corrosion in the Oil and Gas Industry, Proceedings of the Corrosion/83 Symposium, Anaheim, CA, April 18-19, 1983.* Ed. R.H. Hausler. Houston, TX: National Association of Corrosion Engineers. Vol. 1, 10-19.

Schmitt, G. 1983b. "$CO_2$ Corrosion of Steels—An Attempt to Range Parameters and Their Effects," *Advances in $CO_2$ Corrosion in the Oil and Gas Industry, Proceedings of the Corrosion/83 Symposium, Anaheim, CA, April 18-19, 1983.* Ed. R.H. Hausler. Houston, TX: National Association of Corrosion Engineers. Vol. 1, 1-2.

Schutz, R.W. 1986. "Titanium," *Process Industries Corrosion—The Theory and Practice, International Process Industries Corrosion Seminar, New Orleans, LA, 1986.* Eds. B.M. Moniz and W.I. Pollock. Houston, TX: National Association of Corrosion Engineers. 503-527.

Schweitzer, P.A. 1986. *Corrosion Resistance Tables.* New York, NY: Marcel Dekker, Inc. 256.

Seki, N., T. Kotera, T. Nakasawa, Y. Kobayashi, and T. Taira. 1982. "The Evaluation of Environmental Conditions and the Performance of Linepipe Steels Under Wet Sour Gas," *Corrosion '82, International Corrosion Forum, Houston, TX, March 22-26, 1982.* Paper no. 131. Houston, TX: National Association of Corrosion Engineers.

Silman, J.F.B. 1958. "The Stabilities of Some Oxidized Copper Minerals in Aqueous Solutions at 25°C and 1 Atmosphere Total Pressure." Ph.D. dissertation. Cambridge, MA: Harvard University.

Simpson, J.P., and R. Schenk. 1987. "Hydrogen Evolution from Corrosion of Pure Copper," *Corrosion Science.* Vol. 27, no. 12, 1365-1370.

Simpson, J.P., and R. Schenk. 1989. "Corrosion Induced Hydrogen Evolution on High Level Waste Overpack Materials in Synthetic Groundwaters and Chloride Solutions," *Scientific Basis for Nuclear Waste Management XII, Materials Research Society Symposium Proceedings, Berlin, Germany, October 10-13, 1988.* Eds. W. Lutze and R.C. Ewing. Pittsburgh, PA: Materials Research Society. Vol. 127, 389-396.

Soo, P., ed. 1983. *Review of DOE Waste Package Program—Subtask 1.1, National Waste Package Program, April-September 1982.* NUREG/CR-2482, BNL-NUREG-51494. Upton, NY: Department of Nuclear Energy, Brookhaven National Laboratory. Vol. 3, 89.

Southwell, C.R., and A.L. Alexander. 1969. "Corrosion of Structural Ferrous Metals in Tropical Environments—Sixteen Years' Exposure to Sea and Fresh Water," *Proceedings of the 24th Conference, National Association of Corrosion Engineers, Cleveland, OH, March 18-22, 1968.* Houston, TX: National Association of Corrosion Engineers. 685-695.

Syrett, B.C. 1977. "Accelerated Corrosion of Copper in Flowing Pure Water Contaminated with Oxygen and Sulfide," *Corrosion.* Vol. 33, no. 7, 257-262.

Tapping, R.L., P.A. Lavoie, and R.D. Davidson. 1983. "Effect of $H_2S$ Neutralization Methods on Sulfide Films in Heavy Water Plants," *Corrosion '83, Anaheim, CA, April 18-22, 1983.* Paper no. 11. Houston, TX: National Association of Corrosion Engineers.

Tewari, P.H., M.G. Bailey, and A.B. Campbell. 1979. "The Erosion-Corrosion of Carbon Steel in Aqueous $H_2S$ Solutions Up to 120°C and 1.6 MPa Pressure," *Corrosion Science.* Vol. 19, no. 8, 573-585.

Thomason, W.H. 1978. "Formation Rates of Protective Iron Sulfide Films on Mild Steel in $H_2S$-Saturated Brine as a Function of Temperature," *Corrosion '78, Houston, TX, March 6-10, 1978.* Paper no. 41. Houston, TX: National Association of Corrosion Engineers.

Turkdogan, E.T. 1980. *Physical Chemistry of High Temperature Technology.* New York, NY: Academic Press.

Videm, K., and A. Dugstad. 1987. "Effect of Flow Rate, PH, $Fe^{2+}$ Concentration and Steel Quality on the $CO_2$ Corrosion of Carbon Steels," *Corrosion '87, Corrosion Control and Monitoring in Gas Pipelines and Well Systems, Calgary, Alberta, Canada, March 9-10, 1987.* Houston, TX: National Association of Corrosion Engineers. 53-64.

Vreeland, D.C. 1976. "Review of Corrosion Experience with Copper-Nickel Alloys in Sea Water Piping Systems," *Materials Performance.* Vol. 15, no. 10, 38-41.

Westerman, R.E. 1988. "Evaluation of the Corrosion Behavior of Nickel- and Copper-Base Alloys in High-Magnesium Brine," *Joint U.S. DOE/FRG Workshop on Nuclear Package Materials, Albuquerque, NM, March 9, 1988.* PNL/SRP-SA-15685. Richland, WA: Pacific Northwest Laboratory.

Westerman, R.E., J.H. Haberman, S.G. Pitman, K.H. Pool, K.C. Rhoads, and M.R. Telander. 1987. *Corrosion Behavior of A216 Grade WCA Mild Steel and Ti Grade 12 Alloy in Hydrothermal Brines, Salt Repository Project: Annual Report, FY 1986.* PNL-SRP-6221. Richland, WA: Pacific Northwest Laboratory.

Wikjord, A.G., T.E. Rummery, F.E. Doern, and D.G. Owen. 1980. "Corrosion and Deposition During the Exposure of Carbon Steel to Hydrogen Sulfide-Water Solutions," *Corrosion Science.* Vol. 20, 651-671.

# APPENDIX A: PRESSURE HISTORIES, ANOXIC BRINE (BRINE /$N_2$) AND BRINE/$CO_2$ SEAL-WELDED CONTAINER TESTS


Table A-1: 3-Month Tests
Table A-2: 6-Month Tests
Table A-3: 12 Month Tests
Table A-4: 24-Month Tests
Table A-5: Controlled-$CO_2$-Addition Tests (through 309 days test time)

## APPENDIX A. TABLE A-1
## Pressure History, 3-Month Seal-Welded Container Tests

Summary of Container Environments:

Containers 1 and 2: Immersed Specimens, N2 Overpressure
Containers 3 and 4: Immersed Specimens, CO2 Overpressure
Containers 5 and 6: Vapor-Phase Exposure, N2 Overpressure
Containers 7 and 8: Vapor-Phase Exposure, CO2 Overpressure

| | Pressure in Container, psig | | | | | | | |
|---|---|---|---|---|---|---|---|---|
| Time, days | Cont. 1 | Cont. 2 | Cont. 3 | Cont. 4 | Cont. 5 | Cont. 6 | Cont. 7 | Cont. 8 |
| 0 | 138 | 137 | 157 | 175 | 138 | 138 | 149 | 148 |
| 1 | 138 | 138 | 164 | 170 | 138 | 139 | 149 | 147 |
| 5 | 139 | 139 | 167 | 165 | 138 | 138 | 148 | 147 |
| 6 | 139 | 139 | 168 | 166 | 138 | 139 | 148 | 147 |
| 7 | 139 | 140 | 171 | 167 | 138 | 139 | 148 | 147 |
| 8 | 139 | 139 | 171 | 167 | 138 | 138 | 148 | 147 |
| 12 | 140 | 140 | 175 | 173 | 138 | 139 | 148 | 147 |
| 20 | 141 | 142 | 180 | 178 | 138 | 139 | 148 | 147 |
| 27 | 142 | 142 | 183 | 182 | 138 | 138 | 148 | 147 |
| 40 | 145 | 146 | 186 | 186 | 139 | 139 | 149 | 147 |
| 48 | 147 | 148 | 189 | 188 | 140 | 139 | 148 | 148 |
| 55 | 147 | 147 | 191 | 190 | 140 | 139 | 148 | 148 |
| 62 | 149 | 150 | 192 | 192 | 140 | 139 | 148 | 148 |
| 69 | 150 | 150 | 193 | 192 | 140 | 139 | 148 | 148 |
| 83 | 153 | 153 | 198 | 198 | 140 | 140 | 149 | 149 |
| 90 | 155 | 154 | 198 | 198 | 140 | 139 | 148 | 148 |

## APPENDIX A. TABLE A-2
## Pressure History, 6-Month Seal-Welded Container Tests

Summary of Container Environments:

Containers 9 and 10: Immersed Specimens, N2 Overpressure
Containers 11 and 12: Immersed Specimens, CO2 Overpressure
Containers 13 and 14: Vapor-Phase Exposure, N2 Overpressure
Containers 15 and 15: Vapor-Phase Exposure, CO2 Overpressure

| | Pressure in Container, psig | | | | | | | |
|---|---|---|---|---|---|---|---|---|
| Time, days | Cont. 9 | Cont. 10 | Cont. 11 | Cont. 12 | Cont. 13 | Cont. 14 | Cont. 15 | Cont. 16 |
| 0 | 138 | 138 | 183 | 179 | 136 | 135 | 131 | 131 |
| 1 | 139 | 139 | 192 | 170 | --- | --- | --- | --- |
| 4 | 139 | 139 | 160 | 164 | 137 | 137 | 130 | 130 |
| 5 | 140 | 140 | 160 | 165 | 137 | 137 | 130 | 130 |
| 6 | 140 | 140 | 162 | 167 | 136 | 136 | 130 | 130 |
| 7 | 140 | 140 | 165 | 168 | 136 | 136 | 130 | 130 |
| 8 | 140 | 140 | 167 | 169 | 136 | 136 | 130 | 130 |
| 11 | 140 | 141 | 171 | 173 | 137 | 136 | 130 | 130 |
| 18 | 142 | 141 | 179 | 178 | 137 | 136 | 130 | 130 |
| 25 | 143 | 143 | 185 | 183 | 137 | 136 | 130 | 130 |
| 32 | 144 | 144 | 190 | 187 | 137 | 136 | 130 | 130 |
| 39 | 145 | 145 | 194 | 192 | 137 | 135 | 130 | 130 |
| 46 | 147 | 146 | 199 | 197 | 137 | 136 | 131 | 131 |
| 53 | 148 | 147 | 201 | 200 | 137 | 136 | 131 | 132 |
| 60 | 149 | 149 | 204 | 200 | 137 | 136 | 131 | 132 |
| 67 | 150 | 149 | 206 | 201 | 137 | 136 | 131 | 131 |
| 74 | 152 | 151 | 206 | 201 | 137 | 136 | 131 | 131 |
| 81 | 153 | 152 | 210 | 204 | 137 | 136 | 131 | 132 |
| 88 | 155 | 154 | 212 | 204 | 137 | 136 | 131 | 132 |
| 95 | 157 | 156 | 212 | 204 | 138 | 136 | 131 | 132 |
| 102 | 158 | 157 | 214 | 204 | 137 | 136 | 131 | 132 |
| 109 | 160 | 159 | 215 | 206 | 137 | 136 | 131 | 132 |
| 116 | 161 | 160 | 215 | 206 | 137 | 136 | 131 | 132 |
| 123 | 163 | 162 | 215 | 206 | 137 | 136 | 131 | 132 |
| 130 | 165 | 164 | 216 | 206 | 137 | 136 | 131 | 132 |
| 137 | 167 | 166 | 216 | 206 | 137 | 136 | 131 | 132 |
| 144 | 168 | 167 | 216 | 206 | 137 | 136 | 131 | 132 |
| 151 | 170 | 168 | 216 | 206 | 138 | 136 | 131 | 132 |
| 158 | 171 | 169 | 216 | 206 | 138 | 136 | 131 | 132 |
| 168 | 173 | 172 | 216 | 206 | 138 | 136 | 131 | 132 |
| 172 | 174 | 173 | 217 | 207 | 138 | 136 | 131 | 132 |
| 179 | 176 | 174 | 217 | 207 | 138 | 135 | 131 | 132 |
| 183 | 176 | 174 | 217 | 207 | --- | --- | --- | --- |

## APPENDIX A, TABLE A-3
## Pressure History, 12-Month Seal-Welded Container Tests

Summary of Container Environments:
Containers 17 and 18: Immersed Specimens, N2 Overpressure
Containers 19 and 20: Immersed Specimens, CO2 Overpressure
Containers 21 and 22: Vapor-Phase Exposure, N2 Overpressure
Containers 23 and 24: Vapor-Phase Exposure, CO2 Overpressure

| | Pressure in Container, psig | | | | | Pressure in Container, psig | | | |
|---|---|---|---|---|---|---|---|---|---|
| Time, days | Cont. 17 | Cont. 18 | Cont. 19 | Cont. 20 | Time, days | Cont. 21 | Cont. 22 | Cont. 23 | Cont. 24 |
| 0 | 134 | 134 | 191 | 187 | 0 | 137 | 137 | 135 | 135 |
| 3 | 139 | 138 | 158 | 158 | 7 | 141 | 141 | 134 | 135 |
| 5 | 141 | 140 | 163 | 164 | 13 | 141 | 141 | 134 | 135 |
| 10 | 141 | 141 | 172 | 173 | 20 | 141 | 141 | 134 | 135 |
| 18 | 142 | 142 | 178 | 181 | 27 | 141 | 141 | 134 | 135 |
| 24 | 143 | 143 | 182 | 186 | 34 | 141 | 141 | 134 | 135 |
| 31 | 144 | 144 | 187 | 190 | 41 | 141 | 141 | 134 | 135 |
| 38 | 145 | 145 | 190 | 194 | 46 | 141 | 141 | 134 | 135 |
| 45 | 146 | 146 | 193 | 197 | 53 | 141 | 141 | 133 | 134 |
| 52 | 147 | 147 | 194 | 198 | 60 | 141 | 141 | 133 | 134 |
| 57 | 148 | 148 | 196 | 200 | 67 | 141 | 141 | 133 | 134 |
| 64 | 149 | 149 | 197 | 200 | 74 | 141 | 141 | 133 | 134 |
| 71 | 150 | 150 | 198 | 200 | 81 | 141 | 141 | 133 | 134 |
| 78 | 151 | 151 | 198 | 200 | 88 | 141 | 141 | 133 | 134 |
| 85 | 153 | 153 | 198 | 200 | 95 | 141 | 141 | 133 | 134 |
| 92 | 154 | 154 | 200 | 205 | 102 | 141 | 141 | 133 | 134 |
| 99 | 156 | 156 | 200 | 207 | 109 | 141 | 141 | 133 | 134 |
| 106 | 157 | 157 | 200 | 207 | 119 | 141 | 141 | 133 | 134 |
| 113 | 158 | 158 | 200 | 208 | 123 | 141 | 141 | 133 | 134 |
| 120 | 160 | 160 | 201 | 209 | 130 | 141 | 141 | 133 | 134 |
| 130 | 162 | 162 | 201 | 209 | 137 | 141 | 141 | 133 | 133 |
| 134 | 162 | 163 | 201 | 209 | 144 | 141 | 141 | 133 | 133 |
| 141 | 163 | 164 | 201 | 209 | 151 | 141 | 141 | 133 | 133 |
| 148 | 164 | 164 | 201 | 209 | 159 | 141 | 141 | 133 | 133 |
| 165 | 165 | 201 | 209 | 165 | 141 | 141 | 133 | 133 | |
| 162 | 167 | 167 | 201 | 209 | 173 | 141 | 141 | 132 | 133 |
| 170 | 167 | 168 | 200 | 207 | 179 | 141 | 141 | 132 | 133 |
| 176 | 168 | 169 | 200 | 206 | 186 | 141 | 141 | 132 | 133 |
| 184 | 170 | 170 | 200 | 206 | 200 | 141 | 141 | 132 | 133 |
| 190 | 170 | 171 | 200 | 206 | 207 | 141 | 141 | 132 | 133 |
| 197 | 172 | 173 | 200 | 206 | 214 | 141 | 141 | 132 | 133 |
| 211 | 173 | 174 | 200 | 206 | 221 | 141 | 141 | 132 | 133 |
| 218 | 174 | 175 | 200 | 206 | 228 | 141 | 141 | 132 | 133 |
| 225 | 175 | 176 | 200 | 206 | 235 | 141 | 141 | 132 | 133 |
| 232 | 175 | 176 | 200 | 206 | 242 | 141 | 141 | 132 | 133 |

APPENDIX A. TABLE A-3
Pressure History, 12-Month Seal-Welded Container Tests (cont'd)

| | Pressure in Container, psig | | | | | Pressure in Container, psig | | | |
|---|---|---|---|---|---|---|---|---|---|
| Time, days | Cont. 17 | Cont. 18 | Cont. 19 | Cont. 20 | Time, days | Cont. 21 | Cont. 22 | Cont. 23 | Cont. 24 |
| 239 | 176 | 177 | 200 | 206 | 249 | 140 | 140 | 132 | 133 |
| 246 | 177 | 178 | 200 | 206 | 256 | 140 | 140 | 132 | 133 |
| 253 | 178 | 179 | 200 | 206 | 263 | 140 | 140 | 132 | 133 |
| 260 | 179 | 180 | 200 | 206 | 270 | 140 | 140 | 132 | 133 |
| 267 | 180 | 181 | 200 | 206 | 277 | 140 | 140 | 132 | 133 |
| 274 | 181 | 182 | 200 | 206 | 284 | 140 | 140 | 132 | 133 |
| 282 | 182 | 183 | 200 | 206 | 291 | 140 | 140 | 132 | 133 |
| 288 | 183 | 184 | 200 | 206 | 298 | 140 | 140 | 132 | 133 |
| 295 | 183 | 184 | 200 | 206 | 305 | 140 | 140 | 132 | 133 |
| 302 | 184 | 185 | 200 | 206 | 312 | 140 | 140 | 132 | 133 |
| 309 | 185 | 186 | 200 | 206 | 319 | 140 | 140 | 132 | 133 |
| 316 | 186 | 187 | 200 | 206 | 326 | 140 | 140 | 132 | 133 |
| 323 | 187 | 188 | 200 | 206 | 333 | 140 | 141 | 132 | 133 |
| 330 | 187 | 189 | 200 | 206 | 340 | 140 | 141 | 132 | 133 |
| 337 | 188 | 190 | 200 | 206 | 347 | 140 | 140 | 132 | 133 |
| 344 | 189 | 191 | 200 | 206 | 354 | 140 | 140 | 132 | 133 |
| 351 | 190 | 192 | 200 | 206 | | | | | |
| 358 | 191 | 192 | 200 | 206 | | | | | |
| 365 | 192 | 193 | 200 | 206 | | | | | |

## APPENDIX A, TABLE A-4
## Pressure History, 24-Month Seal-Welded Container Tests

Summary of Container Environments:

Containers 25 and 26 Immersed Specimens, N2 Overpressure
Containers 27 and 28: Immersed Specimens, CO2 Overpressure
Containers 29 and 30: Vapor-Phase Exposure, N2 Overpressure
Containers 31 and 32: Vapor-Phase Exposure, CO2 Overpressure

| | Pressure in Container, psig | | | | | Pressure in Container, psig | | | |
|---|---|---|---|---|---|---|---|---|---|
| Time, days | Cont. 25 | Cont. 26 | Cont. 27 | Cont. 28 | Time, days | Cont. 29 | Cont. 30 | Cont. 31 | Cont. 32 |
| 0 | 137 | 135 | 178(a) | 180(a) | 0 | 136 | 136 | 135 | 135 |
| 5 | 142 | 141 | 166 | 164 | 3 | 140 | 140 | 135 | 135 |
| 12 | 143 | 142 | 176 | 175 | 10 | 141 | 141 | 135 | 136 |
| 19 | 144 | 143 | 181 | 180 | 17 | 141 | 141 | 135 | 135 |
| 26 | 146 | 144 | 186 | 184 | 24 | 141 | 141 | 135 | 135 |
| 33 | 147 | 145 | 190 | 188 | 31 | 141 | 141 | 135 | 135 |
| 40 | 148 | 146 | 192 | 191 | 38 | 141 | 141 | 135 | 135 |
| 54 | 151 | 148 | 197 | 197 | 52 | 141 | 141 | 135 | 135 |
| 68 | 153 | 150 | 200 | 199 | 66 | 141 | 141 | 135 | 135 |
| 85 | 157 | 154 | 201 | 202 | 83 | 141 | 141 | 135 | 135 |
| 96 | 160 | 156 | 202 | 203 | 94 | 141 | 141 | 135 | 135 |
| 110 | 163 | 159 | 202 | 203 | 108 | 141 | 141 | 135 | 134 |
| 125 | 167 | 162 | 202 | 204 | 123 | 141 | 141 | 134 | 134 |
| 139 | 169 | 164 | 202 | 204 | 137 | 141 | 141 | 134 | 134 |
| 152 | 172 | 167 | 202 | 204 | 150 | 141 | 141 | 135 | 134 |
| 173 | 175 | 170 | 202 | 204 | 171 | 141 | 141 | 134 | 134 |
| 194 | 178 | 173 | 202 | 204 | 192 | 141 | 141 | 134 | 134 |
| 215 | 181 | 176 | 202 | 204 | 213 | 141 | 140 | 134 | 134 |
| 236 | 184 | 180 | 202 | 204 | 234 | 141 | 140 | 134 | 134 |
| 257 | 188 | 182 | 202 | 204 | 255 | 141 | 140 | 134 | 134 |
| 278 | 191 | 185 | 202 | 204 | 276 | 141 | 140 | 134 | 134 |
| 299 | 195 | 188 | 202 | 204 | 297 | 141 | 140 | 134 | 134 |
| 320 | 197 | 192 | 202 | 204 | 318 | 142 | 141 | 134 | 134 |
| 338 | 200 | 194 | (pressure before venting containers 25 and 26) | | | | | | |
| 338 | 166 | 165 | (pressure after venting containers 25 and 26) | | | | | | |
| 341 | 168 | 167 | 202 | 204 | 339 | 142 | 140 | 134 | 134 |
| 362 | 170 | 169 | 202 | 204 | 360 | 142 | 140 | 134 | 134 |
| 383 | 172 | 172 | 202 | 204 | 381 | 142 | 140 | 134 | 134 |
| 404 | 175 | 174 | 202 | 204 | 402 | 141 | 140 | 134 | 134 |
| 425 | 177 | 176 | 202 | 204 | 423 | 142 | 140 | 134 | 134 |

(a) 155 psig can be used as the hypothetical starting pressure for these tests.

APPENDIX A, TABLE A-4
Pressure History, 24-Month Seal-Welded Container Tests (cont'd)

| | Pressure in Container, psig | | | | | Pressure in Container, psig | | | |
|---|---|---|---|---|---|---|---|---|---|
| Time, days | Cont. 25 | Cont. 26 | Cont. 27 | Cont. 28 | Time, days | Cont. 29 | Cont. 30 | Cont. 31 | Cont. 32 |
| 446 | 180 | 179 | 202 | 204 | 444 | 142 | 140 | 134 | 134 |
| 467 | 182 | 181 | 202 | 204 | 465 | 142 | 140 | 134 | 134 |
| 488 | 184 | 183 | 202 | 204 | 486 | 142 | 140 | 134 | 134 |
| 502 | 186 | 184 | 202 | 204 | 500 | 142 | 140 | 133 | 134 |
| 523 | 188 | 186 | 202 | 204 | 521 | 142 | 140 | 133 | 134 |
| 551 | 190 | 188 | 202 | 204 | 549 | 142 | 140 | 133 | 134 |
| 572 | 192 | 190 | 202 | 204 | 570 | 142 | 140 | 133 | 134 |
| 593 | 194 | 193 | 202 | 204 | 591 | 142 | 140 | 133 | 134 |
| 614 | 195 | 194 | 202 | 204 | 612 | 142 | 140 | 133 | 134 |
| 635 | 198 | 197 | 203 | 205 | 633 | 142 | 140 | 133 | 134 |
| 656 | 199 | 198 | 203 | 205 | 654 | 141 | 140 | 133 | 134 |
| 677 | 201 | 200 | 203 | 205 | 675 | 142 | 140 | 133 | 134 |
| 698 | 203 | 202 | 203 | 205 | 696 | 141 | 140 | 133 | 134 |
| 719 | 204 | 203 | 202 | 204 | 717 | 141 | 140 | 133 | 133 |
| 728 | 206 | 204 | 203 | 205 | 726 | 141 | 140 | 133 | 134 |

## APPENDIX A, TABLE A-5
## Pressure History, Controlled-$CO_2$ Addition Seal-Welded Container Tests

Summary of Container Environments:

All specimens are completely immersed in Brine A in each container
Container 33: 0.32 mol $CO_2$/m2 steel
Container 34: 0.16 mol $CO_2$/m2 steel
Container 35: 0.063 mol $CO_2$/m2 steel
Container 36: 0.032 mol $CO_2$/m2 steel + $N_2$
Container 37: 0.016 mol $CO_2$/m2 steel + $N_2$
Container 38: 0.00 mol $CO_2$/m2 steel ($N_2$ only)

| | Pressure in Container, psig | | | | Pressure in Container, psig | | |
|---|---|---|---|---|---|---|---|
| Time, days | Cont. 33 | Cont. 34 | Cont. 35 | Time, days | Cont. 36 | Cont. 37 | Cont. 38 |
| 0 | 59 | 21 | -2 (est.) | 0 | 22 | 19 | 31 |
| 8 | 69 | 30 | 0 | 6 | 25 | 20 | 34 |
| 14 | 73 | 33 | 4 | 12 | 27 | 21 | 34 |
| 22 | 77 | 37 | 6 | 20 | 28 | 23 | 35 |
| 29 | 80 | 38 | 8 | 27 | 30 | 24 | 36 |
| 36 | 82 | 40 | 10 | 34 | 31 | 25 | 37 |
| 43 | 84 | 42 | 10 | 41 | 31 | 26 | 38 |
| 50 | 85 | 43 | 10 | 48 | 32 | 27 | 39 |
| 71 | 88 | 44 | 12 | 69 | 34 | 30 | 42 |
| 85 | 89 | 45 | 13 | 83 | 34 | 31 | 44 |
| 99 | 90 | 46 | 14 | 97 | 36 | 34 | 46 |
| 113 | 92 | 46 | 15 | 111 | 38 | 35 | 49 |
| 127 | 93 | 46 | 17 | 125 | 41 | 39 | 52 |
| 141 | 94 | 47 | 19 | 139 | 44 | 41 | 56 |
| 155 | 94 | 47 | 21 | 153 | 46 | 43 | 58 |
| 162 | 94 | 47 | 22 | 160 | 48 | 44 | 60 |
| 176 | 94 | 48 | 24 | 174 | 51 | 47 | 63 |
| 190 | 94 | 48 | 26 | 188 | 53 | 50 | 65 |
| 212 | 95 | 48 | 30 | 210 | 57 | 53 | 70 |
| 225 | 95 | 49 | 32 | 223 | 60 | 56 | 72 |
| 239 | 95 | 49 | 34 | 237 | 62 | 58 | 75 |
| 253 | 96 | 49 | 36 | 251 | 64 | 61 | 79 |
| 267 | 95 | 50 | 38 | 265 | 67 | 63 | 81 |
| 281 | 95 | 50 | 40 | 279 | 69 | 65 | 83 |
| 295 | 95 | 50 | 42 | 293 | 72 | 67 | 86 |
| 309 | 95 | 50 | 44 | 307 | 74 | 70 | 88 |

# APPENDIX B-1: INDIVIDUAL SPECIMEN CORROSION-RATE DATA, ANOXIC BRINE ($N_2$/IMMERSED) ENVIRONMENT, SEAL-WELDED-CONTAINER TEST METHOD

## APPENDIX B-1
## Individual Specimen Data, Seal-Welded Container Test No. 1

Test No.: 1
Test Type: Immersion
Test Environment: Simulated WIPP Brine A, N2 Overpressure (10 atm)
Test Temperature: 30 ±5°C
Test Exposure: 3 Months

| Specimen | Material Type | Length, mm | Width, mm | Thickness, mm | Top Hole ID, mm | Bot. Hole ID, mm | Area, dm2 | Initial Wt., g | Final Wt., g | Corrosion Rate, mpy | Corrosion Rate, µm/yr |
|---|---|---|---|---|---|---|---|---|---|---|---|
| J1 | Low-Carbon Steel, Lot J | 190.81 | 86.46 | 0.695 | 8.00 | 8.00 | 3.321 | 87.6936 | 87.5674 | 0.072 | 1.834 |
| J2 | Low-Carbon Steel, Lot J | 190.70 | 86.41 | 0.704 | 8.00 | 8.00 | 3.318 | 89.1819 | 89.0488 | 0.076 | 1.936 |
| J3 | Low-Carbon Steel, Lot J | 191.42 | 86.51 | 0.689 | 7.99 | 7.99 | 3.334 | 88.0226 | 87.8895 | 0.076 | 1.927 |
| J201 | Low-Carbon Steel, Lot J | 190.63 | 51.43 | 0.712 | 7.99 | 8.00 | 1.979 | 52.7773 | 52.7083 | 0.066 | 1.683 |
| J202 | Low-Carbon Steel, Lot J | 190.76 | 51.36 | 0.711 | 8.06 | 7.99 | 1.977 | 52.7223 | 52.6498 | 0.070 | 1.770 |
| J203 | Low-Carbon Steel, Lot J | 190.72 | 51.44 | 0.712 | 8.02 | 8.06 | 1.980 | 52.7432 | SA* | SA | SA |
| K1 | Low-Carbon Steel, Lot K | 190.63 | 86.26 | 0.878 | 7.96 | 7.97 | 3.322 | 110.9676 | 110.8360 | 0.075 | 1.912 |
| K2 | Low-Carbon Steel, Lot K | 190.76 | 86.42 | 0.884 | 7.99 | 7.96 | 3.331 | 111.6249 | 111.4954 | 0.074 | 1.876 |
| K3 | Low-Carbon Steel, Lot K | 190.46 | 86.34 | 0.882 | 7.96 | 7.96 | 3.322 | 111.2495 | 111.1130 | 0.078 | 1.983 |
| K201 | Low-Carbon Steel, Lot K | 190.36 | 51.33 | 0.877 | 7.97 | 7.97 | 1.981 | 64.9559 | 64.8842 | 0.069 | 1.747 |
| K202 | Low-Carbon Steel, Lot K | 190.30 | 51.39 | 0.874 | 7.98 | 7.98 | 1.983 | 65.0662 | 64.9946 | 0.069 | 1.743 |
| K203 | Low-Carbon Steel, Lot K | 190.31 | 51.49 | 0.879 | 7.98 | 7.98 | 1.987 | 65.6125 | SA | SA | SA |
| L1 | Low-Carbon Steel, Lot L | 190.83 | 86.32 | 1.536 | 7.94 | 7.94 | 3.367 | 195.4656 | 195.3277 | 0.078 | 1.976 |
| L2 | Low-Carbon Steel, Lot L | 190.86 | 86.47 | 1.549 | 7.94 | 7.93 | 3.375 | 196.6869 | 196.5469 | 0.079 | 2.002 |
| L3 | Low-Carbon Steel, Lot L | 190.82 | 86.37 | 1.545 | 7.95 | 7.94 | 3.370 | 196.8227 | 196.6862 | 0.077 | 1.955 |
| L201 | Low-Carbon Steel, Lot L | 190.84 | 51.36 | 1.537 | 7.96 | 7.95 | 2.023 | 115.3703 | 115.2924 | 0.073 | 1.859 |
| L202 | Low-Carbon Steel, Lot L | 190.98 | 51.44 | 1.506 | 7.95 | 7.95 | 2.025 | 112.5495 | 112.4681 | 0.076 | 1.939 |
| L203 | Low-Carbon Steel, Lot L | 190.96 | 51.43 | 1.508 | 7.96 | 7.95 | 2.025 | 112.0076 | SA | SA | SA |
| M1 | Low-Carbon Steel, Lot M | 189.75 | 83.66 | 1.605 | 7.96 | 7.96 | 3.251 | 197.7103 | 197.5857 | 0.073 | 1.850 |
| M2 | Low-Carbon Steel, Lot M | 189.91 | 84.32 | 1.615 | 7.99 | 7.99 | 3.279 | 200.2593 | 200.1577 | 0.059 | 1.495 |
| M3 | Low-Carbon Steel, Lot M | 189.76 | 84.32 | 1.597 | 7.98 | 7.97 | 3.276 | 197.5366 | 197.4064 | 0.076 | 1.918 |
| M201 | Low-Carbon Steel, Lot M | 190.31 | 51.48 | 1.610 | 7.98 | 7.98 | 2.025 | 121.0624 | 120.9845 | 0.073 | 1.856 |
| M202 | Low-Carbon Steel, Lot M | 190.55 | 51.38 | 1.630 | 7.98 | 7.98 | 2.025 | 121.8096 | 121.7324 | 0.072 | 1.840 |
| M203 | Low-Carbon Steel, Lot M | 190.33 | 51.33 | 1.583 | 7.98 | 7.96 | 2.018 | 117.6252 | SA | SA | SA |

* SA = Specimen was retained for surface analysis.

## APPENDIX B-1
## Individual Specimen Data, Seal-Welded Container Test No. 2

Test No.: 2
Test Type: Immersion
Test Environment: Simulated WIPP Brine A, N2 Overpressure (10 atm)
Test Temperature: 30 ±5°C
Test Exposure: 3 Months

| Specimen | Material Type | Length, mm | Width, mm | Thickness, mm | Top Hole ID, mm | Bot. Hole ID, mm | Area, dm2 | Initial Wt., g | Final Wt., g | Corrosion Rate, mpy | Corrosion Rate, µm/yr |
|---|---|---|---|---|---|---|---|---|---|---|---|
| J4 | Low-Carbon Steel, Lot J | 191.06 | 86.53 | 0.705 | 7.96 | 7.95 | 3.329 | 89.0290 | 88.8927 | 0.078 | 1.976 |
| J5 | Low-Carbon Steel, Lot J | 190.92 | 86.59 | 0.715 | 7.95 | 7.95 | 3.330 | 90.1033 | 89.9545 | 0.085 | 2.157 |
| J6 | Low-Carbon Steel, Lot J | 190.94 | 86.63 | 0.700 | 7.95 | 7.94 | 3.331 | 88.1796 | 88.0323 | 0.084 | 2.134 |
| J204 | Low-Carbon Steel, Lot J | 189.68 | 51.26 | 0.717 | 7.95 | 7.95 | 1.963 | 52.3102 | 52.2325 | 0.075 | 1.910 |
| J205 | Low-Carbon Steel, Lot J | 190.95 | 51.46 | 0.711 | 7.95 | 7.95 | 1.983 | 52.4953 | 52.4071 | 0.084 | 2.146 |
| J206 | Low-Carbon Steel, Lot J | 190.63 | 51.37 | 0.705 | 7.95 | 7.95 | 1.976 | 52.2646 | SA* | SA | SA |
| K4 | Low-Carbon Steel, Lot K | 190.38 | 86.29 | 0.877 | 7.96 | 7.96 | 3.319 | 111.1520 | 110.9998 | 0.087 | 2.213 |
| K5 | Low-Carbon Steel, Lot K | 190.26 | 86.30 | 0.878 | 7.97 | 7.97 | 3.317 | 111.2736 | 111.1244 | 0.085 | 2.171 |
| K6 | Low-Carbon Steel, Lot K | 190.45 | 86.33 | 0.871 | 7.96 | 7.96 | 3.321 | 110.2407 | 110.0600 | 0.103 | 2.626 |
| K204 | Low-Carbon Steel, Lot K | 190.24 | 51.42 | 0.885 | 7.96 | 7.97 | 1.984 | 66.3359 | 66.2520 | 0.080 | 2.041 |
| K205 | Low-Carbon Steel, Lot K | 190.11 | 51.36 | 0.874 | 7.97 | 7.97 | 1.979 | 64.8904 | 64.8103 | 0.077 | 1.953 |
| K206 | Low-Carbon Steel, Lot K | 190.14 | 51.42 | 0.887 | 7.97 | 7.96 | 1.983 | 66.3186 | SA | SA | SA |
| L4 | Low-Carbon Steel, Lot L | 190.91 | 86.43 | 1.556 | 7.97 | 7.96 | 3.374 | 197.5401 | 197.3664 | 0.098 | 2.484 |
| L5 | Low-Carbon Steel, Lot L | 190.96 | 86.13 | 1.544 | 7.96 | 7.96 | 3.363 | 196.3888 | 196.2330 | 0.088 | 2.236 |
| L6 | Low-Carbon Steel, Lot L | 190.90 | 86.35 | 1.551 | 7.98 | 7.97 | 3.371 | 197.1904 | 197.0352 | 0.087 | 2.222 |
| L204 | Low-Carbon Steel, Lot L | 191.07 | 51.48 | 1.503 | 7.96 | 7.96 | 2.028 | 112.3139 | 112.2253 | 0.083 | 2.109 |
| L205 | Low-Carbon Steel, Lot L | 190.79 | 51.47 | 1.551 | 7.97 | 7.97 | 2.027 | 115.6739 | SA | SA | SA |
| L206 | Low-Carbon Steel, Lot L | 190.75 | 51.53 | 1.539 | 7.97 | 7.97 | 2.028 | 115.0275 | 114.9364 | 0.085 | 2.168 |
| M4 | Low-Carbon Steel, Lot M | 190.01 | 84.38 | 1.594 | 7.96 | 7.96 | 3.282 | 198.2676 | 198.1661 | 0.059 | 1.492 |
| M5 | Low-Carbon Steel, Lot M | 190.12 | 84.39 | 1.607 | 7.96 | 7.96 | 3.285 | 199.5875 | 199.4617 | 0.073 | 1.848 |
| M6 | Low-Carbon Steel, Lot M | 190.02 | 84.39 | 1.605 | 7.97 | 7.96 | 3.283 | 199.4802 | 199.3576 | 0.071 | 1.802 |
| M204 | Low-Carbon Steel, Lot M | 190.50 | 51.16 | 1.612 | 7.97 | 7.97 | 2.015 | 120.5647 | 120.4844 | 0.076 | 1.923 |
| M205 | Low-Carbon Steel, Lot M | 190.51 | 51.19 | 1.628 | 7.96 | 7.96 | 2.017 | 121.5140 | 121.4350 | 0.074 | 1.890 |
| M206 | Low-Carbon Steel, Lot M | 190.48 | 51.23 | 1.582 | 7.97 | 7.96 | 2.016 | 118.7620 | SA | SA | SA |

* SA = Specimen was retained for surface analysis.

## APPENDIX B-1
## Individual Specimen Data, Seal-Welded Container Test No. 9

Test No: 9
Test Type: Immersion
Test Environment: Simulated WIPP Brine A, N2 Overpressure (10 atm)
Test Temperature: 30 ±5°C
Test Exposure: 6 Months

| Specimen | Material Type | Length, mm | Width, mm | Thickness, mm | Top Hole ID, mm | Bot. Hole ID, mm | Area, dm2 | Initial Wt., g | Final Wt., g | Corrosion Rate, mpy | Corrosion Rate, µm/yr |
|---|---|---|---|---|---|---|---|---|---|---|---|
| J25 | Low-Carbon Steel, Lot J | 188.90 | 80.04 | 0.702 | 7.92 | 7.93 | 3.045 | 80.9667 | 80.7737 | 0.0614 | 1.559 |
| J26 | Low-Carbon Steel, Lot J | 188.90 | 80.05 | 0.704 | 7.97 | 7.95 | 3.046 | 80.8076 | 80.5991 | 0.0663 | 1.684 |
| J26 | Low-Carbon Steel, Lot J | 188.90 | 80.06 | 0.704 | 7.96 | 7.95 | 3.046 | 80.7470 | 80.5377 | 0.0666 | 1.691 |
| J225 | Low-Carbon Steel, Lot J | 188.83 | 50.76 | 0.694 | 7.97 | 7.60 | 1.935 | 50.3613 | SA* | SA | SA |
| J226 | Low-Carbon Steel, Lot J | 188.82 | 50.77 | 0.697 | 7.70 | 8.01 | 1.935 | 50.3302 | 50.1976 | 0.0664 | 1.686 |
| J227 | Low-Carbon Steel, Lot J | 188.83 | 50.77 | 0.712 | 7.93 | 7.90 | 1.935 | 51.5671 | 51.4323 | 0.0675 | 1.714 |
| K25 | Low-Carbon Steel, Lot K | 188.90 | 80.05 | 0.882 | 7.97 | 7.98 | 3.056 | 102.9565 | 102.7551 | 0.0638 | 1.622 |
| K26 | Low-Carbon Steel, Lot K | 188.89 | 80.06 | 0.845 | 7.98 | 7.97 | 3.054 | 98.7986 | 98.5901 | 0.0661 | 1.680 |
| K27 | Low-Carbon Steel, Lot K | 188.90 | 80.06 | 0.875 | 7.98 | 7.98 | 3.056 | 101.7641 | 101.5616 | 0.0642 | 1.630 |
| K225 | Low-Carbon Steel, Lot K | 188.83 | 50.65 | 0.856 | 7.97 | 7.97 | 1.938 | 62.3278 | SA | SA | SA |
| K226 | Low-Carbon Steel, Lot K | 188.84 | 50.70 | 0.882 | 7.97 | 7.97 | 1.942 | 64.3067 | 64.1754 | 0.0655 | 1.664 |
| K227 | Low-Carbon Steel, Lot K | 188.83 | 50.72 | 0.870 | 7.97 | 7.97 | 1.942 | 63.6805 | 63.5473 | 0.0665 | 1.688 |
| L25 | Low-Carbon Steel, Lot L | 188.89 | 79.98 | 1.501 | 7.98 | 7.98 | 3.090 | 175.5799 | 175.3297 | 0.0784 | 1.993 |
| L26 | Low-Carbon Steel, Lot L | 188.91 | 79.99 | 1.510 | 7.98 | 7.98 | 3.091 | 175.0349 | 174.8040 | 0.0724 | 1.838 |
| L27 | Low-Carbon Steel, Lot L | 188.92 | 80.00 | 1.496 | 7.97 | 7.97 | 3.091 | 175.1505 | 174.9067 | 0.0764 | 1.941 |
| L225 | Low-Carbon Steel, Lot L | 188.92 | 50.80 | 1.516 | 7.98 | 7.98 | 1.980 | 110.7318 | 110.5803 | 0.0741 | 1.883 |
| L226 | Low-Carbon Steel, Lot L | 188.92 | 50.80 | 1.510 | 7.98 | 7.98 | 1.979 | 110.8363 | 110.6818 | 0.0756 | 1.921 |
| L227 | Low-Carbon Steel, Lot L | 188.93 | 50.78 | 1.503 | 7.98 | 7.98 | 1.978 | 110.1434 | SA | SA | SA |
| M25 | Low-Carbon Steel, Lot M | 188.87 | 80.03 | 1.592 | 7.97 | 7.98 | 3.097 | 186.8781 | 186.6534 | 0.0703 | 1.785 |
| M26 | Low-Carbon Steel, Lot M | 188.89 | 80.03 | 1.624 | 7.98 | 7.98 | 3.099 | 189.3488 | 189.1299 | 0.0684 | 1.738 |
| M27 | Low-Carbon Steel, Lot M | 188.89 | 80.05 | 1.585 | 7.98 | 7.98 | 3.097 | 185.2336 | 185.0096 | 0.0701 | 1.780 |
| M225 | Low-Carbon Steel, Lot M | 188.97 | 50.45 | 1.615 | 7.99 | 7.99 | 1.972 | 118.7449 | 118.6025 | 0.0700 | 1.777 |
| M226 | Low-Carbon Steel, Lot M | 188.97 | 50.56 | 1.593 | 7.98 | 7.98 | 1.975 | 116.9096 | SA | SA | SA |
| M227 | Low-Carbon Steel, Lot M | 188.96 | 50.60 | 1.590 | 7.99 | 7.98 | 1.976 | 116.5333 | 116.3875 | 0.0715 | 1.815 |

* SA = Specimen was retained for surface analysis.

## APPENDIX B-1
## Individual Specimen Data, Seal-Welded Container Test No. 10

Test No: 10
Test Type: Immersion
Test Environment: Simulated WIPP Brine A, N2 Overpressure (10 atm)
Test Temperature: 30 ±5°C
Test Exposure: 6 Months

| Specimen | Material Type | Length, mm | Width, mm | Thickness, mm | Top Hole ID, mm | Bot. Hole ID, mm | Area, dm2 | Initial Wt., g | Final Wt., g | Corrosion Rate, mpy | Corrosion Rate, µm/yr |
|---|---|---|---|---|---|---|---|---|---|---|---|
| J28 | Low-Carbon Steel, Lot J | 188.89 | 80.06 | 0.697 | 7.95 | 7.95 | 3.046 | 80.0200 | 79.8289 | 0.0605 | 1.537 |
| J29 | Low-Carbon Steel, Lot J | 188.90 | 80.07 | 0.694 | 7.99 | 7.99 | 3.046 | 79.8873 | 79.6907 | 0.0623 | 1.581 |
| J30 | Low-Carbon Steel, Lot J | 188.90 | 80.08 | 0.689 | 7.98 | 7.95 | 3.046 | 78.2569 | 78.0661 | 0.0604 | 1.535 |
| J228 | Low-Carbon Steel, Lot J | 188.82 | 50.77 | 0.708 | 7.98 | 7.89 | 1.935 | 51.1553 | SA* | SA | SA |
| J229 | Low-Carbon Steel, Lot J | 188.82 | 50.78 | 0.696 | 7.89 | 7.95 | 1.935 | 50.3692 | 50.2458 | 0.0615 | 1.562 |
| J230 | Low-Carbon Steel, Lot J | 188.82 | 50.79 | 0.716 | 7.89 | 7.91 | 1.936 | 51.6435 | 51.5210 | 0.0610 | 1.550 |
| K28 | Low-Carbon Steel, Lot K | 188.88 | 80.06 | 0.868 | 8.00 | 7.98 | 3.055 | 101.0222 | 100.8198 | 0.0639 | 1.623 |
| K29 | Low-Carbon Steel, Lot K | 188.89 | 80.06 | 0.872 | 7.99 | 7.99 | 3.056 | 101.4461 | 101.2481 | 0.0625 | 1.587 |
| K30 | Low-Carbon Steel, Lot K | 188.89 | 80.07 | 0.873 | 7.99 | 7.99 | 3.056 | 102.0831 | 101.8812 | 0.0637 | 1.618 |
| K228 | Low-Carbon Steel, Lot K | 188.82 | 50.76 | 0.881 | 7.99 | 7.99 | 1.943 | 64.3251 | 64.1936 | 0.0653 | 1.658 |
| K229 | Low-Carbon Steel, Lot K | 188.82 | 50.75 | 0.872 | 7.99 | 7.99 | 1.943 | 63.6800 | SA | SA | SA |
| K230 | Low-Carbon Steel, Lot K | 188.82 | 50.70 | 0.870 | 7.99 | 7.99 | 1.941 | 63.6278 | 63.4930 | 0.0670 | 1.702 |
| L28 | Low-Carbon Steel, Lot L | 188.91 | 80.01 | 1.562 | 8.00 | 8.00 | 3.095 | 182.4419 | 182.2019 | 0.0748 | 1.900 |
| L29 | Low-Carbon Steel, Lot L | 188.91 | 80.02 | 1.557 | 8.00 | 8.00 | 3.095 | 180.9204 | 180.6789 | 0.0753 | 1.912 |
| L30 | Low-Carbon Steel, Lot L | 188.91 | 80.01 | 1.509 | 8.00 | 8.00 | 3.092 | 175.5258 | 175.2851 | 0.0751 | 1.907 |
| L228 | Low-Carbon Steel, Lot L | 188.91 | 50.79 | 1.515 | 8.00 | 8.00 | 1.979 | 110.3849 | SA | SA | SA |
| L229 | Low-Carbon Steel, Lot L | 188.91 | 50.78 | 1.572 | 8.01 | 8.00 | 1.982 | 115.3170 | 115.1635 | 0.0747 | 1.898 |
| L230 | Low-Carbon Steel, Lot L | 188.90 | 50.80 | 1.549 | 8.00 | 8.00 | 1.981 | 113.1697 | 113.0134 | 0.0761 | 1.933 |
| M28 | Low-Carbon Steel, Lot M | 188.39 | 80.05 | 1.612 | 7.99 | 8.00 | 3.091 | 188.3112 | 188.1011 | 0.0656 | 1.665 |
| M29 | Low-Carbon Steel, Lot M | 188.90 | 80.05 | 1.630 | 8.00 | 8.00 | 3.100 | 191.1087 | 190.9019 | 0.0643 | 1.634 |
| M30 | Low-Carbon Steel, Lot M | 188.91 | 80.04 | 1.576 | 8.00 | 8.00 | 3.097 | 183.1318 | 182.9269 | 0.0638 | 1.621 |
| M228 | Low-Carbon Steel, Lot M | 188.96 | 50.70 | 1.596 | 8.00 | 7.99 | 1.980 | 117.1475 | 117.0186 | 0.0628 | 1.594 |
| M229 | Low-Carbon Steel, Lot M | 188.89 | 50.66 | 1.601 | 8.00 | 8.00 | 1.978 | 117.3251 | SA | SA | SA |
| M230 | Low-Carbon Steel, Lot M | 188.96 | 50.80 | 1.587 | 8.00 | 8.00 | 1.984 | 117.2574 | 117.1245 | 0.0646 | 1.641 |

* SA = Specimen was retained for surface analysis.

## APPENDIX B-1
## Individual Specimen Data, Seal-Welded Container Test No. 17

Test No: 17
Test Type: Immersion
Test Environment: Simulated WIPP Brine A, N2 Overpressure (10 atm)
Test Temperature: 30 ±5°C
Test Exposure: 12 Months

| Specimen | Material Type | Length, mm | Width, mm | Thickness, mm | Top Hole ID, mm | Bot. Hole ID, mm | Area, dm2 | Initial Wt., g | Final Wt., g | Corrosion Rate, mpy | Corrosion Rate, µm/yr |
|---|---|---|---|---|---|---|---|---|---|---|---|
| J49 | Low-Carbon Steel, Lot J | 189.09 | 79.94 | 0.701 | 8.00 | 7.96 | 3.044 | 80.8697 | 80.6038 | 0.0423 | 1.075 |
| J50 | Low-Carbon Steel, Lot J | 189.08 | 79.96 | 0.710 | 8.00 | 7.99 | 3.045 | 81.8711 | 81.6146 | 0.0408 | 1.037 |
| J51 | Low-Carbon Steel, Lot J | 189.08 | 79.95 | 0.711 | 7.99 | 7.97 | 3.045 | 82.2706 | 81.9798 | 0.0463 | 1.176 |
| J249 | Low-Carbon Steel, Lot J | 189.05 | 50.71 | 0.713 | 7.95 | 7.88 | 1.935 | 51.6008 | 51.4386 | 0.0406 | 1.032 |
| J250 | Low-Carbon Steel, Lot J | 189.05 | 50.73 | 0.709 | 7.96 | 8.00 | 1.936 | 51.3007 | SA* | SA | SA |
| J251 | Low-Carbon Steel, Lot J | 189.05 | 50.62 | 0.717 | 7.98 | 7.98 | 1.932 | 51.3406 | 51.1739 | 0.0418 | 1.062 |
| K49 | Low-Carbon Steel, Lot K | 189.08 | 79.95 | 0.885 | 7.89 | 7.92 | 3.056 | 102.3283 | 102.0000 | 0.0521 | 1.323 |
| K50 | Low-Carbon Steel, Lot K | 189.09 | 79.96 | 0.884 | 7.86 | 7.88 | 3.056 | 102.3078 | 101.9911 | 0.0502 | 1.276 |
| K51 | Low-Carbon Steel, Lot K | 189.08 | 79.95 | 0.886 | 7.92 | 7.81 | 3.056 | 102.6056 | 102.2900 | 0.0500 | 1.271 |
| K249 | Low-Carbon Steel, Lot K | 189.05 | 50.71 | 0.878 | 7.90 | 7.88 | 1.944 | 64.2702 | 64.0744 | 0.0488 | 1.240 |
| K250 | Low-Carbon Steel, Lot K | 189.05 | 50.71 | 0.867 | 7.93 | 7.92 | 1.944 | 63.8434 | 63.6375 | 0.0513 | 1.304 |
| K251 | Low-Carbon Steel, Lot K | 189.06 | 50.70 | 0.886 | 7.93 | 7.93 | 1.944 | 64.7405 | SA | SA | SA |
| L49 | Low-Carbon Steel, Lot L | 189.22 | 80.02 | 1.511 | 7.93 | 7.93 | 3.097 | 175.6488 | 175.3203 | 0.0514 | 1.306 |
| L50 | Low-Carbon Steel, Lot L | 189.21 | 80.03 | 1.492 | 7.94 | 7.95 | 3.096 | 174.8962 | 174.5729 | 0.0506 | 1.285 |
| L51 | Low-Carbon Steel, Lot L | 189.21 | 80.02 | 1.555 | 7.94 | 7.93 | 3.100 | 181.6679 | 181.3421 | 0.0509 | 1.294 |
| L249 | Low-Carbon Steel, Lot L | 189.19 | 50.72 | 1.511 | 7.95 | 7.93 | 1.979 | 110.2186 | 110.0169 | 0.0494 | 1.254 |
| L250 | Low-Carbon Steel, Lot L | 189.20 | 50.73 | 1.528 | 8.00 | 8.00 | 1.981 | 111.5012 | 111.2935 | 0.0508 | 1.291 |
| L251 | Low-Carbon Steel, Lot L | 189.20 | 50.73 | 1.525 | 8.02 | 7.98 | 1.980 | 111.2591 | SA | SA | SA |
| M49 | Low-Carbon Steel, Lot M | 189.33 | 80.15 | 1.599 | 7.98 | 7.98 | 3.109 | 186.2713 | 185.9466 | 0.0506 | 1.286 |
| M50 | Low-Carbon Steel, Lot M | 189.33 | 80.17 | 1.551 | 8.00 | 8.00 | 3.107 | 182.8244 | 182.4943 | 0.0515 | 1.308 |
| M51 | Low-Carbon Steel, Lot M | 189.34 | 80.17 | 1.557 | 7.99 | 8.00 | 3.108 | 182.4878 | 182.1446 | 0.0535 | 1.360 |
| M249 | Low-Carbon Steel, Lot M | 189.06 | 50.59 | 1.607 | 8.01 | 7.98 | 1.978 | 117.4947 | 117.2953 | 0.0489 | 1.241 |
| M250 | Low-Carbon Steel, Lot M | 189.07 | 50.63 | 1.592 | 7.98 | 7.97 | 1.979 | 116.7827 | SA | SA | SA |
| M251 | Low-Carbon Steel, Lot M | 189.08 | 50.60 | 1.610 | 7.99 | 7.98 | 1.979 | 117.6595 | 117.4538 | 0.0504 | 1.280 |

* SA = Specimen was retained for surface analysis.

## APPENDIX B-1
## Individual Specimen Data, Seal-Welded Container Test No. 18

Test No: 18
Test Type: Immersion
Test Environment: Simulated WIPP Brine A, N2 Overpressure (10 atm)
Test Temperature: 30 ±5°C
Test Exposure: 12 Months

| Specimen | Material Type | Length, mm | Width, mm | Thickness, mm | Top Hole ID, mm | Bot. Hole ID, mm | Area, dm2 | Initial Wt., g | Final Wt., g | Corrosion Rate, mpy | Corrosion Rate, µm/yr |
|---|---|---|---|---|---|---|---|---|---|---|---|
| J52 | Low-Carbon Steel, Lot J | 189.03 | 79.97 | 0.710 | 7.90 | 7.94 | 3.045 | 81.9938 | 81.7411 | 0.0402 | 1.021 |
| J53 | Low-Carbon Steel, Lot J | 189.03 | 79.97 | 0.703 | 7.91 | 7.92 | 3.045 | 81.7066 | 81.4348 | 0.0433 | 1.099 |
| J54 | Low-Carbon Steel, Lot J | 189.09 | 80.00 | 0.707 | 7.95 | 7.94 | 3.047 | 81.8526 | 81.5930 | 0.0413 | 1.049 |
| J252 | Low-Carbon Steel, Lot J | 189.07 | 50.68 | 0.709 | 7.93 | 7.88 | 1.934 | 51.5550 | 51.3992 | 0.0390 | 0.992 |
| J253 | Low-Carbon Steel, Lot J | 189.06 | 50.73 | 0.712 | 7.94 | 7.91 | 1.936 | 52.0054 | 51.8393 | 0.0416 | 1.056 |
| J254 | Low-Carbon Steel, Lot J | 189.07 | 50.73 | 0.714 | 7.93 | 7.90 | 1.936 | 51.7604 | SA* | SA | SA |
| K52 | Low-Carbon Steel, Lot K | 189.09 | 79.99 | 0.879 | 7.85 | 7.89 | 3.057 | 102.0543 | 101.7510 | 0.0481 | 1.221 |
| K53 | Low-Carbon Steel, Lot K | 189.10 | 79.97 | 0.872 | 7.92 | 7.84 | 3.056 | 101.7205 | 101.4067 | 0.0498 | 1.264 |
| K54 | Low-Carbon Steel, Lot K | 189.09 | 79.97 | 0.874 | 7.85 | 7.88 | 3.056 | 101.4722 | 101.1585 | 0.0497 | 1.264 |
| K252 | Low-Carbon Steel, Lot K | 189.06 | 50.77 | 0.885 | 7.93 | 7.90 | 1.947 | 64.8092 | 64.6186 | 0.0474 | 1.205 |
| K253 | Low-Carbon Steel, Lot K | 189.08 | 50.79 | 0.885 | 7.95 | 7.89 | 1.948 | 64.9056 | 64.7110 | 0.0484 | 1.230 |
| K254 | Low-Carbon Steel, Lot K | 189.07 | 50.74 | 0.885 | 7.95 | 7.93 | 1.946 | 65.0250 | SA | SA | SA |
| L52 | Low-Carbon Steel, Lot L | 189.21 | 80.02 | 1.534 | 7.95 | 7.96 | 3.099 | 179.1034 | 178.7480 | 0.0556 | 1.412 |
| L53 | Low-Carbon Steel, Lot L | 189.23 | 80.04 | 1.551 | 7.96 | 7.95 | 3.101 | 180.9391 | 180.6093 | 0.0515 | 1.309 |
| L54 | Low-Carbon Steel, Lot L | 189.21 | 80.03 | 1.552 | 7.94 | 7.93 | 3.100 | 181.8081 | 181.4741 | 0.0522 | 1.326 |
| L252 | Low-Carbon Steel, Lot L | 189.21 | 50.75 | 1.544 | 7.97 | 7.95 | 1.982 | 112.8618 | SA | SA | SA |
| L253 | Low-Carbon Steel, Lot L | 189.20 | 50.73 | 1.499 | 7.97 | 7.93 | 1.979 | 109.7198 | 109.5079 | 0.0519 | 1.318 |
| L254 | Low-Carbon Steel, Lot L | 189.19 | 50.72 | 1.545 | 7.96 | 7.95 | 1.981 | 112.0234 | 111.8130 | 0.0515 | 1.307 |
| M52 | Low-Carbon Steel, Lot M | 189.36 | 80.20 | 1.544 | 7.93 | 7.93 | 3.109 | 182.6694 | 182.3404 | 0.0513 | 1.303 |
| M53 | Low-Carbon Steel, Lot M | 189.35 | 80.24 | 1.555 | 7.93 | 7.93 | 3.111 | 182.9135 | 182.5880 | 0.0507 | 1.288 |
| M54 | Low-Carbon Steel, Lot M | 189.38 | 80.18 | 1.557 | 7.93 | 7.94 | 3.109 | 182.9513 | 182.6276 | 0.0505 | 1.282 |
| M252 | Low-Carbon Steel, Lot M | 189.11 | 50.67 | 1.606 | 7.94 | 7.95 | 1.982 | 117.3912 | SA | SA | SA |
| M253 | Low-Carbon Steel, Lot M | 189.11 | 50.69 | 1.591 | 7.95 | 7.94 | 1.982 | 116.5208 | 116.3211 | 0.0488 | 1.241 |
| M254 | Low-Carbon Steel, Lot M | 189.12 | 50.62 | 1.596 | 7.96 | 7.95 | 1.979 | 116.7564 | 116.5523 | 0.0500 | 1.269 |

* SA = Specimen was retained for surface analysis.

## APPENDIX B-1
## Individual Specimen Data, Seal-Welded Container Test No. 25

Test No.: 25
Test Type: Immersion
Test Environment: Simulated WIPP Brine A, N2 Overpressure (10 atm)
Test Temperature: 30 ±5°C
Test Exposure: 24 Months

| Specimen | Material Type | Length, mm | Width, mm | Thickness, mm | Top Hole ID, mm | Bot. Hole ID, mm | Area, dm2 | Initial Wt., g | Final Wt., g | Corrosion Rate, mpy | Corrosion Rate, µm/yr |
|---|---|---|---|---|---|---|---|---|---|---|---|
| J73 | Low-Carbon Steel, Lot J | 188.86 | 79.90 | 0.709 | 7.89 | 7.92 | 3.040 | 81.9915 | 81.5206 | 0.0381 | 0.967 |
| J74 | Low-Carbon Steel, Lot J | 188.89 | 79.92 | 0.718 | 7.89 | 7.88 | 3.042 | 82.8456 | 82.3799 | 0.0376 | 0.956 |
| J75 | Low-Carbon Steel, Lot J | 188.86 | 79.89 | 0.703 | 7.89 | 7.89 | 3.039 | 81.6919 | 81.2330 | 0.0371 | 0.943 |
| J273 | Low-Carbon Steel, Lot J | 189.04 | 50.83 | 0.709 | 7.86 | 7.85 | 1.940 | 51.7868 | 51.4873 | 0.0380 | 0.964 |
| J274 | Low-Carbon Steel, Lot J | 189.06 | 50.84 | 0.692 | 7.87 | 7.87 | 1.940 | 50.6111 | SA* | SA | SA |
| J275 | Low-Carbon Steel, Lot J | 189.09 | 50.85 | 0.717 | 7.89 | 7.88 | 1.941 | 52.2689 | 51.9801 | 0.0366 | 0.929 |
| K73 | Low-Carbon Steel, Lot K | 188.89 | 79.94 | 0.858 | 7.88 | 7.88 | 3.051 | 99.8946 | 99.2461 | 0.0523 | 1.327 |
| K74 | Low-Carbon Steel, Lot K | 188.86 | 79.89 | 0.858 | 7.89 | 7.88 | 3.048 | 99.8410 | 99.2438 | 0.0482 | 1.223 |
| K75 | Low-Carbon Steel, Lot K | 188.90 | 79.94 | 0.870 | 7.94 | 7.94 | 3.051 | 101.1830 | 100.6200 | 0.0454 | 1.152 |
| K273 | Low-Carbon Steel, Lot K | 189.04 | 50.82 | 0.877 | 7.91 | 7.92 | 1.948 | 64.3493 | 63.9994 | 0.0442 | 1.121 |
| K274 | Low-Carbon Steel, Lot K | 189.05 | 50.84 | 0.867 | 7.93 | 7.94 | 1.948 | 63.4702 | 63.1022 | 0.0464 | 1.179 |
| K275 | Low-Carbon Steel, Lot K | 189.04 | 50.82 | 0.864 | 7.91 | 7.92 | 1.947 | 63.4661 | SA | SA | SA |
| L73 | Low-Carbon Steel, Lot L | 188.91 | 79.96 | 1.559 | 7.92 | 7.96 | 3.093 | 180.6934 | 180.2229 | 0.0374 | 0.950 |
| L74 | Low-Carbon Steel, Lot L | 188.96 | 80.00 | 1.568 | 7.85 | 7.92 | 3.096 | 182.0639 | 181.5921 | 0.0375 | 0.952 |
| L75 | Low-Carbon Steel, Lot L | 188.97 | 79.98 | 1.518 | 7.90 | 7.86 | 3.092 | 177.1573 | 176.7111 | 0.0355 | 0.901 |
| L273 | Low-Carbon Steel, Lot L | 189.18 | 50.79 | 1.503 | 7.94 | 7.88 | 1.982 | 109.3805 | SA | SA | SA |
| L274 | Low-Carbon Steel, Lot L | 189.19 | 50.82 | 1.554 | 7.92 | 7.88 | 1.986 | 113.2251 | 112.9405 | 0.0352 | 0.895 |
| L275 | Low-Carbon Steel, Lot L | 189.18 | 50.88 | 1.558 | 7.90 | 7.91 | 1.988 | 113.9692 | 113.6746 | 0.0364 | 0.925 |
| M73 | Low-Carbon Steel, Lot M | 189.04 | 80.15 | 1.578 | 7.90 | 7.90 | 3.103 | 185.8791 | 185.4481 | 0.0341 | 0.867 |
| M74 | Low-Carbon Steel, Lot M | 189.03 | 80.10 | 1.586 | 7.92 | 7.91 | 3.102 | 186.1507 | 185.6994 | 0.0358 | 0.908 |
| M75 | Low-Carbon Steel, Lot M | 189.02 | 80.13 | 1.601 | 7.93 | 7.94 | 3.104 | 187.5477 | 187.0784 | 0.0372 | 0.944 |
| M273 | Low-Carbon Steel, Lot M | 189.09 | 50.79 | 1.552 | 7.92 | 7.94 | 1.983 | 114.4320 | 114.1137 | 0.0395 | 1.002 |
| M274 | Low-Carbon Steel, Lot M | 189.14 | 50.81 | 1.576 | 7.94 | 7.91 | 1.986 | 115.8318 | SA | SA | SA |
| M275 | Low-Carbon Steel, Lot M | 189.16 | 50.98 | 1.581 | 7.91 | 7.89 | 1.993 | 116.7991 | 116.4833 | 0.0390 | 0.989 |

*SA = Specimen was retained for surface analysis.

## APPENDIX B-1
## Individual Specimen Data, Seal-Welded Container Test No. 26

Test No.: 26
Test Type: Immersion
Test Environment: Simulated WIPP Brine A, N2 Overpressure (10 atm)
Test Temperature: 30 ±5°C
Test Exposure: 24 Months

| Specimen | Material Type | Length, mm | Width, mm | Thickness, mm | Top Hole ID, mm | Bot. Hole ID, mm | Area, dm2 | Initial Wt., g | Final Wt., g | Corrosion Rate, mpy | Corrosion Rate, µm/yr |
|---|---|---|---|---|---|---|---|---|---|---|---|
| J76 | Low-Carbon Steel, Lot J | 188.95 | 79.99 | 0.704 | 7.93 | 7.95 | 3.044 | 81.5207 | 81.0630 | 0.0369 | 0.938 |
| J77 | Low-Carbon Steel, Lot J | 188.96 | 79.99 | 0.708 | 7.94 | 7.94 | 3.045 | 82.1630 | 81.6953 | 0.0377 | 0.959 |
| J78 | Low-Carbon Steel, Lot J | 188.99 | 79.98 | 0.706 | 7.94 | 7.95 | 3.045 | 81.4929 | 81.0709 | 0.0341 | 0.865 |
| J276 | Low-Carbon Steel, Lot J | 189.15 | 50.89 | 0.714 | 7.95 | 7.96 | 1.943 | 52.1371 | 51.8144 | 0.0408 | 1.037 |
| J277 | Low-Carbon Steel, Lot J | 189.14 | 50.90 | 0.699 | 7.94 | 7.94 | 1.943 | 51.5245 | 51.2103 | 0.0397 | 1.010 |
| J278 | Low-Carbon Steel, Lot J | 189.15 | 50.93 | 0.712 | 7.96 | 7.93 | 1.945 | 51.9054 | SA* | SA | SA |
| K76 | Low-Carbon Steel, Lot K | 188.98 | 79.97 | 0.861 | 7.94 | 7.96 | 3.053 | 100.3056 | 99.7797 | 0.0423 | 1.075 |
| K77 | Low-Carbon Steel, Lot K | 188.95 | 79.99 | 0.872 | 7.95 | 7.93 | 3.054 | 101.3347 | 100.7793 | 0.0447 | 1.135 |
| K78 | Low-Carbon Steel, Lot K | 188.95 | 79.99 | 0.870 | 7.95 | 7.93 | 3.054 | 101.0741 | 100.5218 | 0.0444 | 1.129 |
| K276 | Low-Carbon Steel, Lot K | 189.10 | 50.90 | 0.863 | 7.95 | 7.95 | 1.951 | 63.6048 | SA | SA | SA |
| K277 | Low-Carbon Steel, Lot K | 189.09 | 50.86 | 0.869 | 7.94 | 7.95 | 1.950 | 63.8011 | 63.4727 | 0.0414 | 1.051 |
| K278 | Low-Carbon Steel, Lot K | 189.08 | 50.88 | 0.877 | 7.93 | 7.94 | 1.951 | 64.4909 | 64.1461 | 0.0434 | 1.103 |
| L76 | Low-Carbon Steel, Lot L | 189.01 | 80.05 | 1.539 | 7.92 | 7.93 | 3.097 | 179.1690 | 178.7389 | 0.0341 | 0.867 |
| L77 | Low-Carbon Steel, Lot L | 189.02 | 80.05 | 1.546 | 7.93 | 7.91 | 3.097 | 180.9903 | 180.5484 | 0.0351 | 0.891 |
| L78 | Low-Carbon Steel, Lot L | 189.00 | 80.06 | 1.539 | 7.95 | 7.95 | 3.097 | 180.3304 | 179.9089 | 0.0334 | 0.850 |
| L276 | Low-Carbon Steel, Lot L | 189.25 | 50.70 | 1.490 | 7.95 | 7.94 | 1.978 | 108.9996 | 108.7177 | 0.0350 | 0.890 |
| L277 | Low-Carbon Steel, Lot L | 189.24 | 50.69 | 1.563 | 7.96 | 7.94 | 1.981 | 113.9647 | SA | SA | SA |
| L278 | Low-Carbon Steel, Lot L | 189.25 | 50.73 | 1.510 | 7.95 | 7.96 | 1.980 | 110.1100 | 109.8020 | 0.0382 | 0.971 |
| M76 | Low-Carbon Steel, Lot M | 189.07 | 80.15 | 1.592 | 7.93 | 7.95 | 3.105 | 186.8068 | 186.3409 | 0.0369 | 0.937 |
| M77 | Low-Carbon Steel, Lot M | 189.05 | 80.17 | 1.573 | 7.93 | 7.93 | 3.104 | 184.7843 | 184.3148 | 0.0372 | 0.944 |
| M78 | Low-Carbon Steel, Lot M | 189.06 | 80.18 | 1.581 | 7.92 | 7.93 | 3.105 | 186.2283 | 185.7450 | 0.0383 | 0.972 |
| M276 | Low-Carbon Steel, Lot M | 189.20 | 50.89 | 1.598 | 7.95 | 7.96 | 1.991 | 117.7083 | 117.3963 | 0.0385 | 0.978 |
| M277 | Low-Carbon Steel, Lot M | 189.21 | 50.88 | 1.578 | 7.96 | 7.91 | 1.989 | 116.8505 | SA | SA | SA |
| M278 | Low-Carbon Steel, Lot M | 189.22 | 50.75 | 1.594 | 7.96 | 7.97 | 1.985 | 117.3540 | 117.0425 | 0.0386 | 0.979 |

*SA = Specimen was retained for surface analysis.

# APPENDIX B-2: INDIVIDUAL SPECIMEN CORROSION-RATE DATA, ANOXIC BRINE ($N_2$/VAPOR) ENVIRONMENT, SEAL-WELDED-CONTAINER TEST METHOD

## APPENDIX B-2
## Individual Specimen Data, Seal-Welded Container Test No. 5

Test No.: 5
Test Type: Vapor Phase Exposure
Test Environment: Simulated WIPP Brine A Vapor + N2 (12 atm)
Test Temperature: 30 ±5°C
Test Exposure: 3 Months

| Specimen | Material Type | Length, mm | Width, mm | Thickness, mm | Top Hole ID, mm | Bot. Hole ID, mm | Area, dm2 | Initial Wt., g | Final Wt., g | Corrosion Rate, mpy | Corrosion Rate, µm/yr |
|---|---|---|---|---|---|---|---|---|---|---|---|
| J13 | Low-Carbon Steel, Lot J | 190.72 | 86.48 | 0.721 | 8.01 | 8.01 | 3.322 | 89.7014 | 89.6852 | 0.010 | 0.246 |
| J14 | Low-Carbon Steel, Lot J | 190.86 | 86.15 | 0.699 | 8.00 | 8.00 | 3.311 | 88.0915 | 88.0757 | 0.009 | 0.240 |
| J15 | Low-Carbon Steel, Lot J | 190.48 | 86.53 | 0.708 | 8.01 | 8.02 | 3.319 | 89.0198 | 89.0032 | 0.010 | 0.252 |
| J213 | Low-Carbon Steel, Lot J | 190.22 | 51.26 | 0.710 | 8.00 | 8.00 | 1.968 | 51.7779 | SA* | SA | SA |
| J214 | Low-Carbon Steel, Lot J | 189.00 | 51.18 | 0.714 | 8.02 | 8.01 | 1.952 | 51.6697 | 51.6596 | 0.010 | 0.261 |
| J215 | Low-Carbon Steel, Lot J | 190.78 | 51.31 | 0.714 | 8.01 | 8.01 | 1.976 | 52.5299 | 52.5174 | 0.013 | 0.319 |
| K13 | Low-Carbon Steel, Lot K | 190.63 | 86.12 | 0.877 | 7.96 | 7.96 | 3.316 | 110.5081 | 110.4738 | 0.021 | 0.521 |
| K14 | Low-Carbon Steel, Lot K | 189.15 | 86.02 | 0.866 | 7.97 | 7.96 | 3.286 | 108.6067 | 108.5912 | 0.009 | 0.238 |
| K15 | Low-Carbon Steel, Lot K | 190.69 | 86.29 | 0.868 | 7.98 | 7.98 | 3.323 | 109.8060 | 109.7874 | 0.011 | 0.282 |
| K213 | Low-Carbon Steel, Lot K | 189.21 | 51.27 | 0.881 | 7.98 | 7.97 | 1.967 | 64.8458 | 64.8327 | 0.013 | 0.336 |
| K214 | Low-Carbon Steel, Lot K | 189.94 | 51.19 | 0.879 | 7.98 | 7.97 | 1.971 | 64.9311 | 64.9156 | 0.016 | 0.396 |
| K215 | Low-Carbon Steel, Lot K | 188.87 | 51.31 | 0.874 | 7.98 | 7.99 | 1.965 | 64.4635 | SA | SA | SA |
| L13 | Low-Carbon Steel, Lot L | 190.72 | 86.54 | 1.547 | 7.97 | 7.96 | 3.375 | 196.6486 | 196.6070 | 0.024 | 0.621 |
| L14 | Low-Carbon Steel, Lot L | 190.12 | 86.22 | 1.528 | 7.98 | 7.97 | 3.351 | 194.8468 | 194.8260 | 0.012 | 0.313 |
| L15 | Low-Carbon Steel, Lot L | 190.85 | 86.54 | 1.532 | 7.98 | 7.97 | 3.376 | 196.7299 | 196.7094 | 0.012 | 0.306 |
| L213 | Low-Carbon Steel, Lot L | 191.75 | 51.42 | 1.496 | 7.97 | 7.97 | 2.032 | 112.0215 | SA | SA | SA |
| L214 | Low-Carbon Steel, Lot L | 190.77 | 51.38 | 1.504 | 7.98 | 7.98 | 2.021 | 112.0013 | 111.9888 | 0.012 | 0.312 |
| L215 | Low-Carbon Steel, Lot L | 189.97 | 51.45 | 1.551 | 7.98 | 7.97 | 2.017 | 115.0684 | 115.0554 | 0.013 | 0.325 |
| M13 | Low-Carbon Steel, Lot M | 189.93 | 84.29 | 1.597 | 7.97 | 7.97 | 3.277 | 197.9004 | 197.8821 | 0.011 | 0.281 |
| M14 | Low-Carbon Steel, Lot M | 190.37 | 84.37 | 1.576 | 7.97 | 7.97 | 3.287 | 197.9424 | 197.9222 | 0.012 | 0.310 |
| M15 | Low-Carbon Steel, Lot M | 189.98 | 84.36 | 1.576 | 7.96 | 7.96 | 3.280 | 197.0945 | 197.0710 | 0.014 | 0.361 |
| M213 | Low-Carbon Steel, Lot M | 190.47 | 51.49 | 1.611 | 7.97 | 7.96 | 2.028 | 121.3102 | 121.2944 | 0.015 | 0.393 |
| M214 | Low-Carbon Steel, Lot M | 190.45 | 51.34 | 1.624 | 7.97 | 7.96 | 2.022 | 121.8258 | SA | SA | SA |
| M215 | Low-Carbon Steel, Lot M | 190.45 | 51.39 | 1.621 | 7.98 | 7.96 | 2.024 | 121.4284 | 121.4114 | 0.017 | 0.423 |

* SA = Specimen was retained for surface analysis.

## APPENDIX B-2
## Individual Specimen Data, Seal-Welded Container Test No. 6

Test No.: 6
Test Type: Vapor Phase Exposure
Test Environment: Simulated WIPP Brine A Vapor + N2 (10 atm)
Test Temperature: 30 ±5°C
Test Exposure: 3 Months

| Specimen | Material Type | Length, mm | Width, mm | Thickness, mm | Top Hole ID, mm | Bot. Hole ID, mm | Area, dm2 | Initial Wt., g | Final Wt., g | Corrosion Rate, mpy | Corrosion Rate, µm/yr |
|---|---|---|---|---|---|---|---|---|---|---|---|
| J16 | Low-Carbon Steel, Lot J | 189.13 | 85.78 | 0.701 | 7.96 | 7.96 | 3.267 | 87.5332 | 87.5126 | 0.013 | 0.318 |
| J17 | Low-Carbon Steel, Lot J | 189.15 | 85.78 | 0.706 | 7.96 | 7.95 | 3.268 | 87.2655 | 87.2528 | 0.008 | 0.196 |
| J18 | Low-Carbon Steel, Lot J | 189.14 | 85.78 | 0.712 | 7.95 | 7.95 | 3.268 | 88.6485 | 88.6354 | 0.008 | 0.202 |
| J216 | Low-Carbon Steel, Lot J | 189.60 | 50.98 | 0.713 | 7.96 | 7.96 | 1.951 | 51.6486 | 51.6404 | 0.008 | 0.212 |
| J217 | Low-Carbon Steel, Lot J | 189.60 | 50.98 | 0.702 | 7.97 | 7.96 | 1.951 | 51.0916 | 51.0824 | 0.009 | 0.238 |
| J218 | Low-Carbon Steel, Lot J | 189.60 | 50.98 | 0.716 | 7.96 | 7.96 | 1.951 | 52.1835 | SA* | SA | SA |
| K16 | Low-Carbon Steel, Lot K | 189.13 | 85.78 | 0.874 | 7.96 | 7.95 | 3.277 | 109.1842 | 109.1557 | 0.017 | 0.438 |
| K17 | Low-Carbon Steel, Lot K | 189.14 | 85.78 | 0.871 | 7.96 | 7.95 | 3.277 | 108.9417 | 108.9199 | 0.013 | 0.335 |
| K18 | Low-Carbon Steel, Lot K | 189.14 | 85.78 | 0.876 | 7.97 | 7.96 | 3.278 | 109.3402 | 109.3300 | 0.006 | 0.157 |
| K216 | Low-Carbon Steel, Lot K | 189.60 | 50.98 | 0.874 | 7.97 | 7.96 | 1.960 | 64.4479 | 64.4418 | 0.006 | 0.157 |
| K217 | Low-Carbon Steel, Lot K | 189.61 | 50.98 | 0.885 | 7.97 | 7.96 | 1.960 | 65.5893 | 65.5844 | 0.005 | 0.126 |
| K218 | Low-Carbon Steel, Lot K | 189.60 | 50.98 | 0.886 | 7.97 | 7.97 | 1.960 | 65.4429 | SA | SA | SA |
| L16 | Low-Carbon Steel, Lot L | 189.14 | 85.80 | 1.561 | 7.96 | 7.95 | 3.319 | 195.4773 | 195.4522 | 0.015 | 0.381 |
| L17 | Low-Carbon Steel, Lot L | 189.14 | 85.79 | 1.543 | 7.97 | 7.96 | 3.318 | 192.9296 | 192.9102 | 0.012 | 0.295 |
| L18 | Low-Carbon Steel, Lot L | 189.14 | 85.78 | 1.536 | 7.97 | 7.96 | 3.317 | 192.8766 | 192.8570 | 0.012 | 0.298 |
| L216 | Low-Carbon Steel, Lot L | 189.62 | 50.98 | 1.543 | 7.98 | 7.97 | 1.995 | 115.2451 | 115.2340 | 0.011 | 0.280 |
| L217 | Low-Carbon Steel, Lot L | 189.61 | 50.98 | 1.559 | 7.98 | 7.98 | 1.996 | 115.3136 | 115.3033 | 0.010 | 0.260 |
| L218 | Low-Carbon Steel, Lot L | 189.61 | 50.99 | 1.546 | 7.97 | 7.97 | 1.996 | 113.7260 | SA | SA | SA |
| M16 | Low-Carbon Steel, Lot M | 189.16 | 84.36 | 1.600 | 7.96 | 7.96 | 3.267 | 199.1066 | 199.0927 | 0.008 | 0.214 |
| M17 | Low-Carbon Steel, Lot M | 189.15 | 84.31 | 1.560 | 7.97 | 7.96 | 3.263 | 193.9453 | 193.9291 | 0.010 | 0.250 |
| M18 | Low-Carbon Steel, Lot M | 189.15 | 84.31 | 1.555 | 7.97 | 7.97 | 3.262 | 193.5659 | 193.5514 | 0.009 | 0.224 |
| M216 | Low-Carbon Steel, Lot M | 189.60 | 50.98 | 1.560 | 7.98 | 7.97 | 1.996 | 115.6005 | SA | SA | SA |
| M217 | Low-Carbon Steel, Lot M | 189.62 | 50.99 | 1.595 | 7.97 | 7.97 | 1.999 | 118.5693 | 118.5622 | 0.007 | 0.179 |
| M218 | Low-Carbon Steel, Lot M | 189.61 | 50.98 | 1.618 | 7.97 | 7.97 | 1.999 | 119.9987 | 119.9914 | 0.007 | 0.184 |

* SA = Specimen was retained for surface analysis.

## APPENDIX B-2
## Individual Specimen Data, Seal-Welded Container Test No. 13

Test No: 13
Test Type: Vapor Phase Exposure
Test Environment: Simulated WIPP Brine A Vapor + N2 (10 atm)
Test Temperature: 30 ±5°C
Test Exposure: 6 Months

| Specimen | Material Type | Length, mm | Width, mm | Thickness, mm | Top Hole ID, mm | Bot. Hole ID, mm | Area, dm2 | Initial Wt., g | Final Wt., g | Corrosion Rate, mpy | Corrosion Rate, µm/yr |
|---|---|---|---|---|---|---|---|---|---|---|---|
| J37 | Low-Carbon Steel, Lot J | 188.99 | 80.14 | 0.710 | 7.82 | 7.80 | 3.052 | 80.4475 | 80.4279 | 0.0062 | 0.158 |
| J38 | Low-Carbon Steel, Lot J | 188.96 | 80.12 | 0.706 | 7.84 | 7.80 | 3.050 | 80.3535 | 80.3360 | 0.0056 | 0.141 |
| J39 | Low-Carbon Steel, Lot J | 188.98 | 80.12 | 0.705 | 7.86 | 7.79 | 3.050 | 80.5772 | 80.5568 | 0.0065 | 0.165 |
| J237 | Low-Carbon Steel, Lot J | 188.86 | 50.79 | 0.720 | 7.82 | 7.81 | 1.937 | 51.5181 | 51.5082 | 0.0050 | 0.126 |
| J238 | Low-Carbon Steel, Lot J | 188.85 | 50.79 | 0.720 | 7.73 | 7.74 | 1.938 | 51.8347 | SA* | SA | SA |
| J239 | Low-Carbon Steel, Lot J | 188.85 | 50.79 | 0.709 | 7.90 | 7.60 | 1.937 | 51.1926 | 51.1795 | 0.0066 | 0.166 |
| K37 | Low-Carbon Steel, Lot K | 188.96 | 80.13 | 0.890 | 7.88 | 7.89 | 3.061 | 102.6192 | 102.5993 | 0.0063 | 0.160 |
| K38 | Low-Carbon Steel, Lot K | 188.95 | 80.13 | 0.885 | 7.89 | 7.89 | 3.061 | 102.3975 | 102.3796 | 0.0057 | 0.144 |
| K39 | Low-Carbon Steel, Lot K | 188.96 | 80.12 | 0.887 | 7.89 | 7.80 | 3.061 | 102.3473 | 102.3294 | 0.0057 | 0.144 |
| K237 | Low-Carbon Steel, Lot K | 188.90 | 50.63 | 0.873 | 7.85 | 7.89 | 1.939 | 63.1282 | 63.1211 | 0.0035 | 0.090 |
| K238 | Low-Carbon Steel, Lot K | 188.90 | 50.77 | 0.877 | 7.86 | 7.90 | 1.945 | 63.4326 | 63.4181 | 0.0072 | 0.183 |
| K239 | Low-Carbon Steel, Lot K | 188.90 | 50.70 | 0.877 | 7.87 | 7.89 | 1.942 | 63.5664 | SA | SA | SA |
| L37 | Low-Carbon Steel, Lot L | 188.90 | 80.00 | 1.554 | 7.88 | 7.89 | 3.094 | 179.5847 | 179.5643 | 0.0064 | 0.162 |
| L38 | Low-Carbon Steel, Lot L | 188.90 | 80.02 | 1.499 | 7.89 | 7.80 | 3.092 | 173.7574 | 173.7341 | 0.0073 | 0.185 |
| L39 | Low-Carbon Steel, Lot L | 188.91 | 80.01 | 1.500 | 7.81 | 7.84 | 3.092 | 173.4066 | 173.3820 | 0.0077 | 0.196 |
| L237 | Low-Carbon Steel, Lot L | 188.88 | 50.75 | 1.560 | 7.86 | 7.89 | 1.980 | 113.7850 | SA | SA | SA |
| L238 | Low-Carbon Steel, Lot L | 188.89 | 50.78 | 1.570 | 7.86 | 7.88 | 1.982 | 114.5543 | 114.5352 | 0.0093 | 0.237 |
| L239 | Low-Carbon Steel, Lot L | 188.92 | 50.78 | 1.564 | 7.86 | 7.85 | 1.982 | 113.8630 | 113.8443 | 0.0091 | 0.232 |
| M37 | Low-Carbon Steel, Lot M | 188.87 | 80.02 | 1.554 | 7.78 | 7.86 | 3.095 | 181.2015 | 181.1747 | 0.0084 | 0.213 |
| M38 | Low-Carbon Steel, Lot M | 188.92 | 80.04 | 1.554 | 7.84 | 7.85 | 3.096 | 181.1371 | 181.1088 | 0.0089 | 0.225 |
| M39 | Low-Carbon Steel, Lot M | 188.90 | 80.06 | 1.608 | 7.83 | 7.86 | 3.100 | 187.6152 | 187.5916 | 0.0074 | 0.187 |
| M237 | Low-Carbon Steel, Lot M | 188.93 | 50.78 | 1.601 | 7.89 | 7.88 | 1.984 | 117.4677 | 117.4507 | 0.0083 | 0.211 |
| M238 | Low-Carbon Steel, Lot M | 188.94 | 50.77 | 1.608 | 7.89 | 7.89 | 1.984 | 117.6713 | 117.6583 | 0.0063 | 0.161 |
| M239 | Low-Carbon Steel, Lot M | 188.94 | 50.77 | 1.602 | 7.86 | 7.88 | 1.984 | 116.7488 | SA | SA | SA |

* SA = Specimen was retained for surface analysis.

## APPENDIX B-2
## Individual Specimen Data, Seal-Welded Container Test No. 14

Test No: 14
Test Type: Vapor Phase Exposure
Test Environment: Simulated WIPP Brine A Vapor + N2 (10 atm)
Test Temperature: 30 ±5°C
Test Exposure: 6 Months

| Specimen | Material Type | Length, mm | Width, mm | Thickness, mm | Top Hole ID, mm | Bot. Hole ID, mm | Area, dm2 | Initial Wt., g | Final Wt., g | Corrosion Rate, mpy | Corrosion Rate, µm/yr |
|---|---|---|---|---|---|---|---|---|---|---|---|
| J40 | Low-Carbon Steel, Lot J | 188.97 | 80.09 | 0.699 | 7.82 | 7.84 | 3.049 | 80.4540 | 80.4293 | 0.0078 | 0.199 |
| J41 | Low-Carbon Steel, Lot J | 188.96 | 80.10 | 0.706 | 7.84 | 7.84 | 3.049 | 80.3870 | 80.3624 | 0.0078 | 0.199 |
| J42 | Low-Carbon Steel, Lot J | 188.95 | 80.10 | 0.685 | 7.82 | 7.85 | 3.048 | 78.4684 | 78.4421 | 0.0084 | 0.212 |
| J240 | Low-Carbon Steel, Lot J | 188.83 | 50.75 | 0.697 | 7.58 | 7.84 | 1.935 | 50.7707 | SA* | SA | SA |
| J241 | Low-Carbon Steel, Lot J | 188.83 | 50.73 | 0.697 | 7.76 | 7.82 | 1.934 | 50.7602 | 50.7460 | 0.0071 | 0.181 |
| J242 | Low-Carbon Steel, Lot J | 188.83 | 50.75 | 0.692 | 7.81 | 7.82 | 1.934 | 50.3101 | 50.2961 | 0.0070 | 0.178 |
| K40 | Low-Carbon Steel, Lot K | 188.96 | 80.13 | 0.884 | 7.85 | 7.87 | 3.061 | 102.6329 | 102.6003 | 0.0103 | 0.262 |
| K41 | Low-Carbon Steel, Lot K | 188.95 | 80.14 | 0.866 | 7.88 | 7.81 | 3.060 | 100.0001 | 99.9826 | 0.0055 | 0.141 |
| K42 | Low-Carbon Steel, Lot K | 188.95 | 80.13 | 0.887 | 7.88 | 7.86 | 3.061 | 102.7006 | 102.6789 | 0.0069 | 0.174 |
| K240 | Low-Carbon Steel, Lot K | 188.89 | 50.77 | 0.879 | 7.88 | 7.86 | 1.945 | 63.9198 | 63.9039 | 0.0079 | 0.201 |
| K241 | Low-Carbon Steel, Lot K | 188.90 | 50.77 | 0.875 | 7.87 | 7.87 | 1.945 | 63.6705 | SA | SA | SA |
| K242 | Low-Carbon Steel, Lot K | 188.90 | 50.79 | 0.878 | 7.88 | 7.85 | 1.946 | 63.5059 | 63.4963 | 0.0048 | 0.121 |
| L40 | Low-Carbon Steel, Lot L | 188.90 | 80.01 | 1.505 | 7.81 | 7.85 | 3.092 | 174.7145 | 174.6882 | 0.0082 | 0.209 |
| L41 | Low-Carbon Steel, Lot L | 188.91 | 80.02 | 1.524 | 7.86 | 7.86 | 3.093 | 175.8240 | 175.7930 | 0.0097 | 0.247 |
| L42 | Low-Carbon Steel, Lot L | 188.94 | 80.03 | 1.493 | 7.84 | 7.86 | 3.092 | 174.3934 | 174.3593 | 0.0107 | 0.271 |
| L240 | Low-Carbon Steel, Lot L | 188.91 | 50.80 | 1.511 | 7.86 | 7.90 | 1.980 | 110.2232 | 110.2082 | 0.0073 | 0.186 |
| L241 | Low-Carbon Steel, Lot L | 188.89 | 50.79 | 1.560 | 7.87 | 7.83 | 1.982 | 114.3206 | SA | SA | SA |
| L242 | Low-Carbon Steel, Lot L | 188.92 | 50.78 | 1.552 | 7.85 | 7.88 | 1.981 | 113.5412 | 113.5162 | 0.0122 | 0.310 |
| M40 | Low-Carbon Steel, Lot M | 188.91 | 80.06 | 1.620 | 7.88 | 7.88 | 3.100 | 188.5504 | 188.5181 | 0.0101 | 0.256 |
| M41 | Low-Carbon Steel, Lot M | 188.90 | 80.07 | 1.623 | 7.85 | 7.83 | 3.101 | 187.0956 | 187.0698 | 0.0081 | 0.205 |
| M42 | Low-Carbon Steel, Lot M | 188.86 | 80.08 | 1.611 | 7.86 | 7.88 | 3.100 | 187.7237 | 187.6942 | 0.0092 | 0.234 |
| M240 | Low-Carbon Steel, Lot M | 188.94 | 50.74 | 1.585 | 7.87 | 7.83 | 1.982 | 116.4061 | 116.3939 | 0.0060 | 0.151 |
| M241 | Low-Carbon Steel, Lot M | 188.94 | 50.76 | 1.619 | 7.88 | 7.86 | 1.984 | 119.0870 | SA | SA | SA |
| M242 | Low-Carbon Steel, Lot M | 188.95 | 50.76 | 1.615 | 7.89 | 7.87 | 1.984 | 119.1614 | 119.1458 | 0.0076 | 0.193 |

* SA = Specimen was retained for surface analysis.

## APPENDIX B-2
## Individual Specimen Data, Seal-Welded Container Test No. 21

Test No: 21
Test Type: Vapor Phase Exposure
Test Environment: Simulated WIPP Brine A Vapor +N2 (10 atm)
Test Temperature: 30 ±5°C
Test Exposure: 12 Months

| Specimen | Material Type | Length, mm | Width, mm | Thickness, mm | Top Hole ID, mm | Bot. Hole ID, mm | Area, dm2 | Initial Wt., g | Final Wt., g | Corrosion Rate, mpy | Corrosion Rate, µm/yr |
|---|---|---|---|---|---|---|---|---|---|---|---|
| J61 | Low-Carbon Steel, Lot J | 189.10 | 79.98 | 0.708 | 7.88 | 7.92 | 3.047 | 81.9678 | 81.9551 | 0.0021 | 0.053 |
| J62 | Low-Carbon Steel, Lot J | 189.09 | 79.99 | 0.699 | 7.86 | 7.89 | 3.047 | 81.4793 | 81.4631 | 0.0027 | 0.067 |
| J63 | Low-Carbon Steel, Lot J | 189.05 | 80.01 | 0.700 | 7.84 | 7.86 | 3.047 | 81.2433 | 81.2270 | 0.0027 | 0.068 |
| J261 | Low-Carbon Steel, Lot J | 189.09 | 50.67 | 0.713 | 7.90 | 7.88 | 1.934 | 51.9571 | 51.9463 | 0.0028 | 0.071 |
| J262 | Low-Carbon Steel, Lot J | 189.11 | 50.75 | 0.711 | 7.88 | 7.91 | 1.938 | 51.8130 | SA* | SA | SA |
| J263 | Low-Carbon Steel, Lot J | 189.14 | 50.66 | 0.704 | 7.91 | 7.89 | 1.934 | 51.0897 | 51.0800 | 0.0025 | 0.064 |
| K61 | Low-Carbon Steel, Lot K | 189.15 | 79.98 | 0.870 | 7.86 | 7.92 | 3.057 | 101.5718 | 101.5529 | 0.0031 | 0.078 |
| K62 | Low-Carbon Steel, Lot K | 189.14 | 80.09 | 0.869 | 7.88 | 7.81 | 3.061 | 101.4023 | 101.3854 | 0.0028 | 0.070 |
| K63 | Low-Carbon Steel, Lot K | 189.16 | 80.00 | 0.865 | 7.85 | 7.89 | 3.058 | 100.5147 | 100.4987 | 0.0026 | 0.066 |
| K261 | Low-Carbon Steel, Lot K | 189.10 | 50.67 | 0.864 | 7.94 | 7.87 | 1.942 | 63.1254 | SA | SA | SA |
| K262 | Low-Carbon Steel, Lot K | 189.10 | 50.68 | 0.864 | 7.91 | 7.92 | 1.943 | 63.4264 | 63.4183 | 0.0021 | 0.053 |
| K263 | Low-Carbon Steel, Lot K | 189.10 | 50.75 | 0.871 | 7.93 | 7.88 | 1.946 | 63.8094 | 63.7969 | 0.0032 | 0.081 |
| L61 | Low-Carbon Steel, Lot L | 189.15 | 80.03 | 1.553 | 7.94 | 7.91 | 3.099 | 181.1958 | 181.1687 | 0.0044 | 0.111 |
| L62 | Low-Carbon Steel, Lot L | 189.17 | 79.98 | 1.498 | 7.95 | 7.92 | 3.094 | 176.1699 | 176.1470 | 0.0037 | 0.094 |
| L63 | Low-Carbon Steel, Lot L | 189.20 | 80.01 | 1.504 | 7.94 | 7.91 | 3.096 | 176.0578 | 176.0357 | 0.0036 | 0.090 |
| L261 | Low-Carbon Steel, Lot L | 189.15 | 50.68 | 1.557 | 7.94 | 7.90 | 1.980 | 113.9161 | 113.8993 | 0.0042 | 0.108 |
| L262 | Low-Carbon Steel, Lot L | 189.17 | 50.70 | 1.488 | 7.94 | 7.93 | 1.977 | 109.7299 | SA | SA | SA |
| L263 | Low-Carbon Steel, Lot L | 189.19 | 50.72 | 1.566 | 7.94 | 7.94 | 1.982 | 114.3665 | 114.3471 | 0.0049 | 0.124 |
| M61 | Low-Carbon Steel, Lot M | 189.23 | 80.11 | 1.612 | 7.93 | 7.92 | 3.107 | 189.3613 | 189.3410 | 0.0033 | 0.083 |
| M62 | Low-Carbon Steel, Lot M | 189.27 | 80.11 | 1.626 | 7.91 | 7.91 | 3.109 | 190.4287 | 190.4079 | 0.0033 | 0.085 |
| M63 | Low-Carbon Steel, Lot M | 189.29 | 80.16 | 1.612 | 7.92 | 7.93 | 3.110 | 189.8820 | 189.8629 | 0.0031 | 0.078 |
| M261 | Low-Carbon Steel, Lot M | 189.06 | 50.69 | 1.604 | 7.92 | 7.93 | 1.982 | 118.1401 | 118.1283 | 0.0030 | 0.075 |
| M262 | Low-Carbon Steel, Lot M | 189.05 | 50.67 | 1.608 | 7.93 | 7.92 | 1.981 | 118.0343 | SA | SA | SA |
| M263 | Low-Carbon Steel, Lot M | 189.06 | 50.52 | 1.580 | 7.92 | 7.93 | 1.974 | 114.3347 | 114.3188 | 0.0040 | 0.102 |

* SA = Specimen was retained for surface analysis.

## APPENDIX B-2
## Individual Specimen Data, Seal-Welded Container Test No. 22

Test No: 22
Test Type: Vapor Phase Exposure
Test Environment: Simulated WIPP Brine A Vapor +N2 (10 atm)
Test Temperature: 30 ±5°C
Test Exposure: 12 Months

| Specimen | Material Type | Length, mm | Width, mm | Thickness, mm | Top Hole ID, mm | Bot. Hole ID, mm | Area, dm2 | Initial Wt., g | Final Wt., g | Corrosion Rate, mpy | Corrosion Rate, µm/yr |
|---|---|---|---|---|---|---|---|---|---|---|---|
| J64 | Low-Carbon Steel, Lot J | 189.11 | 79.96 | 0.705 | 7.86 | 7.89 | 3.046 | 81.5597 | 81.5417 | 0.0029 | 0.075 |
| J65 | Low-Carbon Steel, Lot J | 189.10 | 79.95 | 0.709 | 7.92 | 7.83 | 3.046 | 81.8360 | 81.8160 | 0.0033 | 0.083 |
| J66 | Low-Carbon Steel, Lot J | 189.09 | 79.94 | 0.705 | 7.90 | 7.82 | 3.045 | 81.4581 | 81.4403 | 0.0029 | 0.074 |
| J264 | Low-Carbon Steel, Lot J | 189.13 | 50.75 | 0.722 | 7.85 | 7.86 | 1.938 | 52.4947 | 52.4859 | 0.0023 | 0.058 |
| J265 | Low-Carbon Steel, Lot J | 189.14 | 50.75 | 0.705 | 7.90 | 7.91 | 1.937 | 50.9732 | 50.9641 | 0.0023 | 0.060 |
| J266 | Low-Carbon Steel, Lot J | 189.13 | 50.71 | 0.702 | 7.86 | 7.85 | 1.936 | 50.6710 | SA* | SA | SA |
| K64 | Low-Carbon Steel, Lot K | 189.14 | 79.98 | 0.867 | 7.90 | 7.85 | 3.057 | 100.9647 | 100.9289 | 0.0058 | 0.148 |
| K65 | Low-Carbon Steel, Lot K | 189.14 | 79.98 | 0.896 | 7.90 | 7.90 | 3.059 | 103.8692 | 103.8507 | 0.0030 | 0.077 |
| K66 | Low-Carbon Steel, Lot K | 189.14 | 79.98 | 0.897 | 7.90 | 7.87 | 3.059 | 103.1913 | 103.1758 | 0.0025 | 0.064 |
| K264 | Low-Carbon Steel, Lot K | 189.08 | 50.74 | 0.869 | 7.87 | 7.91 | 1.945 | 63.8704 | 63.8585 | 0.0031 | 0.078 |
| K265 | Low-Carbon Steel, Lot K | 189.07 | 50.75 | 0.873 | 7.91 | 7.92 | 1.946 | 63.8454 | SA | SA | SA |
| K266 | Low-Carbon Steel, Lot K | 189.08 | 50.69 | 0.873 | 7.89 | 7.92 | 1.943 | 63.5818 | 63.5688 | 0.0033 | 0.085 |
| L64 | Low-Carbon Steel, Lot L | 189.17 | 80.00 | 1.501 | 7.95 | 7.93 | 3.095 | 175.2797 | 175.2388 | 0.0066 | 0.168 |
| L65 | Low-Carbon Steel, Lot L | 189.17 | 80.00 | 1.538 | 7.92 | 7.93 | 3.097 | 179.6310 | 179.6042 | 0.0043 | 0.110 |
| L66 | Low-Carbon Steel, Lot L | 189.19 | 80.00 | 1.534 | 7.94 | 7.95 | 3.097 | 178.8025 | 178.7730 | 0.0048 | 0.121 |
| L264 | Low-Carbon Steel, Lot L | 189.19 | 50.72 | 1.547 | 7.96 | 7.92 | 1.981 | 112.9342 | 112.9185 | 0.0040 | 0.100 |
| L265 | Low-Carbon Steel, Lot L | 189.19 | 50.74 | 1.498 | 7.97 | 7.93 | 1.979 | 109.8000 | 109.7840 | 0.0040 | 0.102 |
| L266 | Low-Carbon Steel, Lot L | 189.21 | 50.72 | 1.541 | 7.96 | 7.93 | 1.981 | 113.1228 | SA | SA | SA |
| M64 | Low-Carbon Steel, Lot M | 189.34 | 80.15 | 1.548 | 7.93 | 7.94 | 3.106 | 182.5703 | 182.5497 | 0.0033 | 0.084 |
| M65 | Low-Carbon Steel, Lot M | 189.36 | 80.18 | 1.607 | 7.93 | 7.93 | 3.111 | 189.1902 | 189.1695 | 0.0033 | 0.084 |
| M66 | Low-Carbon Steel, Lot M | 189.37 | 80.19 | 1.584 | 7.95 | 7.92 | 3.111 | 185.9014 | 185.8767 | 0.0040 | 0.101 |
| M264 | Low-Carbon Steel, Lot M | 189.08 | 50.62 | 1.567 | 7.96 | 7.96 | 1.977 | 115.0593 | 115.0463 | 0.0033 | 0.083 |
| M265 | Low-Carbon Steel, Lot M | 189.11 | 50.44 | 1.582 | 7.96 | 7.96 | 1.972 | 114.8420 | 114.8296 | 0.0031 | 0.080 |
| M266 | Low-Carbon Steel, Lot M | 189.12 | 50.60 | 1.557 | 7.94 | 7.93 | 1.977 | 114.2275 | SA | SA | SA |

* SA = Specimen was retained for surface analysis.

## APPENDIX B-2
## Individual Specimen Data, Seal-Welded Container Test No. 29

Test No.: 29
Test Type: Vapor Phase Exposure
Test Environment: Simulated WIPP Brine A Vapor + N2 (10 atm)
Test Temperature: 30 ±5°C
Test Exposure: 24 Months

| Specimen | Material Type | Length, mm | Width, mm | Thickness, mm | Top Hole ID, mm | Bot. Hole ID, mm | Area, dm2 | Initial Wt., g | Final Wt., g | Corrosion Rate, mpy | Corrosion Rate, µm/yr |
|---|---|---|---|---|---|---|---|---|---|---|---|
| J85 | Low-Carbon Steel, Lot J | 188.96 | 79.97 | 0.702 | 7.91 | 7.91 | 3.044 | 81.0579 | 81.0232 | 0.0028 | 0.071 |
| J86 | Low-Carbon Steel, Lot J | 188.96 | 79.98 | 0.709 | 7.93 | 7.94 | 3.045 | 81.3179 | 81.2897 | 0.0023 | 0.058 |
| J87 | Low-Carbon Steel, Lot J | 188.95 | 79.95 | 0.706 | 7.92 | 7.93 | 3.043 | 81.1321 | 81.1059 | 0.0021 | 0.054 |
| J285 | Low-Carbon Steel, Lot J | 189.12 | 50.88 | 0.711 | 7.90 | 7.90 | 1.943 | 51.7369 | SA* | SA | SA |
| J286 | Low-Carbon Steel, Lot J | 189.10 | 50.89 | 0.701 | 7.92 | 7.92 | 1.942 | 51.5338 | 51.5150 | 0.0024 | 0.061 |
| J287 | Low-Carbon Steel, Lot J | 189.14 | 50.88 | 0.714 | 7.91 | 7.93 | 1.943 | 52.3371 | 52.3199 | 0.0022 | 0.055 |
| K85 | Low-Carbon Steel, Lot K | 188.83 | 79.96 | 0.873 | 7.92 | 7.92 | 3.051 | 101.5585 | 101.5376 | 0.0017 | 0.043 |
| K86 | Low-Carbon Steel, Lot K | 188.91 | 79.96 | 0.862 | 7.94 | 7.91 | 3.052 | 100.3989 | 100.3758 | 0.0019 | 0.047 |
| K87 | Low-Carbon Steel, Lot K | 189.93 | 79.95 | 0.878 | 7.91 | 7.94 | 3.069 | 102.0867 | 102.0592 | 0.0022 | 0.056 |
| K285 | Low-Carbon Steel, Lot K | 189.10 | 50.92 | 0.864 | 7.92 | 7.92 | 1.952 | 63.2837 | 63.2640 | 0.0025 | 0.063 |
| K286 | Low-Carbon Steel, Lot K | 189.11 | 50.88 | 0.868 | 7.91 | 7.93 | 1.951 | 64.0563 | SA | SA | SA |
| K287 | Low-Carbon Steel, Lot K | 189.12 | 50.84 | 0.863 | 7.91 | 7.94 | 1.949 | 63.6442 | 63.6221 | 0.0028 | 0.071 |
| L85 | Low-Carbon Steel, Lot L | 188.87 | 79.92 | 1.549 | 7.92 | 7.93 | 3.090 | 179.8499 | 179.8074 | 0.0034 | 0.086 |
| L86 | Low-Carbon Steel, Lot L | 188.87 | 79.91 | 1.509 | 7.94 | 7.92 | 3.087 | 175.4831 | 175.4435 | 0.0032 | 0.080 |
| L87 | Low-Carbon Steel, Lot L | 188.87 | 79.91 | 1.508 | 7.95 | 7.95 | 3.087 | 175.2537 | 175.2074 | 0.0037 | 0.094 |
| L285 | Low-Carbon Steel, Lot L | 189.07 | 50.83 | 1.560 | 7.93 | 7.91 | 1.985 | 113.3798 | 113.3477 | 0.0040 | 0.101 |
| L286 | Low-Carbon Steel, Lot L | 189.08 | 50.83 | 1.522 | 7.93 | 7.92 | 1.983 | 110.3635 | SA | SA | SA |
| L287 | Low-Carbon Steel, Lot L | 189.07 | 50.81 | 1.555 | 7.93 | 7.93 | 1.984 | 113.2895 | 113.2535 | 0.0045 | 0.114 |
| M85 | Low-Carbon Steel, Lot M | 188.89 | 79.99 | 1.571 | 7.91 | 7.90 | 3.095 | 183.9039 | 183.8634 | 0.0032 | 0.082 |
| M86 | Low-Carbon Steel, Lot M | 188.87 | 80.00 | 1.609 | 7.90 | 7.90 | 3.097 | 188.5787 | 188.5526 | 0.0021 | 0.053 |
| M87 | Low-Carbon Steel, Lot M | 188.96 | 80.02 | 1.585 | 7.89 | 7.91 | 3.098 | 185.7263 | 185.7002 | 0.0021 | 0.053 |
| M285 | Low-Carbon Steel, Lot M | 189.03 | 50.70 | 1.601 | 7.91 | 7.90 | 1.982 | 117.4508 | 117.4300 | 0.0026 | 0.066 |
| M286 | Low-Carbon Steel, Lot M | 189.03 | 50.67 | 1.582 | 7.92 | 7.90 | 1.980 | 115.8337 | 115.8150 | 0.0023 | 0.059 |
| M287 | Low-Carbon Steel, Lot M | 189.04 | 50.71 | 1.559 | 7.94 | 7.92 | 1.980 | 114.3128 | SA | SA | SA |

*SA = Specimen was retained for surface analysis.

## APPENDIX B-2
## Individual Specimen Data, Seal-Welded Container Test No. 30

Test No.: 30
Test Type: Vapor Phase Exposure
Test Environment: Simulated WIPP Brine A Vapor + N2 (10 atm)
Test Temperature: 30 ±5°C
Test Exposure: 24 Months

| Specimen | Material Type | Length, mm | Width, mm | Thickness, mm | Top Hole ID, mm | Bot. Hole ID, mm | Area, dm2 | Initial Wt., g | Final Wt., g | Corrosion Rate, mpy | Corrosion Rate, µm/yr |
|---|---|---|---|---|---|---|---|---|---|---|---|
| J88 | Low-Carbon Steel, Lot J | 188.96 | 79.97 | 0.702 | 7.92 | 7.93 | 3.044 | 80.7136 | 80.6792 | 0.0028 | 0.071 |
| J89 | Low-Carbon Steel, Lot J | 189.00 | 79.94 | 0.706 | 7.92 | 7.94 | 3.043 | 81.3005 | 81.2809 | 0.0016 | 0.040 |
| J90 | Low-Carbon Steel, Lot J | 189.02 | 79.96 | 0.715 | 7.93 | 7.93 | 3.045 | 81.9655 | 81.9459 | 0.0016 | 0.040 |
| J288 | Low-Carbon Steel, Lot J | 189.13 | 50.89 | 0.711 | 7.91 | 7.94 | 1.943 | 52.1447 | SA* | SA | SA |
| J289 | Low-Carbon Steel, Lot J | 189.12 | 50.91 | 0.717 | 7.91 | 7.90 | 1.944 | 52.5598 | 52.5481 | 0.0015 | 0.038 |
| J290 | Low-Carbon Steel, Lot J | 189.17 | 50.92 | 0.721 | 7.92 | 7.90 | 1.945 | 52.5694 | 52.5554 | 0.0018 | 0.045 |
| K88 | Low-Carbon Steel, Lot K | 188.90 | 79.94 | 0.860 | 7.93 | 7.91 | 3.051 | 99.9478 | 99.9259 | 0.0018 | 0.045 |
| K89 | Low-Carbon Steel, Lot K | 188.91 | 80.03 | 0.881 | 7.94 | 7.92 | 3.056 | 102.1515 | 102.1301 | 0.0017 | 0.044 |
| K90 | Low-Carbon Steel, Lot K | 188.91 | 79.96 | 0.875 | 7.92 | 7.93 | 3.053 | 101.8537 | 101.8308 | 0.0018 | 0.047 |
| K288 | Low-Carbon Steel, Lot K | 189.14 | 50.86 | 0.870 | 8.36 | 7.91 | 1.949 | 63.8811 | SA | SA | SA |
| K289 | Low-Carbon Steel, Lot K | 189.13 | 50.93 | 0.866 | 7.93 | 7.91 | 1.953 | 63.9961 | 63.9851 | 0.0014 | 0.035 |
| K290 | Low-Carbon Steel, Lot K | 189.13 | 50.85 | 0.869 | 7.95 | 7.91 | 1.950 | 63.9998 | 63.9822 | 0.0022 | 0.056 |
| L88 | Low-Carbon Steel, Lot L | 188.88 | 79.91 | 1.500 | 7.92 | 7.93 | 3.087 | 174.4848 | 174.4534 | 0.0025 | 0.064 |
| L89 | Low-Carbon Steel, Lot L | 188.87 | 79.94 | 1.555 | 7.93 | 7.92 | 3.091 | 180.0901 | 180.0611 | 0.0023 | 0.059 |
| L90 | Low-Carbon Steel, Lot L | 188.91 | 79.94 | 1.561 | 7.93 | 7.94 | 3.092 | 180.6883 | 180.6564 | 0.0025 | 0.064 |
| L288 | Low-Carbon Steel, Lot L | 189.09 | 50.85 | 1.562 | 7.93 | 7.93 | 1.986 | 114.1488 | 114.1286 | 0.0025 | 0.064 |
| L289 | Low-Carbon Steel, Lot L | 189.13 | 50.84 | 1.513 | 7.93 | 7.91 | 1.984 | 111.2062 | SA | SA | SA |
| L290 | Low-Carbon Steel, Lot L | 189.14 | 50.82 | 1.524 | 7.92 | 7.94 | 1.983 | 111.1832 | 111.1619 | 0.0026 | 0.067 |
| M88 | Low-Carbon Steel, Lot M | 188.94 | 80.06 | 1.604 | 7.93 | 7.92 | 3.100 | 187.6189 | 187.5772 | 0.0033 | 0.084 |
| M89 | Low-Carbon Steel, Lot M | 188.95 | 80.03 | 1.614 | 7.91 | 7.93 | 3.099 | 189.2799 | 189.2551 | 0.0020 | 0.050 |
| M90 | Low-Carbon Steel, Lot M | 188.95 | 80.05 | 1.581 | 7.92 | 7.94 | 3.098 | 185.6152 | 185.5892 | 0.0021 | 0.052 |
| M288 | Low-Carbon Steel, Lot M | 189.12 | 50.69 | 1.582 | 7.93 | 7.94 | 1.981 | 115.9691 | 115.9532 | 0.0020 | 0.050 |
| M289 | Low-Carbon Steel, Lot M | 189.07 | 50.70 | 1.585 | 7.93 | 7.90 | 1.981 | 115.4328 | SA | SA | SA |
| M290 | Low-Carbon Steel, Lot M | 189.09 | 50.77 | 1.549 | 7.92 | 7.93 | 1.982 | 113.4237 | 113.4066 | 0.0021 | 0.054 |

*SA = Specimen was retained for surface analysis.

## APPENDIX B-3: INDIVIDUAL SPECIMEN CORROSION-RATE DATA, ANOXIC BRINE ($CO_2$/IMMERSED) ENVIRONMENT, SEAL-WELDED-CONTAINER TEST METHOD

## APPENDIX B-3
## Individual Specimen Data, Seal-Welded Container Test No. 3

Test No.: 3
Test Type: Immersion
Test Environment: Simulated WIPP Brine A, CO2 Overpressure (12 atm)
Test Temperature: 30 ±5°C
Test Exposure: 3 Months

| Specimen | Material Type | Length, mm | Width, mm | Thickness, mm | Top Hole ID, mm | Bot. Hole ID, mm | Area, dm2 | Initial Wt., g | Final Wt., g | Corrosion Rate, mpy | Corrosion Rate, µm/yr |
|---|---|---|---|---|---|---|---|---|---|---|---|
| J7 | Low-Carbon Steel, Lot J | 191.14 | 86.60 | 0.706 | 7.96 | 7.96 | 3.333 | 89.6822 | 88.9643 | 0.423 | 10.739 |
| J8 | Low-Carbon Steel, Lot J | 190.90 | 86.49 | 0.703 | 7.96 | 7.95 | 3.325 | 88.8109 | 88.0909 | 0.425 | 10.798 |
| J9 | Low-Carbon Steel, Lot J | 191.22 | 86.56 | 0.698 | 7.96 | 7.97 | 3.333 | 88.5780 | 87.8283 | 0.442 | 11.217 |
| J207 | Low-Carbon Steel, Lot J | 190.82 | 51.42 | 0.708 | 7.94 | 7.93 | 1.980 | 52.9288 | SA* | SA | SA |
| J208 | Low-Carbon Steel, Lot J | 191.09 | 51.41 | 0.715 | 7.99 | 8.00 | 1.983 | 53.3468 | 53.0005 | 0.343 | 8.708 |
| J209 | Low-Carbon Steel, Lot J | 190.70 | 51.42 | 0.719 | 8.11 | 8.10 | 1.979 | 52.5722 | 51.8871 | 0.680 | 17.262 |
| K7 | Low-Carbon Steel, Lot K | 190.59 | 86.26 | 0.877 | 7.97 | 7.96 | 3.321 | 111.2580 | 110.6618 | 0.352 | 8.952 |
| K8 | Low-Carbon Steel, Lot K | 190.58 | 86.15 | 0.868 | 7.96 | 7.94 | 3.316 | 109.7743 | 109.2249 | 0.325 | 8.261 |
| K9 | Low-Carbon Steel, Lot K | 190.54 | 86.32 | 0.873 | 7.96 | 7.96 | 3.322 | 110.3311 | 109.6990 | 0.374 | 9.487 |
| K207 | Low-Carbon Steel, Lot K | 190.38 | 51.36 | 0.885 | 7.96 | 7.96 | 1.983 | 65.9886 | 65.6516 | 0.334 | 8.475 |
| K208 | Low-Carbon Steel, Lot K | 190.25 | 51.35 | 0.869 | 7.97 | 7.96 | 1.980 | 64.4717 | 64.1096 | 0.359 | 9.118 |
| K209 | Low-Carbon Steel, Lot K | 190.29 | 51.30 | 0.888 | 7.96 | 7.96 | 1.980 | 65.6494 | SA | SA | SA |
| L7 | Low-Carbon Steel, Lot L | 190.88 | 86.35 | 1.549 | 7.97 | 7.96 | 3.370 | 197.1697 | 196.7695 | 0.233 | 5.921 |
| L8 | Low-Carbon Steel, Lot L | 190.82 | 86.41 | 1.556 | 7.97 | 7.96 | 3.372 | 197.3520 | 197.0446 | 0.179 | 4.546 |
| L9 | Low-Carbon Steel, Lot L | 190.65 | 86.37 | 1.556 | 7.97 | 7.95 | 3.367 | 197.4031 | 197.0804 | 0.188 | 4.779 |
| L207 | Low-Carbon Steel, Lot L | 190.49 | 51.31 | 1.523 | 7.96 | 7.96 | 2.016 | 113.0462 | 112.7509 | 0.288 | 7.303 |
| L208 | Low-Carbon Steel, Lot L | 190.59 | 51.32 | 1.556 | 7.97 | 7.97 | 2.019 | 115.4697 | SA | SA | SA |
| L209 | Low-Carbon Steel, Lot L | 190.69 | 51.31 | 1.536 | 7.97 | 7.97 | 2.019 | 114.5975 | 114.4094 | 0.183 | 4.646 |
| M7 | Low-Carbon Steel, Lot M | 189.83 | 84.32 | 1.588 | 7.99 | 8.00 | 3.276 | 196.7823 | 195.8714 | 0.546 | 13.864 |
| M8 | Low-Carbon Steel, Lot M | 189.96 | 84.34 | 1.607 | 8.00 | 8.00 | 3.280 | 199.3454 | 198.8286 | 0.309 | 7.856 |
| M9 | Low-Carbon Steel, Lot M | 190.92 | 84.33 | 1.588 | 8.00 | 8.00 | 3.295 | 198.0555 | 197.5907 | 0.277 | 7.033 |
| M207 | Low-Carbon Steel, Lot M | 190.77 | 51.21 | 1.591 | 8.00 | 8.00 | 2.019 | 118.7277 | 118.4063 | 0.313 | 7.939 |
| M208 | Low-Carbon Steel, Lot M | 190.30 | 51.21 | 1.595 | 8.01 | 8.00 | 2.014 | 120.4206 | 120.1534 | 0.260 | 6.616 |
| M209 | Low-Carbon Steel, Lot M | 190.71 | 51.23 | 1.602 | 8.01 | 8.00 | 2.019 | 119.8208 | SA | SA | SA |

* SA = Specimen was retained for surface analysis.

## APPENDIX B-3
## Individual Specimen Data, Seal-Welded Container Test No. 4

Test No.: 4
Test Type: Immersion
Test Environment: Simulated WIPP Brine A, CO2 Overpressure (12 atm)
Test Temperature: 30 ±5°C
Test Exposure: 3 Months

| Specimen | Material Type | Length, mm | Width, mm | Thickness, mm | Top Hole ID, mm | Bot. Hole ID, mm | Area, dm2 | Initial Wt., g | Final Wt., g | Corrosion Rate, mpy | Corrosion Rate, µm/yr |
|---|---|---|---|---|---|---|---|---|---|---|---|
| J10 | Low-Carbon Steel, Lot J | 191.13 | 86.74 | 0.701 | 7.96 | 7.96 | 3.338 | 88.7716 | 87.8619 | 0.535 | 13.588 |
| J11 | Low-Carbon Steel, Lot J | 190.72 | 86.78 | 0.704 | 7.97 | 7.96 | 3.333 | 89.1730 | 88.3056 | 0.511 | 12.978 |
| J12 | Low-Carbon Steel, Lot J | 190.61 | 86.24 | 0.708 | 7.95 | 7.95 | 3.311 | 89.4414 | 88.7932 | 0.384 | 9.763 |
| J210 | Low-Carbon Steel, Lot J | 190.40 | 51.15 | 0.716 | 7.97 | 7.96 | 1.966 | 52.5713 | 52.0152 | 0.555 | 14.104 |
| J211 | Low-Carbon Steel, Lot J | 190.55 | 51.47 | 0.711 | 7.98 | 7.97 | 1.980 | 52.9630 | 52.2422 | 0.715 | 18.157 |
| J212 | Low-Carbon Steel, Lot J | 190.68 | 51.47 | 0.710 | 7.96 | 7.96 | 1.981 | 52.6438 | SA* | SA | SA |
| K10 | Low-Carbon Steel, Lot K | 189.59 | 86.22 | 0.866 | 8.00 | 7.99 | 3.301 | 108.7415 | 108.0088 | 0.436 | 11.067 |
| K11 | Low-Carbon Steel, Lot K | 190.02 | 86.15 | 0.867 | 8.00 | 7.99 | 3.306 | 108.8873 | 108.2597 | 0.373 | 9.465 |
| K12 | Low-Carbon Steel, Lot K | 190.23 | 86.22 | 0.868 | 8.01 | 8.00 | 3.313 | 109.3152 | 108.6920 | 0.369 | 9.381 |
| K210 | Low-Carbon Steel, Lot K | 189.40 | 51.20 | 0.875 | 8.01 | 8.00 | 1.966 | 64.7175 | 64.3014 | 0.416 | 10.555 |
| K211 | Low-Carbon Steel, Lot K | 189.50 | 51.30 | 0.868 | 8.00 | 8.00 | 1.970 | 64.5583 | SA | SA | SA |
| K212 | Low-Carbon Steel, Lot K | 188.88 | 51.17 | 0.872 | 8.01 | 8.00 | 1.959 | 64.2470 | 63.8068 | 0.441 | 11.204 |
| L10 | Low-Carbon Steel, Lot L | 190.53 | 86.49 | 1.537 | 7.95 | 7.95 | 3.369 | 195.4332 | 195.1021 | 0.193 | 4.901 |
| L11 | Low-Carbon Steel, Lot L | 190.24 | 86.33 | 1.540 | 7.97 | 7.96 | 3.358 | 195.1232 | 194.8036 | 0.187 | 4.746 |
| L12 | Low-Carbon Steel, Lot L | 190.39 | 86.37 | 1.538 | 7.97 | 7.95 | 3.362 | 195.3679 | 194.9886 | 0.222 | 5.626 |
| L210 | Low-Carbon Steel, Lot L | 190.44 | 51.18 | 1.496 | 7.97 | 7.97 | 2.009 | 111.1462 | 110.9507 | 0.191 | 4.852 |
| L211 | Low-Carbon Steel, Lot L | 190.73 | 51.42 | 1.492 | 7.98 | 7.97 | 2.021 | 111.6578 | SA | SA | SA |
| L212 | Low-Carbon Steel, Lot L | 190.27 | 51.40 | 1.552 | 7.98 | 7.97 | 2.019 | 115.5176 | 115.2931 | 0.218 | 5.545 |
| M10 | Low-Carbon Steel, Lot M | 190.22 | 84.31 | 1.576 | 8.01 | 8.00 | 3.282 | 197.0038 | 196.5995 | 0.242 | 6.143 |
| M11 | Low-Carbon Steel, Lot M | 190.08 | 84.43 | 1.612 | 8.00 | 8.00 | 3.286 | 200.1839 | 199.8368 | 0.207 | 5.267 |
| M12 | Low-Carbon Steel, Lot M | 190.36 | 84.43 | 1.550 | 8.01 | 8.01 | 3.287 | 193.6257 | 193.2085 | 0.249 | 6.329 |
| M210 | Low-Carbon Steel, Lot M | 190.34 | 51.41 | 1.616 | 8.02 | 8.01 | 2.023 | 121.3934 | 121.1619 | 0.225 | 5.706 |
| M211 | Low-Carbon Steel, Lot M | 190.85 | 51.33 | 1.603 | 8.03 | 8.02 | 2.025 | 120.0643 | SA | SA | SA |
| M212 | Low-Carbon Steel, Lot M | 190.60 | 51.30 | 1.599 | 8.03 | 8.03 | 2.021 | 119.5115 | 119.2148 | 0.288 | 7.321 |

* SA = Specimen was retained for surface analysis.

## APPENDIX B-3
## Individual Specimen Data, Seal-Welded Container Test No. 11

Test No: 11
Test Type: Immersion
Test Environment: Simulated WIPP Brine A, CO2 Overpressure (12 atm)
Test Temperature: 30 ±5°C
Test Exposure: 6 Months

| Specimen | Material Type | Length, mm | Width, mm | Thickness, mm | Top Hole ID, mm | Bot. Hole ID, mm | Area, dm2 | Initial Wt., g | Final Wt., g | Corrosion Rate, mpy | Corrosion Rate, µm/yr |
|---|---|---|---|---|---|---|---|---|---|---|---|
| J31 | Low-Carbon Steel, Lot J | 188.93 | 80.08 | 0.702 | 7.95 | 7.91 | 3.047 | 80.0602 | 78.9040 | 0.3679 | 9.344 |
| J32 | Low-Carbon Steel, Lot J | 188.93 | 80.09 | 0.713 | 7.95 | 7.96 | 3.048 | 81.3335 | 80.4336 | 0.2862 | 7.270 |
| J33 | Low-Carbon Steel, Lot J | 188.93 | 80.09 | 0.708 | 7.97 | 7.94 | 3.048 | 81.3839 | 80.3414 | 0.3316 | 8.423 |
| J231 | Low-Carbon Steel, Lot J | 188.83 | 50.78 | 0.709 | 7.95 | 7.95 | 1.935 | 50.9416 | SA* | SA | SA |
| J232 | Low-Carbon Steel, Lot J | 188.83 | 50.78 | 0.715 | 7.94 | 7.91 | 1.936 | 51.2092 | 50.4458 | 0.3824 | 9.712 |
| J233 | Low-Carbon Steel, Lot J | 188.83 | 50.78 | 0.710 | 8.05 | 7.70 | 1.936 | 51.2145 | 50.2643 | 0.4759 | 12.089 |
| K31 | Low-Carbon Steel, Lot K | 188.91 | 80.09 | 0.864 | 7.98 | 7.97 | 3.057 | 100.2633 | 99.5902 | 0.2135 | 5.423 |
| K32 | Low-Carbon Steel, Lot K | 188.92 | 80.09 | 0.884 | 7.98 | 7.98 | 3.058 | 102.5432 | 101.8378 | 0.2237 | 5.681 |
| K33 | Low-Carbon Steel, Lot K | 188.91 | 80.10 | 0.876 | 7.98 | 7.97 | 3.058 | 101.6378 | 100.4497 | 0.3767 | 9.569 |
| K231 | Low-Carbon Steel, Lot K | 188.83 | 50.74 | 0.875 | 7.99 | 7.97 | 1.943 | 63.6236 | SA | SA | SA |
| K232 | Low-Carbon Steel, Lot K | 188.84 | 50.73 | 0.875 | 7.99 | 7.98 | 1.942 | 63.7375 | 62.7541 | 0.4909 | 12.470 |
| K233 | Low-Carbon Steel, Lot K | 188.85 | 50.67 | 0.869 | 7.99 | 7.98 | 1.940 | 63.3250 | 62.6792 | 0.3228 | 8.199 |
| L31 | Low-Carbon Steel, Lot L | 188.91 | 80.02 | 1.554 | 7.99 | 7.98 | 3.095 | 180.6953 | 180.1964 | 0.1563 | 3.970 |
| L32 | Low-Carbon Steel, Lot L | 188.91 | 80.02 | 1.508 | 7.99 | 7.97 | 3.092 | 173.7476 | 173.2288 | 0.1627 | 4.132 |
| L33 | Low-Carbon Steel, Lot L | 188.91 | 80.02 | 1.503 | 7.98 | 7.97 | 3.092 | 173.7478 | 173.2274 | 0.1632 | 4.145 |
| L231 | Low-Carbon Steel, Lot L | 188.90 | 50.27 | 1.567 | 7.98 | 7.98 | 1.962 | 112.5016 | 112.1628 | 0.1674 | 4.253 |
| L232 | Low-Carbon Steel, Lot L | 188.89 | 50.76 | 1.559 | 7.99 | 7.98 | 1.980 | 113.8185 | SA | SA | SA |
| L233 | Low-Carbon Steel, Lot L | 188.87 | 50.78 | 1.555 | 7.98 | 7.98 | 1.980 | 113.1084 | 112.6689 | 0.2152 | 5.465 |
| M31 | Low-Carbon Steel, Lot M | 188.90 | 80.04 | 1.606 | 7.99 | 7.98 | 3.098 | 188.5694 | 187.7950 | 0.2423 | 6.156 |
| M32 | Low-Carbon Steel, Lot M | 188.88 | 80.03 | 1.576 | 7.98 | 7.98 | 3.096 | 183.0774 | 182.4466 | 0.1976 | 5.018 |
| M33 | Low-Carbon Steel, Lot M | 188.87 | 80.01 | 1.586 | 7.98 | 7.98 | 3.096 | 184.6954 | 184.0358 | 0.2066 | 5.248 |
| M231 | Low-Carbon Steel, Lot M | 188.94 | 50.79 | 1.619 | 7.98 | 7.98 | 1.985 | 118.1074 | SA | SA | SA |
| M232 | Low-Carbon Steel, Lot M | 188.92 | 50.78 | 1.586 | 7.98 | 7.98 | 1.983 | 117.2962 | 116.8442 | 0.2210 | 5.615 |
| M233 | Low-Carbon Steel, Lot M | 188.91 | 50.70 | 1.565 | 7.99 | 7.99 | 1.978 | 114.3836 | 113.9568 | 0.2092 | 5.313 |

* SA = Specimen was retained for surface analysis.

## APPENDIX B-3
## Individual Specimen Data, Seal-Welded Container Test No. 12

Test No: 12
Test Type: Immersion
Test Environment: Simulated WIPP Brine A, CO2 Overpressure (12 atm)
Test Temperature: 30 ±5°C
Test Exposure: 6 Months

| Specimen | Material Type | Length, mm | Width, mm | Thickness, mm | Top Hole ID, mm | Bot. Hole ID, mm | Area, dm2 | Initial Wt., g | Final Wt., g | Corrosion Rate, mpy | Corrosion Rate, µm/yr |
|---|---|---|---|---|---|---|---|---|---|---|---|
| J34 | Low-Carbon Steel, Lot J | 188.94 | 80.10 | 0.692 | 8.01 | 8.00 | 3.047 | 80.2577 | 79.4066 | 0.2706 | 6.872 |
| J35 | Low-Carbon Steel, Lot J | 188.92 | 80.10 | 0.689 | 7.99 | 7.91 | 3.047 | 79.4202 | 78.7872 | 0.2012 | 5.112 |
| J36 | Low-Carbon Steel, Lot J | 188.95 | 80.10 | 0.711 | 8.01 | 8.02 | 3.049 | 80.9811 | 80.0300 | 0.3022 | 7.676 |
| J234 | Low-Carbon Steel, Lot J | 188.85 | 50.79 | 0.698 | 7.77 | 8.03 | 1.936 | 50.3958 | 49.7281 | 0.3342 | 8.488 |
| J235 | Low-Carbon Steel, Lot J | 188.85 | 50.79 | 0.713 | 8.09 | 7.80 | 1.936 | 51.6316 | SA* | SA | SA |
| J236 | Low-Carbon Steel, Lot J | 188.85 | 50.73 | 0.709 | 7.78 | 8.05 | 1.934 | 51.1730 | 50.4057 | 0.3844 | 9.763 |
| K34 | Low-Carbon Steel, Lot K | 188.95 | 80.11 | 0.883 | 8.03 | 8.03 | 3.059 | 102.4166 | 101.3527 | 0.3369 | 8.558 |
| K35 | Low-Carbon Steel, Lot K | 188.95 | 80.11 | 0.891 | 8.04 | 8.04 | 3.060 | 103.6533 | 102.7167 | 0.2966 | 7.533 |
| K36 | Low-Carbon Steel, Lot K | 188.96 | 80.11 | 0.884 | 8.04 | 8.03 | 3.059 | 102.5319 | 101.2962 | 0.3913 | 9.939 |
| K234 | Low-Carbon Steel, Lot K | 188.87 | 50.76 | 0.882 | 8.03 | 8.03 | 1.944 | 64.1602 | 63.8577 | 0.1508 | 3.829 |
| K235 | Low-Carbon Steel, Lot K | 188.87 | 50.77 | 0.872 | 8.04 | 8.04 | 1.944 | 63.5034 | 62.8671 | 0.3171 | 8.055 |
| K236 | Low-Carbon Steel, Lot K | 188.88 | 50.77 | 0.882 | 8.04 | 8.04 | 1.944 | 64.0895 | SA | SA | SA |
| L34 | Low-Carbon Steel, Lot L | 188.94 | 80.03 | 1.556 | 8.04 | 8.04 | 3.095 | 180.1520 | 179.7073 | 0.1392 | 3.535 |
| L35 | Low-Carbon Steel, Lot L | 188.92 | 80.02 | 1.553 | 8.04 | 8.03 | 3.095 | 180.3099 | 179.9042 | 0.1270 | 3.226 |
| L36 | Low-Carbon Steel, Lot L | 188.92 | 80.01 | 1.552 | 8.05 | 8.04 | 3.094 | 179.5812 | 179.1778 | 0.1263 | 3.208 |
| L234 | Low-Carbon Steel, Lot L | 188.90 | 50.75 | 1.561 | 8.05 | 8.04 | 1.980 | 113.7402 | 113.5039 | 0.1156 | 2.937 |
| L235 | Low-Carbon Steel, Lot L | 188.93 | 50.80 | 1.559 | 8.04 | 8.04 | 1.982 | 113.7897 | 113.5187 | 0.1325 | 3.365 |
| L236 | Low-Carbon Steel, Lot L | 188.89 | 50.78 | 1.546 | 8.04 | 8.04 | 1.980 | 113.1743 | SA | SA | SA |
| M34 | Low-Carbon Steel, Lot M | 188.87 | 80.02 | 1.553 | 8.04 | 8.04 | 3.094 | 181.5511 | 180.9146 | 0.1993 | 5.062 |
| M35 | Low-Carbon Steel, Lot M | 188.88 | 80.00 | 1.599 | 8.04 | 8.04 | 3.096 | 185.5557 | 185.0397 | 0.1615 | 4.101 |
| M36 | Low-Carbon Steel, Lot M | 188.88 | 80.00 | 1.589 | 8.04 | 8.05 | 3.095 | 184.9131 | 184.1543 | 0.2375 | 6.032 |
| M234 | Low-Carbon Steel, Lot M | 188.92 | 50.74 | 1.569 | 8.05 | 8.04 | 1.980 | 114.8283 | SA | SA | SA |
| M235 | Low-Carbon Steel, Lot M | 188.92 | 50.79 | 1.604 | 8.05 | 8.04 | 1.984 | 118.3917 | 118.1223 | 0.1316 | 3.342 |
| M236 | Low-Carbon Steel, Lot M | 188.92 | 50.79 | 1.578 | 8.05 | 8.03 | 1.982 | 115.3701 | 115.0396 | 0.1615 | 4.102 |

* SA = Specimen was retained for surface analysis.

## APPENDIX B-3
## Individual Specimen Data, Seal-Welded Container Test No. 19

Test No: 19
Test Type: Immersion
Test Environment: Simulated WIPP Brine A, CO2 Overpressure (12 atm)
Test Temperature: 30 ±5°C
Test Exposure: 12 Months

| Specimen | Material Type | Length, mm | Width, mm | Thickness, mm | Top Hole ID, mm | Bot. Hole ID, mm | Area, dm2 | Initial Wt., g | Final Wt., g | Corrosion Rate, mpy | Corrosion Rate, µm/yr |
|---|---|---|---|---|---|---|---|---|---|---|---|
| J55 | Low-Carbon Steel, Lot J | 189.11 | 79.96 | 0.706 | 7.83 | 7.86 | 3.046 | 81.5981 | 80.7627 | 0.1329 | 3.376 |
| J56 | Low-Carbon Steel, Lot J | 189.09 | 79.95 | 0.708 | 7.84 | 7.84 | 3.046 | 81.8740 | 81.3033 | 0.0908 | 2.307 |
| J57 | Low-Carbon Steel, Lot J | 189.09 | 79.96 | 0.711 | 7.80 | 7.85 | 3.042 | 81.8164 | 81.1144 | 0.1118 | 2.840 |
| J255 | Low-Carbon Steel, Lot J | 189.08 | 50.72 | 0.719 | 7.84 | 7.88 | 1.937 | 51.7608 | SA* | SA | SA |
| J256 | Low-Carbon Steel, Lot J | 189.10 | 50.60 | 0.713 | 7.92 | 7.88 | 1.932 | 51.5461 | 50.9211 | 0.1568 | 3.983 |
| J257 | Low-Carbon Steel, Lot J | 189.11 | 50.70 | 0.709 | 7.91 | 7.91 | 1.935 | 51.5252 | 50.8732 | 0.1633 | 4.147 |
| K55 | Low-Carbon Steel, Lot K | 189.10 | 79.95 | 0.866 | 7.78 | 7.79 | 3.056 | 101.0552 | 100.3553 | 0.1110 | 2.820 |
| K56 | Low-Carbon Steel, Lot K | 189.11 | 79.95 | 0.885 | 7.83 | 7.83 | 3.057 | 103.1937 | 102.2030 | 0.1571 | 3.990 |
| K57 | Low-Carbon Steel, Lot K | 189.12 | 79.97 | 0.854 | 7.89 | 7.92 | 3.055 | 99.7712 | 98.6927 | 0.1711 | 4.345 |
| K255 | Low-Carbon Steel, Lot K | 189.09 | 50.71 | 0.884 | 7.91 | 7.84 | 1.945 | 65.1223 | 64.7259 | 0.0988 | 2.509 |
| K256 | Low-Carbon Steel, Lot K | 189.09 | 50.74 | 0.878 | 7.88 | 7.80 | 1.946 | 64.8900 | 64.2907 | 0.1493 | 3.791 |
| K257 | Low-Carbon Steel, Lot K | 189.08 | 50.74 | 0.876 | 7.84 | 7.88 | 1.946 | 64.7653 | SA | SA | SA |
| L55 | Low-Carbon Steel, Lot L | 189.17 | 80.00 | 1.562 | 7.93 | 7.94 | 3.099 | 182.0185 | 181.5973 | 0.0659 | 1.673 |
| L56 | Low-Carbon Steel, Lot L | 189.15 | 79.99 | 1.549 | 7.94 | 7.93 | 3.097 | 180.2001 | 179.6670 | 0.0834 | 2.119 |
| L57 | Low-Carbon Steel, Lot L | 189.14 | 79.98 | 1.553 | 7.93 | 7.95 | 3.097 | 181.4972 | 181.0665 | 0.0674 | 1.712 |
| L255 | Low-Carbon Steel, Lot L | 189.14 | 50.71 | 1.569 | 7.96 | 7.95 | 1.981 | 114.5227 | SA | SA | SA |
| L256 | Low-Carbon Steel, Lot L | 189.12 | 50.68 | 1.511 | 7.94 | 7.93 | 1.977 | 110.4609 | 110.2196 | 0.0591 | 1.502 |
| L257 | Low-Carbon Steel, Lot L | 189.12 | 50.67 | 1.496 | 7.94 | 7.94 | 1.976 | 109.6952 | 109.4363 | 0.0635 | 1.613 |
| M55 | Low-Carbon Steel, Lot M | 189.31 | 80.12 | 1.601 | 7.95 | 7.95 | 3.108 | 187.0912 | 186.4560 | 0.0991 | 2.516 |
| M56 | Low-Carbon Steel, Lot M | 189.29 | 80.12 | 1.548 | 7.94 | 7.90 | 3.105 | 182.6324 | 182.0434 | 0.0919 | 2.335 |
| M57 | Low-Carbon Steel, Lot M | 189.25 | 80.10 | 1.553 | 7.92 | 7.92 | 3.103 | 183.5540 | 182.8145 | 0.1155 | 2.933 |
| M255 | Low-Carbon Steel, Lot M | 189.31 | 50.62 | 1.602 | 7.94 | 7.92 | 1.982 | 117.8308 | 117.3415 | 0.1197 | 3.039 |
| M256 | Low-Carbon Steel, Lot M | 189.29 | 50.48 | 1.583 | 7.94 | 7.96 | 1.975 | 116.4617 | 116.1487 | 0.0768 | 1.951 |
| M257 | Low-Carbon Steel, Lot M | 189.26 | 50.59 | 1.610 | 7.95 | 7.96 | 1.980 | 117.9880 | SA | SA | SA |

* SA = Specimen was retained for surface analysis.

## APPENDIX B-3
## Individual Specimen Data, Seal-Welded Container Test No. 20

Test No: 20
Test Type: Immersion
Test Environment: Simulated WIPP Brine A, CO2 Overpressure (12 atm)
Test Temperature: 30 ±5°C
Test Exposure: 12 Months

| Specimen | Material Type | Length, mm | Width, mm | Thickness, mm | Top Hole ID, mm | Bot. Hole ID, mm | Area, dm2 | Initial Wt., g | Final Wt., g | Corrosion Rate, mpy | Corrosion Rate, µm/yr |
|---|---|---|---|---|---|---|---|---|---|---|---|
| J58 | Low-Carbon Steel, Lot J | 189.12 | 80.01 | 0.702 | 7.89 | 7.86 | 3.048 | 80.9211 | 79.8984 | 0.1626 | 4.130 |
| J59 | Low-Carbon Steel, Lot J | 189.12 | 79.98 | 0.704 | 7.87 | 7.92 | 3.047 | 81.8872 | 80.8236 | 0.1692 | 4.297 |
| J60 | Low-Carbon Steel, Lot J | 189.11 | 79.97 | 0.690 | 7.85 | 7.92 | 3.046 | 80.5422 | 79.7011 | 0.1338 | 3.400 |
| J258 | Low-Carbon Steel, Lot J | 189.12 | 50.66 | 0.731 | 7.92 | 7.90 | 1.935 | 52.2297 | 51.6413 | 0.1474 | 3.743 |
| J259 | Low-Carbon Steel, Lot J | 189.14 | 50.68 | 0.726 | 7.87 | 7.89 | 1.936 | 52.3322 | 51.6187 | 0.1786 | 4.537 |
| J260 | Low-Carbon Steel, Lot J | 189.13 | 50.69 | 0.724 | 7.92 | 7.90 | 1.936 | 52.3393 | SA* | SA | SA |
| K58 | Low-Carbon Steel, Lot K | 189.14 | 79.97 | 0.860 | 7.89 | 7.89 | 3.056 | 100.5629 | 99.3321 | 0.1952 | 4.958 |
| K59 | Low-Carbon Steel, Lot K | 189.14 | 79.98 | 0.865 | 7.89 | 7.88 | 3.057 | 100.9443 | 99.9581 | 0.1564 | 3.971 |
| K60 | Low-Carbon Steel, Lot K | 189.14 | 79.98 | 0.869 | 7.88 | 7.90 | 3.057 | 102.3157 | 101.4593 | 0.1358 | 3.449 |
| K258 | Low-Carbon Steel, Lot K | 189.09 | 50.32 | 0.889 | 7.86 | 7.86 | 1.931 | 65.0805 | SA | SA | SA |
| K259 | Low-Carbon Steel, Lot K | 189.09 | 50.70 | 0.886 | 7.92 | 7.88 | 1.945 | 65.1449 | 64.6333 | 0.1275 | 3.238 |
| K260 | Low-Carbon Steel, Lot K | 189.10 | 50.68 | 0.860 | 7.90 | 7.87 | 1.943 | 63.1326 | 62.7096 | 0.1055 | 2.680 |
| L58 | Low-Carbon Steel, Lot L | 189.13 | 79.98 | 1.557 | 7.92 | 7.90 | 3.097 | 180.6159 | 180.2452 | 0.0580 | 1.473 |
| L59 | Low-Carbon Steel, Lot L | 189.15 | 79.98 | 1.548 | 7.93 | 7.90 | 3.097 | 180.0252 | 179.6116 | 0.0647 | 1.644 |
| L60 | Low-Carbon Steel, Lot L | 189.16 | 79.97 | 1.566 | 7.93 | 7.93 | 3.098 | 181.7287 | 181.2482 | 0.0752 | 1.909 |
| L258 | Low-Carbon Steel, Lot L | 189.15 | 50.69 | 1.558 | 7.95 | 7.90 | 1.980 | 113.6880 | 113.4177 | 0.0661 | 1.680 |
| L259 | Low-Carbon Steel, Lot L | 189.15 | 50.73 | 1.486 | 7.95 | 7.91 | 1.978 | 109.3001 | SA | SA | SA |
| L260 | Low-Carbon Steel, Lot L | 189.15 | 50.71 | 1.551 | 7.95 | 7.91 | 1.981 | 110.2340 | 109.9352 | 0.0731 | 1.857 |
| M58 | Low-Carbon Steel, Lot M | 189.27 | 80.10 | 1.557 | 7.90 | 7.84 | 3.104 | 183.3880 | 182.9589 | 0.0670 | 1.702 |
| M59 | Low-Carbon Steel, Lot M | 189.25 | 80.09 | 1.620 | 7.89 | 7.89 | 3.107 | 188.9110 | 188.3172 | 0.0926 | 2.353 |
| M60 | Low-Carbon Steel, Lot M | 189.24 | 80.10 | 1.616 | 7.86 | 7.90 | 3.107 | 188.9908 | 188.1878 | 0.1252 | 3.181 |
| M258 | Low-Carbon Steel, Lot M | 189.09 | 50.21 | 1.606 | 7.93 | 7.94 | 1.964 | 115.8765 | SA | SA | SA |
| M259 | Low-Carbon Steel, Lot M | 189.10 | 50.65 | 1.605 | 7.91 | 7.92 | 1.981 | 117.7221 | 117.1470 | 0.1407 | 3.574 |
| M260 | Low-Carbon Steel, Lot M | 189.08 | 50.68 | 1.599 | 7.90 | 7.86 | 1.982 | 117.5165 | 116.9818 | 0.1308 | 3.322 |

* SA = Specimen was retained for surface analysis.

## APPENDIX B-3
## Individual Specimen Data, Seal-Welded Container Test No. 27

Test No.: 27
Test Type: Immersion
Test Environment: Simulated WIPP Brine A, CO2 Overpressure (12 atm)
Test Temperature: 30 ±5°C
Test Exposure: 24 Months

| Specimen | Material Type | Length, mm | Width, mm | Thickness, mm | Top Hole ID, mm | Bot. Hole ID, mm | Area, dm2 | Initial Wt., g | Final Wt., g | Corrosion Rate, mpy | Corrosion Rate, µm/yr |
|---|---|---|---|---|---|---|---|---|---|---|---|
| J79 | Low-Carbon Steel, Lot J | 188.98 | 80.01 | 0.714 | 7.97 | 7.97 | 3.046 | 81.9966 | 81.0910 | 0.0731 | 1.856 |
| J80 | Low-Carbon Steel, Lot J | 188.99 | 80.03 | 0.709 | 7.96 | 7.94 | 3.047 | 82.0435 | 81.2813 | 0.0615 | 1.562 |
| J81 | Low-Carbon Steel, Lot J | 189.00 | 80.01 | 0.705 | 7.94 | 7.96 | 3.046 | 81.9907 | 81.0176 | 0.0785 | 1.995 |
| J279 | Low-Carbon Steel, Lot J | 189.15 | 50.93 | 0.719 | 7.95 | 7.98 | 1.945 | 52.2287 | 51.7101 | 0.0655 | 1.665 |
| J280 | Low-Carbon Steel, Lot J | 189.17 | 50.92 | 0.702 | 7.96 | 7.96 | 1.944 | 51.3165 | 50.9371 | 0.0480 | 1.219 |
| J281 | Low-Carbon Steel, Lot J | 189.18 | 50.89 | 0.702 | 7.96 | 7.95 | 1.943 | 51.3331 | SA* | SA | SA |
| K79 | Low-Carbon Steel, Lot K | 188.94 | 79.97 | 0.861 | 7.98 | 7.96 | 3.053 | 99.9204 | 99.2529 | 0.0538 | 1.365 |
| K80 | Low-Carbon Steel, Lot K | 188.97 | 79.98 | 0.863 | 7.96 | 7.94 | 3.054 | 100.5006 | 99.5972 | 0.0727 | 1.847 |
| K81 | Low-Carbon Steel, Lot K | 188.99 | 79.99 | 0.855 | 7.94 | 7.97 | 3.054 | 99.7339 | 98.9676 | 0.0617 | 1.567 |
| K279 | Low-Carbon Steel, Lot K | 189.08 | 50.85 | 0.871 | 7.95 | 7.96 | 1.949 | 64.4807 | SA | SA | SA |
| K280 | Low-Carbon Steel, Lot K | 189.10 | 50.86 | 0.878 | 7.96 | 7.91 | 1.950 | 64.7214 | 64.2372 | 0.0610 | 1.550 |
| K281 | Low-Carbon Steel, Lot K | 189.09 | 50.86 | 0.860 | 7.98 | 7.96 | 1.949 | 63.4749 | 62.9064 | 0.0717 | 1.821 |
| L79 | Low-Carbon Steel, Lot L | 189.00 | 80.03 | 1.499 | 7.98 | 7.96 | 3.093 | 175.0865 | 174.6950 | 0.0311 | 0.790 |
| L80 | Low-Carbon Steel, Lot L | 189.00 | 80.03 | 1.544 | 7.96 | 7.94 | 3.096 | 180.8945 | 180.5277 | 0.0291 | 0.740 |
| L81 | Low-Carbon Steel, Lot L | 188.97 | 80.02 | 1.550 | 7.94 | 7.93 | 3.096 | 181.0917 | 180.0015 | 0.0866 | 2.199 |
| L279 | Low-Carbon Steel, Lot L | 189.24 | 50.77 | 1.566 | 7.94 | 7.97 | 1.985 | 113.9270 | 113.6557 | 0.0336 | 0.854 |
| L280 | Low-Carbon Steel, Lot L | 189.25 | 50.80 | 1.544 | 7.84 | 7.94 | 1.985 | 113.2527 | 112.7035 | 0.0680 | 1.728 |
| L281 | Low-Carbon Steel, Lot L | 189.21 | 50.73 | 1.580 | 7.91 | 7.96 | 1.984 | 115.3752 | SA | SA | SA |
| M79 | Low-Carbon Steel, Lot M | 189.04 | 80.16 | 1.574 | 7.92 | 7.94 | 3.104 | 185.3045 | 184.6508 | 0.0518 | 1.315 |
| M80 | Low-Carbon Steel, Lot M | 189.04 | 80.15 | 1.583 | 7.96 | 7.93 | 3.104 | 186.6548 | 186.1674 | 0.0386 | 0.981 |
| M81 | Low-Carbon Steel, Lot M | 189.03 | 80.13 | 1.573 | 7.95 | 7.98 | 3.102 | 183.0341 | 182.5454 | 0.0387 | 0.984 |
| M279 | Low-Carbon Steel, Lot M | 189.22 | 50.92 | 1.597 | 7.97 | 7.96 | 1.992 | 118.3555 | SA | SA | SA |
| M280 | Low-Carbon Steel, Lot M | 189.19 | 50.92 | 1.605 | 7.92 | 7.92 | 1.992 | 118.4153 | 118.0134 | 0.0496 | 1.260 |
| M281 | Low-Carbon Steel, Lot M | 189.20 | 50.88 | 1.598 | 7.91 | 7.94 | 1.990 | 118.0693 | 117.7003 | 0.0456 | 1.158 |

*SA = Specimen was retained for surface analysis.

## APPENDIX B-3
## Individual Specimen Data, Seal-Welded Container Test No. 28

Test No.: 28
Test Type: Immersion
Test Environment: Simulated WIPP Brine A, CO2 Overpressure (12 atm)
Test Temperature: 30 ±5°C
Test Exposure: 24 Months

| Specimen | Material Type | Length, mm | Width, mm | Thickness, mm | Top Hole ID, mm | Bot. Hole ID, mm | Area, dm2 | Initial Wt., g | Final Wt., g | Corrosion Rate, mpy | Corrosion Rate, µm/yr |
|---|---|---|---|---|---|---|---|---|---|---|---|
| J82 | Low-Carbon Steel, Lot J | 189.04 | 80.06 | 0.702 | 7.99 | 7.97 | 3.048 | 82.0773 | 81.3106 | 0.0617 | 1.568 |
| J83 | Low-Carbon Steel, Lot J | 189.04 | 80.05 | 0.694 | 7.97 | 7.97 | 3.047 | 80.3571 | 79.3098 | 0.0844 | 2.143 |
| J84 | Low-Carbon Steel, Lot J | 189.05 | 80.05 | 0.701 | 7.96 | 7.97 | 3.048 | 81.1452 | 80.2389 | 0.0730 | 1.854 |
| J282 | Low-Carbon Steel, Lot J | 189.23 | 50.95 | 0.713 | 7.98 | 7.98 | 1.946 | 52.0976 | SA* | SA | SA |
| J283 | Low-Carbon Steel, Lot J | 189.22 | 50.96 | 0.699 | 7.96 | 7.96 | 1.946 | 51.0211 | 50.6394 | 0.0482 | 1.223 |
| J284 | Low-Carbon Steel, Lot J | 189.22 | 50.96 | 0.703 | 7.99 | 7.96 | 1.946 | 51.3464 | 50.9825 | 0.0459 | 1.166 |
| K82 | Low-Carbon Steel, Lot K | 188.99 | 80.03 | 0.860 | 7.97 | 7.95 | 3.056 | 100.4228 | 99.4067 | 0.0816 | 2.073 |
| K83 | Low-Carbon Steel, Lot K | 189.00 | 80.02 | 0.877 | 7.97 | 7.96 | 3.056 | 101.9646 | 100.6979 | 0.1017 | 2.584 |
| K84 | Low-Carbon Steel, Lot K | 189.01 | 80.05 | 0.870 | 7.95 | 7.96 | 3.057 | 101.3292 | 100.4551 | 0.0702 | 1.783 |
| K282 | Low-Carbon Steel, Lot K | 189.18 | 50.90 | 0.865 | 7.96 | 7.98 | 1.952 | 63.8153 | SA | SA | SA |
| K283 | Low-Carbon Steel, Lot K | 189.18 | 50.93 | 0.859 | 7.95 | 7.96 | 1.953 | 63.3199 | 62.8758 | 0.0558 | 1.418 |
| K284 | Low-Carbon Steel, Lot K | 189.21 | 50.94 | 0.859 | 7.95 | 7.94 | 1.953 | 63.2987 | 62.5052 | 0.0997 | 2.533 |
| L82 | Low-Carbon Steel, Lot L | 188.98 | 80.02 | 1.565 | 8.00 | 7.98 | 3.096 | 182.3109 | 181.8291 | 0.0382 | 0.970 |
| L83 | Low-Carbon Steel, Lot L | 188.94 | 79.98 | 1.552 | 7.98 | 7.96 | 3.094 | 181.0362 | 180.7109 | 0.0258 | 0.656 |
| L84 | Low-Carbon Steel, Lot L | 188.94 | 79.98 | 1.571 | 7.97 | 7.98 | 3.095 | 182.1545 | 181.7372 | 0.0331 | 0.841 |
| L282 | Low-Carbon Steel, Lot L | 189.22 | 50.89 | 1.567 | 7.95 | 7.93 | 1.989 | 115.4343 | 115.0263 | 0.0504 | 1.279 |
| L283 | Low-Carbon Steel, Lot L | 189.18 | 50.81 | 1.497 | 7.95 | 7.95 | 1.982 | 109.6492 | 109.3121 | 0.0418 | 1.061 |
| L284 | Low-Carbon Steel, Lot L | 189.17 | 50.80 | 1.508 | 7.96 | 7.96 | 1.982 | 110.1402 | SA | SA | SA |
| M82 | Low-Carbon Steel, Lot M | 189.00 | 80.12 | 1.584 | 7.96 | 7.98 | 3.102 | 186.4713 | 185.6583 | 0.0643 | 1.634 |
| M83 | Low-Carbon Steel, Lot M | 188.97 | 80.10 | 1.545 | 7.96 | 8.01 | 3.098 | 181.7548 | 181.1451 | 0.0483 | 1.227 |
| M84 | Low-Carbon Steel, Lot M | 188.98 | 80.08 | 1.588 | 7.99 | 7.97 | 3.100 | 186.5229 | 185.7996 | 0.0573 | 1.455 |
| M282 | Low-Carbon Steel, Lot M | 189.19 | 50.83 | 1.569 | 7.96 | 7.96 | 1.987 | 116.1085 | SA | SA | SA |
| M283 | Low-Carbon Steel, Lot M | 189.16 | 50.84 | 1.601 | 7.96 | 7.95 | 1.988 | 118.8486 | 118.4332 | 0.0513 | 1.303 |
| M284 | Low-Carbon Steel, Lot M | 189.14 | 50.81 | 1.535 | 7.96 | 7.94 | 1.984 | 113.8922 | 113.4784 | 0.0512 | 1.301 |

*SA = Specimen was retained for surface analysis.

## APPENDIX B-4: INDIVIDUAL SPECIMEN CORROSION-RATE DATA, ANOXIC BRINE ($CO_2$/VAPOR) ENVIRONMENT, SEAL-WELDED-CONTAINER TEST METHOD

## APPENDIX B-4
## Individual Specimen Data, Seal-Welded Container Test No. 7

Test No.: 7
Test Type: Vapor Phase Exposure
Test Environment: Simulated WIPP Brine A Vapor + CO2 (10 atm)
Test Temperature: 30 ±5°C
Test Exposure: 3 Months

| Specimen | Material Type | Length, mm | Width, mm | Thickness, mm | Top Hole ID, mm | Bot. Hole ID, mm | Area, dm2 | Initial Wt., g | Final Wt., g | Corrosion Rate, mpy | Corrosion Rate, µm/yr |
|---|---|---|---|---|---|---|---|---|---|---|---|
| J19 | Low-Carbon Steel, Lot J | 189.13 | 85.78 | 0.701 | 8.09 | 8.10 | 3.266 | 87.4959 | 87.4712 | 0.015 | 0.373 |
| J20 | Low-Carbon Steel, Lot J | 189.13 | 85.78 | 0.711 | 8.01 | 8.00 | 3.267 | 88.4081 | 88.3855 | 0.013 | 0.341 |
| J21 | Low-Carbon Steel, Lot J | 189.13 | 85.78 | 0.710 | 8.01 | 8.01 | 3.267 | 87.8460 | 87.8149 | 0.018 | 0.470 |
| J219 | Low-Carbon Steel, Lot J | 189.58 | 50.98 | 0.720 | 8.01 | 8.01 | 1.951 | 52.7502 | 52.7276 | 0.022 | 0.571 |
| J220 | Low-Carbon Steel, Lot J | 189.59 | 50.98 | 0.720 | 8.02 | 8.01 | 1.951 | 52.6166 | SA* | SA | SA |
| J221 | Low-Carbon Steel, Lot J | 189.59 | 50.98 | 0.682 | 8.03 | 8.02 | 1.949 | 50.7769 | 50.7373 | 0.039 | 1.002 |
| K19 | Low-Carbon Steel, Lot K | 189.11 | 85.77 | 0.862 | 7.99 | 8.00 | 3.276 | 108.7068 | 108.6909 | 0.009 | 0.239 |
| K20 | Low-Carbon Steel, Lot K | 189.11 | 85.77 | 0.867 | 8.00 | 8.00 | 3.276 | 109.4164 | 109.4028 | 0.008 | 0.205 |
| K21 | Low-Carbon Steel, Lot K | 189.11 | 85.78 | 0.875 | 8.00 | 8.00 | 3.277 | 109.3517 | 109.3401 | 0.007 | 0.175 |
| K219 | Low-Carbon Steel, Lot K | 189.58 | 50.97 | 0.889 | 8.00 | 8.00 | 1.960 | 65.5730 | 65.5643 | 0.009 | 0.219 |
| K220 | Low-Carbon Steel, Lot K | 189.58 | 50.97 | 0.888 | 8.00 | 8.00 | 1.960 | 65.5550 | 65.5480 | 0.007 | 0.176 |
| K221 | Low-Carbon Steel, Lot K | 189.58 | 50.97 | 0.877 | 8.01 | 8.00 | 1.959 | 64.7891 | SA | SA | SA |
| L19 | Low-Carbon Steel, Lot L | 189.13 | 85.80 | 1.490 | 7.98 | 7.97 | 3.315 | 187.2841 | 187.2598 | 0.014 | 0.362 |
| L20 | Low-Carbon Steel, Lot L | 189.13 | 85.80 | 1.532 | 7.97 | 7.96 | 3.317 | 192.5109 | 192.4857 | 0.015 | 0.375 |
| L21 | Low-Carbon Steel, Lot L | 189.13 | 85.80 | 1.490 | 7.98 | 7.97 | 3.315 | 187.9035 | 187.8749 | 0.017 | 0.426 |
| L219 | Low-Carbon Steel, Lot L | 189.60 | 50.99 | 1.538 | 7.97 | 7.98 | 1.995 | 113.3141 | 113.2979 | 0.016 | 0.401 |
| L220 | Low-Carbon Steel, Lot L | 189.60 | 50.99 | 1.544 | 7.99 | 7.99 | 1.996 | 113.9537 | 113.9315 | 0.022 | 0.549 |
| L221 | Low-Carbon Steel, Lot L | 189.60 | 50.98 | 1.559 | 7.99 | 7.98 | 1.996 | 115.4085 | SA | SA | SA |
| M19 | Low-Carbon Steel, Lot M | 189.12 | 84.35 | 1.613 | 7.97 | 7.97 | 3.267 | 200.1505 | 200.1297 | 0.012 | 0.314 |
| M20 | Low-Carbon Steel, Lot M | 189.12 | 84.35 | 1.620 | 7.98 | 7.98 | 3.267 | 200.4969 | 200.4733 | 0.014 | 0.356 |
| M21 | Low-Carbon Steel, Lot M | 189.13 | 85.81 | 1.575 | 7.98 | 7.98 | 3.320 | 198.1883 | 198.1654 | 0.013 | 0.340 |
| M219 | Low-Carbon Steel, Lot M | 189.61 | 50.98 | 1.552 | 7.98 | 7.98 | 1.996 | 115.2150 | 115.2049 | 0.010 | 0.250 |
| M220 | Low-Carbon Steel, Lot M | 189.60 | 50.98 | 1.592 | 7.99 | 7.98 | 1.998 | 118.3897 | SA | SA | SA |
| M221 | Low-Carbon Steel, Lot M | 189.60 | 50.98 | 1.579 | 7.98 | 7.98 | 1.997 | 117.9729 | 117.9509 | 0.021 | 0.543 |

* SA = Specimen was retained for surface analysis.

## APPENDIX B-4
## Individual Specimen Data, Seal-Welded Container Test No. 8

Test No.: 8
Test Type: Vapor Phase Exposure
Test Environment: Simulated WIPP Brine A Vapor + CO2 (10 atm)
Test Temperature: 30 ±5°C
Test Exposure: 3 Months

| Specimen | Material Type | Length, mm | Width, mm | Thickness, mm | Top Hole ID, mm | Bot. Hole ID, mm | Area, dm2 | Initial Wt., g | Final Wt., g | Corrosion Rate, mpy | Corrosion Rate, µm/yr |
|---|---|---|---|---|---|---|---|---|---|---|---|
| J22 | Low-Carbon Steel, Lot J | 189.14 | 85.79 | 0.718 | 7.99 | 7.99 | 3.268 | 88.1511 | 88.1247 | 0.016 | 0.398 |
| J23 | Low-Carbon Steel, Lot J | 189.14 | 85.78 | 0.709 | 7.99 | 7.99 | 3.267 | 88.5012 | 88.4797 | 0.013 | 0.325 |
| J24 | Low-Carbon Steel, Lot J | 189.14 | 85.79 | 0.705 | 7.99 | 7.99 | 3.268 | 87.4136 | 87.3831 | 0.018 | 0.460 |
| J222 | Low-Carbon Steel, Lot J | 189.62 | 50.98 | 0.685 | 7.99 | 7.99 | 1.950 | 50.6810 | SA* | SA | SA |
| J223 | Low-Carbon Steel, Lot J | 189.63 | 50.99 | 0.692 | 8.00 | 8.00 | 1.951 | 50.7238 | 50.7028 | 0.021 | 0.531 |
| J224 | Low-Carbon Steel, Lot J | 189.61 | 50.98 | 0.695 | 8.00 | 7.99 | 1.950 | 51.3646 | 51.3354 | 0.029 | 0.739 |
| K22 | Low-Carbon Steel, Lot K | 189.15 | 85.78 | 0.872 | 7.97 | 7.97 | 3.277 | 109.1905 | 109.1701 | 0.012 | 0.307 |
| K23 | Low-Carbon Steel, Lot K | 189.14 | 85.79 | 0.872 | 7.97 | 7.96 | 3.278 | 109.0113 | 108.9867 | 0.015 | 0.370 |
| K24 | Low-Carbon Steel, Lot K | 189.14 | 85.78 | 0.875 | 7.97 | 7.96 | 3.277 | 109.4165 | 109.3997 | 0.010 | 0.253 |
| K222 | Low-Carbon Steel, Lot K | 189.60 | 50.98 | 0.886 | 7.97 | 7.97 | 1.960 | 65.5292 | 65.5115 | 0.018 | 0.445 |
| K223 | Low-Carbon Steel, Lot K | 189.59 | 50.98 | 0.884 | 7.98 | 7.97 | 1.960 | 65.4462 | 65.4335 | 0.013 | 0.320 |
| K224 | Low-Carbon Steel, Lot K | 189.59 | 50.98 | 0.870 | 7.98 | 7.98 | 1.959 | 64.5470 | SA | SA | SA |
| L22 | Low-Carbon Steel, Lot L | 189.14 | 85.79 | 1.484 | 7.98 | 7.97 | 3.314 | 185.6642 | 185.6345 | 0.017 | 0.442 |
| L23 | Low-Carbon Steel, Lot L | 189.14 | 85.79 | 1.543 | 7.98 | 7.97 | 3.318 | 194.4421 | 194.4154 | 0.016 | 0.397 |
| L24 | Low-Carbon Steel, Lot L | 189.15 | 85.79 | 1.539 | 7.99 | 7.98 | 3.318 | 192.8785 | 192.8516 | 0.016 | 0.400 |
| L222 | Low-Carbon Steel, Lot L | 189.59 | 50.99 | 1.545 | 7.98 | 7.99 | 1.996 | 114.0443 | SA | SA | SA |
| L223 | Low-Carbon Steel, Lot L | 189.59 | 50.98 | 1.552 | 7.98 | 7.98 | 1.996 | 115.1881 | 115.1557 | 0.032 | 0.801 |
| L224 | Low-Carbon Steel, Lot L | 189.58 | 50.99 | 1.513 | 7.99 | 7.99 | 1.994 | 112.1181 | 112.0915 | 0.026 | 0.658 |
| M22 | Low-Carbon Steel, Lot M | 189.14 | 84.39 | 1.587 | 7.98 | 7.98 | 3.267 | 196.0964 | 196.0682 | 0.017 | 0.426 |
| M23 | Low-Carbon Steel, Lot M | 189.14 | 84.39 | 1.580 | 7.99 | 7.98 | 3.267 | 194.8490 | 194.8226 | 0.016 | 0.399 |
| M24 | Low-Carbon Steel, Lot M | 189.15 | 84.39 | 1.626 | 7.98 | 7.98 | 3.270 | 200.8466 | 200.8174 | 0.017 | 0.441 |
| M222 | Low-Carbon Steel, Lot M | 189.58 | 50.99 | 1.614 | 7.99 | 7.98 | 1.999 | 120.0831 | SA | SA | SA |
| M223 | Low-Carbon Steel, Lot M | 189.59 | 50.99 | 1.609 | 8.00 | 7.99 | 1.999 | 120.3188 | 120.3062 | 0.012 | 0.311 |
| M224 | Low-Carbon Steel, Lot M | 189.58 | 50.99 | 1.587 | 8.00 | 7.98 | 1.998 | 118.2353 | 118.2107 | 0.024 | 0.608 |

* SA = Specimen was retained for surface analysis.

## APPENDIX B-4
## Individual Specimen Data, Seal-Welded Container Test No. 15

Test No: 15
Test Type: Vapor Phase Exposure
Test Environment: Simulated WIPP Brine A Vapor + CO2 (10 atm)
Test Temperature: 30 ±5°C
Test Exposure: 6 Months

| Specimen | Material Type | Length, mm | Width, mm | Thickness, mm | Top Hole ID, mm | Bot. Hole ID, mm | Area, dm2 | Initial Wt., g | Final Wt., g | Corrosion Rate, mpy | Corrosion Rate, µm/yr |
|---|---|---|---|---|---|---|---|---|---|---|---|
| J43 | Low-Carbon Steel, Lot J | 188.94 | 80.09 | 0.711 | 8.00 | 7.98 | 3.048 | 81.6922 | 81.6774 | 0.0047 | 0.119 |
| J44 | Low-Carbon Steel, Lot J | 188.95 | 80.08 | 0.704 | 8.00 | 7.95 | 3.048 | 81.1870 | 81.1682 | 0.0060 | 0.152 |
| J45 | Low-Carbon Steel, Lot J | 188.94 | 80.07 | 0.702 | 8.02 | 7.99 | 3.047 | 80.4568 | 80.4208 | 0.0114 | 0.291 |
| J243 | Low-Carbon Steel, Lot J | 188.80 | 50.74 | 0.710 | 8.02 | 7.98 | 1.933 | 51.2853 | 51.2567 | 0.0143 | 0.364 |
| J244 | Low-Carbon Steel, Lot J | 188.80 | 50.73 | 0.712 | 8.08 | 7.88 | 1.933 | 51.5502 | SA* | SA | SA |
| J245 | Low-Carbon Steel, Lot J | 188.77 | 50.72 | 0.714 | 7.95 | 8.05 | 1.933 | 51.4095 | 51.3405 | 0.0346 | 0.879 |
| K43 | Low-Carbon Steel, Lot K | 188.91 | 80.09 | 0.864 | 8.01 | 8.01 | 3.057 | 100.0602 | 99.9801 | 0.0254 | 0.645 |
| K44 | Low-Carbon Steel, Lot K | 188.91 | 80.09 | 0.868 | 8.01 | 8.01 | 3.057 | 100.7607 | 100.6312 | 0.0410 | 1.042 |
| K45 | Low-Carbon Steel, Lot K | 188.91 | 80.08 | 0.866 | 8.01 | 8.00 | 3.056 | 100.2789 | 100.2519 | 0.0086 | 0.217 |
| K243 | Low-Carbon Steel, Lot K | 188.88 | 50.78 | 0.879 | 8.01 | 8.01 | 1.945 | 64.1399 | 64.1197 | 0.0101 | 0.256 |
| K244 | Low-Carbon Steel, Lot K | 188.89 | 50.71 | 0.885 | 8.01 | 8.01 | 1.942 | 64.5459 | 64.4956 | 0.0251 | 0.637 |
| K245 | Low-Carbon Steel, Lot K | 188.89 | 50.20 | 0.874 | 8.02 | 8.02 | 1.922 | 63.0785 | SA | SA | SA |
| L43 | Low-Carbon Steel, Lot L | 188.90 | 80.01 | 1.501 | 8.02 | 8.01 | 3.091 | 175.6515 | 175.5875 | 0.0201 | 0.509 |
| L44 | Low-Carbon Steel, Lot L | 188.90 | 80.02 | 1.507 | 8.02 | 8.01 | 3.092 | 176.2958 | 176.2439 | 0.0163 | 0.413 |
| L45 | Low-Carbon Steel, Lot L | 188.91 | 80.02 | 1.509 | 8.01 | 8.01 | 3.092 | 175.1453 | 175.1023 | 0.0135 | 0.342 |
| L243 | Low-Carbon Steel, Lot L | 188.87 | 50.77 | 1.548 | 8.02 | 8.02 | 1.980 | 113.2535 | SA | SA | SA |
| L244 | Low-Carbon Steel, Lot L | 188.87 | 50.75 | 1.506 | 8.02 | 8.01 | 1.977 | 109.3093 | 109.2521 | 0.0280 | 0.712 |
| L245 | Low-Carbon Steel, Lot L | 188.87 | 50.27 | 1.543 | 8.02 | 8.02 | 1.960 | 111.7084 | 111.6328 | 0.0374 | 0.949 |
| M43 | Low-Carbon Steel, Lot M | 188.89 | 80.05 | 1.608 | 8.02 | 8.01 | 3.099 | 188.2269 | 188.1949 | 0.0100 | 0.254 |
| M44 | Low-Carbon Steel, Lot M | 188.90 | 80.04 | 1.584 | 8.02 | 8.01 | 3.097 | 184.9015 | 184.8665 | 0.0109 | 0.278 |
| M45 | Low-Carbon Steel, Lot M | 188.89 | 80.05 | 1.619 | 8.01 | 8.01 | 3.099 | 189.3780 | 189.3368 | 0.0129 | 0.327 |
| M243 | Low-Carbon Steel, Lot M | 188.91 | 50.77 | 1.559 | 8.02 | 8.01 | 1.981 | 114.0451 | 114.0240 | 0.0103 | 0.262 |
| M244 | Low-Carbon Steel, Lot M | 188.89 | 50.76 | 1.558 | 8.02 | 8.02 | 1.980 | 114.1413 | 114.0999 | 0.0203 | 0.515 |
| M245 | Low-Carbon Steel, Lot M | 188.90 | 50.76 | 1.562 | 8.01 | 8.01 | 1.980 | 113.7145 | SA | SA | SA |

* SA = Specimen was retained for surface analysis.

## APPENDIX B-4
## Individual Specimen Data, Seal-Welded Container Test No. 16

Test No: 16
Test Type: Vapor Phase Exposure
Test Environment: Simulated WIPP Brine A Vapor + CO2 (10 atm)
Test Temperature: 30 ±5°C
Test Exposure: 6 Months

| Specimen | Material Type | Length, mm | Width, mm | Thickness, mm | Top Hole ID, mm | Bot. Hole ID, mm | Area, dm2 | Initial Wt., g | Final Wt., g | Corrosion Rate, mpy | Corrosion Rate, µm/yr |
|---|---|---|---|---|---|---|---|---|---|---|---|
| J46 | Low-Carbon Steel, Lot J | 188.95 | 80.07 | 0.704 | 8.00 | 8.00 | 3.047 | 80.5476 | 80.5206 | 0.0086 | 0.218 |
| J47 | Low-Carbon Steel, Lot J | 188.95 | 80.07 | 0.708 | 7.98 | 7.94 | 3.048 | 81.2328 | 81.1523 | 0.0256 | 0.650 |
| J48 | Low-Carbon Steel, Lot J | 188.94 | 80.06 | 0.713 | 7.98 | 7.98 | 3.047 | 81.5028 | 81.4719 | 0.0098 | 0.250 |
| J246 | Low-Carbon Steel, Lot J | 188.78 | 50.72 | 0.711 | 8.00 | 8.00 | 1.933 | 51.5578 | 51.5449 | 0.0065 | 0.164 |
| J247 | Low-Carbon Steel, Lot J | 188.78 | 50.72 | 0.706 | 8.00 | 8.00 | 1.932 | 50.9101 | SA* | SA | SA |
| J248 | Low-Carbon Steel, Lot J | 188.78 | 50.68 | 0.710 | 7.95 | 8.03 | 1.931 | 51.4672 | 51.4508 | 0.0082 | 0.209 |
| K46 | Low-Carbon Steel, Lot K | 188.89 | 80.07 | 0.863 | 8.02 | 8.02 | 3.055 | 100.1253 | 100.0712 | 0.0172 | 0.436 |
| K47 | Low-Carbon Steel, Lot K | 188.86 | 80.04 | 0.885 | 8.02 | 8.02 | 3.055 | 102.7517 | 102.6885 | 0.0200 | 0.509 |
| K48 | Low-Carbon Steel, Lot K | 188.85 | 80.03 | 0.882 | 8.02 | 8.02 | 3.054 | 102.1519 | 102.0891 | 0.0199 | 0.506 |
| K246 | Low-Carbon Steel, Lot K | 188.90 | 50.66 | 0.865 | 8.02 | 8.01 | 1.940 | 63.1837 | 63.0895 | 0.0470 | 1.195 |
| K247 | Low-Carbon Steel, Lot K | 188.91 | 50.70 | 0.877 | 8.02 | 8.02 | 1.942 | 63.4839 | SA | SA | SA |
| K248 | Low-Carbon Steel, Lot K | 188.91 | 50.76 | 0.869 | 8.02 | 8.01 | 1.944 | 63.0387 | 63.0012 | 0.0187 | 0.475 |
| L46 | Low-Carbon Steel, Lot L | 188.91 | 80.03 | 1.512 | 8.02 | 8.02 | 3.092 | 176.3947 | 176.3588 | 0.0112 | 0.286 |
| L47 | Low-Carbon Steel, Lot L | 188.91 | 80.02 | 1.509 | 8.03 | 8.02 | 3.092 | 175.6374 | 175.5947 | 0.0134 | 0.340 |
| L48 | Low-Carbon Steel, Lot L | 188.92 | 80.01 | 1.509 | 8.02 | 8.02 | 3.092 | 175.4664 | 175.4066 | 0.0187 | 0.476 |
| L246 | Low-Carbon Steel, Lot L | 188.88 | 50.49 | 1.562 | 8.03 | 8.02 | 1.970 | 112.9453 | 112.8699 | 0.0371 | 0.942 |
| L247 | Low-Carbon Steel, Lot L | 188.84 | 50.75 | 1.500 | 8.03 | 8.03 | 1.976 | 109.7192 | 109.6457 | 0.0360 | 0.915 |
| L248 | Low-Carbon Steel, Lot L | 188.84 | 50.75 | 1.555 | 8.04 | 8.03 | 1.979 | 113.1176 | SA | SA | SA |
| M46 | Low-Carbon Steel, Lot M | 188.89 | 80.03 | 1.582 | 8.03 | 8.02 | 3.096 | 185.4076 | 185.3686 | 0.0122 | 0.310 |
| M47 | Low-Carbon Steel, Lot M | 188.86 | 80.00 | 1.590 | 8.02 | 8.02 | 3.095 | 186.6108 | 186.5414 | 0.0217 | 0.552 |
| M48 | Low-Carbon Steel, Lot M | 188.83 | 79.98 | 1.590 | 8.02 | 8.02 | 3.094 | 185.7308 | 185.6967 | 0.0107 | 0.271 |
| M246 | Low-Carbon Steel, Lot M | 188.90 | 50.76 | 1.604 | 8.03 | 8.02 | 1.982 | 117.9382 | 117.9264 | 0.0058 | 0.146 |
| M247 | Low-Carbon Steel, Lot M | 188.87 | 50.74 | 1.611 | 8.02 | 8.02 | 1.982 | 117.2196 | SA | SA | SA |
| M248 | Low-Carbon Steel, Lot M | 188.87 | 50.73 | 1.609 | 8.03 | 8.02 | 1.981 | 118.2908 | 118.2547 | 0.0177 | 0.448 |

* SA = Specimen was retained for surface analysis.

## APPENDIX B-4
## Individual Specimen Data, Seal-Welded Container Test No. 23

Test No: 23
Test Type: Vapor Phase Exposure
Test Environment: Simulated WIPP Brine A Vapor +CO2 (10 atm)
Test Temperature: 30 ±5°C
Test Exposure: 12 Months

| Specimen | Material Type | Length, mm | Width, mm | Thickness, mm | Top Hole ID, mm | Bot. Hole ID, mm | Area, dm2 | Initial Wt., g | Final Wt., g | Corrosion Rate, mpy | Corrosion Rate, µm/yr |
|---|---|---|---|---|---|---|---|---|---|---|---|
| J67 | Low-Carbon Steel, Lot J | 189.08 | 79.96 | 0.701 | 7.88 | 7.93 | 3.045 | 81.3418 | 81.3227 | 0.0031 | 0.080 |
| J68 | Low-Carbon Steel, Lot J | 189.09 | 79.98 | 0.710 | 7.86 | 7.88 | 3.047 | 81.9931 | 81.9693 | 0.0039 | 0.099 |
| J69 | Low-Carbon Steel, Lot J | 189.08 | 79.96 | 0.705 | 7.90 | 7.88 | 3.046 | 81.7696 | 81.7274 | 0.0069 | 0.176 |
| J267 | Low-Carbon Steel, Lot J | 189.15 | 50.67 | 0.720 | 7.92 | 7.89 | 1.935 | 51.7629 | 51.7503 | 0.0032 | 0.083 |
| J268 | Low-Carbon Steel, Lot J | 189.14 | 50.65 | 0.731 | 7.89 | 7.90 | 1.935 | 52.1323 | 52.1189 | 0.0035 | 0.088 |
| J269 | Low-Carbon Steel, Lot J | 189.14 | 50.74 | 0.708 | 7.86 | 7.90 | 1.937 | 51.1253 | SA* | SA | SA |
| K67 | Low-Carbon Steel, Lot K | 189.13 | 80.01 | 0.866 | 7.91 | 7.92 | 3.058 | 100.4655 | 100.4378 | 0.0045 | 0.115 |
| K68 | Low-Carbon Steel, Lot K | 189.14 | 80.00 | 0.879 | 7.89 | 7.90 | 3.058 | 102.1231 | 102.1036 | 0.0032 | 0.081 |
| K69 | Low-Carbon Steel, Lot K | 189.14 | 80.00 | 0.871 | 7.91 | 7.93 | 3.058 | 101.5011 | 101.4825 | 0.0030 | 0.077 |
| K267 | Low-Carbon Steel, Lot K | 189.08 | 50.63 | 0.871 | 7.92 | 7.89 | 1.941 | 63.5558 | SA | SA | SA |
| K268 | Low-Carbon Steel, Lot K | 189.08 | 50.77 | 0.881 | 7.83 | 7.86 | 1.947 | 64.0648 | 64.0547 | 0.0026 | 0.066 |
| K269 | Low-Carbon Steel, Lot K | 189.08 | 50.60 | 0.874 | 7.89 | 7.89 | 1.940 | 63.6321 | 63.6177 | 0.0037 | 0.094 |
| L67 | Low-Carbon Steel, Lot L | 189.18 | 80.02 | 1.496 | 7.94 | 7.93 | 3.096 | 174.6833 | 174.6585 | 0.0040 | 0.102 |
| L68 | Low-Carbon Steel, Lot L | 189.18 | 80.02 | 1.498 | 7.95 | 7.95 | 3.096 | 174.8022 | 174.7669 | 0.0057 | 0.145 |
| L69 | Low-Carbon Steel, Lot L | 189.18 | 80.02 | 1.544 | 7.97 | 7.96 | 3.099 | 179.6399 | 179.5993 | 0.0065 | 0.166 |
| L267 | Low-Carbon Steel, Lot L | 189.18 | 50.75 | 1.493 | 7.99 | 7.98 | 1.979 | 109.5154 | 109.4940 | 0.0054 | 0.137 |
| L268 | Low-Carbon Steel, Lot L | 189.17 | 50.76 | 1.531 | 7.96 | 7.97 | 1.982 | 112.6513 | 112.6285 | 0.0057 | 0.146 |
| L269 | Low-Carbon Steel, Lot L | 189.19 | 50.79 | 1.561 | 7.98 | 7.98 | 1.985 | 114.6015 | SA | SA | SA |
| M67 | Low-Carbon Steel, Lot M | 189.35 | 80.19 | 1.576 | 7.97 | 7.96 | 3.110 | 185.1187 | 185.1020 | 0.0027 | 0.068 |
| M68 | Low-Carbon Steel, Lot M | 189.38 | 80.20 | 1.608 | 7.95 | 7.96 | 3.113 | 189.0036 | 188.9802 | 0.0038 | 0.095 |
| M69 | Low-Carbon Steel, Lot M | 189.37 | 80.21 | 1.557 | 7.98 | 7.98 | 3.110 | 182.6606 | 182.6320 | 0.0046 | 0.117 |
| M267 | Low-Carbon Steel, Lot M | 189.12 | 50.68 | 1.565 | 7.95 | 7.97 | 1.980 | 113.6987 | 113.6856 | 0.0033 | 0.084 |
| M268 | Low-Carbon Steel, Lot M | 189.12 | 50.35 | 1.551 | 8.00 | 7.99 | 1.966 | 112.6640 | 112.6483 | 0.0040 | 0.101 |
| M269 | Low-Carbon Steel, Lot M | 189.13 | 50.29 | 1.546 | 7.99 | 8.00 | 1.964 | 112.4100 | SA | SA | SA |

* SA = Specimen was retained for surface analysis.

## APPENDIX B-4
## Individual Specimen Data, Seal-Welded Container Test No. 24

Test No: 24
Test Type: Vapor Phase Exposure
Test Environment: Simulated WIPP Brine A Vapor +CO2 (10 atm)
Test Temperature: 30 ±5°C
Test Exposure: 12 Months

| Specimen | Material Type | Length, mm | Width, mm | Thickness, mm | Top Hole ID, mm | Bot. Hole ID, mm | Area, dm2 | Initial Wt., g | Final Wt., g | Corrosion Rate, mpy | Corrosion Rate, µm/yr |
|---|---|---|---|---|---|---|---|---|---|---|---|
| J70 | Low-Carbon Steel, Lot J | 189.10 | 79.98 | 0.703 | 7.91 | 7.92 | 3.046 | 81.6353 | 81.6148 | 0.0034 | 0.085 |
| J71 | Low-Carbon Steel, Lot J | 189.11 | 80.00 | 0.700 | 7.94 | 7.90 | 3.047 | 81.6443 | 81.6218 | 0.0037 | 0.094 |
| J72 | Low-Carbon Steel, Lot J | 189.10 | 79.98 | 0.708 | 7.93 | 7.92 | 3.047 | 81.4066 | 81.3738 | 0.0054 | 0.136 |
| J270 | Low-Carbon Steel, Lot J | 189.18 | 50.76 | 0.729 | 7.92 | 7.96 | 1.939 | 51.2001 | 51.1890 | 0.0029 | 0.073 |
| J271 | Low-Carbon Steel, Lot J | 189.20 | 50.47 | 0.703 | 7.89 | 7.92 | 1.927 | 50.2557 | 50.2402 | 0.0040 | 0.102 |
| J272 | Low-Carbon Steel, Lot J | 189.21 | 50.78 | 0.710 | 7.88 | 7.93 | 1.940 | 51.4334 | SA* | SA | SA |
| K70 | Low-Carbon Steel, Lot K | 189.18 | 80.02 | 0.884 | 7.93 | 7.96 | 3.060 | 101.7218 | 101.6887 | 0.0054 | 0.137 |
| K71 | Low-Carbon Steel, Lot K | 189.17 | 80.09 | 0.875 | 7.90 | 7.88 | 3.062 | 101.5879 | 101.5657 | 0.0036 | 0.092 |
| K72 | Low-Carbon Steel, Lot K | 189.18 | 80.04 | 0.869 | 7.90 | 7.90 | 3.060 | 101.1717 | 101.1494 | 0.0036 | 0.092 |
| K270 | Low-Carbon Steel, Lot K | 189.09 | 50.77 | 0.865 | 7.90 | 7.89 | 1.946 | 63.2157 | SA | SA | SA |
| K271 | Low-Carbon Steel, Lot K | 189.10 | 50.79 | 0.856 | 7.98 | 7.96 | 1.946 | 62.7625 | 62.7484 | 0.0036 | 0.092 |
| K272 | Low-Carbon Steel, Lot K | 189.07 | 50.70 | 0.870 | 7.94 | 7.95 | 1.943 | 63.1447 | 63.1213 | 0.0060 | 0.153 |
| L70 | Low-Carbon Steel, Lot L | 189.21 | 80.02 | 1.556 | 7.96 | 7.94 | 3.100 | 181.4153 | 181.3846 | 0.0049 | 0.126 |
| L71 | Low-Carbon Steel, Lot L | 189.20 | 80.03 | 1.533 | 7.93 | 7.94 | 3.099 | 178.5215 | 178.4916 | 0.0048 | 0.122 |
| L72 | Low-Carbon Steel, Lot L | 189.19 | 80.03 | 1.559 | 7.94 | 7.95 | 3.100 | 181.3424 | 181.2958 | 0.0075 | 0.191 |
| L270 | Low-Carbon Steel, Lot L | 189.21 | 50.81 | 1.550 | 7.96 | 7.94 | 1.985 | 113.4394 | 113.4151 | 0.0061 | 0.155 |
| L271 | Low-Carbon Steel, Lot L | 189.20 | 50.76 | 1.501 | 7.95 | 7.95 | 1.980 | 110.3922 | 110.3708 | 0.0054 | 0.137 |
| L272 | Low-Carbon Steel, Lot L | 189.18 | 50.75 | 1.545 | 7.97 | 7.96 | 1.982 | 112.9268 | SA | SA | SA |
| M70 | Low-Carbon Steel, Lot M | 189.35 | 80.16 | 1.573 | 7.95 | 7.94 | 3.108 | 184.6148 | 184.5301 | 0.0136 | 0.345 |
| M71 | Low-Carbon Steel, Lot M | 189.32 | 80.16 | 1.602 | 7.96 | 7.96 | 3.110 | 187.4471 | 187.4000 | 0.0076 | 0.192 |
| M72 | Low-Carbon Steel, Lot M | 189.30 | 80.13 | 1.601 | 7.94 | 7.94 | 3.108 | 187.0564 | 187.0282 | 0.0045 | 0.115 |
| M270 | Low-Carbon Steel, Lot M | 189.12 | 50.38 | 1.545 | 7.94 | 7.94 | 1.967 | 112.9702 | SA | SA | SA |
| M271 | Low-Carbon Steel, Lot M | 189.13 | 50.47 | 1.550 | 7.95 | 7.95 | 1.971 | 113.1766 | 113.1569 | 0.0050 | 0.127 |
| M272 | Low-Carbon Steel, Lot M | 189.13 | 50.29 | 1.608 | 7.95 | 7.94 | 1.967 | 116.7650 | 116.7324 | 0.0083 | 0.210 |

* SA = Specimen was retained for surface analysis.

## APPENDIX B-4
## Individual Specimen Data, Seal-Welded Container Test No. 31

Test No.: 31
Test Type: Vapor Phase Exposure
Test Environment: Simulated WIPP Brine A Vapor + CO2 (10 atm)
Test Temperature: 30 ±5°C
Test Exposure: 24 Months

| Specimen | Material Type | Length, mm | Width, mm | Thickness, mm | Top Hole ID, mm | Bot. Hole ID, mm | Area, dm2 | Initial Wt., g | Final Wt., g | Corrosion Rate, mpy | Corrosion Rate, µm/yr |
|---|---|---|---|---|---|---|---|---|---|---|---|
| J91 | Low-Carbon Steel, Lot J | 189.00 | 79.96 | 0.690 | 7.93 | 7.93 | 3.043 | 80.2830 | 80.2563 | 0.0022 | 0.055 |
| J92 | Low-Carbon Steel, Lot J | 189.02 | 79.96 | 0.701 | 7.93 | 7.93 | 3.044 | 81.7406 | 81.7196 | 0.0017 | 0.043 |
| J93 | Low-Carbon Steel, Lot J | 189.02 | 79.94 | 0.701 | 7.91 | 7.94 | 3.044 | 80.9974 | 80.9676 | 0.0024 | 0.061 |
| J291 | Low-Carbon Steel, Lot J | 189.16 | 50.90 | 0.718 | 7.93 | 7.90 | 1.944 | 52.7647 | SA* | SA | SA |
| J292 | Low-Carbon Steel, Lot J | 189.12 | 50.87 | 0.717 | 7.91 | 7.92 | 1.942 | 52.8664 | 52.8493 | 0.0022 | 0.055 |
| J293 | Low-Carbon Steel, Lot J | 189.11 | 50.87 | 0.712 | 7.93 | 7.91 | 1.942 | 51.8954 | 51.8661 | 0.0037 | 0.094 |
| K91 | Low-Carbon Steel, Lot K | 188.91 | 79.97 | 0.856 | 7.92 | 7.92 | 3.052 | 99.7789 | 99.7595 | 0.0016 | 0.040 |
| K92 | Low-Carbon Steel, Lot K | 188.92 | 79.97 | 0.881 | 7.93 | 7.93 | 3.054 | 101.8044 | 101.7821 | 0.0018 | 0.046 |
| K93 | Low-Carbon Steel, Lot K | 188.91 | 79.95 | 0.887 | 7.92 | 7.94 | 3.053 | 103.4581 | 103.4119 | 0.0037 | 0.095 |
| K291 | Low-Carbon Steel, Lot K | 189.14 | 50.84 | 0.870 | 7.95 | 7.92 | 1.949 | 64.1470 | 64.1277 | 0.0024 | 0.062 |
| K292 | Low-Carbon Steel, Lot K | 189.10 | 50.84 | 0.865 | 7.94 | 7.90 | 1.949 | 63.8962 | SA | SA | SA |
| K293 | Low-Carbon Steel, Lot K | 189.16 | 50.82 | 0.874 | 7.94 | 7.92 | 1.949 | 64.5834 | 64.5633 | 0.0025 | 0.065 |
| L91 | Low-Carbon Steel, Lot L | 188.92 | 79.94 | 1.571 | 7.92 | 7.93 | 3.093 | 181.4198 | 181.3852 | 0.0028 | 0.070 |
| L92 | Low-Carbon Steel, Lot L | 188.91 | 79.94 | 1.556 | 7.93 | 7.94 | 3.092 | 180.3477 | 180.3136 | 0.0027 | 0.069 |
| L93 | Low-Carbon Steel, Lot L | 188.89 | 79.93 | 1.563 | 7.93 | 7.92 | 3.092 | 181.6635 | 181.6275 | 0.0029 | 0.073 |
| L291 | Low-Carbon Steel, Lot L | 189.15 | 50.82 | 1.506 | 7.94 | 7.92 | 1.983 | 110.2253 | SA | SA | SA |
| L292 | Low-Carbon Steel, Lot L | 189.16 | 50.84 | 1.535 | 7.94 | 7.93 | 1.985 | 112.9923 | 112.9612 | 0.0039 | 0.098 |
| L293 | Low-Carbon Steel, Lot L | 189.16 | 50.80 | 1.567 | 7.94 | 7.93 | 1.985 | 114.4277 | 114.3849 | 0.0053 | 0.135 |
| M91 | Low-Carbon Steel, Lot M | 188.89 | 80.06 | 1.579 | 7.93 | 7.92 | 3.098 | 185.8753 | 185.8465 | 0.0023 | 0.058 |
| M92 | Low-Carbon Steel, Lot M | 188.91 | 80.05 | 1.595 | 7.93 | 7.93 | 3.098 | 185.6871 | 185.6585 | 0.0023 | 0.058 |
| M93 | Low-Carbon Steel, Lot M | 188.89 | 80.05 | 1.597 | 7.92 | 7.92 | 3.098 | 186.3069 | 186.2770 | 0.0024 | 0.060 |
| M291 | Low-Carbon Steel, Lot M | 189.08 | 50.75 | 1.601 | 7.94 | 7.92 | 1.984 | 117.9399 | 117.9213 | 0.0023 | 0.059 |
| M292 | Low-Carbon Steel, Lot M | 189.11 | 50.79 | 1.609 | 7.93 | 7.93 | 1.986 | 118.5022 | SA | SA | SA |
| M293 | Low-Carbon Steel, Lot M | 189.13 | 50.79 | 1.608 | 7.93 | 7.92 | 1.987 | 118.4315 | 118.4123 | 0.0024 | 0.061 |

*SA = Specimen was retained for surface analysis.

## APPENDIX B-4
## Individual Specimen Data, Seal-Welded Container Test No. 32

Test No.: 32
Test Type: Vapor Phase Exposure
Test Environment: Simulated WIPP Brine A Vapor + CO2 (10 atm)
Test Temperature: 30 ±5°C
Test Exposure: 24 Months

| Specimen | Material Type | Length, mm | Width, mm | Thickness, mm | Top Hole ID, mm | Bot. Hole ID, mm | Area, dm2 | Initial Wt., g | Final Wt., g | Corrosion Rate, mpy | Corrosion Rate, µm/yr |
|---|---|---|---|---|---|---|---|---|---|---|---|
| J94 | Low-Carbon Steel, Lot J | 189.02 | 79.97 | 0.697 | 7.91 | 7.95 | 3.044 | 80.8992 | 80.8710 | 0.0023 | 0.058 |
| J95 | Low-Carbon Steel, Lot J | 189.04 | 79.95 | 0.709 | 7.94 | 7.94 | 3.045 | 82.5590 | 82.5361 | 0.0019 | 0.047 |
| J96 | Low-Carbon Steel, Lot J | 189.07 | 79.93 | 0.696 | 7.94 | 7.92 | 3.044 | 80.5701 | 80.5428 | 0.0022 | 0.056 |
| J294 | Low-Carbon Steel, Lot J | 189.11 | 50.85 | 0.711 | 7.93 | 7.93 | 1.941 | 51.3962 | SA* | SA | SA |
| J295 | Low-Carbon Steel, Lot J | 189.00 | 50.86 | 0.702 | 7.92 | 7.90 | 1.940 | 51.6423 | 51.6307 | 0.0015 | 0.037 |
| J296 | Low-Carbon Steel, Lot J | 189.03 | 50.85 | 0.706 | 7.93 | 7.92 | 1.940 | 51.5334 | 51.5161 | 0.0022 | 0.056 |
| K94 | Low-Carbon Steel, Lot K | 188.91 | 80.00 | 0.863 | 7.91 | 7.94 | 3.054 | 100.8548 | 100.8176 | 0.0030 | 0.076 |
| K95 | Low-Carbon Steel, Lot K | 188.93 | 79.95 | 0.872 | 7.92 | 7.94 | 3.052 | 101.1040 | 101.0148 | 0.0072 | 0.183 |
| K96 | Low-Carbon Steel, Lot K | 188.91 | 79.95 | 0.864 | 7.91 | 7.92 | 3.052 | 100.6818 | 100.5488 | 0.0107 | 0.272 |
| K294 | Low-Carbon Steel, Lot K | 189.18 | 50.83 | 0.866 | 7.92 | 7.92 | 1.949 | 64.1060 | SA | SA | SA |
| K295 | Low-Carbon Steel, Lot K | 189.13 | 50.84 | 0.862 | 7.92 | 7.93 | 1.949 | 63.6030 | 63.5816 | 0.0027 | 0.069 |
| K296 | Low-Carbon Steel, Lot K | 189.12 | 50.81 | 0.878 | 7.93 | 7.90 | 1.949 | 64.2733 | 64.2490 | 0.0031 | 0.078 |
| L94 | Low-Carbon Steel, Lot L | 188.94 | 79.94 | 1.557 | 7.93 | 7.93 | 3.093 | 180.8542 | 180.8178 | 0.0029 | 0.074 |
| L95 | Low-Carbon Steel, Lot L | 188.90 | 79.94 | 1.557 | 7.95 | 7.93 | 3.092 | 181.5524 | 181.5187 | 0.0027 | 0.068 |
| L96 | Low-Carbon Steel, Lot L | 188.92 | 79.96 | 1.573 | 7.94 | 7.92 | 3.094 | 181.8120 | 181.7717 | 0.0032 | 0.081 |
| L294 | Low-Carbon Steel, Lot L | 189.17 | 50.79 | 1.559 | 7.94 | 7.94 | 1.984 | 113.6946 | 113.6669 | 0.0034 | 0.087 |
| L295 | Low-Carbon Steel, Lot L | 189.20 | 50.89 | 1.549 | 7.93 | 7.95 | 1.988 | 113.6312 | 113.6047 | 0.0033 | 0.083 |
| L296 | Low-Carbon Steel, Lot L | 189.16 | 50.85 | 1.546 | 7.93 | 7.95 | 1.986 | 113.3702 | SA | SA | SA |
| M94 | Low-Carbon Steel, Lot M | 188.94 | 80.05 | 1.595 | 7.93 | 7.93 | 3.099 | 187.1926 | SA | SA | SA |
| M95 | Low-Carbon Steel, Lot M | 188.94 | 80.03 | 1.592 | 7.91 | 7.90 | 3.098 | 186.8385 | 186.5938 | 0.0194 | 0.494 |
| M96 | Low-Carbon Steel, Lot M | 188.91 | 79.99 | 1.610 | 7.93 | 7.92 | 3.097 | 189.2964 | 189.2558 | 0.0032 | 0.082 |
| M294 | Low-Carbon Steel, Lot M | 189.12 | 50.79 | 1.607 | 7.95 | 7.96 | 1.986 | 118.3168 | 118.2919 | 0.0031 | 0.078 |
| M295 | Low-Carbon Steel, Lot M | 189.12 | 50.74 | 1.568 | 7.94 | 7.93 | 1.982 | 115.7260 | SA | SA | SA |
| M296 | Low-Carbon Steel, Lot M | 189.11 | 50.76 | 1.606 | 7.94 | 7.94 | 1.985 | 118.4649 | 118.4357 | 0.0036 | 0.092 |

*SA = Specimen was retained for surface analysis.

## APPENDIX B-5: INDIVIDUAL SPECIMEN CORROSION-RATE DATA, AUTOCLAVE TEST AUT-1

## APPENDIX B-5
## Individual Specimen Corrosion-Rate Data, Autoclave Test AUT-1

Test No.: AUT-1
Test Type: Immersion
Test Environment: Simulated WIPP Brine A, H2 Overpressure (70 atm)
Test Temperature: 30 ±5°C
Test Exposure: 6 Months

| Specimen | Material Type | Length, mm | Width, mm | Thickness, mm | Top Hole ID, mm | Bot. Hole ID, mm | Area, dm2 | Initial Wt., g | Final Wt., g | Corrosion Rate, mpy | Corrosion Rate, µm/yr |
|---|---|---|---|---|---|---|---|---|---|---|---|
| J297 | Low-Carbon Steel, Lot J | 191.05 | 51.49 | 0.677 | 7.98 | 7.97 | 1.984 | 49.8704 | 49.8447 | 0.013 | 0.331 |
| J298 | Low-Carbon Steel, Lot J | 191.30 | 51.50 | 0.671 | 7.98 | 7.98 | 1.986 | 50.1519 | 50.1270 | 0.013 | 0.320 |
| J299 | Low-Carbon Steel, Lot J | 191.24 | 51.38 | 0.690 | 7.98 | 7.98 | 1.982 | 51.2650 | 51.2408 | 0.012 | 0.312 |
| J300 | Low-Carbon Steel, Lot J | 190.93 | 51.50 | 0.700 | 7.98 | 7.98 | 1.984 | 51.9040 | 51.8808 | 0.012 | 0.299 |
| J301 | Low-Carbon Steel, Lot J | 192.91 | 51.57 | 0.710 | 7.98 | 7.98 | 2.008 | 52.7437 | 52.7189 | 0.012 | 0.316 |
| K297 | Low-Carbon Steel, Lot K | 190.31 | 51.41 | 0.876 | 7.97 | 7.96 | 1.984 | 64.4697 | 64.4349 | 0.018 | 0.448 |
| K298 | Low-Carbon Steel, Lot K | 190.44 | 51.34 | 0.862 | 7.98 | 7.97 | 1.981 | 63.9087 | 63.8803 | 0.014 | 0.366 |
| K299 | Low-Carbon Steel, Lot K | 190.52 | 51.38 | 0.863 | 7.98 | 7.97 | 1.984 | 64.4015 | 64.3738 | 0.014 | 0.357 |
| K300 | Low-Carbon Steel, Lot K | 190.53 | 51.33 | 0.854 | 7.99 | 7.97 | 1.982 | 62.8801 | 62.8484 | 0.016 | 0.409 |
| K301 | Low-Carbon Steel, Lot K | 190.39 | 51.38 | 0.837 | 7.98 | 7.98 | 1.981 | 61.1923 | 61.1603 | 0.016 | 0.413 |

## APPENDIX B-6: INDIVIDUAL SPECIMEN CORROSION-RATE DATA, AUTOCLAVE TEST AUT-3

## APPENDIX B-6
## Individual Specimen Corrosion-Rate Data, Autoclave Test AUT-3

Test No.: AUT-3
Test Type: Immersion
Test Environment: Simulated WIPP Brine A, H2 Overpressure (36 atm)
Test Temperature: 30 ±5°C
Test Exposure: 12 Months

| Specimen | Material Type | Length, mm | Width, mm | Thickness, mm | Top Hole ID, mm | Bot. Hole ID, mm | Area, dm2 | Initial Wt., g | Final Wt., g | Corrosion Rate, mpy | Corrosion Rate, µm/yr |
|---|---|---|---|---|---|---|---|---|---|---|---|
| J307 | Low-Carbon Steel, Lot J | 191.26 | 51.48 | 0.679 | 7.96 | 7.96 | 1.986 | 50.5868 | 50.5549 | 0.008 | 0.204 |
| J308 | Low-Carbon Steel, Lot J | 191.43 | 51.41 | 0.683 | 7.97 | 7.96 | 1.985 | 50.8966 | 50.8672 | 0.007 | 0.188 |
| J309 | Low-Carbon Steel, Lot J | 191.24 | 51.44 | 0.672 | 7.98 | 7.97 | 1.983 | 50.4018 | 50.3710 | 0.008 | 0.197 |
| J310 | Low-Carbon Steel, Lot J | 191.10 | 51.47 | 0.674 | 7.96 | 7.96 | 1.983 | 50.3097 | 50.2783 | 0.008 | 0.201 |
| J311 | Low-Carbon Steel, Lot J | 190.95 | 51.49 | 0.704 | 7.97 | 7.97 | 1.984 | 51.8678 | 51.8360 | 0.008 | 0.203 |
| K307 | Low-Carbon Steel, Lot K | 190.32 | 51.31 | 0.870 | 7.98 | 7.98 | 1.979 | 64.5367 | 64.5000 | 0.009 | 0.235 |
| K308 | Low-Carbon Steel, Lot K | 190.52 | 51.32 | 0.864 | 7.98 | 7.97 | 1.982 | 64.4370 | 64.3978 | 0.010 | 0.251 |
| K309 | Low-Carbon Steel, Lot K | 190.35 | 51.33 | 0.862 | 7.99 | 7.98 | 1.980 | 64.1058 | 64.0708 | 0.009 | 0.224 |
| K310 | Low-Carbon Steel, Lot K | 190.39 | 51.32 | 0.862 | 7.99 | 7.97 | 1.980 | 63.8059 | 63.7624 | 0.011 | 0.278 |
| K311 | Low-Carbon Steel, Lot K | 190.48 | 51.32 | 0.855 | 8.00 | 7.98 | 1.981 | 62.8852 | 62.8440 | 0.010 | 0.264 |

## APPENDIX B-7: INDIVIDUAL SPECIMEN CORROSION-RATE DATA, AUTOCLAVE TEST AUT-4

## APPENDIX B-7
## Individual Specimen Corrosion-Rate Data, Autoclave Test AUT-4

Test No.: AUT-4
Test Type: Immersion
Test Environment: Simulated WIPP Brine A, H2 Overpressure (70 atm)
Test Temperature: 30 ±5°C
Test Exposure: 12 Months

| Specimen | Material Type | Length, mm | Width, mm | Thickness, mm | Top Hole ID, mm | Bot. Hole ID, mm | Area, dm2 | Initial Wt., g | Final Wt., g | Corrosion Rate, mpy | Corrosion Rate, µm/yr |
|---|---|---|---|---|---|---|---|---|---|---|---|
| J312 | Low-Carbon Steel, Lot J | 191.24 | 51.44 | 0.689 | 7.96 | 7.97 | 1.984 | 50.9004 | 50.8725 | 0.007 | 0.178 |
| J313 | Low-Carbon Steel, Lot J | 190.97 | 51.51 | 0.711 | 7.99 | 7.97 | 1.985 | 52.4448 | 52.4148 | 0.008 | 0.191 |
| J314 | Low-Carbon Steel, Lot J | 190.96 | 51.49 | 0.694 | 7.98 | 7.97 | 1.984 | 51.4439 | 51.4127 | 0.008 | 0.199 |
| J315 | Low-Carbon Steel, Lot J | 191.00 | 51.49 | 0.699 | 7.97 | 7.96 | 1.984 | 52.1348 | 52.1020 | 0.008 | 0.209 |
| J316 | Low-Carbon Steel, Lot J | 191.04 | 51.45 | 0.694 | 7.96 | 7.96 | 1.983 | 51.4726 | 51.4402 | 0.008 | 0.207 |
| K312 | Low-Carbon Steel, Lot K | 190.54 | 51.06 | 0.863 | 7.98 | 7.98 | 1.972 | 63.4063 | 63.3721 | 0.009 | 0.220 |
| K313 | Low-Carbon Steel, Lot K | 190.38 | 51.35 | 0.865 | 7.99 | 7.98 | 1.981 | 63.2425 | 63.1963 | 0.012 | 0.295 |
| K314 | Low-Carbon Steel, Lot K | 190.57 | 51.07 | 0.860 | 7.97 | 7.97 | 1.972 | 63.6838 | 63.6391 | 0.011 | 0.287 |
| K315 | Low-Carbon Steel, Lot K | 190.46 | 51.32 | 0.865 | 7.99 | 7.98 | 1.981 | 64.0279 | 63.9831 | 0.011 | 0.287 |
| K316 | Low-Carbon Steel, Lot K | 190.50 | 51.42 | 0.873 | 7.98 | 7.97 | 1.986 | 64.4769 | 64.4353 | 0.010 | 0.265 |

## APPENDIX B-8: INDIVIDUAL SPECIMEN CORROSION-RATE DATA, AUTOCLAVE TEST AUT-2

## APPENDIX B-8
## Individual Specimen Corrosion-Rate Data, Autoclave Test AUT-2

Test No.: AUT-2
Test Type: Immersion
Test Environment: Simulated WIPP Brine A, N2 Overpressure (73 atm)
Test Temperature: 30 ±5°C
Test Exposure: 6 Months

| Specimen | Material Type | Length, mm | Width, mm | Thickness, mm | Top Hole ID, mm | Bot. Hole ID, mm | Area, dm2 | Initial Wt., g | Final Wt., g | Corrosion Rate, mpy | Corrosion Rate, µm/yr |
|---|---|---|---|---|---|---|---|---|---|---|---|
| J302 | Low-Carbon Steel, Lot J | 191.14 | 51.49 | 0.679 | 7.98 | 7.98 | 1.985 | 50.8021 | 50.5661 | 0.120 | 3.038 |
| J303 | Low-Carbon Steel, Lot J | 191.19 | 51.50 | 0.691 | 7.98 | 7.97 | 1.986 | 51.9241 | 51.6993 | 0.114 | 2.892 |
| J304 | Low-Carbon Steel, Lot J | 191.92 | 51.50 | 0.704 | 7.98 | 7.97 | 1.995 | 52.5896 | 52.3900 | 0.101 | 2.557 |
| J305 | Low-Carbon Steel, Lot J | 191.27 | 51.47 | 0.719 | 7.98 | 7.98 | 1.987 | 53.9753 | 53.7833 | 0.097 | 2.468 |
| J306 | Low-Carbon Steel, Lot J | 191.22 | 51.47 | 0.692 | 7.99 | 7.97 | 1.985 | 51.3828 | 51.1608 | 0.112 | 2.857 |
| K302 | Low-Carbon Steel, Lot K | 190.55 | 51.37 | 0.846 | 7.98 | 7.97 | 1.983 | 62.0946 | 61.8530 | 0.123 | 3.113 |
| K303 | Low-Carbon Steel, Lot K | 190.48 | 51.35 | 0.849 | 7.97 | 7.96 | 1.982 | 62.5359 | 62.2916 | 0.124 | 3.150 |
| K304 | Low-Carbon Steel, Lot K | 190.44 | 51.39 | 0.853 | 7.97 | 7.96 | 1.983 | 62.9778 | 62.7334 | 0.124 | 3.149 |
| K305 | Low-Carbon Steel, Lot K | 190.51 | 51.36 | 0.851 | 7.97 | 7.96 | 1.982 | 63.1314 | 62.8827 | 0.126 | 3.206 |
| K306 | Low-Carbon Steel, Lot K | 190.48 | 51.37 | 0.855 | 7.99 | 7.97 | 1.983 | 62.9294 | 62.6801 | 0.126 | 3.213 |

# APPENDIX B-9: INDIVIDUAL SPECIMEN CORROSION-RATE DATA, AUTOCLAVE TEST AUT-7

## APPENDIX B-9
## Individual Specimen Corrosion-Rate Data, Autoclave Test AUT-7

Test No.: AUT-7
Test Type: Immersion
Test Environment: Simulated WIPP Brine A, CO2 Overpressure (36 atm)
Test Temperature: 30 ±5°C
Test Exposure: 6 Months

| Specimen | Material Type | Length, mm | Width, mm | Thickness, mm | Top Hole ID, mm | Bot. Hole ID, mm | Area, dm2 | Initial Wt., g | Final Wt., g | Corrosion Rate, mpy | Corrosion Rate, µm/yr |
|---|---|---|---|---|---|---|---|---|---|---|---|
| J7 1 | Low-Carbon Steel, Lot J | 76.49 | 37.93 | 0.702 | 8.01 | 0.00 | 0.588 | 15.4834 | 14.9355 | 0.933 | 23.705 |
| J7 2 | Low-Carbon Steel, Lot J | 76.48 | 37.94 | 0.699 | 8.01 | 0.00 | 0.588 | 15.4601 | SA* | SA | SA |
| J7 3 | Low-Carbon Steel, Lot J | 76.21 | 36.99 | 0.691 | 8.00 | 0.00 | 0.571 | 14.8239 | 14.3717 | 0.793 | 20.143 |
| J7 4 | Low-Carbon Steel, Lot J | 76.06 | 37.69 | 0.702 | 7.99 | 0.00 | 0.581 | 15.1808 | 14.6658 | 0.888 | 22.549 |
| K7 1 | Low-Carbon Steel, Lot K | 76.31 | 37.27 | 0.849 | 7.94 | 0.00 | 0.580 | 18.1103 | 17.5727 | 0.928 | 23.568 |
| K7 2 | Low-Carbon Steel, Lot K | 75.91 | 37.64 | 0.851 | 7.92 | 0.00 | 0.583 | 18.3776 | 17.7992 | 0.994 | 25.238 |
| K7 3 | Low-Carbon Steel, Lot K | 76.13 | 37.77 | 0.842 | 8.00 | 0.00 | 0.586 | 18.1748 | 17.5995 | 0.983 | 24.962 |
| K7 4 | Low-Carbon Steel, Lot K | 76.10 | 37.89 | 0.842 | 7.94 | 0.00 | 0.588 | 18.3229 | 17.7267 | 1.015 | 25.792 |
| L7 1 | Low-Carbon Steel, Lot L | 76.11 | 37.64 | 1.485 | 7.97 | 0.00 | 0.600 | 31.5138 | 30.7021 | 1.354 | 34.389 |
| L7 2 | Low-Carbon Steel, Lot L | 76.26 | 37.93 | 1.474 | 7.93 | 0.00 | 0.606 | 32.3544 | 31.4590 | 1.480 | 37.592 |
| L7 3 | Low-Carbon Steel, Lot L | 76.09 | 37.99 | 1.450 | 7.98 | 0.00 | 0.605 | 31.7096 | 30.8561 | 1.413 | 35.899 |
| L7 4 | Low-Carbon Steel, Lot L | 76.00 | 37.69 | 1.474 | 7.99 | 0.00 | 0.600 | 31.7864 | 30.9307 | 1.428 | 36.278 |
| M7 1 | Low-Carbon Steel, Lot M | 76.42 | 37.93 | 1.541 | 7.93 | 0.00 | 0.609 | 34.1713 | 33.2661 | 1.489 | 37.819 |
| M7 2 | Low-Carbon Steel, Lot M | 76.21 | 36.80 | 1.545 | 7.98 | 0.00 | 0.590 | 33.1634 | 32.3331 | 1.410 | 35.821 |
| M7 3 | Low-Carbon Steel, Lot M | 76.38 | 37.71 | 1.565 | 7.96 | 0.00 | 0.606 | 34.5017 | 33.6498 | 1.409 | 35.780 |
| M7 4 | Low-Carbon Steel, Lot M | 76.02 | 37.81 | 1.542 | 7.96 | 0.00 | 0.604 | 33.9293 | 33.1291 | 1.327 | 33.712 |

* SA = Specimen was retained for surface analysis.

# APPENDIX B-10: INDIVIDUAL SPECIMEN CORROSION-RATE DATA, AUTOCLAVE TEST AUT-5

## APPENDIX B-10
## Individual Specimen Corrosion-Rate Data, Autoclave Test AUT-5

Test No.: AUT-5
Test Type: Wicking
Test Environment: Specimens were in contact with coarse particulate WIPP salt. The salt was held in a mesh basket contacting WIPP Brine A, permitting some degree of wicking of the liquid. The autoclave had a N2 overpressure of 10 atm.
Test Temperature: 30 ±5°C
Test Exposure: 3 Months

| Specimen | Material Type | Length, mm | Width, mm | Thickness, mm | Top Hole ID*, mm | Bot. Hole ID*, mm | Area, dm2 | Initial Wt., g | Final Wt., g | Corrosion Rate, mpy | Corrosion Rate, µm/yr |
|---|---|---|---|---|---|---|---|---|---|---|---|
| JW1 | Low-Carbon Steel, Lot J | 49.73 | 25.41 | 0.717 | 0.00 | 0.00 | 0.264 | 7.0397 | 7.0342 | 0.041 | 1.049 |
| JW2 | Low-Carbon Steel, Lot J | 49.97 | 25.70 | 0.706 | 0.00 | 0.00 | 0.268 | 6.9837 | 6.9774 | 0.047 | 1.184 |
| JW3 | Low-Carbon Steel, Lot J | 50.00 | 23.95 | 0.707 | 0.00 | 0.00 | 0.250 | 6.5473 | 6.5407 | 0.052 | 1.327 |
| JW4 | Low-Carbon Steel, Lot J | 50.57 | 25.18 | 0.711 | 0.00 | 0.00 | 0.265 | 6.9600 | 6.9560 | 0.030 | 0.758 |
| JW5 | Low-Carbon Steel, Lot J | 52.62 | 25.34 | 0.697 | 0.00 | 0.00 | 0.278 | 7.1422 | 7.1352 | 0.050 | 1.268 |
| JW6 | Low-Carbon Steel, Lot J | 49.91 | 26.82 | 0.709 | 0.00 | 0.00 | 0.279 | 7.3286 | 7.3214 | 0.051 | 1.299 |
| JW7 | Low-Carbon Steel, Lot J | 51.29 | 25.97 | 0.705 | 0.00 | 0.00 | 0.277 | 7.2698 | 7.2573 | 0.089 | 2.266 |
| JW8 | Low-Carbon Steel, Lot J | 52.28 | 27.46 | 0.717 | 0.00 | 0.00 | 0.299 | 7.9249 | 7.9101 | 0.098 | 2.492 |
| JW9 | Low-Carbon Steel, Lot J | 52.33 | 23.44 | 0.714 | 0.00 | 0.00 | 0.256 | 6.7602 | 6.7538 | 0.049 | 1.256 |
| JW10 | Low-Carbon Steel, Lot J | 51.01 | 25.06 | 0.708 | 0.00 | 0.00 | 0.266 | 6.9991 | 6.9881 | 0.082 | 2.075 |
| JW11 | Low-Carbon Steel, Lot J | 51.50 | 25.16 | 0.704 | 0.00 | 0.00 | 0.270 | 7.0981 | 7.0894 | 0.064 | 1.620 |
| JW12 | Low-Carbon Steel, Lot J | 52.16 | 25.44 | 0.709 | 0.00 | 0.00 | 0.276 | 7.3294 | 7.3196 | 0.070 | 1.782 |

* = Specimens were simple rectangular coupons without holes.

# APPENDIX B-11: INDIVIDUAL SPECIMEN CORROSION-RATE DATA, AUTOCLAVE TEST AUT-6

## APPENDIX B-11
## Individual Specimen Corrosion-Rate Data, Autoclave Test AUT-6

Test No.: AUT-6
Test Type: Vapor
Test Environment: Specimens were in contact with coarse particulate WIPP salt. The salt was held in a mesh basket above the level of the simulated WIPP Brine A in the autoclave. Condensing water dripped onto the salt. The autoclave had a N2 overpressure of 10 atm.
Test Temperature: 30 ±5°C
Test Exposure: 3 Months

| Specimen | Material Type | Length, mm | Width, mm | Thickness, mm | Top Hole ID*, mm | Bot. Hole ID*, mm | Area, dm2 | Initial Wt., g | Final Wt., g | Corrosion Rate, mpy | Corrosion Rate, µm/yr |
|---|---|---|---|---|---|---|---|---|---|---|---|
| JV1 | Low-Carbon Steel, Lot J | 50.60 | 25.69 | 0.704 | 0.00 | 0.00 | 0.271 | 7.0583 | 7.0543 | 0.029 | 0.743 |
| JV2 | Low-Carbon Steel, Lot J | 50.34 | 25.45 | 0.705 | 0.00 | 0.00 | 0.267 | 7.0030 | 6.9989 | 0.030 | 0.772 |
| JV3 | Low-Carbon Steel, Lot J | 50.27 | 25.30 | 0.724 | 0.00 | 0.00 | 0.265 | 6.8805 | 6.8761 | 0.033 | 0.834 |
| JV4 | Low-Carbon Steel, Lot J | 50.66 | 25.78 | 0.708 | 0.00 | 0.00 | 0.272 | 7.0851 | 7.0809 | 0.031 | 0.776 |
| JV5 | Low-Carbon Steel, Lot J | 50.76 | 26.00 | 0.693 | 0.00 | 0.00 | 0.275 | 7.1300 | 7.1255 | 0.032 | 0.824 |
| JV6 | Low-Carbon Steel, Lot J | 51.08 | 25.09 | 0.704 | 0.00 | 0.00 | 0.267 | 6.9594 | 6.9553 | 0.030 | 0.772 |
| JV7 | Low-Carbon Steel, Lot J | 51.80 | 25.73 | 0.706 | 0.00 | 0.00 | 0.278 | 7.2946 | 7.2902 | 0.031 | 0.797 |
| JV8 | Low-Carbon Steel, Lot J | 51.84 | 25.35 | 0.712 | 0.00 | 0.00 | 0.274 | 7.2510 | 7.2475 | 0.025 | 0.643 |
| JV9 | Low-Carbon Steel, Lot J | 49.64 | 25.31 | 0.702 | 0.00 | 0.00 | 0.262 | 6.7814 | 6.7785 | 0.022 | 0.557 |
| JV10 | Low-Carbon Steel, Lot J | 51.26 | 25.73 | 0.708 | 0.00 | 0.00 | 0.275 | 7.2437 | 7.2403 | 0.024 | 0.622 |
| JV11 | Low-Carbon Steel, Lot J | 51.59 | 25.30 | 0.698 | 0.00 | 0.00 | 0.272 | 7.0797 | 7.0766 | 0.023 | 0.573 |
| JV12 | Low-Carbon Steel, Lot J | 51.98 | 25.79 | 0.710 | 0.00 | 0.00 | 0.279 | 7.3686 | 7.3650 | 0.026 | 0.648 |

* = Specimens were simple retangular coupons without holes.

## APPENDIX B-12: INDIVIDUAL SPECIMEN CORROSION-RATE DATA, COPPER-BASE MATERIALS, ANOXIC BRINE ENVIRONMENT, SEAL-WELDED-CONTAINER TEST 7A

## APPENDIX B-12
## Individual Specimen Data, Seal-Welded Container Test No. 7A

Test No: 7A
Test Type: Immersion
Test Environment: Simulated WIPP Brine A, N2 Overpressure (10 atm)
Test Temperature: 30 ±5°C
Test Exposure: 15 Months

These specimens were considered essentially free of attack during the corrosion test, based on (a) absence of reaction-product gas and (b) post-test appearance of specimens (clean, shiny).

| Specimen | Material Type | Outer Diameter, mm | Hole ID, mm | Thickness, mm | Area, dm2 | Initial Wt., g | Final Wt.*, g | Wt. Loss, g |
|---|---|---|---|---|---|---|---|---|
| C25 | Unalloyed copper | 38.01 | 7.84 | 1.522 | 0.239 | 14.4214 | 14.4214 | 0.0000 |
| C26 | Unalloyed copper | 38.01 | 7.85 | 1.536 | 0.239 | 14.5758 | -- | -- |
| C27 | Unalloyed copper | 38.01 | 7.79 | 1.513 | 0.239 | 14.3556 | -- | -- |
| C28 | Unalloyed copper | 38.01 | 7.83 | 1.516 | 0.239 | 14.3839 | -- | -- |
| C29 | Unalloyed copper | 38.01 | 7.81 | 1.526 | 0.239 | 14.4894 | -- | -- |
| C30 | Unalloyed copper | 38.01 | 7.74 | 1.523 | 0.239 | 14.4357 | -- | -- |
| C31 | Unalloyed copper | 38.03 | 7.81 | 1.535 | 0.240 | 14.5734 | 14.5733 | 0.0001 |
| C32 | Unalloyed copper | 38.01 | 7.86 | 1.549 | 0.239 | 14.7899 | 14.7896 | 0.0003 |
| CN25 | Cupronickel 90-10 | 37.71 | 7.87 | 1.512 | 0.235 | 14.1479 | -- | -- |
| CN26 | Cupronickel 90-10 | 38.14 | 7.88 | 1.514 | 0.241 | 14.5297 | -- | -- |
| CN27 | Cupronickel 90-10 | 38.09 | 7.86 | 1.515 | 0.240 | 14.4596 | 14.4597 | -0.0001 |
| CN28 | Cupronickel 90-10 | 37.74 | 7.86 | 1.507 | 0.235 | 14.1334 | 14.1336 | -0.0002 |
| CN29 | Cupronickel 90-10 | 38.16 | 7.89 | 1.512 | 0.241 | 14.5506 | -- | -- |
| CN30 | Cupronickel 90-10 | 37.97 | 7.86 | 1.521 | 0.239 | 14.4965 | -- | -- |
| CN31 | Cupronickel 90-10 | 37.66 | 7.88 | 1.480 | 0.234 | 13.7473 | -- | -- |
| CN32 | Cupronickel 90-10 | 37.70 | 7.88 | 1.507 | 0.235 | 14.0880 | 14.0878 | 0.0002 |

* Final weight was determined after rinsing specimen in deionized water and denatured alcohol. No chemical etching of specimen was performed.

## APPENDIX B-12
## Individual Specimen Data, Seal-Welded Container Test No. 7A (cont'd)

Test No: 7A
Test Type: Immersion
Test Environment: Simulated WIPP Brine A, N2 Overpressure (10 atm)
Test Temperature: 30 ±5°C
Test Exposure: 15 Months

These specimens were considered essentially free of attack during the corrosion test, based on (a) absence of reaction-product gas and (b) post-test appearance of specimens (clean, shiny).

| Specimen | Material Type | Length, mm | Width, mm | Thickness, mm | Top Hole ID, mm | Bot. Hole ID, mm | Area, dm2 | Initial Wt., g | Final Wt.*, g | Wt. Loss, g |
|---|---|---|---|---|---|---|---|---|---|---|
| C225 | Unalloyed copper | 190.25 | 63.31 | 1.574 | 7.95 | 7.96 | 2.477 | 165.1700 | 165.1694 | 0.0006 |
| C226 | Unalloyed copper | 190.26 | 63.36 | 1.575 | 7.85 | 7.82 | 2.479 | 165.1703 | 165.1713 | -0.0010 |
| C227 | Unalloyed copper | 190.08 | 63.13 | 1.577 | 7.76 | 7.85 | 2.468 | 165.2828 | -- | -- |
| C228 | Unalloyed copper | 190.39 | 63.33 | 1.574 | 7.98 | 7.94 | 2.479 | 165.1163 | -- | -- |
| C229 | Unalloyed copper | 190.21 | 63.24 | 1.580 | 7.85 | 7.84 | 2.474 | 166.1690 | -- | -- |
| C230 | Unalloyed copper | 190.09 | 63.22 | 1.566 | 7.81 | 7.88 | 2.471 | 165.0357 | -- | -- |
| C231 | Unalloyed copper | 190.19 | 63.20 | 1.576 | 7.86 | 7.85 | 2.472 | 165.5649 | -- | -- |
| C232 | Unalloyed copper | 190.19 | 63.19 | 1.573 | 7.87 | 7.86 | 2.472 | 164.5055 | 164.5064 | -0.0009 |
| CN225 | Cupronickel 90-10 | 190.25 | 63.13 | 1.561 | 7.91 | 7.86 | 2.469 | 163.7170 | -- | -- |
| CN226 | Cupronickel 90-10 | 190.36 | 63.16 | 1.570 | 7.98 | 7.94 | 2.472 | 164.8880 | -- | -- |
| CN227 | Cupronickel 90-10 | 190.27 | 63.17 | 1.533 | 7.94 | 7.95 | 2.469 | 160.8346 | 160.8397 | -0.0051 |
| CN228 | Cupronickel 90-10 | 190.18 | 63.14 | 1.554 | 7.93 | 7.97 | 2.468 | 162.9847 | -- | -- |
| CN229 | Cupronickel 90-10 | 190.20 | 63.16 | 1.557 | 7.95 | 7.93 | 2.469 | 162.8367 | 162.8385 | -0.0018 |
| CN230 | Cupronickel 90-10 | 190.26 | 63.35 | 1.562 | 7.93 | 7.96 | 2.478 | 163.1214 | -- | -- |
| CN231 | Cupronickel 90-10 | 190.21 | 63.15 | 1.551 | 7.96 | 7.98 | 2.469 | 161.1034 | 161.1151 | -0.0117 |
| CN232 | Cupronickel 90-10 | 190.26 | 63.20 | 1.564 | 7.99 | 7.96 | 2.472 | 162.9246 | -- | -- |

* Final weight was determined after rinsing specimen in deionized water and denatured alcohol. No chemical etching of specimen was performed.

## APPENDIX B-13: INDIVIDUAL SPECIMEN CORROSION-RATE DATA, COPPER-BASE MATERIALS, BRINE/$CO_2$ ENVIRONMENT, SEAL-WELDED-CONTAINER TEST 8A

## APPENDIX B-13
## Individual Specimen Data, Seal-Welded Container Test No. 8A

Test No: 8A
Test Type: Immersion
Test Environment: Simulated WIPP Brine A, CO2 Overpressure (10 atm)
Test Temperature: 30 ±5°C
Test Exposure: 15 Months

These specimens were considered essentially free of attack during the corrosion test, based on (a) absence of reaction-product gas and (b) post-test appearance of specimens (clean, shiny).

| Specimen | Material Type | Outer Diameter, mm | Hole ID, mm | Thickness, mm | Area, dm2 | Initial Wt., g | Final Wt.*, g | Wt. Loss, g |
|---|---|---|---|---|---|---|---|---|
| C33 | Unalloyed copper | 38.02 | 7.82 | 1.537 | 0.239 | 14.6355 | -- | -- |
| C34 | Unalloyed copper | 38.02 | 7.81 | 1.550 | 0.240 | 14.7608 | -- | -- |
| C35 | Unalloyed copper | 37.99 | 7.84 | 1.553 | 0.239 | 14.7727 | -- | -- |
| C36 | Unalloyed copper | 38.00 | 7.82 | 1.551 | 0.239 | 14.7803 | 14.7798 | 0.0005 |
| C37 | Unalloyed copper | 38.00 | 7.85 | 1.541 | 0.239 | 14.6795 | -- | -- |
| C38 | Unalloyed copper | 38.03 | 7.82 | 1.531 | 0.240 | 14.5731 | 14.5724 | 0.0007 |
| C39 | Unalloyed copper | 38.01 | 7.86 | 1.540 | 0.239 | 14.6600 | 14.6595 | 0.0005 |
| C40 | Unalloyed copper | 38.07 | 7.82 | 1.536 | 0.240 | 14.5996 | -- | -- |
| CN33 | Cupronickel 90-10 | 38.16 | 7.86 | 1.516 | 0.241 | 14.5368 | 14.5362 | 0.0006 |
| CN34 | Cupronickel 90-10 | 38.11 | 7.85 | 1.527 | 0.240 | 14.5600 | -- | -- |
| CN35 | Cupronickel 90-10 | 37.70 | 7.85 | 1.521 | 0.235 | 14.2382 | -- | -- |
| CN36 | Cupronickel 90-10 | 38.06 | 7.88 | 1.465 | 0.239 | 13.9062 | 13.9057 | 0.0005 |
| CN37 | Cupronickel 90-10 | 38.11 | 7.87 | 1.537 | 0.240 | 14.7243 | 14.7236 | 0.0007 |
| CN38 | Cupronickel 90-10 | 38.05 | 7.87 | 1.536 | 0.240 | 14.7037 | -- | -- |
| CN39 | Cupronickel 90-10 | 38.09 | 7.86 | 1.533 | 0.240 | 14.6807 | -- | -- |
| CN40 | Cupronickel 90-10 | 37.66 | 7.93 | 1.532 | 0.235 | 14.3520 | -- | -- |

* Final weight was determined after rinsing specimen in deionized water and denatured alcohol. No chemical etching of specimen was performed.

## APPENDIX B-13
## Individual Specimen Data, Seal-Welded Container Test No. 8A (cont'd)

Test No: 8A
Test Type: Immersion
Test Environment: Simulated WIPP Brine A, CO2 Overpressure (10 atm)
Test Temperature: 30 ±5°C
Test Exposure:15 Months

These specimens were considered essentially free of attack during the corrosion test, based on (a) absence of reaction-product gas and (b) post-test appearance of specimens (clean, shiny).

| Specimen | Material Type | Length, mm | Width, mm | Thickness, mm | Top Hole ID, mm | Bot. Hole ID, mm | Area, dm2 | Initial Wt., g | Final Wt.*, g | Wt. Loss, g |
|---|---|---|---|---|---|---|---|---|---|---|
| C233 | Unalloyed copper | 190.34 | 63.18 | 1.592 | 7.88 | 7.82 | 2.474 | 166.2625 | 166.2527 | 0.0098 |
| C234 | Unalloyed copper | 190.32 | 63.14 | 1.595 | 7.84 | 7.84 | 2.473 | 166.2143 | -- | -- |
| C235 | Unalloyed copper | 190.30 | 63.17 | 1.588 | 7.86 | 7.76 | 2.473 | 165.5987 | -- | -- |
| C236 | Unalloyed copper | 190.22 | 63.23 | 1.593 | 7.85 | 7.88 | 2.475 | 165.3475 | 165.3406 | 0.0069 |
| C237 | Unalloyed copper | 190.16 | 63.14 | 1.583 | 7.87 | 7.78 | 2.470 | 165.0830 | -- | -- |
| C238 | Unalloyed copper | 190.18 | 63.12 | 1.584 | 7.90 | 7.83 | 2.469 | 165.1274 | -- | -- |
| C239 | Unalloyed copper | 190.17 | 63.29 | 1.591 | 7.87 | 7.90 | 2.476 | 166.9182 | -- | -- |
| C240 | Unalloyed copper | 190.11 | 63.26 | 1.579 | 7.88 | 7.79 | 2.474 | 166.1039 | 166.0932 | 0.0107 |
| CN233 | Cupronickel 90-10 | 190.17 | 63.21 | 1.565 | 7.95 | 7.93 | 2.471 | 162.7382 | 162.7287 | 0.0095 |
| CN234 | Cupronickel 90-10 | 190.23 | 63.13 | 1.534 | 7.94 | 7.96 | 2.467 | 161.0609 | 161.0555 | 0.0054 |
| CN235 | Cupronickel 90-10 | 190.35 | 63.18 | 1.564 | 7.95 | 7.96 | 2.473 | 162.9677 | 162.9616 | 0.0061 |
| CN236 | Cupronickel 90-10 | 190.19 | 63.10 | 1.516 | 7.97 | 7.92 | 2.465 | 157.6580 | -- | -- |
| CN237 | Cupronickel 90-10 | 190.20 | 63.30 | 1.559 | 7.91 | 7.98 | 2.475 | 162.8907 | -- | -- |
| CN238 | Cupronickel 90-10 | 190.25 | 63.17 | 1.550 | 7.98 | 7.95 | 2.470 | 162.8537 | -- | -- |
| CN239 | Cupronickel 90-10 | 190.26 | 63.30 | 1.563 | 7.92 | 7.95 | 2.476 | 164.3112 | -- | -- |
| CN240 | Cupronickel 90-10 | 190.31 | 63.20 | 1.527 | 7.55 | 7.94 | 2.472 | 159.7624 | -- | -- |

r rinsing specimen in deionized water and denatured alcohol.
al etching of specimen was performed.

## APPENDIX B-14: INDIVIDUAL SPECIMEN CORROSION-RATE DATA, COPPER-BASE MATERIALS, BRINE/$H_2S$ ENVIRONMENT, SEAL-WELDED-CONTAINER TEST 3A and 9A

## APPENDIX B-14
## Individual Specimen Data, Seal-Welded Container Test No. 3A

Test No: 3A
Test Type: Immersion
Test Environment: Simulated WIPP Brine A, H2S Overpressure (5 atm)
Test Temperature: 30 ±5°C
Test Exposure: 9 Months

| Specimen | Material Type | Outer Diameter, mm | Hole ID, mm | Thickness, mm | Area, dm2 | Initial Wt., g | Final Wt., g | Corrosion Rate, mpy | Corrosion Rate, µm/yr |
|---|---|---|---|---|---|---|---|---|---|
| C17 | Unalloyed copper | 38.03 | 7.81 | 1.539 | 0.240 | 14.6381 | -- | -- | -- |
| C18 | Unalloyed copper | 38.02 | 7.79 | 1.544 | 0.240 | 14.6917 | 14.5120 | 0.421 | 10.689 |
| C19 | Unalloyed copper | 38.03 | 7.80 | 1.547 | 0.240 | 14.7740 | -- | -- | -- |
| C20 | Unalloyed copper | 38.04 | 7.78 | 1.534 | 0.240 | 14.6482 | -- | -- | -- |
| C21 | Unalloyed copper | 38.01 | 7.81 | 1.539 | 0.239 | 14.6511 | 14.4760 | 0.410 | 10.426 |
| C22 | Unalloyed copper | 38.01 | 7.78 | 1.536 | 0.239 | 14.6423 | -- | -- | -- |
| C23 | Unalloyed copper | 38.02 | 7.80 | 1.538 | 0.240 | 14.6244 | 14.4410 | 0.430 | 10.914 |
| C24 | Unalloyed copper | 38.01 | 7.84 | 1.534 | 0.239 | 14.5921 | 14.3980 | 0.455 | 11.563 |
| CN17 | Cupronickel 90-10 | 37.67 | 7.88 | 1.468 | 0.234 | 13.6371 | -- | -- | -- |
| CN18 | Cupronickel 90-10 | 38.16 | 7.81 | 1.500 | 0.241 | 14.3909 | 14.2200 | 0.396 | 10.063 |
| CN19 | Cupronickel 90-10 | 38.11 | 7.86 | 1.452 | 0.239 | 13.8900 | 13.7170 | 0.403 | 10.247 |
| CN20 | Cupronickel 90-10 | 37.70 | 7.87 | 1.509 | 0.235 | 14.0748 | -- | -- | -- |
| CN21 | Cupronickel 90-10 | 38.17 | 7.85 | 1.497 | 0.241 | 14.3535 | -- | -- | -- |
| CN22 | Cupronickel 90-10 | 37.73 | 7.87 | 1.501 | 0.235 | 14.0362 | -- | -- | -- |
| CN23 | Cupronickel 90-10 | 38.09 | 7.87 | 1.462 | 0.239 | 13.9145 | -- | -- | -- |
| CN24 | Cupronickel 90-10 | 38.17 | 7.86 | 1.508 | 0.241 | 14.4819 | -- | -- | -- |

## APPENDIX B-14
## Individual Specimen Data, Seal-Welded Container Test No. 3A (cont'd)

Test No: 3A
Test Type: Immersion
Test Environment: Simulated WIPP Brine A, H2S Overpressure (5 atm)
Test Temperature: 30 ±5°C
Test Exposure: 9 Months

| Specimen | Material Type | Length, mm | Width, mm | Thickness, mm | Top Hole ID, mm | Bot. Hole ID, mm | Area, dm2 | Initial Wt., g | Final Wt., g | Corrosion Rate, mpy | Corrosion Rate, µm/yr |
|---|---|---|---|---|---|---|---|---|---|---|---|
| C217 | Unalloyed copper | 190.23 | 63.10 | 1.557 | 7.89 | 7.79 | 2.468 | 164.1836 | -- | -- | -- |
| C218 | Unalloyed copper | 190.15 | 63.17 | 1.560 | 7.91 | 7.90 | 2.470 | 163.8577 | -- | -- | -- |
| C219 | Unalloyed copper | 190.33 | 63.43 | 1.567 | 7.88 | 7.90 | 2.482 | 166.7513 | -- | -- | -- |
| C220 | Unalloyed copper | 190.43 | 63.34 | 1.557 | 7.90 | 7.86 | 2.480 | 164.4625 | -- | -- | -- |
| C221 | Unalloyed copper | 190.19 | 63.31 | 1.553 | 7.88 | 7.87 | 2.475 | 163.2704 | -- | -- | -- |
| C222 | Unalloyed copper | 190.33 | 63.35 | 1.554 | 7.98 | 7.99 | 2.478 | 163.1701 | -- | -- | -- |
| C223 | Unalloyed copper | 190.25 | 63.11 | 1.568 | 7.86 | 7.85 | 2.469 | 164.8691 | 162.4500 | 0.550 | 13.965 |
| C224 | Unalloyed copper | 190.05 | 63.55 | 1.569 | 7.88 | 7.81 | 2.484 | 165.5393 | 162.9500 | 0.585 | 14.861 |
| CN217 | Cupronickel 90-10 | 190.33 | 63.05 | 1.554 | 7.98 | 7.97 | 2.467 | 161.4721 | -- | -- | -- |
| CN218 | Cupronickel 90-10 | 190.18 | 63.09 | 1.534 | 7.95 | 7.97 | 2.465 | 160.9541 | -- | -- | -- |
| CN219 | Cupronickel 90-10 | 190.16 | 63.23 | 1.526 | 7.97 | 7.95 | 2.470 | 158.7918 | -- | -- | -- |
| CN220 | Cupronickel 90-10 | 190.31 | 63.22 | 1.553 | 7.82 | 7.92 | 2.473 | 161.7179 | -- | -- | -- |
| CN221 | Cupronickel 90-10 | 190.27 | 63.20 | 1.551 | 7.93 | 7.95 | 2.472 | 163.5478 | -- | -- | -- |
| CN222 | Cupronickel 90-10 | 190.26 | 63.17 | 1.540 | 7.95 | 7.96 | 2.470 | 162.6259 | -- | -- | -- |
| CN223 | Cupronickel 90-10 | 190.24 | 63.20 | 1.550 | 7.95 | 7.96 | 2.471 | 162.6998 | 159.1500 | 0.802 | 20.360 |
| CN224 | Cupronickel 90-10 | 190.32 | 63.19 | 1.551 | 7.94 | 7.78 | 2.472 | 162.8219 | 159.2000 | 0.818 | 20.765 |

## APPENDIX B-14
## Individual Specimen Data, Seal-Welded Container Test No. 9A

Test No: 9A
Test Type: Immersion
Test Environment: Simulated WIPP Brine A, H2S Overpressure (5 atm)
Test Temperature: 30 ±5°C
Test Exposure: 15 Months

| Specimen | Material Type | Outer Diameter, mm | Hole ID, mm | Thickness, mm | Area, dm2 | Initial Wt., g | Final Wt., g | Corrosion Rate, mpy | Corrosion Rate, µm/yr |
|---|---|---|---|---|---|---|---|---|---|
| C41 | Unalloyed copper | 38.03 | 7.84 | 1.545 | 0.240 | 14.6777 | -- | -- | -- |
| C42 | Unalloyed copper | 38.03 | 7.82 | 1.536 | 0.240 | 14.6333 | 14.4135 | 0.330 | 8.376 |
| C43 | Unalloyed copper | 38.01 | 7.81 | 1.544 | 0.239 | 14.7425 | 14.5598 | 0.274 | 6.965 |
| C44 | Unalloyed copper | 38.02 | 7.85 | 1.542 | 0.239 | 14.7385 | 14.5364 | 0.303 | 7.704 |
| C45 | Unalloyed copper | 37.99 | 7.86 | 1.535 | 0.239 | 14.6024 | -- | -- | -- |
| C46 | Unalloyed copper | 37.98 | 7.82 | 1.530 | 0.239 | 14.5370 | -- | -- | -- |
| C47 | Unalloyed copper | 37.98 | 7.82 | 1.524 | 0.239 | 14.4762 | -- | -- | -- |
| C48 | Unalloyed copper | 38.00 | 7.85 | 1.512 | 0.239 | 14.4013 | -- | -- | -- |
| CN41 | Cupronickel 90-10 | 37.62 | 7.89 | 1.531 | 0.234 | 14.2846 | -- | -- | -- |
| CN42 | Cupronickel 90-10 | 37.60 | 7.86 | 1.517 | 0.234 | 14.0981 | -- | -- | -- |
| CN43 | Cupronickel 90-10 | 37.74 | 7.87 | 1.523 | 0.236 | 14.3340 | -- | -- | -- |
| CN44 | Cupronickel 90-10 | 37.67 | 7.89 | 1.535 | 0.235 | 14.3814 | -- | -- | -- |
| CN45 | Cupronickel 90-10 | 38.10 | 7.89 | 1.538 | 0.240 | 14.7412 | 14.5416 | 0.297 | 7.539 |
| CN46 | Cupronickel 90-10 | 38.09 | 7.86 | 1.524 | 0.240 | 14.6116 | 14.4270 | 0.275 | 6.980 |
| CN47 | Cupronickel 90-10 | 38.11 | 7.89 | 1.540 | 0.240 | 14.7696 | -- | -- | -- |
| CN48 | Cupronickel 90-10 | 38.07 | 7.88 | 1.540 | 0.240 | 14.7513 | -- | -- | -- |

## APPENDIX B-14
## Individual Specimen Data, Seal-Welded Container Test No. 9A (cont'd)

Test No: 9A
Test Type: Immersion
Test Environment: Simulated WIPP Brine A, H2S Overpressure (5 atm)
Test Temperature: 30 ±5°C
Test Exposure: 15 Months

| Specimen | Material Type | Length, mm | Width, mm | Thickness, mm | Top Hole ID, mm | Bot. Hole ID, mm | Area, dm2 | Initial Wt., g | Final Wt., g | Corrosion Rate, mpy | Corrosion Rate, µm/yr |
|---|---|---|---|---|---|---|---|---|---|---|---|
| C241 | Unalloyed copper | 190.27 | 63.13 | 1.544 | 7.86 | 7.86 | 2.469 | 162.8408 | -- | -- | -- |
| C242 | Unalloyed copper | 190.25 | 63.26 | 1.563 | 7.90 | 7.84 | 2.475 | 165.6610 | -- | -- | -- |
| C243 | Unalloyed copper | 190.15 | 63.24 | 1.554 | 7.89 | 7.83 | 2.472 | 164.6624 | -- | -- | -- |
| C244 | Unalloyed copper | 190.10 | 63.33 | 1.551 | 7.86 | 7.88 | 2.475 | 164.2470 | -- | -- | -- |
| C245 | Unalloyed copper | 190.42 | 63.25 | 1.560 | 7.86 | 7.79 | 2.476 | 164.2390 | -- | -- | -- |
| C246 | Unalloyed copper | 190.04 | 63.25 | 1.576 | 7.87 | 7.86 | 2.472 | 165.2658 | -- | -- | -- |
| C247 | Unalloyed copper | 190.14 | 63.19 | 1.570 | 7.85 | 7.86 | 2.471 | 165.3727 | 159.3332 | 0.879 | 22.314 |
| C248 | Unalloyed copper | 190.00 | 63.25 | 1.570 | 7.85 | 7.86 | 2.471 | 165.4518 | 159.1513 | 0.916 | 23.274 |
| CN241 | Cupronickel 90-10 | 190.26 | 63.25 | 1.522 | 7.99 | 7.96 | 2.472 | 160.9265 | -- | -- | -- |
| CN242 | Cupronickel 90-10 | 190.20 | 63.25 | 1.524 | 7.97 | 7.94 | 2.471 | 160.0673 | -- | -- | -- |
| CN243 | Cupronickel 90-10 | 190.34 | 63.28 | 1.570 | 7.94 | 7.94 | 2.477 | 163.8679 | -- | -- | -- |
| CN244 | Cupronickel 90-10 | 190.35 | 63.33 | 1.549 | 7.92 | 7.93 | 2.478 | 162.2167 | -- | -- | -- |
| CN245 | Cupronickel 90-10 | 190.35 | 63.16 | 1.423 | 7.90 | 7.92 | 2.464 | 149.3230 | -- | -- | -- |
| CN246 | Cupronickel 90-10 | 190.29 | 63.21 | 1.555 | 7.95 | 7.96 | 2.472 | 162.2631 | -- | -- | -- |
| CN247 | Cupronickel 90-10 | 190.16 | 63.17 | 1.517 | 7.96 | 7.94 | 2.467 | 158.4790 | 152.9509 | 0.801 | 20.341 |
| CN248 | Cupronickel 90-10 | 190.25 | 63.16 | 1.501 | 7.94 | 7.96 | 2.467 | 158.7949 | 152.8068 | 0.868 | 22.035 |

# APPENDIX B-15: INDIVIDUAL SPECIMEN CORROSION-RATE DATA, TITANIUM-BASE MATERIALS, ANOXIC BRINE ENVIRONMENT, SEAL-WELDED-CONTAINER TEST 10A

## APPENDIX B-15
## Individual Specimen Data, Seal-Welded Container Test No. 10A

Test No: 10A
Test Type: Immersion
Test Environment: Simulated WIPP Brine A, N2 Overpressure (10 atm)
Test Temperature: 30 ±5°C
Test Exposure: 15 Months

These specimens were considered essentially free of attack during the corrosion test, based on (a) absence of reaction-product gas and (b) post-test appearance of specimens (clean, shiny).

| Specimen | Material Type | Outer Diameter, mm | Hole ID, mm | Thickness, mm | Area, dm2 | Initial Wt., g | Final Wt.*, g | Wt. Loss, g |
|---|---|---|---|---|---|---|---|---|
| T25 | Titanium, Gr 2 | 38.23 | 7.77 | 1.562 | 0.243 | 7.6314 | 7.6320 | -0.0006 |
| T26 | Titanium, Gr 2 | 38.24 | 7.74 | 1.568 | 0.243 | 7.6317 | 7.6319 | -0.0002 |
| T27 | Titanium, Gr 2 | 38.30 | 7.73 | 1.535 | 0.243 | 7.4539 | -- | -- |
| T28 | Titanium, Gr 2 | 38.25 | 7.72 | 1.517 | 0.242 | 7.3115 | 7.3127 | -0.0012 |
| T29 | Titanium, Gr 2 | 38.26 | 7.77 | 1.575 | 0.243 | 7.6711 | -- | -- |
| T30 | Titanium, Gr 2 | 38.20 | 7.81 | 1.558 | 0.242 | 7.5792 | -- | -- |
| T31 | Titanium, Gr 2 | 38.22 | 7.76 | 1.567 | 0.243 | 7.5611 | -- | -- |
| T32 | Titanium, Gr 2 | 38.25 | 7.78 | 1.567 | 0.243 | 7.6222 | -- | -- |
| TN25 | Titanium, Gr 12 | 38.12 | 7.73 | 1.553 | 0.241 | 7.4928 | -- | -- |
| TN26 | Titanium, Gr 12 | 38.17 | 7.76 | 1.478 | 0.241 | 7.1120 | 7.1125 | -0.0005 |
| TN27 | Titanium, Gr 12 | 38.16 | 7.81 | 1.591 | 0.242 | 7.6496 | 7.6498 | -0.0002 |
| TN28 | Titanium, Gr 12 | 38.16 | 7.77 | 1.539 | 0.241 | 7.4599 | -- | -- |
| TN29 | Titanium, Gr 12 | 38.10 | 7.84 | 1.552 | 0.241 | 7.4932 | -- | -- |
| TN30 | Titanium, Gr 12 | 38.14 | 7.86 | 1.532 | 0.241 | 7.4409 | -- | -- |
| TN31 | Titanium, Gr 12 | 38.13 | 7.84 | 1.568 | 0.241 | 7.6198 | 7.6205 | -0.0007 |
| TN32 | Titanium, Gr 12 | 38.16 | 7.84 | 1.551 | 0.241 | 7.4843 | -- | -- |

* Final weight was determined after rinsing specimen in deionized water and denatured alcohol. No chemical etching of specimen was performed.

## APPENDIX B-15
## Individual Specimen Data, Seal-Welded Container Test No. 10A (cont'd)

Test No: 10A
Test Type: Immersion
Test Environment: Simulated WIPP Brine A, N2 Overpressure (10 atm)
Test Temperature: 30 ±5°C
Test Exposure: 15 Months

These specimens were considered essentially free of attack during the corrosion test, based on (a) absence of reaction-product gas and (b) post-test appearance of specimens (clean, shiny).

| Specimen | Material Type | Length, mm | Width, mm | Thickness, mm | ID, mm | ID, mm | Area, dm2 | Initial Wt., g | Final Wt.*, g | Wt. Loss, g |
|---|---|---|---|---|---|---|---|---|---|---|
| T225 | Titanium, Gr 2 | 190.45 | 63.38 | 1.569 | 7.95 | 7.94 | 2.482 | 83.9200 | 83.9203 | -0.0003 |
| T226 | Titanium, Gr 2 | 190.44 | 63.47 | 1.609 | 8.00 | 7.98 | 2.487 | 86.4833 | 86.4851 | -0.0018 |
| T227 | Titanium, Gr 2 | 190.40 | 63.46 | 1.591 | 7.97 | 8.00 | 2.485 | 84.9097 | -- | -- |
| T228 | Titanium, Gr 2 | 190.50 | 63.46 | 1.570 | 7.98 | 7.98 | 2.485 | 84.4365 | -- | -- |
| T229 | Titanium, Gr 2 | 190.52 | 63.43 | 1.606 | 7.98 | 7.98 | 2.487 | 86.1846 | -- | -- |
| T230 | Titanium, Gr 2 | 190.42 | 63.38 | 1.445 | 8.00 | 7.99 | 2.474 | 77.1828 | 77.1852 | -0.0024 |
| T231 | Titanium, Gr 2 | 190.48 | 63.49 | 1.584 | 7.96 | 8.00 | 2.487 | 85.0025 | -- | -- |
| T232 | Titanium, Gr 2 | 190.42 | 63.42 | 1.591 | 8.00 | 7.98 | 2.484 | 85.0660 | -- | -- |
| TN225 | Titanium, Gr 12 | 190.62 | 63.45 | 1.533 | 7.86 | 7.86 | 2.485 | 83.7261 | -- | -- |
| TN226 | Titanium, Gr 12 | 190.66 | 63.47 | 1.487 | 7.90 | 7.90 | 2.484 | 80.9096 | 80.9107 | -0.0011 |
| TN227 | Titanium, Gr 12 | 190.65 | 63.42 | 1.493 | 7.87 | 7.88 | 2.482 | 80.7866 | 80.7873 | -0.0007 |
| TN228 | Titanium, Gr 12 | 190.43 | 63.32 | 1.558 | 7.86 | 7.84 | 2.479 | 84.3618 | 84.3612 | 0.0006 |
| TN229 | Titanium, Gr 12 | 190.38 | 63.20 | 1.558 | 7.83 | 7.83 | 2.474 | 83.5710 | -- | -- |
| TN230 | Titanium, Gr 12 | 190.59 | 63.27 | 1.533 | 7.83 | 7.82 | 2.478 | 82.6462 | -- | -- |
| TN231 | Titanium, Gr 12 | 190.25 | 63.23 | 1.508 | 7.80 | 7.81 | 2.471 | 79.5766 | -- | -- |
| TN232 | Titanium, Gr 12 | 190.59 | 63.43 | 1.564 | 7.88 | 7.89 | 2.486 | 84.0623 | -- | -- |

* Final weight was determined after rinsing specimen in deionized water and denatured alcohol. No chemical etching of specimen was performed.

## APPENDIX B-16: INDIVIDUAL SPECIMEN CORROSION-RATE DATA, TITANIUM-BASE MATERIALS, BRINE/$CO_2$ ENVIRONMENT, SEAL-WELDED-CONTAINER TEST 11A

## APPENDIX B-16
## Individual Specimen Data, Seal-Welded Container Test No. 11A

Test No: 11A
Test Type: Immersion
Test Environment: Simulated WIPP Brine A, CO2 Overpressure (10 atm)
Test Temperature: 30 ±5°C
Test Exposure: 15 Months

These specimens were considered essentially free of attack during the corrosion test, based on (a) absence of reaction-product gas and (b) post-test appearance of specimens (clean, shiny).

| Specimen | Material Type | Outer Diameter, mm | Hole ID, mm | Thickness, mm | Area, dm2 | Initial Wt., g | Final Wt.*, g | Wt. Loss, g |
|---|---|---|---|---|---|---|---|---|
| T33 | Titanium, Gr 2 | 38.27 | 7.73 | 1.545 | 0.243 | 7.4816 | -- | -- |
| T34 | Titanium, Gr 2 | 38.30 | 7.75 | 1.552 | 0.243 | 7.5228 | -- | -- |
| T35 | Titanium, Gr 2 | 38.25 | 7.79 | 1.556 | 0.243 | 7.5527 | -- | -- |
| T36 | Titanium, Gr 2 | 38.27 | 7.73 | 1.561 | 0.243 | 7.5981 | -- | -- |
| T37 | Titanium, Gr 2 | 38.26 | 7.78 | 1.528 | 0.242 | 7.4339 | 7.4338 | 0.0001 |
| T38 | Titanium, Gr 2 | 38.22 | 7.75 | 1.555 | 0.242 | 7.5714 | 7.5713 | 0.0001 |
| T39 | Titanium, Gr 2 | 38.25 | 7.74 | 1.560 | 0.243 | 7.6052 | 7.6052 | 0.0000 |
| T40 | Titanium, Gr 2 | 38.26 | 7.72 | 1.556 | 0.243 | 7.5716 | -- | -- |
| TN33 | Titanium, Gr 12 | 38.22 | 7.88 | 1.570 | 0.242 | 7.6008 | -- | -- |
| TN34 | Titanium, Gr 12 | 38.16 | 7.89 | 1.566 | 0.241 | 7.5923 | -- | -- |
| TN35 | Titanium, Gr 12 | 38.15 | 7.89 | 1.503 | 0.240 | 7.2845 | -- | -- |
| TN36 | Titanium, Gr 12 | 38.15 | 7.87 | 1.576 | 0.242 | 7.6427 | 7.6426 | 0.0001 |
| TN37 | Titanium, Gr 12 | 38.17 | 7.87 | 1.499 | 0.241 | 7.2705 | -- | -- |
| TN38 | Titanium, Gr 12 | 38.13 | 7.85 | 1.491 | 0.240 | 7.2341 | -- | -- |
| TN39 | Titanium, Gr 12 | 38.14 | 7.84 | 1.450 | 0.240 | 6.9732 | 6.9732 | 0.0000 |
| TN40 | Titanium, Gr 12 | 38.15 | 7.83 | 1.505 | 0.241 | 7.2528 | 7.2528 | 0.0000 |

* Final weight was determined after rinsing specimen in deionized water and denatured alcohol. No chemical etching of specimen was performed.

## APPENDIX B-16
## Individual Specimen Data, Seal-Welded Container Test No. 11A (cont'd)

Test No: 11A
Test Type: Immersion
Test Environment: Simulated WIPP Brine A, CO2 Overpressure (10 atm)
Test Temperature: 30 ±5°C
Test Exposure: 15 Months

These specimens were considered essentially free of attack during the corrosion test, based on (a) absence of reaction-product gas and (b) post-test appearance of specimens (clean, shiny).

| Specimen | Material Type | Length, mm | Width, mm | Thickness, mm | ID, mm | ID, mm | Area, dm2 | Initial Wt., g | Final Wt.*, g | Wt. Loss, g |
|---|---|---|---|---|---|---|---|---|---|---|
| T233 | Titanium, Gr 2 | 190.44 | 63.35 | 1.608 | 7.88 | 7.96 | 2.483 | 85.5785 | -- | -- |
| T234 | Titanium, Gr 2 | 190.45 | 63.44 | 1.600 | 8.00 | 7.99 | 2.486 | 85.8362 | -- | -- |
| T235 | Titanium, Gr 2 | 190.47 | 63.44 | 1.608 | 7.99 | 7.98 | 2.486 | 86.2818 | 86.2805 | 0.0013 |
| T236 | Titanium, Gr 2 | 190.56 | 63.46 | 1.609 | 7.97 | 7.98 | 2.488 | 86.0296 | -- | -- |
| T237 | Titanium, Gr 2 | 190.42 | 63.42 | 1.604 | 7.98 | 8.02 | 2.485 | 86.0700 | 86.0686 | 0.0014 |
| T238 | Titanium, Gr 2 | 190.49 | 63.52 | 1.593 | 8.01 | 8.04 | 2.489 | 85.3463 | 85.3456 | 0.0007 |
| T239 | Titanium, Gr 2 | 190.36 | 63.42 | 1.597 | 7.99 | 7.98 | 2.484 | 85.3794 | -- | -- |
| T240 | Titanium, Gr 2 | 190.45 | 63.38 | 1.594 | 8.01 | 7.96 | 2.483 | 85.3181 | -- | -- |
| TN233 | Titanium, Gr 12 | 190.57 | 63.41 | 1.557 | 7.88 | 7.88 | 2.484 | 83.7172 | -- | -- |
| TN234 | Titanium, Gr 12 | 190.39 | 63.43 | 1.554 | 7.86 | 7.86 | 2.482 | 83.3396 | -- | -- |
| TN235 | Titanium, Gr 12 | 190.40 | 63.62 | 1.527 | 7.86 | 7.87 | 2.488 | 81.8190 | -- | -- |
| TN236 | Titanium, Gr 12 | 190.61 | 63.67 | 1.547 | 7.86 | 7.86 | 2.494 | 84.3176 | 84.3172 | 0.0004 |
| TN237 | Titanium, Gr 12 | 190.81 | 63.32 | 1.569 | 7.85 | 7.86 | 2.485 | 84.0329 | 84.0321 | 0.0008 |
| TN238 | Titanium, Gr 12 | 190.47 | 63.29 | 1.508 | 7.85 | 7.86 | 2.476 | 80.0610 | -- | -- |
| TN239 | Titanium, Gr 12 | 190.48 | 63.58 | 1.509 | 7.86 | 7.87 | 2.487 | 81.1324 | -- | -- |
| TN240 | Titanium, Gr 12 | 190.63 | 63.44 | 1.484 | 7.86 | 7.89 | 2.482 | 80.6646 | 80.6639 | 0.0007 |

* Final weight was determined after rinsing specimen in deionized water and denatured alcohol. No chemical etching of specimen was performed.

## APPENDIX B-17: INDIVIDUAL SPECIMEN CORROSION-RATE DATA, TITANIUM-BASE MATERIALS, BRINE/$H_2S$ ENVIRONMENT, SEAL-WELDED-CONTAINER TEST 12A

## APPENDIX B-17
## Individual Specimen Data, Seal-Welded Container Test No. 12A

Test No: 12A
Test Type: Immersion
Test Environment: Simulated WIPP Brine A, H2S Overpressure (5 atm)
Test Temperature: 30 ±5°C
Test Exposure: 15 Months

These specimens were considered essentially free of attack during the corrosion test, based on (a) absence of reaction-product gas and (b) post-test appearance of specimens (clean, shiny).

| Specimen | Material Type | Outer Diameter, mm | Hole ID, mm | Thickness, mm | Area, dm2 | Initial Wt., g | Final Wt.*, g | Wt. Loss, g |
|---|---|---|---|---|---|---|---|---|
| T41 | Titanium, Gr 2 | 38.24 | 7.77 | 1.557 | 0.243 | 7.5548 | -- | -- |
| T42 | Titanium, Gr 2 | 38.23 | 7.76 | 1.542 | 0.242 | 7.4892 | -- | -- |
| T43 | Titanium, Gr 2 | 38.24 | 7.73 | 1.573 | 0.243 | 7.6494 | 7.6493 | 0.0001 |
| T44 | Titanium, Gr 2 | 38.24 | 7.78 | 1.543 | 0.242 | 7.4582 | -- | -- |
| T45 | Titanium, Gr 2 | 38.20 | 7.79 | 1.512 | 0.241 | 7.3003 | 7.3001 | 0.0002 |
| T46 | Titanium, Gr 2 | 38.20 | 7.79 | 1.528 | 0.242 | 7.3614 | -- | -- |
| T47 | Titanium, Gr 2 | 38.20 | 7.79 | 1.535 | 0.242 | 7.4042 | 7.4043 | -0.0001 |
| T48 | Titanium, Gr 2 | 38.25 | 7.76 | 1.547 | 0.243 | 7.5067 | -- | -- |
| TN41 | Titanium, Gr 12 | 38.10 | 7.82 | 1.539 | 0.240 | 7.3482 | -- | -- |
| TN42 | Titanium, Gr 12 | 38.10 | 7.89 | 1.540 | 0.240 | 7.3484 | 7.3485 | -0.0001 |
| TN43 | Titanium, Gr 12 | 38.10 | 7.91 | 1.557 | 0.241 | 7.4566 | 7.4566 | 0.0000 |
| TN44 | Titanium, Gr 12 | 38.09 | 7.90 | 1.516 | 0.240 | 7.2560 | -- | -- |
| TN45 | Titanium, Gr 12 | 38.10 | 7.83 | 1.564 | 0.241 | 7.5030 | -- | -- |
| TN46 | Titanium, Gr 12 | 38.12 | 7.85 | 1.526 | 0.240 | 7.3176 | -- | -- |
| TN47 | Titanium, Gr 12 | 38.16 | 7.81 | 1.506 | 0.241 | 7.3057 | -- | -- |
| TN48 | Titanium, Gr 12 | 38.12 | 7.87 | 1.477 | 0.240 | 7.1354 | 7.1354 | 0.0000 |

* Final weight was determined after rinsing specimen in deionized water and denatured alcohol. No chemical etching of specimen was performed.

## APPENDIX B-17
## Individual Specimen Data, Seal-Welded Container Test No. 12A (cont'd)

Test No: 12A
Test Type: Immersion
Test Environment: Simulated WIPP Brine A, H2S Overpressure (5 atm)
Test Temperature: 30 ±5°C
Test Exposure: 15 Months

These specimens were considered essentially free of attack during the corrosion test, based on (a) absence of reaction-product gas and (b) post-test appearance of specimens (clean, shiny).

| Specimen | Material Type | Length, mm | Width, mm | Thickness, mm | Top Hole ID, mm | Bot. Hole ID, mm | Area, dm2 | Initial Wt., g | Final Wt.*, g | Wt. Loss, g |
|---|---|---|---|---|---|---|---|---|---|---|
| T241 | Titanium, Gr 2 | 190.46 | 63.36 | 1.560 | 7.97 | 7.97 | 2.481 | 83.7408 | 83.7397 | 0.0011 |
| T242 | Titanium, Gr 2 | 190.45 | 63.37 | 1.603 | 7.99 | 7.98 | 2.483 | 85.7788 | 85.7784 | 0.0004 |
| T243 | Titanium, Gr 2 | 190.48 | 63.37 | 1.576 | 7.99 | 7.96 | 2.482 | 84.0563 | -- | -- |
| T244 | Titanium, Gr 2 | 190.42 | 63.29 | 1.593 | 7.97 | 7.97 | 2.479 | 85.4843 | -- | -- |
| T245 | Titanium, Gr 2 | 190.45 | 63.34 | 1.598 | 7.98 | 8.00 | 2.482 | 85.4462 | 85.4457 | 0.0005 |
| T246 | Titanium, Gr 2 | 190.55 | 63.39 | 1.600 | 7.96 | 7.98 | 2.485 | 85.6183 | -- | -- |
| T247 | Titanium, Gr 2 | 190.43 | 63.38 | 1.596 | 7.97 | 7.96 | 2.483 | 85.2410 | -- | -- |
| T248 | Titanium, Gr 2 | 190.50 | 63.46 | 1.604 | 7.98 | 7.99 | 2.487 | 86.1754 | -- | -- |
| TN241 | Titanium, Gr 12 | 190.53 | 63.61 | 1.568 | 7.86 | 7.86 | 2.492 | 83.7340 | 83.7328 | 0.0012 |
| TN242 | Titanium, Gr 12 | 190.76 | 63.39 | 1.443 | 7.85 | 7.85 | 2.480 | 77.6584 | -- | -- |
| TN243 | Titanium, Gr 12 | 190.62 | 63.45 | 1.555 | 7.85 | 7.61 | 2.487 | 83.4980 | -- | -- |
| TN244 | Titanium, Gr 12 | 190.55 | 63.41 | 1.544 | 7.83 | 7.83 | 2.483 | 83.3203 | 83.3195 | 0.0008 |
| TN245 | Titanium, Gr 12 | 190.83 | 63.37 | 1.526 | 7.84 | 7.84 | 2.484 | 83.0038 | 83.0030 | 0.0008 |
| TN246 | Titanium, Gr 12 | 190.46 | 63.52 | 1.560 | 7.84 | 7.83 | 2.487 | 83.0839 | -- | -- |
| TN247 | Titanium, Gr 12 | 190.29 | 63.27 | 1.428 | 7.86 | 7.87 | 2.468 | 77.6856 | -- | -- |
| TN248 | Titanium, Gr 12 | 190.54 | 63.39 | 1.554 | 7.86 | 7.87 | 2.483 | 84.3729 | -- | -- |

* Final weight was determined after rinsing specimen in deionized water and denatured alcohol. No chemical etching of specimen was performed.

# APPENDIX C: METHOD OF DETERMINING DEGREE OF MOLAR EQUIVALENCE BETWEEN $H_2$ FORMED AND FE REACTED IN ANOXIC BRINE (BRINE/$N_2$) AND BRINE/$CO_2$ SEAL-WELDED-CONTAINER TESTS

# APPENDIX C: METHOD OF DETERMINING DEGREE OF MOLAR EQUIVALENCE BETWEEN $H_2$ FORMED AND Fe REACTED IN ANOXIC BRINE (BRINE/$N_2$) AND BRINE/$CO_2$ SEAL-WELDED-CONTAINER TESTS

The method of determining the degree of molar equivolence between $H_2$ formed and Fe reacted in the anoxic brine (brine/$N_2$) and the brine/$CO_2$ seal-welded-container tests is presented here. The results of the calculations are shown here and in Tables 6.4 and 6.7. The "Average Corrosion" rates are the mean value rates for all steel lots from Tables 6.2 and 6.6. The "Final P ($P_f$)" values are from either the pressure history curves or the raw data summations of Appendix A. The "Fraction $H_2$" values are from Tables 6.1 and 6.5.

The corrosion rate of steel in $\mu$m/yr is converted to mol/m$^2$-yr of Fe by the conversion factor 0.141 mol/$\mu$m-$m_2$, as 0.141 mol Fe is contained in a piece of Fe (steel) having an area of 1 m$^2$ and a thickness of 1 $\mu$m.

Moles Fe Consumed by the Corrosion Reaction (Gravimetric Analysis)

| | Test Duration, months | Containers | Average Corrosion Rate, $\mu$m/yr | Fe Reacted, mol/m$^2$-yr |
|---|---|---|---|---|
| Brine/$N_2$ | 3 | 1,2 | 1.96 | 0.276 |
| | 6 | 9,10 | 1.72 | 0.243 |
| | 12 | 17,18 | 1.23 | 0.173 |
| | 24 | 25,26 | 0.99 | 0.140 |
| Brine/$CO_2$ | 3 | 3,4 | 8.76 | 1.24 |
| | 6 | 11,12 | 6.31 | 0.890 |
| | 12 | 19,20 | 2.91 | 0.410 |
| | 24 | 27,28 | 1.46 | 0.206 |

Moles $H_2$ Formed by the Corrosion Reaction (Gas Pressure and Compositon)

| | Test Duration, months | Final P ($P_f$) psig | Final P ($P_f$) psia | Fraction $H_2$ | Atm $H_2$ | $H_2$,[a] mol/$m^2$-yr | moles $H_2$ / moles Fe |
|---|---|---|---|---|---|---|---|
| Brine/$N_2$ | 3 | 155 | 170 | 0.103 | 1.19 | 0.190 | 0.69 |
| | 6 | 175 | 190 | 0.191 | 2.47 | 0.209 | 0.86 |
| | 12 | 193 | 208 | 0.262 | 3.71 | 0.156 | 0.90 |
| | 24 | 236 | 251 | 0.391 | 6.68 | 0.141 | 1.0 |
| Brine/$CO_2$ | 3 | 198 | 213 | 0.478 | 6.94 | 1.11 | 0.89 |
| | 6 | 212 | 227 | 0.673 | 10.4 | 0.877 | 0.98 |
| | 12 | 203 | 218 | 0.617 | 9.18 | 0.386 | 0.94 |
| | 24 | 204 | 219 | 0.595 | 8.84 | 0.186 | 0.90 |

[a]

$$\text{moles } H_2 = \frac{PV}{RT} = \frac{P_f \text{ atm} \cdot 0.634\text{L}}{0.0821 \frac{\text{atm-L}}{\text{mole-°K}} \cdot 303\text{°K}} \cdot \frac{12 \text{ months/yr}}{\Delta t \text{ months}} \cdot \frac{1}{Am^2}$$

where 0.634L = plenum volume of container
$\Delta t$ = test duration, months
A = area of steel in test (from Appendix D)

# APPENDIX D: TOTAL STEEL SPECIMEN AREA, SEAL-WELDED-CONTAINER TESTS

## APPENDIX D: TOTAL STEEL SPECIMEN AREA, SEAL-WELDED-CONTAINER TESTS

Low-Carbon Steel

| Test Container | Area, $m^2$ | Test Container | Area, $m^2$ | Test Container | Area, $m^2$ |
|---|---|---|---|---|---|
| 1 | 0.639 | 15 | 0.603 | 29 | 0.604 |
| 2 | 0.639 | 16 | 0.604 | 30 | 0.604 |
| 3 | 0.639 | 17 | 0.604 | 31 | 0.604 |
| 4 | 0.638 | 18 | 0.605 | 32 | 0.604 |
| 5 | 0.638 | 19 | 0.604 | 33 | 0.630 |
| 6 | 0.631 | 20 | 0.604 | 34 | 0.629 |
| 7 | 0.631 | 21 | 0.604 | 35 | 0.629 |
| 8 | 0.631 | 22 | 0.604 | 36 | 0.629 |
| 9 | 0.604 | 23 | 0.604 | 37 | 0.630 |
| 10 | 0.604 | 24 | 0.604 | 38 | 0.629 |
| 11 | 0.604 | 25 | 0.604 | 40 | 0.497 |
| 12 | 0.604 | 26 | 0.605 | 41 | 0.498 |
| 13 | 0.604 | 27 | 0.605 | 42 | 0.497 |
| 14 | 0.604 | 28 | 0.605 | 43 | 0.498 |

Alternative Materials

| Test Container | Area, $m^2$ | Test Container | Area, $m^2$ |
|---|---|---|---|
| 1A | 0.434 | 10A | 0.436 |
| 2A | 0.433 | 11A | 0.436 |
| 3A | 0.434 | 12A | 0.436 |
| 4A | 0.436 | 13A | 0.434 |
| 5A | 0.436 | 14A | 0.434 |
| 6A | 0.436 | 15A | 0.434 |
| 7A | 0.433 | 16A | 0.436 |
| 8A | 0.434 | 17A | 0.436 |
| 9A | 0.434 | 18A | 0.436 |

# DISTRIBUTION

## Federal Agencies

US Department of Energy (6)
Office of Civilian Radioactive Waste Management
Attn: Deputy Director, RW-2
Associate Director, RW-10/50
Office of Program and Resources Management
Office of Contract Business Management
Director, Analysis and Verification Division, RW-22
Associate Director, RW-30
Office of Systems and Compliance
Associate Director, RW-40
Office of Storage and Transportation
Director, RW-4/5
Office of Strategic Planning and International Programs
Office of External Relations
Forrestal Building
Washington, DC 20585

US Department of Energy
Albuquerque Operations Office
Attn: National Atomic Museum Library
PO Box 5400
Albuquerque, NM 87185-5400

US Department of Energy (4)
WIPP Project Integration Office
Attn: W.J. Arthur III
L.W. Gage
P.J. Higgins
D.A. Olona
PO Box 5400
Albuquerque, NM 87115-5400

US Department of Energy (2)
WIPP Project Integration Satellite Office
Attn: R. Batra
R. Becker
PO Box 3090, Mail Stop 525
Carlsbad, NM 88221-3090

US Department of Energy (3)
WIPP Project Site Office (Carlsbad)
Attn: V. Daub
J. Lippis
J.A. Mewhinney
PO Box 3090
Carlsbad, NM 88221-3090

US Department of Energy
Research & Waste Management Division
Attn: Director
PO Box E
Oak Ridge, TN 37831

US Department of Energy
Attn: E. Young
Room E-178
GAO/RCED/GTN
Washington, DC 20545

US Department of Energy
Office of Environmental Restoration and Waste Management
Attn: J. Lytle, EM-30,
Trevion II
Washington, DC 20585-0002

US Department of Energy (3)
Office of Environmental Restoration and Waste Management
Attn: M. Frei, EM-34,
Trevion II
Washington, DC 20585-0002

US Department of Energy
Office of Environmental Restoration and Waste Management
Attn: S. Schneider, EM-342,
Trevion II
Washington, DC 20585-0002

US Department of Energy (2)
Office of Environment, Safety and Health
Attn: C. Borgstrom, EH-25
R. Pelletier, EH-231
Washington, DC 20585

US Department of Energy (2)
Idaho Operations Office
Fuel Processing and Waste
Management Division
785 DOE Place
Idaho Falls, ID 83402

US Environmental Protection
Agency (2)
Radiation Programs (ANR-460)
Attn: M. Oge
r. Guimond
Washington, DC 20460

US Geological Survey (2)
Water Resources Division
Attn: R. Livingston
4501 Indian School NE
Suite 200
Albuquerque, NM 87110

US Nuclear Regulatory Commission
Division of Waste Management
Attn: H. Marson
Mail Stop 623SS
Washington, DC 20555

## Boards

Defense Nuclear Facilities Safety Board
Attn: D. Winters
625 Indiana Ave. NW, Suite 700
Washington, DC 20004

Nuclear Waste Technical Review
Board (2)
Attn: D.A. Deere
S.J.S. Parry
1100 Wilson Blvd., Suite 910
Arlington, VA 22209-2297

Advisory Committee on Nuclear Waste
Nuclear Regulatory Commission
Attn: R. Major
7920 Norfolk Ave.
Bethesda, MD 20814

## State Agencies

Environmental Evaluation Group (3)
Attn: Library
7007 Wyoming NE
Suite F-2
Albuquerque, NM 87109

NM Bureau of Mines and Mineral
Resources
Socorro, NM 87801

NM Energy, Minerals, and Natural
Resources Department
Attn: Library
2040 S. Pacheco
Santa Fe, NM 87505

NM Environment Department (3)
Secretary of the Environment
Attn: J. Espinosa
1190 St. Francis Drive
Santa Fe, NM 87503-0968

NM Environment Department
WIPP Project Site
Attn: P. McCasland
PO Box 3090
Carlsbad, NM 88221

## Laboratories/Corporations

Battelle Pacific Northwest Laboratories (36)
Attn: S.M.Bruemmer, P8-16
H.C. Burkholder, P7-41
P.G. Doctor, K6-96
R.E. Einziger, P7-14
P.W. Eslinger, K6-96
W.W. Laity, K2-50
G.L. McVay, K2-45
K.H. Pool, P8-44
R.L. Skaggs, K6-77
P. Silva, P8-44
M.T. Smith, P8-35
M.R. Telander, P8-44 (10)
R.E. Westerman, P8-44 (10)
Publishing Coordination Technical
Report Files (5)
Battelle Blvd.
Richland, WA 99352

INTERA Inc.
Attn: J.F. Pickens
6850 Austin Center Blvd.
Suite 300
Austin, TX 78731

INTERA Inc.
Attn: W. Stensrud
PO Box 2123
Carlsbad, NM 88221

IT Corporation
Attn: R.F. McKinney
Regional Office
5301 Central NE
Suite 700
Albuquerque, NM 87108

Los Alamos National Laboratory
Attn: B. Erdal, CNC-11
PO Box 1663
Los Alamos, NM 87544

RE/SPEC, Inc.
Attn: W. Coons
4775 Indian School NE
Suite 300
Albuquerque, NM 87110-3927

RE/SPEC, Inc.
Attn: J.L. Ratigan
PO Box 725
Rapid City, SD 57709

Southwest Research Institute (2)
Center for Nuclear Waste
Regulatory Analysis
Attn: P.K. Nair
6220 Culebra Road
San Antonio, TX 78228-0510

SAIC
Attn: D.C. Royer
101 Convention Center Dr.
Las Vegas, NV 89109

SAIC
Attn: H.R. Pratt
10260 Campus Point Dr.
San Diego, CA 92121

SAIC (2)
Attn: M. Davis
J. Tollison
2109 Air Park Rd. SE
Albuquerque, NM 87106

Tech Reps Inc. (3)
Attn: J. Chapman
C. Crawford
T. Peterson
5000 Marble NE
Suite 222
Albuquerque, NM 87110

TRW Environmental Safety Systems
Attn: L. Wildman
2650 Park Tower Dr., Suite 1300
Vienna, VA 22180-7306

Westinghouse Electric Corporation (5)
Attn: Library
C. Cox
L. Fitch
B.A. Howard
R. Kehrman
PO Box 2078
Carlsbad, NM 88221

Westinghouse–Savannah River Technology
Center (4)
Attn: N. Bibler
J.R. Harbour
M.J. Plodinec
G.G. Wicks
Aiken, SC 29802

## National Academy of Sciences, WIPP Panel

Howard Adler
Oak Ridge Associated Universities
Medical Sciences Division
PO Box 117
Oak Ridge, TN 37831-0117

Ina Alterman
Board on Radioactive
Waste Management, GF456
2101 Constitution Ave.
Washington, DC 20418

John D. Bredehoeft
Western Region Hydrologist
Water Resources Division
US Geological Survey (M/S 439)
345 Middlefield Road
Menlo Park, CA 94025

Fred M. Ernsberger
250 Old Mill Road
Pittsburgh, PA 15238

Rodney C. Ewing
Department of Geology
University of New Mexico
Albuquerque, NM 87131

Charles Fairhurst, Chairman
Department of Civil and
Mineral Engineering
University of Minnesota
500 Pillsbury Dr. SE
Minneapolis, MN 55455-0220

B. John Garrick
PLG Incorporated
4590 MacArthur Blvd., Suite 400
Newport Beach, CA 92660-2027

Leonard F. Konikow
US Geological Survey
431 National Center
Reston, VA 22092

Peter B. Myers
National Academy of Sciences
Board on Radioactive
Waste Management
2101 Constitution Ave.
Washington, DC 20418

Jeremiah O'Driscoll
Jody Incorporated
505 Valley Hill Drive
Atlanta, GA 30350

Christopher G. Whipple
Clement International
160 Spear St., Suite 1380
San Francisco, CA 94105

## Individuals

P. Drez
8816 Cherry Hills Rd. NE
Albuquerque, NM 87111

D.W. Powers
Star Route Box 87
Anthony, TX 79821

## Universities

University of New Mexico
Geology Department
Attn: Library
Albuquerque, NM 87131

University of Washington
College of Ocean
and Fishery Sciences
Attn: G.R.Heath
583 Henderson Hall
Seattle, WA 98195

## Libraries

Thomas Brannigan Library
Attn: D. Dresp
106 W. Hadley St.
Las Cruces, NM 88001

Government Publications Department
Zimmerman Library
University of New Mexico
Albuquerque, NM 87131

New Mexico Junior College
Pannell Library
Attn: R. Hill
Lovington Highway
Hobbs, NM 88240

New Mexico State Library
Attn: N. McCallan
325 Don Gaspar
Santa Fe, NM 87503

New Mexico Tech
Martin Speere Memorial Library
Campus Street
Socorro, NM 87810

WIPP Public Reading Room
Carlsbad Public Library
Attn: Director
101 S. Halagueno St.
Carlsbad, NM 88220

## Foreign Addresses

Studiecentrum Voor Kernenergie
Centre D'Energie Nucleaire
Attn: A. Bonne
SCK/CEN Boeretang 200
B-2400 Mol, BELGIUM

Atomic Energy of Canada, Ltd. (3)
Whiteshell Research Estab.
Attn: B. Goodwin
M. Stevens
D. Wushke
Pinewa, Manitoba, CANADA R0E 1L0

Francois Chenevier (2)
ANDRA
Route du Panorama Robert Schumann
B.P. 38
92266 Fontenay-aux-Roses, Cedex
FRANCE

Jean-Pierre Olivier
OECD Nuclear Energy Agency
Division of Radiation Protection
and Waste Management
38, Boulevard Suchet
75016 Paris, FRANCE

Claude Sombret
Centre D'Etudes Nucleaires
De La Vallee Rhone
CEN/VALRHO
S.D.H.A. B.P. 171
30205 Bagnols-Sur-Ceze, FRANCE

Gesellschaft fur Reaktorsicherheit (GRS)
(2)
Attn: B. Baltes
W. Muller
Schwertnergasse 1
D-5000 Cologne, GERMANY

Bundesanstalt fur Geowissenschaften
und Rohstoffe
Attn: M. Langer
Postfach 510 153
3000 Hanover 51, GERMANY

Bundesministerium fur Forschung und
Technologie
Postfach 200 706
5300 Bonn 2, GERMANY

Institut fur Tieflagerung (2)
Attn: K. Kuhn
Theodor-Heuss-Strasse 4
D-3300 Braunschweig, GERMANY

Kerforschungszentrum Karlsruhe GmbH
Institut fur Nukleare Entsorgungstechnik (2)
Attn: W. Lutze
E. Smailos
Postfach 3640
D-7500 Karlsruhe 1
GERMANY

Physikalisch-Technische Bundesanstalt
Attn: P. Brenneke
Postfach 3345
D-3300 Braunschweig, GERMANY

Shingo Tashiro
Japan Atomic Energy Research Inst.
Tokai-Mura, Ibaraki-Ken, 319-11
JAPAN

Netherlands Energy Research Foundation
ECN
Attn: L.H. Vons
3 Westerduinweg
PO Box 1
1755 ZG Petten, THE NETHERLANDS

Svensk Karnbransleforsorjning AB
Attn: F. Karlsson
Project KBS
Karnbranslesakerhet
Box 5864
10248 Stockholm, SWEDEN

Nationale Genossenschaft für die Lagerung
Radioaktiver Abfälle (2)
Attn: S. Vomvoris
P. Zuidema
Hardstrasse 73
CH-5430 Wettingen, SWITZERLAND

AEA Technology
Attn: J.H. Rees
D5W/29 Culham Laboratory
Abington, Oxfordshire OX14 3DB
UNITED KINGDOM

AEA Technology
Attn: W.R. Rodwell
O44/A31 Winfrith Technical Centre
Dorchester, Dorset DT2 8DH
UNITED KINGDOM

AEA Technology
Attn: J.E. Tinson
B4244 Harwell Laboratory
Didcot, Oxfordshire OX11 0RA
UNITED KINGDOM

D.R. Knowles
British Nuclear Fuels, plc
Risley, Warrington, Cheshire WA3 6AS
1002607 UNITED KINGDOM

## Internal

| | |
|---|---|
| 1502 | J.C. Cummings |
| 6000 | D.L. Hartley |
| 6100 | R.W. Lynch |
| 6101 | P.J. Hommert |
| 6119 | E.D. Gorham |
| 6119 | S.W. Webb (10) |
| 6119 | Staff (14) |
| 6121 | J.R. Tillerson |
| 6121 | Staff (7) |
| 6300 | D.E. Ellis |
| 6302 | L.E. Shephard |
| 6303 | S.Y. Pickering |
| 6303 | W.D. Weart |
| 6305 | S.A. Goldstein |
| 6305 | A.R. Lappin |
| 6306 | A.L. Stevens |
| 6342 | D.R. Anderson |
| 6342 | Staff (20) |
| 6343 | V. Harper-Slaboszewicz |
| 6343 | Staff (2) |
| 6345 | R.C. Lincoln |
| 6345 | Staff (9) |
| 6347 | D.R. Schafer |
| 6348 | J.T. Holmes |
| 6348 | Staff (4) |
| 6348 | M.A. Molecke (10) |
| 6348 | L.H. Brush |
| 6351 | R.E. Thompson |
| 6352 | D.P. Garber |
| 6352 | S.E. Sharpton |
| 6352 | WIPP Central Files (RC/AC, 1.1.1.1.3) (10) |
| 7141 | Technical Library (5) |
| 7151 | Technical Publications |
| 7613-2 | Document Processing for DOE/OSTI (10) |
| 8523-2 | Central Technical Files |

* U.S. GOVERNMENT PRINTING OFFICE 1993—774-122/80232